GEOLOGY OF GREENLAND SURVEY BULLETIN 177 • 1997

Accretion and evolution of an Archaean high-grade grey gneiss – amphibolite complex: the Fiskefjord area, southern West Greenland

Adam A. Garde

GEOLOGICAL SURVEY OF DENMARK AND GREENLAND
MINISTRY OF ENVIRONMENT AND ENERGY

GEUS

GEOLOGY OF GREENLAND SURVEY BULLETIN 177 • 1997

Accretion and evolution of an Archaean high-grade grey gneiss – amphibolite complex: the Fiskefjord area, southern West Greenland

Adam A. Garde

GEOLOGICAL SURVEY OF DENMARK AND GREENLAND
MINISTRY OF ENVIRONMENT AND ENERGY

Geology of Greenland Survey Bulletin 177

Keywords
Archaean grey gneiss, West Greenland, supracrustal amphibolite, Akia terrane, tonalite-trondhjemite-granodiorite, granulite facies, retrogression, element mobility, oceanic crust, layered complex, REE fractionation.

Cover
Coastal exposure of purplish grey orthogneiss retrogressed from granulite facies, with angular fragments of homogeneous amphibolite. The purplish grey orthogneiss displays indistinct foliation and migmatisation fabrics, which have been blurred during recrystallisation under granulite facies *P-T* conditions and subsequent static hydrous retrogression in amphibolite facies. Outer coast north of Fiskefjord, point west of Pâtôq. The island Talerulik is visible in the far distance.

Adam A. Garde
Geological Survey of Denmark and Greenland
Thoravej 8, DK-2400 Copenhagen NV, Denmark

Chief editor of this series: Peter R. Dawes
Scientific editor: W. Stuart Watt
Editorial secretary: Esben W. Glendal
Critical readers: Clark R. L. Friend (United Kingdom) and David Bridgwater (Denmark)
Drawing work: Adam A. Garde
Graphic production: Egestal Illustration, Copenhagen, Denmark
Reproduction: Salomon & Roussell AS Grafisk, Søborg, Denmark
Manuscript submitted: 20th November, 1995
Final version approved: 11th June, 1997
Printed: 10th October, 1997

This publication inclusive of colour reproductions is partly financed by the Danish Natural Science Research Council.

ISBN 87-7871-019-7
ISSN 1397-1905

Geology of Greenland Survey Bulletin
The series *Geology of Greenland Survey Bulletin* is a continuation of *Bulletin Grønlands Geologiske Undersøgelse* and incorporates *Rapport Grønlands Geologiske Undersøgelse*.

Citation of the name of this series:
It is recommended that the name of this series is cited in full, viz. *Geology of Greenland Survey Bulletin*
If abbreviation of this volume is necessary the following form is suggested: *Geol. Greenland Surv. Bull.* 177, 115 pp.

Available from:
Geological Survey of Denmark and Greenland
Thoravej 8, DK-2400 Copenhagen NV, Denmark
Phone: +45 38 14 20 00, fax: +45 38 14 20 50, e-mail: geus@geus.dk
or
Geografforlaget Aps
Fruerhøjvej 43, DK-5464 Brenderup, Denmark
Phone: +45 64 44 26 83, fax: +45 64 44 16 97

Contents

Abstract

Garde, A. A. 1997: Accretion and evolution of an Archaean high-grade grey gneiss – amphibolite complex: the Fiskefjord area, southern West Greenland. *Geology of Greenland Survey Bulletin* 177, 115 pp.

The Fiskefjord area in southern West Greenland, part of the Akia tectono-stratigraphic terrane, comprises a supracrustal association and two groups of grey quartzo-feldspathic orthogneises *c*. 3200 and 3000 Ma old. The supracrustal association forms layers and enclaves in grey gneiss and may comprise two or more age groups. Homogeneous amphibolite with MORB-like but LIL element enriched tholeiitic composition predominates; part, associated with cumulate noritic and dunitic rocks, represents fragments of layered complexes. Heterogeneous amphibolite of likely submarine volcanic origin, (basaltic) andesitic amphibolite, leucogabbro-anorthosite, and minor pelitic metasediment occur. Disruption by magmatic and tectonic events and geochemical alteration have obscured primary origin: the supracrustal association may represent oceanic crust.

Grey orthogneiss of the tonalite-trondhjemite-granodiorite (TTG) association was generated during continental accretion at *c*. 3000 Ma, most likely by partial melting of wet and hot tholeiitic basaltic rocks subducted in a convergent plate setting. Most dioritic gneiss is *c*. 220 Ma older. A 3040 Ma dioritic to tonalitic phase, enriched in P_2O_5, Ba, Sr, K, Pb, Rb and LREE, probably was derived from metasomatised mantle.

Intense deformation and metamorphism accompanied the 3000 Ma magmatic accretion. Thrusts along amphibolite-orthogneiss contacts were succeeded by large recumbent isoclines, upright to overturned folds, and local domes with granitic cores. Syntectonic granulite facies metamorphism is thought to be due to heat accumulation by repeated injection of tonalitic magma. Strong ductile deformation produced steep linear belts before the thermal maximum ceased, whereby folds were reorientated into upright south-plunging isoclines. Two large TTG complexes were then emplaced, followed by granodiorite and granite.

Post-kinematic diorite plugs with unusually high MgO, Cr and Ni, and low LIL and immobile incompatible element contents, terminated the 3000 Ma accretion. Hybrid border zones and orbicular textures suggest rapid crystallisation from superheated magma. The diorites most likely formed from ultramafic magma contaminated with continental crust.

Widespread high-grade retrogression preserved a granulite facies core in the south-west; to the east the retrogressed gneiss grades into amphibolite facies gneiss not affected by granulite facies metamorphism and retrogression. LIL elements were depleted during granulite facies metamorphism and reintroduced during retrogression, probably transported in anatectic silicate melts and in fluids. Rb-Sr isotope data, and relationships between retrogression, high-strain zones and granite emplacement, show that retrogression took place shortly after the granulite facies metamorphism, before terrane assembly at *c*. 2720 Ma, probably by movement of melts and fluids into the upper, marginal zone of granulite facies rocks from deeper crust still being dehydrated. Retrogression during Late Archaean terrane assembly was in narrow reactivated zones of ductile deformation; in the Proterozoic it occurred with faulting and dyke emplacement.

Geochemical data are presented for Early Proterozoic high-Mg and mafic dykes. A rare 2085 Ma microgranite dyke strongly enriched in incompatible trace elements was formed by partial anatexis of Archaean continental crust.

Author's address:
Geological Survey of Denmark and Greenland, Thoravej 8, DK-2400 Copenhagen NV, Denmark.

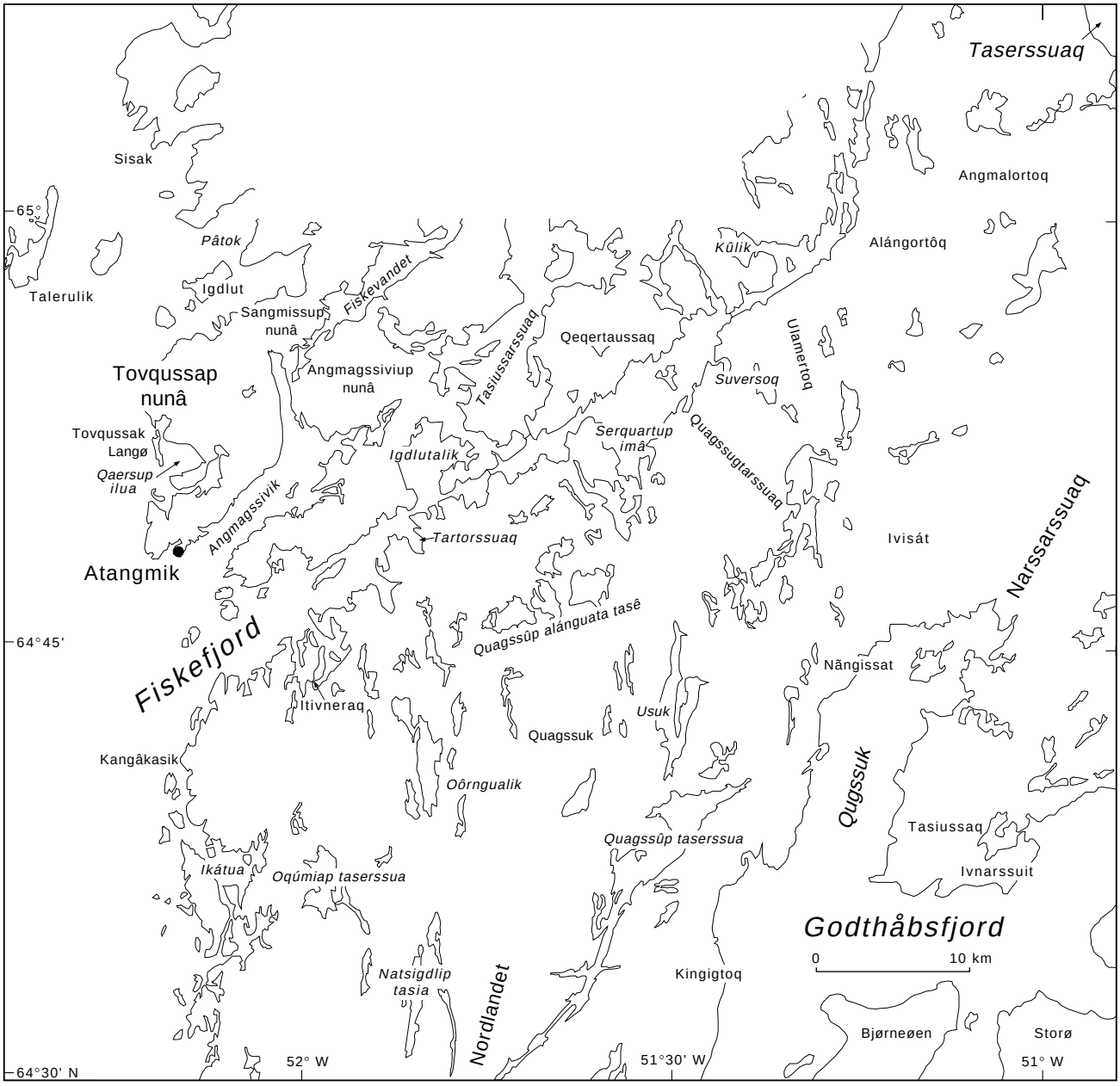

Fig. 1. Outline map of the Fiskefjord area showing place names used in the text. Finnefjeld lies 15 km to the north of the map, and Qôrqût 30 km to the south in Godthåbsfjord.

Introduction

Much of the Archaean crust presently exposed on Earth is traditionally considered to belong to either of two major associations: low-grade granite–greenstone terrains and high-grade grey gneiss – amphibolite terrains (e.g. Windley, 1984; Passchier, 1995). There is growing evidence from both types of associations that 'plate tectonics' in some form was important at least as early as the middle Archaean. Granite–greenstone terrains can provide detailed information about volcanic and sedimentary environments and upper crustal structure, but they may represent specific geotectonic settings where only rather thin continental crust was developed (e.g. Shackleton, 1995), and arguably they do not contain any remnants of oceanic crust (Bickle *et al.*, 1994). There is also new evidence from geophysical studies that most greenstone belts do not extend deep into the underlying continental crust (de Wit & Ashwal, 1995). By contrast, high-grade grey gneiss – amphibolite terrains represent environments where thick Archaean continental crust was rapidly accreted, and the uppermost crust therefore quickly removed by isostatic uplift and erosion. These terrains display the results of mid-crustal metamorphic and tectonic processes, but their supracrustal rock associations are commonly rather poorly preserved. The grey gneiss – amphibolite terrains are sometimes interpreted as the root zones of granite–greenstone terrains, and it is as yet uncertain if they comprise fragments of oceanic crust.

The Fiskefjord area examined in this paper is a type example of a middle Archaean high grade grey gneiss – amphibolite terrain. An early development of supracrustal rocks was followed by magmatic accretion of quartzo-feldspathic rocks in two separate episodes, the first of which took place at around 3200 Ma. A second major episode at *c.* 3000 Ma was short-lived but resulted in the establishment of thick continental crust and subsequent mid-crustal differentiation, and was accompanied by major metamorphic and tectonic activity.

The Fiskefjord area (Figs 1, 2) is located in the northern part of the Archaean block, southern West Greenland (Bridgwater *et al.*, 1976; Kalsbeek & Garde, 1989), which is bounded by the Proterozoic Nagssugtoqidian and Ketilidian orogens to the north and south, respectively. The Fiskefjord area forms a large part of the Akia terrane (Friend *et al.*, 1988a), see Fig. 2, which is juxtaposed to the south-east against the Akulleq terrane

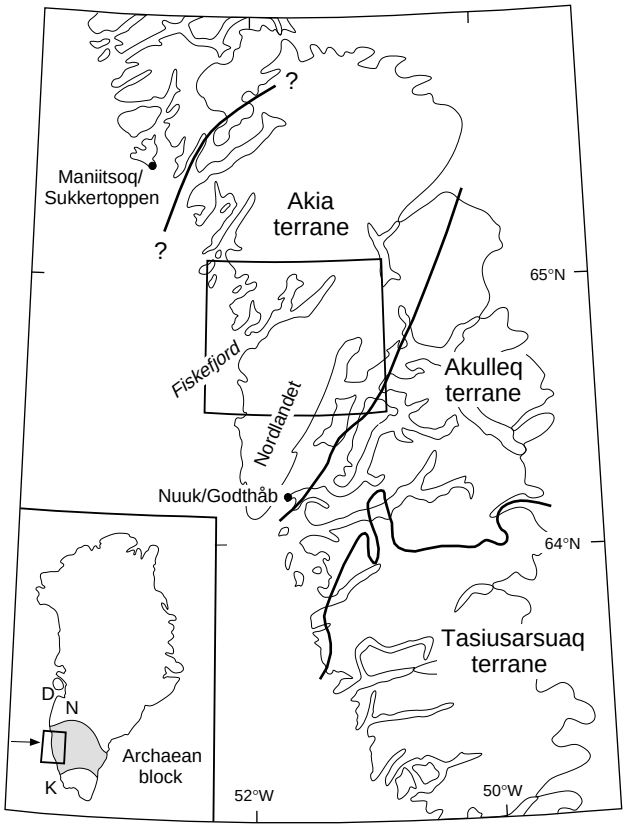

Fig. 2. Positions of three Archaean tectono-stratigraphic terranes: Akia, Akulleq and Tasiusarsuaq in the northern part of the Archaean block of southern West Greenland (inset map), with frame showing location of the Fiskefjord area in the southern part of the Akia terrane. The terranes were assembled around 2750–2650 Ma. D = Disko Bugt. N and K mark the position of the Proterozoic Nagssugtoqidian and Ketilidian orogens, respectively. See the main text for discussion and references.

in Godthåbsfjord (McGregor *et al.*, 1991). The northern boundary of the Akia terrane has not been identified in the field, but recent isotope work suggests that it is located south-east of Maniitsoq (Friend & Nutman, 1994). Plate 1 shows a simplified geological map of the Fiskefjord area, and Fig. 1 shows place names.

The geological history of the Fiskefjord area, summarised in Table 1 together with pertinent isotopic age data, comprises the following main stages: (1) formation of mafic, ultrabasic to ultramafic and minor pelitic supracrustal rocks, perhaps in an oceanic environment; (2) magmatic accretion of large volumes of first dioritic and then dioritic, tonalitic, trondhjemitic and grano-

Table 1. Magmatic, tectonic and metamorphic events in the Fiskefjord area, southern West Greenland

Igneous activity	Tectonic events	Metamorphism	Isotopic age data	Reference
Middle Archaean				
Oceanic? supracrustal association				
Accretion of Nordlandet dioritic gneiss precursors (number of phases unknown)	Early deformation of supracrustal association and dioritic gneiss		3221 ±13 Ma, SHRIMP zircon U-Pb Nordlandet dioritic gneiss	This paper
Second (oceanic?) supracrustal association?	Folding and thrusting within the supracrustal package	Early thermal event (?granulite facies)	*c.* 3180 Ma, SHRIMP zircon U-Pb, Nordlandet dioritic gneiss	This paper
Accretion of Qeqertaussaq diorite precursors (number of intrusive phases unknown) Accretion of main grey gneiss precursors (numerous intrusive phases)	Assembly of Nordlandet dioritic gneiss, dioritic-tonalitic-trondhjemitic gneiss (each with supracrustal enclaves), and possibly larger supracrustal bodies		3112 ±40 Ma?, w.r. Pb-Pb (composite from several units) 3044 ±7 Ma, SHRIMP zircon U-Pb Qeqertaussaq diorite	Garde (1989a, 1990), This paper
	Thrusting at high crustal levels along amphibolite – grey gneiss contacts (e.g. on Angmagssi-viup nunâ)	Prograde metamorphism		
Continued magmatic crustal accretion	Midterhøj phase of deformation (recumbent isoclinal folds) in central Fiskefjord area and possibly on Tovqussap nunâ	Granulite facies conditions possibly reached in the southern and western parts of the Fiskefjord area	2954 ±120 Ma, w. r. Rb-Sr Amphibolite facies grey gneiss, Qugssuk	Garde (1989a, 1990)
	Smalledal phase of deformation (widespread recumbent, E–W trending isoclinal folds)			
Intrusion of mesoperthite granite sheets	Pâkitsoq phase of deformation (widespread upright to overturned, S-plunging folds)	Granulite facies metamorphism outlasting Pâkitsoq phase of deformation		
Intrusion of trondhjemitic and granitic rocks	Early doming, e.g. on Tovqussap nunâ and south of Fiskefjord			
	Ductile deformation in linear N–S trending high strain zones	Late stage of granulite facies metamorphism		
		Widespread high-grade (regional) retrogression	3137 ±172 Ma, w. r. Rb-Sr Grey gneiss, inner Fiskefjord	This paper
Intrusion of Finnefjeld gneiss complex (few large intrusive phases, four of which identified)	Ductile deformation along the south-eastern margin of the Finnefjeld gneiss complex		3067 $^{+62}_{-42}$ Ma, zircon U-Pb 3058 ±123 Ma, w. r. Rb-Sr 3034 ±134 Ma, w. r. Rb-Sr Finnefjeld gneiss complex	Garde (1990) This paper
Middle to Late Archaean				
Intrusion of Taserssuaq tonalite complex (few and large intrusive phases)	Doming	Local granulite facies conditions reached in western Taserssuaq tonalite complex	2982 ±7 Ma, zircon U-Pb 2882 ±36 Ma, w. r. Rb-Sr 2930 ±100 Ma, w.r. Rb-Sr Taserssuaq tonalite complex	Garde *et al.* (1986) This paper
Intrusion of Igánánguit granodiorite	Formation of Igánánguit dome		2935 ± 240 Ma, w. r. Rb-Sr 3092 ±48 Ma (?), w. r. Pb-Pb Igánánguit granodiorite	Garde *et al.* (1986) This paper
Intrusion of Qugssuk granite and related granite sheets, e.g. in northern Nordlandet	Localised doming Localised ductile deformation along N–S trending zones	Local retrogression caused by granite emplacement	2969 ±32 Ma, w. r. Rb-Sr 2842 ±85 Ma, w. r. Rb-Sr Qugssuk granite	Garde *et al.* (1986) This paper
Intrusion of post-kinematic diorite plugs, mainly in the north-western part of the area	End of regional deformation	Auto-retrogression in diorites; possibly also affected by regional retrogression	3017 $^{+12}_{-10}$ Ma, zircon U-Pb (zircons interpreted as cogenetic). Rb-Sr data, Post-kinematic diorite	Garde (1991) This paper

Table 1. Magmatic, tectonic and metamorphic events in the Fiskefjord area (continued)

Igneous activity	Tectonic events	Metamorphism	Isotopic age data	Reference
Late Archaean				
Pegmatite intrusion?	Terrane assembly Reactivation of high-strain zones	Renewed local retrogression along reactivated zones	*c.* 2720 Ma	McGregor *et al.* (1991), Friend *et al.* (1996)
Pegmatite intrusion? (Intrusion of Qôrqut granite complex in Akulleq terrane)		Thermal event	*c.* 2500 Ma, plagioclase, titanite, apatite, Rb-Sr Taserssuaq tonalite complex	Garde *et al.* (1986)
Proterozoic				
Intrusion of N–S trending high-Mg and related dykes, followed by mafic dykes in other directions	Faulting along the Fiskefjord fault and a related conjugate system of NE- and WNW-trending faults	Localised retrogression along dykes and faults	*c.* 2200 Ma, w. r. Rb-Sr SHRIMP zircon U-Pb High-Mg and mafic dykes	Bridgwater *et al.* (1995) Nutman *et al.* (1995)
Intrusion of microgranite dyke at Qugssuk		Weak thermal event	2085^{+55}_{-65} Ma, zircon U-Pb Microgranite dyke at Qugssuk	This paper
		Weak thermal event	*c.* 1690 Ma, epidote and biotite Rb-Sr Taserssuaq tonalite complex	Garde *et al.* (1986)

Note the concentration of events at *c.* 3000 Ma, with overlapping ages. Specific listed events need not be synchronous over the entire area. w. r. = whole rock.

dioritic grey orthogneiss and related rocks at *c.* 3225 and *c.* 3040–2980 Ma, probably in convergent plate-tectonic environments, and culmination of associated ductile deformation and high-grade metamorphism (Garde, 1989a, 1990); (3) partial remobilisation of newly formed grey gneiss, leading to the emplacement of sheets and domes of younger granitoid rocks (Garde *et al.*, 1986); (4) emplacement of local post-kinematic diorite plugs (probably at *c.* 3000 Ma, Garde, 1991), which mark the end of regional Archaean deformation and metamorphism in the Akia terrane. (5) Towards the end of the Archaean (at around 2720 Ma) the Akia terrane was amalgamated with other terranes in the Godthåbsfjord region (Nutman *et al.*, 1989; McGregor *et al.*, 1991; Friend *et al.*, 1996) and became part of the Archaean craton of southern West Greenland. (6) In the Early Proterozoic, contemporaneously with Nagssugtoqidian and Ketilidian orogenic activity north and south of the Archaean craton, block faulting occurred along the NE–SW trending Fiskefjord fault and related faults. Mafic dykes were emplaced, and thermal episodes resulted in injection of rare acid dykes of crustal anatectic origin (Kalsbeek & Taylor, 1983; this paper) and resetting of Rb-Sr biotite ages (Garde *et al.*, 1986).

The present study is based on investigations in the Fiskefjord map area (Garde, 1989b) with its predominant grey orthogneiss and amphibolite, and in two adjacent areas: an inland area to the north-east within the Isukasia map area (Garde, 1987) that includes a younger granitic dome, and a coastal area to the north-west (Marker & Garde, 1988). In the latter area the border zone is exposed between the orthogneiss–amphibolite terrain and the Finnefjeld gneiss complex, a large composite tonalitic pluton that also post-dates the formation of the grey gneisses. The field work was carried out in the period 1980–1987 during a systematic mapping project by the Geological Survey of Greenland (Garde & McGregor, 1982; Garde, 1984, 1986; Garde *et al.*, 1983, 1987; Marker & Garde, 1988).

Previous geological investigations include an early coastal reconnaissance of West Greenland by Noe-Nygaard & Ramberg (1961) and – within the Fiskefjord map area – detailed studies of Tovqussap nunâ and adjacent areas (Berthelsen, 1951, 1960, 1962), and the area west of Qugssuk (Lauerma, 1964). Besides, Sørensen (1953) carried out a detailed petrographic study of ultrabasic rocks at Tovqussap nunâ. In the 1970s B. F. Windley undertook a coastal reconnaissance survey along Fiskefjord and adjacent fjords in preparation for the 1:500 000 map sheet Frederikshåb Isblink – Søndre Strømfjord (Allaart, 1982), and the exploration company Kryolitselskabet Øresund A/S carried out an extensive geological and geophysical mineral exploration programme. Dymek (1978, 1984) and Pillar (1985) studied metamorphism at Langø west of Tovqussap nunâ and in the southern part of the Fiskefjord area, respectively (and elsewhere in the region), and Riciputi *et al.* (1990) determined peak metamorphic conditions in Nordlandet.

Supracrustal rock association: field characteristics and petrography

Amphibolite of presumed volcanic origin and related basic and ultrabasic intrusive rocks, besides very minor pelitic metasediments, form an important component of the Fiskefjord area and constitute about 10 per cent of the outcrop. For convenience these lithologies are collectively referred to as the supracrustal rocks in the following, although this is not strictly correct. The supracrustal rocks form both layers and enclaves of very variable size in most parts of the dioritic, tonalitic and trondhjemitic orthogneiss, and the intrusive relationships of the latter rocks (described later) show that the supracrustal rocks as a whole are older than the grey gneiss, although they may well consist of originally independent sequences of different age.

Supracrustal rocks in the Fiskefjord area have been referred to in previous papers as equivalent to Malene supracrustal rocks in the adjacent Godthåbsfjord region. All supracrustal rocks of supposed Middle Archaean age in the latter region were originally called the Malene supracrustal rocks by McGregor (1969), although he realised that they might belong to more than one group. Subsequent dating of Malene metasedimentary rocks (Hamilton *et al.*, 1983; Schiøtte *et al.*, 1988) showed that they comprise several Middle to Late Archaean age populations. At about the same time it was discovered that the Godthåbsfjord region consists of several terranes with different histories and different ages, and the term 'Malene supracrustal rocks' is no longer used.

None of the supracrustal rocks in the Fiskefjord area have been dated, and their preservation as scattered, fragmented layers and rafts in younger rocks complicates an assessment of their mutual relationships and stratigraphy. In addition, the post-magmatic history of the supracrustal rocks with repeated deformation and metamorphism as enclaves in the grey gneiss has obliterated most primary structures and hindered geochemical identification of their origin due to likely element mobility (see p. 21). Besides, some supracrustal rocks were not surveyed in detail due to limited time available in the field. Therefore this account is not entirely comprehensive.

For descriptive purposes the supracrustal rocks of the Fiskefjord area can be divided into two main groups. Homogeneous, in places porphyroblastic amphibolite forms the bulk of the supracrustal rocks with additional leuco-amphibolite, heterogeneous calc-silicate-bearing amphibolite and minor pelitic metasediment. The second group comprises various ultrabasic rocks. Some ultrabasic bodies have outcrop dimensions of 2–3 km and occur as ovoid or lens-shaped mega-enclaves in either amphibolite or orthogneiss. They predominantly consist of dunite and peridotite and locally display rhythmic magmatic layering. Other ultrabasic and noritic rocks form stratiform, up to a few hundred metres thick bodies overlain by thick sequences of homogeneous amphibolite. Collectively the latter rocks outline at least two layered intrusive complexes, the largest of which is more than 25 km long in its present deformed state.

Homogeneous amphibolite

The most common amphibolite forms homogeneous, fine- to medium-grained, granulite facies rocks with plagioclase, hornblende, ortho- and clinopyroxene (the pyribolites of Berthelsen, 1960), and equivalent plagioclase-hornblende rocks in amphibolite facies in the easternmost part of the Fiskefjord area. Accessory biotite and magnetite-ilmenite intergrowths may occur in rocks of both facies, and titanite is present in some amphibolite facies rocks. Finely disseminated iron sulphide (less than one per cent) is common, and chalcopyrite has occasionally been observed. The amphibolite commonly has a moderate to strong tectono-metamorphic schistosity, combined with distinct rodding and hornblende lineation in hinge zones of larger folds. Mineral textures observed in thin section may be equigranular, but hornblende commonly developed a preferred planar or linear orientation during regional deformation. Pyroxene-bearing amphibolite may be variably retrogressed, whereby hypersthene is partially altered to fibrous orthoamphibole or replaced by symplectitic hornblende-quartz aggregates, and clinopyroxene replaced by epidote-clinozoisite. In some samples the latter mineral also forms coronas around, or completely replaces hornblende. Chemical aspects of this retrogression are examined in a later section.

The homogeneous amphibolite forms layers up to several hundreds of metres thick (rarely up to *c.* 2 km)

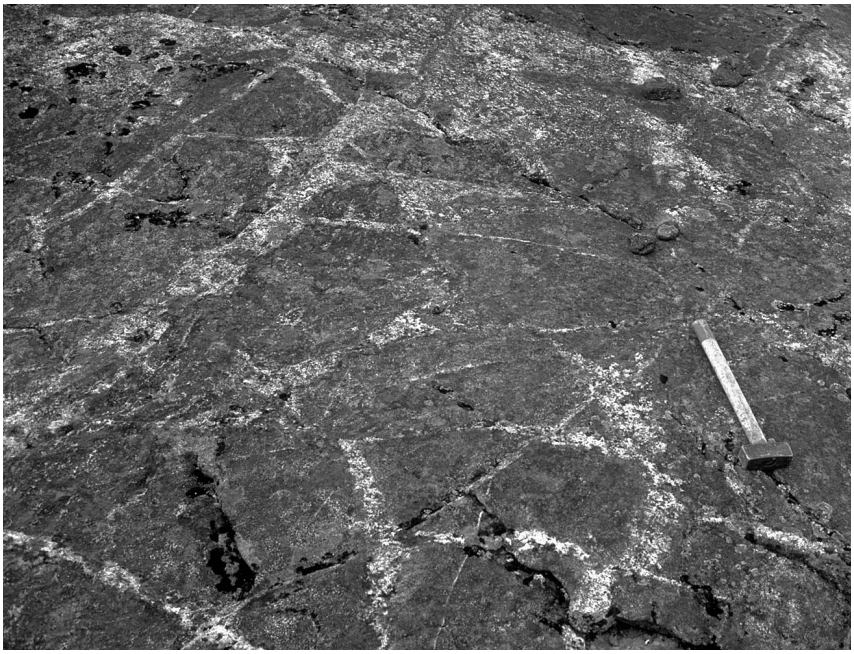

Fig. 3. Homogeneous amphibolite cut by numerous thin quartzo-feldspathic sheets. 10 km east of the head of Fiskefjord.

Fig. 4. Homogeneous medium-grained amphibolite with hornblende-blastic texture. East coast of Qugssuk, *c.* 5 km from the head of the fjord.

in the orthogneiss, and in its present state of preservation it generally appears to be very uniform, without lithological variations that can be ascribed to origin or mode of emplacement (Fig. 3). However, particularly in the lower grade, eastern part of the area there are local porphyroblastic varieties (Fig. 4) characterised by scattered hornblende or plagioclase crystals up to *c.* 1 cm, which may be pseudomorphs of porphyritic magmatic precursors. In this area a *c.* 500 m thick horizon of homogeneous, leucocratic, grey, fine-grained amphibolite also occurs adjacent to a more mafic amphibolite layer. The homogeneous and porphyroblastic amphibolites may have originated as volcanic flows or, more likely, as subvolcanic intrusive rocks (see p. 15).

Heterogeneous amphibolite

Thin horizons of heterogeneous, commonly calc-silicate-bearing amphibolite as well as pelitic metasediment alternate with homogeneous amphibolite in some parts of the Fiskefjord area. Such rocks occur in the western part of the peninsula east of Qugssuk, at the head of Qugssuk, east of the ridge Ulamertoq north of Qugssuk,

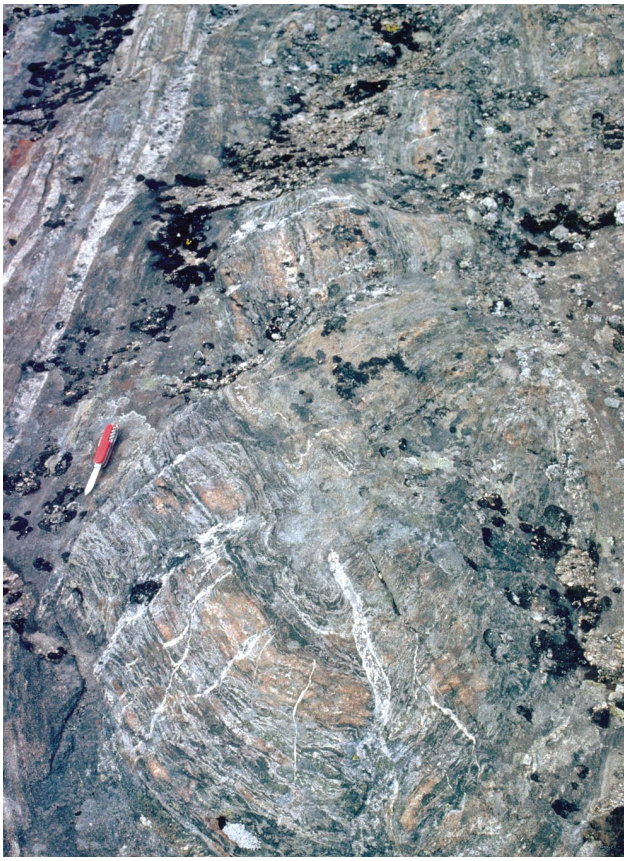

Fig. 5. Heterogeneous amphibolite with a *c.* 1 m thick calc-silicate horizon rich in diopside and garnet. The competent calc-silicate horizon is broken up into *c.* 50–80 cm large, in places folded, boudins and thinner slabs, which show anticlockwise rotation. 10 km north-east of Ulamertoq.

Fig. 6. Heterogeneous, thinly banded amphibolite cut by successive phases of diorite (right of the hammer) and tonalite, and subsequently folded. 8 km east of Ulamertoq.

on both sides of central Fiskefjord in the vicinity of the embayment Suversoq, at Tovqussaq (west of Tovqussap nunâ), and north of Tovqussap nunâ. The heterogeneous amphibolite mainly forms horizons up to a few metres thick with decimetre-sized lenses and irregular patches or, in strongly deformed varieties, distinct centimetre-thick bands of diopside, calcic plagioclase, hornblende, garnet and epidote besides local scapolite or calcite (Fig. 5). Other varieties of heterogeneous amphibolite consist of alternating layers a few centimetres to decimetres thick with variable proportions of hornblende, pyroxene and plagioclase (Figs 6, 7). Some of the heterogeneous, commonly calc-silicate-bearing amphibolite resembles strongly deformed varieties of pillowed lava sequences described from other parts of West Greenland (e.g. Hall & Hughes, 1982; Chadwick, 1990; McGregor, 1993). Besides, the common occurrence of heterogeneous amphibolite interlayered with pelitic metasediment also indicates a submarine extrusive, rather than subaerial or intrusive origin. Other units such as shown in Fig. 7 may originally have been tuffs or tuffites.

A different type of heterogeneous, banded amphibolite contains thin seams of quartz and pyrrhotite and forms rusty-weathering zones a few metres thick within homogeneous or calc-silicate-bearing amphibolite.

Bengaard (1988) described rare matrix-supported amphibolitic conglomerate or agglomerate, poor in calc-silicate minerals, in the Suversoq area south of inner Fiskefjord. Also calc-silicate-banded amphibolite and micaceous metasediment are present in this area. South of outer Fiskefjord there are local occurrences of another type of strongly deformed fragmental amphibolite consisting of closely packed, up to *c.* 1 m long, cigar-shaped or flattened lenses with diffuse margins to an indistinct quartzo-feldspathic matrix (Fig. 8). This type of fragmental amphibolite may represent strongly deformed pillow lava, or it could be an unusual type of agmatite.

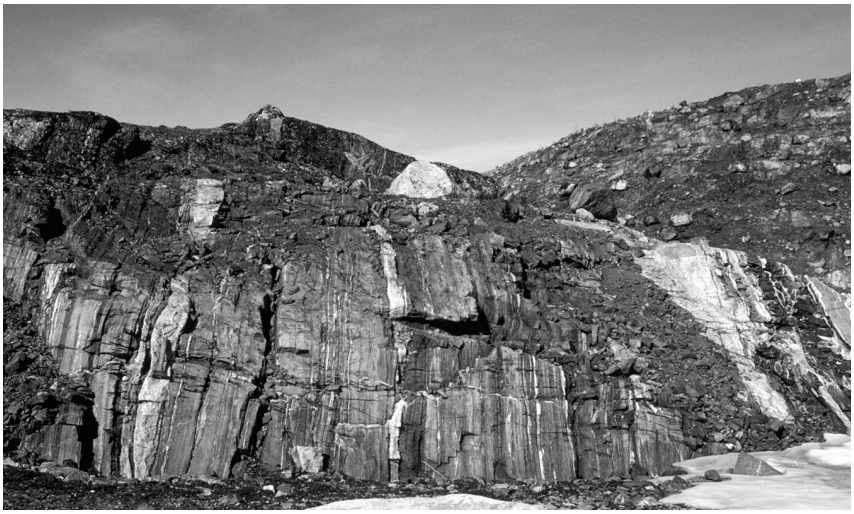

Fig. 7. Succession of strongly deformed, heterogeneous amphibolite with horizons of leuco-amphibolite, perhaps meta-andesitic tuff or tuffite. 7 km east of Ulamertoq.

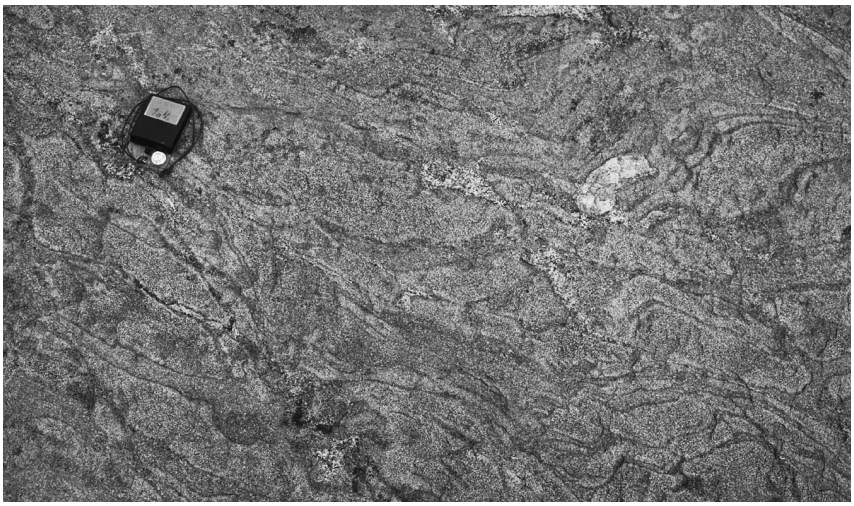

Fig. 8. Strongly deformed fragmental amphibolite consisting of closely packed, up to *c.* 1 m long, cigar-shaped or flattened lenses with diffuse margins to an indistinct quartzo-feldspathic matrix. South of outer Fiskefjord, *c.* 7 km north-east of Itivneraq.

Ultrabasic rocks

Large dunitic bodies

Several ovoid or lens-shaped ultrabasic bodies associated with amphibolite occur in the Fiskefjord area, the largest ones being 2–3 km long (Plate 1). Two of them, north-east of Fiskevandet and north-east of Tasiussarssuaq, are embedded in amphibolite and largely consist of granular, medium-grained dunite, olivine-rich peridotite and smaller irregular bodies of orthopyroxene-rich peridotite with a gradational transition into the dunitic rock. Well-developed rhythmic magmatic layering of olivine and orthopyroxene (locally of olivine and chromite) has been observed in both of these bodies. A third ultrabasic body occurs *c.* 5 km west of the head of Fiskefjord just north of 65°, at the boundary between amphibolite and leucocratic orthogneiss. It is in part covered by a lake and may be longer than the *c.* 1 km long outcrop. Like the two other ultrabasic bodies it consists predominantly of dunite, but its northernmost part adjacent to the amphibolite also contains noritic rocks. Irregular sheets of granite up to *c.* 100 m thick cut the ultrabasic bodies (see p. 14).

A fourth, large ultrabasic body is located 5 km east of Ulamertoq, forming a 1 by 1.5 km large enclave in grey orthogneiss (Fig. 9; Plate 1) at the northern tip of a *c.* 100 m thick amphibolite layer. This was investigated in some detail, and a sketch map is shown in Fig. 10. The ultrabasic body has a partial shell of biotite- and garnet-rich metasediment with thin bands of amphibolite and leuco-amphibolite. The orthogneiss host just south of the ultrabasic body contains numerous metre-sized and larger rafts of amphibolite, biotite schist and ultrabasic rock, which dip steeply inwards to the centre of the body and commonly outline tight N-plunging small scale folds. The ultrabasic body predominantly consists of granular, very uniform, medium-grained

Fig. 9. Large, pale brown ultrabasic body *c.* 5 km east of Ulamertoq, viewed towards the west. The ultrabasic body mostly consists of granular dunite and forms a mega-enclave in the orthogneiss. Part of the body is covered by many small lakes.

dunitic rock with pale brown weathering colours. Variable proportions of ortho- and clinopyroxene may be present and locally dark green spinel or chromite. Thin veins of hydrated phases such as anthophyllite, tremolite, chlorite and phlogopite are quite common (Fig. 11). In the southern, most olivine-rich part of the body there are small areas where centimetre-scale indistinct chromitite layering occurs in the dunite; the chromite occurrence was investigated in the 1970s by Kryolitselskabet Øresund A/S, but it was found to be of no economic interest.

The north-eastern part contains ultrabasic rocks which are less magnesian (Fig. 10). Red-brown weathering harzburgite and locally orthopyroxenite with *c.* 2 cm large pale brown equidimensional, poikilitic orthopyroxene covers an irregular area of *c.* 250 by 600 m. This is bounded to the north-east by a 150 by 500 m large sheet of grey-brown weathering, medium- to coarse-grained norite consisting of calcic plagioclase and magnesian orthopyroxene with accessory hornblende and phlogopite. There are also small pods of granular, medium-grained, greenish brown weathering clinopyroxene-rich rocks. These different rock types generally have gradational contacts; their orientations are difficult to determine due to their gradational nature and the flat topography, but moderately steep to subvertical contacts appear to be common.

Distinct magmatic layering with orientations varying from flat-lying to almost vertical has been observed locally along the contacts. A *c.* 40 m thick norite lens 300 m from the southern end of the ultrabasic body is separated from the dunite by a subvertical, metre-thick layer of coarse-grained orthopyroxenite, followed towards the norite by several parallel, few centimetres thick, alternating layers of orthopyroxenite and plagioclase-rich leuconorite (Fig. 12). The adjacent dunite contains several series of parallel, 0.5–2 cm thick, pale pyroxene-bearing horizons (Fig. 11), traceable over a few metres.

The ultrabasic body contains several irregular sheets and pods of white to pale pinkish granite, which are up to *c.* 150 m thick (Fig. 10). The granite sheets locally cut into the surrounding grey gneiss but are essentially confined to their ultrabasic host. The granites, which are probably of local anatectic origin, appear to have been emplaced along fractures in the competent ultrabasic body during regional deformation. Similar granites are also present in the other large ultrabasic bodies of the Fiskefjord area.

Layered complexes with stratiform ultrabasic and noritic rocks

Two large, layered complexes consisting of ultrabasic, noritic and metagabbroic rocks are embedded within supracrustal rocks. One complex extends for *c.* 25 km in N–S direction across central Fiskefjord, from west of

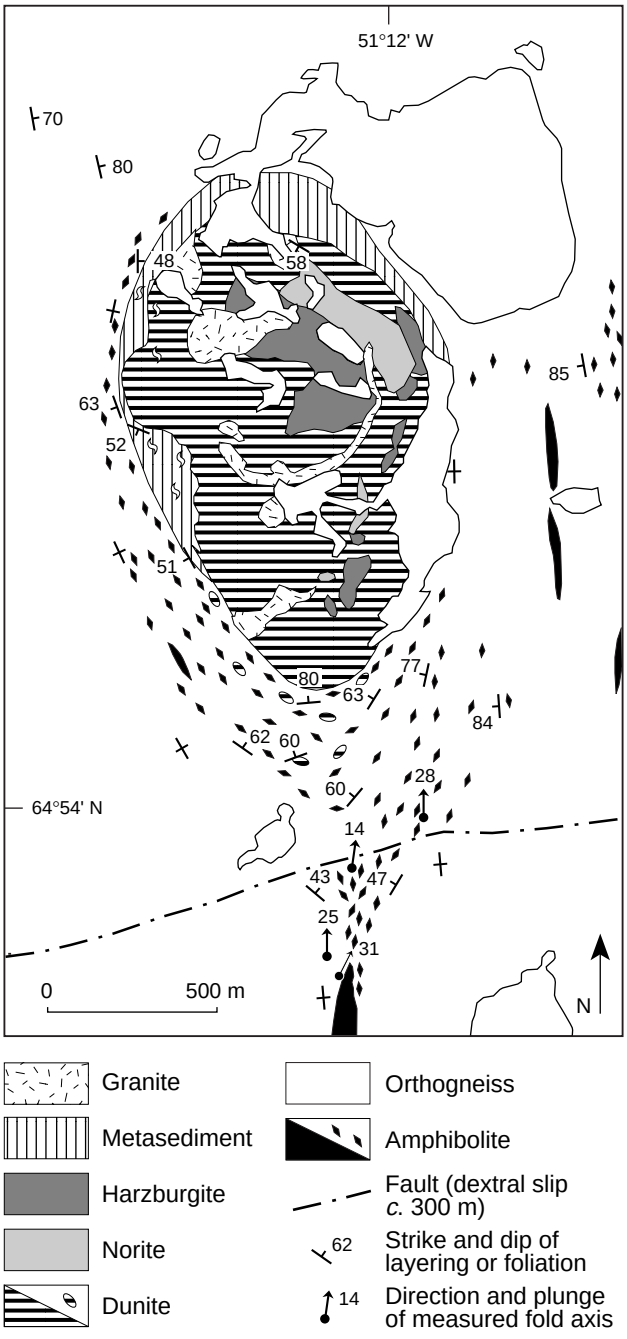

Fig. 10. Sketch map of the ultramafic body east of Ulamertoq.

Quagssugtarssuaq through Suversoq and northwards to the embayment Kûlik. Another occurs at Sangmissup nunâ, north-east of Tovqussap nunâ (Plate 1). Their exact boundaries have not been located as it is not known how much of the overlying homogeneous amphibolite they comprise. These kilometre-sized bodies of ultrabasic rocks may be fragments of larger layered complexes.

The best preserved complex, that across Fiskefjord, consists of elongate lenses and layers of olivine-rich ultrabasic rocks which either pass laterally or grade upwards into norite which, in turn, is overlain by homogeneous amphibolite (see also Bengaard, 1988). The ultrabasic and noritic rocks together form discontinuous, 10–50 m (locally up to *c.* 150 m) thick sheets along the base of a major unit of massive, homogeneous amphibolite (Fig. 13). This amphibolite outlines an elongate, doubly-plunging synform with closures south-west of Quagssugtarssuaq and north of Kûlik. The ultrabasic and noritic rocks occur both along the flanks and in the two hinge zones of this fold; the longest norite sheet can be traced for at least 15 km.

Most of the exposed lower boundary of the layered complex comprises intrusive or tectonic contacts with grey orthogneiss, and both the orthogneiss and ultrabasic-noritic rocks are commonly appreciably deformed along them. In places a *c.* 10 m thick layer of flaggy, strongly schistose, biotite- and garnet-rich pelitic sediment occurs along the lower contact of the layered complex. At one locality Bengaard (1988) observed little-deformed norite cutting compositional banding in the metasediment, suggesting an intrusive relationship. At the mouth of Suversoq steep isoclinal folds occur in the layered complex and adjacent supracrustal rocks, including thin horizons of 'infolded' metasediment. These folds pre-date the emplacement of the surrounding orthogneiss.

Fig. 11. Magmatic layering in olivine-rich ultrabasic rock, and a tremolite-phlogopite-diopside vein. Ultrabasic body east of Ulamertoq.

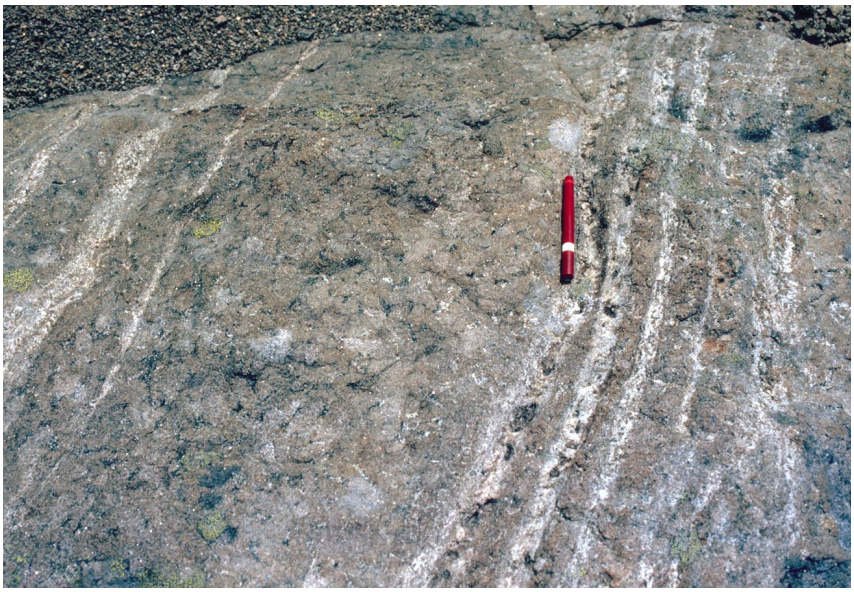

Fig. 12. Layered orthopyroxenite and plagioclase-rich leuconorite. Ultrabasic body east of Ulamertoq.

In the field the norite typically appears as a sugary, grey, very homogeneous rock, not unlike homogeneous tonalitic-dioritic granulite facies orthogneiss, but rare igneous layering consisting of metre-thick orthopyroxene-rich horizons alternating with norite has also been noted. Whereas contacts between dunitic and noritic rocks are sharp or gradational over less than *c.* 5 m, the boundaries between the noritic rocks and overlying homogeneous amphibolite is typically very gradual, with transitions over several tens of metres marked by increasing hornblende.

The norite has metamorphic textures. Orthopyroxene mostly forms equidimensional, *c.* 2–5 mm large anhedral grains, commonly replaced by up to 1–2 mm green hornblende in rounded embayments. Matrix calcic plagioclase (about An_{75}) forms large anhedral grains (up to 10 mm) with frequent tiny hornblende inclusions. Metamorphic equilibrium is suggested by common triple junctions between plagioclase, orthopyroxene or hornblende, and by the absence of mineral zoning.

The deformed margins of the norite bodies contain a distinct schistosity. Elongate, poikiloblastic orthopyroxene crystals up to 10 mm, intergrown with hornblende and subordinate pale brown phlogopite, are orientated parallel to schistosity and surrounded by a mosaic of equant to elongate plagioclase grains. The orthopyroxene grains are commonly composite, consisting of smaller lensoid domains with slightly different optical orientations.

Fig. 13. Dunitic ultrabasic rock (left, marked u) overlain by grey norite (at the lake, marked n) and homogeneous amphibolite in the far distance (marked a). West of Quagssugtarssuaq, 5 km south-east of Serquartup imâ.

Origin of the ultrabasic and noritic rocks

Komatiites in the sense of Arndt (1994) – volcanic, commonly spinifex-textured rocks of picritic to ultrabasic composition, crystallised from previously superheated magmas, have so far not been identified within the Archaean block of southern West Greenland, although Hall (1980) described ultrabasic pillow lavas from the Ivisârtoq area in southern West Greenland. However, komatiites are common constituents of many Mid Archaean supracrustal sequences and may also comprise cumulate rocks. For instance, in the generally well preserved Late Archaean Norseman–Wiluna Greenstone Belt, Yilgarn Block, Western Australia (Hill *et al.*, 1990), the thickest komatiitic flows can commonly be demonstrated to have differentiated, and they may contain cumulate dunitic rocks at their bases, which may rarely reach thicknesses up to a couple of hundred metres. The ultrabasic volcanic units very commonly alternate with basaltic units of similar thickness.

All the larger ultrabasic bodies in the Fiskefjord area predominantly consist of granular, medium-grained, olivine-rich, locally chromite-bearing dunitic rocks, in which magmatic layering and orthocumulus textures are fairly common features. There is a common association with noritic cumulates and, west of Quagssugtarssuaq there is a thick overlying sequence of homogeneous amphibolite. In spite of strong deformation and flattening which has resulted in disruption of the ultrabasic bodies (e.g. south of Quagssugtarssuaq) rather than tectonic repetition, some of them retain thicknesses in the order of 1 km. The available observations from the Fiskefjord area thus suggest that the large ultrabasic bodies are cumulate rocks which were formed at the bases of large magma chambers. This is also supported by geochemical data (see p. 24) but is difficult to substantiate because the apparent absence of spinifex-textured rocks or pillowed lavas in the ultrabasic rocks is not positive evidence that there are no volcanic components among them: former spinifex textures might have been destroyed by high-grade metamorphism and strong penetrative deformation. On the other hand olivine-rich ultrabasic rocks are very competent and resistant to deformation if not hydrated, and do not readily recrystallise even at granulite facies metamorphic conditions.

Fig. 14. Coastal exposure of leucogabbroic to gabbroic enclave in granulite facies orthogneiss, on a small island 5 km south-south-west of Atangmik.

Anorthosite and leucogabbro

Anorthosite and leucogabbro are commonly associated with Archaean supracrustal sequences in West Greenland (e.g. Myers, 1985) and also occur in the relatively poorly exposed south-western part of the Fiskefjord area, forming the continuation of a larger unit in Nordlandet (see McGregor, 1993). At the outer coast south-east of Íkátua, leucogabbro is associated with a large body of amphibolite in the core of a major refolded fold. Along both flanks of this fold the unit continues as several parallel, up to about 1 km wide tracts of closely packed leucogabbroic and gabbroic enclaves in dioritic and tonalitic gneiss, and similar enclaves occur sporadically e.g. around outer Fiskefjord (Plate 1; Fig. 14). The leucogabbro is mostly a medium-grained, pale, homogeneous rock consisting of calcic plagioclase and hornblende with granoblastic metamorphic texture. Smaller units of medium- to coarse grained anorthosite and leucogabbro associated with amphibolite were described by Berthelsen (1960) from Tovqussap nunâ and also occur on a small island north-west of this peninsula.

The anorthosite and leucogabbro occurrences in the Fiskefjord area may be members of disrupted layered complexes, but it has not been possible to demonstrate this in the field.

Fig. 15. Biotite-garnet-sillimanite schist with flattened, up to *c.* 50 cm long calc-silicate lenses, and cut by thin sheets of garnet-bearing granite which is presumably of local anatectic origin (see the main text). North coast of the island Igdlut, *c.* 5 km south of Pâtok.

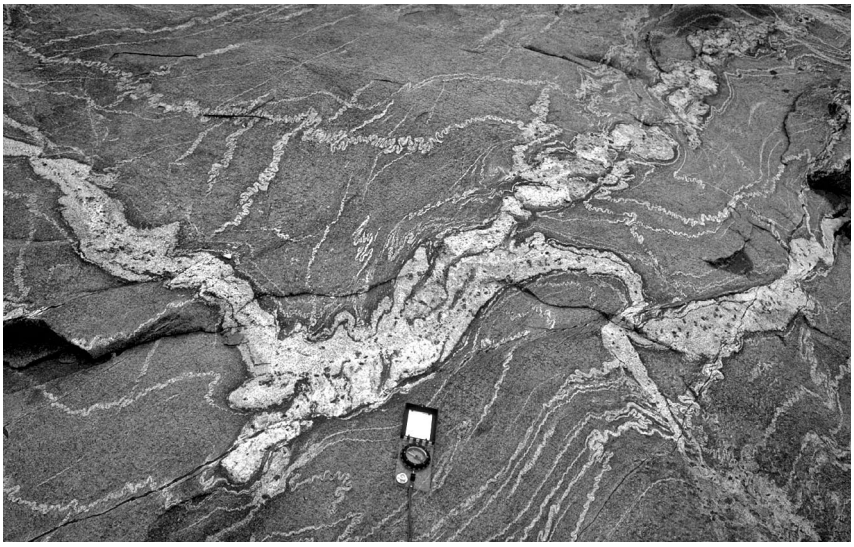

Fig. 16. Folded biotite schist with local anatectic vein of garnet-bearing granite; note the dark selvage rims. East coast of Qugssuk, *c.* 3 km from the head of the fjord.

Metasediments and altered felsic volcanic rocks

Metasediments are volumetrically very insignificant among the supracrustal rocks. They form thin, discontinuous horizons of fine- to medium-grained rocks, commonly strongly schistose with characteristic rusty brown weathering colours (Fig. 15). They exclusively occur within or along the margins of amphibolite, or along ultrabasic bodies. Pelitic schists are most common and consist of plagioclase, quartz, biotite, commonly garnet, and in places additional sillimanite or cordierite. Thin anatectic sheets of garnet-bearing granite (granulite *s.s.*, Berthelsen, 1960), are commonly associated with the pelitic schists (Figs 15, 16). Fine-grained, brownish-grey, quartzo-feldspathic rocks of intermediate composition are locally intercalated with biotite-garnet schist or occur adjacent to amphibolite and ultrabasic rocks. These rocks may be closely related to leuco-amphibolite as suggested by their composition (see p. 24) and are probably of volcano-sedimentary origin. Quartzite or quartz-rich clastic rocks are almost absent from the metasediments of the Fiskefjord area.

On a small island off the outer coast *c.* 2 km north of Kangâkasik, less than 1 m thick horizons of garnet- and magnetite-rich siliceous rocks are intercalated with biotite-garnet-cordierite schist. Berthelsen (1960) and Dymek (1984) described magnetite-diopside-quartz rocks from Langø west of Tovqussap nunâ, associated with calc-silicate rocks and biotite-garnet schist. These rare rock types are interpreted as chemical metasediments (silicate facies iron formation).

Cordierite- and anthophyllite-cummingtonite-rich siliceous rocks form a significant proportion of the thin supracrustal horizons in the south-western part of the Fiskefjord area (between Íkátua and Oqúmiap taserssua and west of Natsigdlip tasia), which also include impure quartzites. Sporadic cordierite-bearing supracrustal rocks also occur, e.g. at Tovqussap nunâ (Berthelsen, 1960). Similar rocks in the Godthåbsfjord region have been interpreted by Beech & Chadwick (1980) and Dymek & Smith (1990) as hydrothermally altered siliceous metavolcanic rocks.

Supracrustal rock association: geochemistry

The analysed samples were collected from many different enclaves of supracrustal rocks mostly in the northern part of the Fiskefjord area (Plate 1; Fig. 17); the groups correspond to those introduced in the previous descriptions. The large geographical coverage is considered to provide a reasonable overview of rock compositions, although limited knowledge about primary relationships between various types of supracrustal rocks, uncertain correlation between geographically separate units, and absence of radiometric age deter-

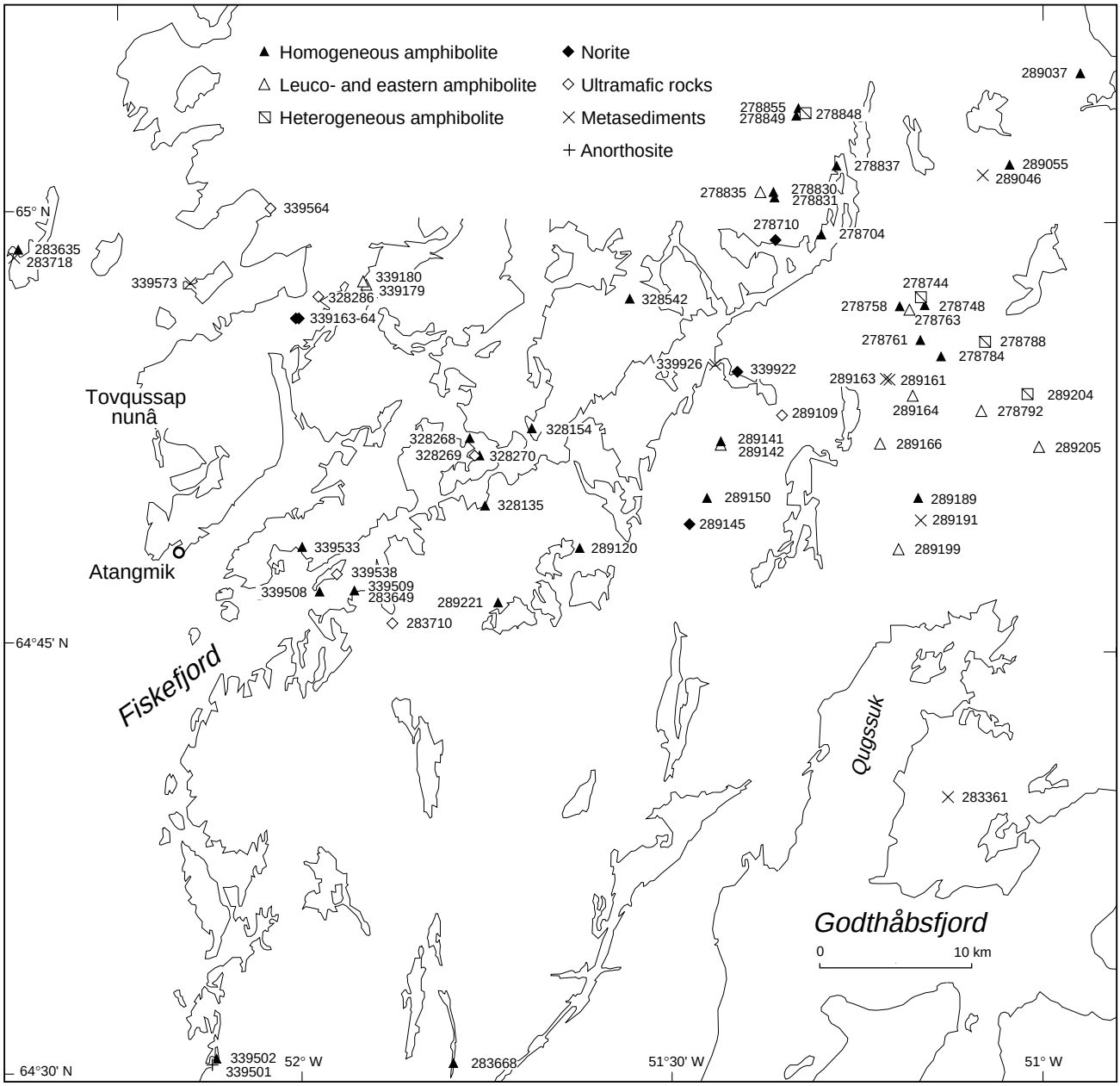

Fig. 17. Locations of analysed amphibolites, metasediments, norites, ultramafic rocks and anorthosite in the Fiskefjord area, with GGU sample numbers.

minations suggest that the analyses may well represent several originally independent sequences.

Modification of original compositions

The compositions of the supracrustal rocks are likely to have been modified from those of their original precursors at various stages of their geological history. Amphibolite precursor magmas may have been contaminated during their emplacement, e.g. by assimilation of crustal rocks, and their products affected by hydrous sea floor alteration. Subsequent metasomatism may have occurred during late diagenesis, during the emplacement of sialic magmas while the continental crust was building up around the supracrustal association, during prograde metamorphic dehydration reactions, and during localised retrogressive rehydration. Only the latest of possible alteration events can now be examined directly; obviously examples of pristine amphibolite precursors are not available for comparison. However, in contrast to the grey gneiss (Garde, 1990 and pp. 55-65), metasomatic changes associated with retrogressive hydration do not seem to have been significant in the case of the amphibolites. Geochemical data from homogeneous amphibolites (Appendix 1) include averages of 22 amphibolites with granulite facies parageneses and 9 similar rocks with textural evidence of partial rehydration. The two groups have almost identical compositions, except that the latter group has higher contents of trivalent iron and volatiles (about 1.0 and 0.5 per cent, respectively), and perhaps slightly different LREE (see below). Elements like K, Na, Rb, Sr, and Pb, which were mobile in intermediate and leucocratic orthogneisses in the Fiskefjord area during both the prograde granulite facies event and the subsequent retrogression (Garde, 1990; this paper), occur in similar concentrations in granulite facies and partially retrogressed amphibolites. A likely explanation is that whereas retrogression of intermediate orthogneisses was commonly complete and involved total replacement of pyroxene by secondary amphibole and biotite, retrogression in most amphibolites was incomplete, biotite was rarely involved, and a stable hydrated phase (mainly hornblende) that could accommodate LIL elements was present throughout the process.

Nevertheless, both the LIL elements and Ca show large variations in the amphibolites (see below), and several LIL elements occur in concentrations that are higher than in unaltered modern basaltic rocks of common geotectonic settings (see p. 25). Besides the LIL elements

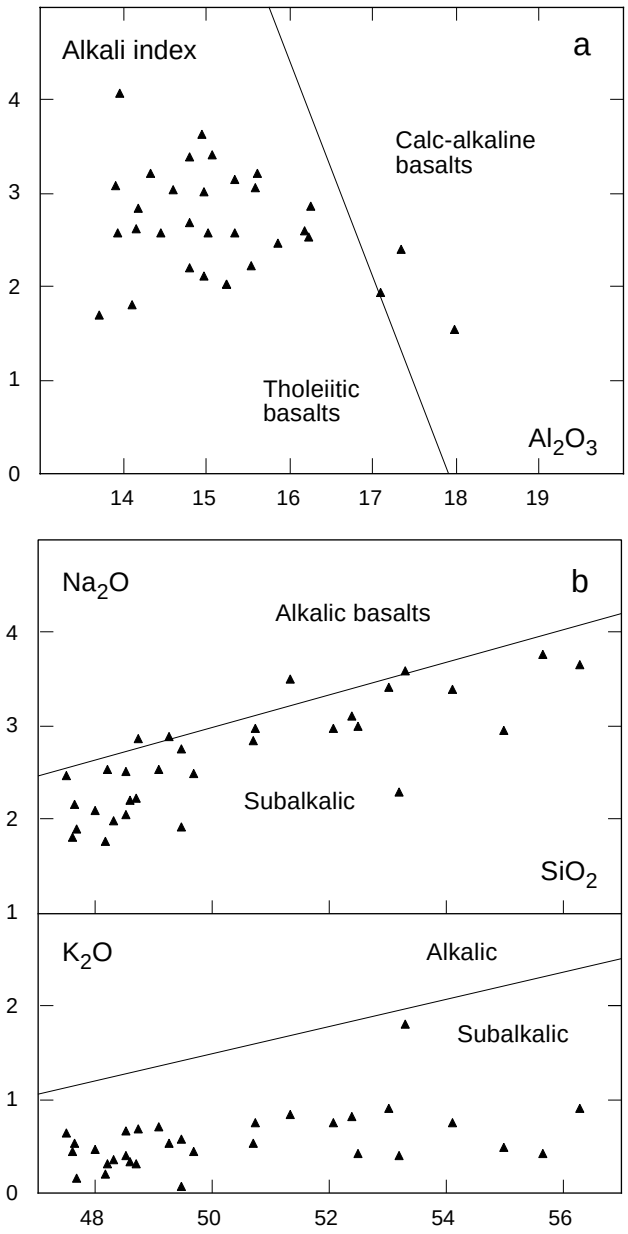

Fig. 18. (**a**) Alkali index *v.* Al_2O_3 (after Middlemost, 1975). (**b**) Variation diagrams of Na_2O and K_2O *v.* SiO_2 of homogeneous amphibolite, Fiskefjord area, illustrating its tholeiitic character. Locations of samples in Fig. 17; analytical details in Appendix.

Ca is also known to be mobile in many diagenetic environments (e.g. during interaction with sea water or carbonate rocks). In addition LIL element exchange may have occurred later between the supracrustal rocks and their orthogneiss hosts. It is therefore likely that amphibolite compositions have been modified by secondary processes, especially with regard to the high and variable concentrations of LIL elements and Ca presented below.

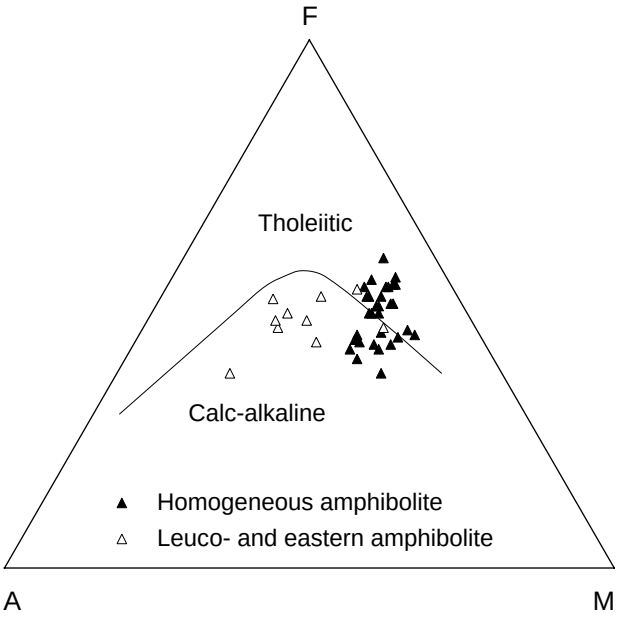

Fig. 19. AFM diagram (Na_2O + K_2O, FeO + Fe_2O_3, MgO) of amphibolites from the Fiskefjord area. Alkali element metasomatism may have shifted some samples of homogeneous amphibolite into the calc-alkaline field. See Fig. 17 for locations of samples and Appendix for analytical details.

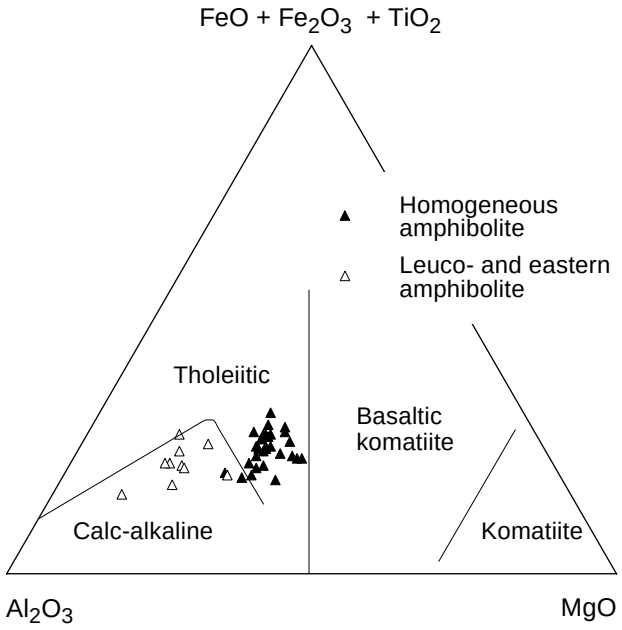

Fig. 20. Jensen diagram (Jensen, 1976) of amphibolites from the Fiskefjord area. Note the absence of samples in the field of basaltic komatiite. See Fig. 17 for locations of samples and Appendix for analytical details.

Amphibolites

Homogeneous amphibolite

The most widespread amphibolite group, homogeneous amphibolite, has a tholeiitic, basaltic major element composition (average *c.* 50.4 wt.% SiO_2, 15.2% Al_2O_3, 10.4% total FeO, 8.4% MgO, 9.9% CaO, 2.7% Na_2O and 0.6% K_2O; Appendix 1). Despite granulite facies metamorphism most samples are significantly hydrated (loss on ignition about 1%, compared to less than 0.5% in modern unaltered basaltic and gabbroic rocks). Most oxide compositions of homogeneous amphibolite are fairly uniform (Appendix 1), except CaO and K_2O which have relative standard deviations of *c.* 20 and 50%, respectively.

Variation diagrams of (a) alkali index *v.* Al_2O_3 and (b) Na_2O and K_2O *v.* SiO_2 (Fig. 18) illustrate the general subalkalic character of the homogeneous amphibolites, irrespective of whether some K_2O has been added or removed during diagenesis and metamorphism. On the AFM diagram (Fig. 19) a small majority of the homogeneous amphibolites plot in the tholeiitic field but do not show significant iron enrichment, whereas the leucocratic group (see section below) plots in the calc-alkaline field; in this plot the alkali content (i.e. possible alteration) is rather critical. The same division is more pronounced in the Jensen plot (Fig. 20), which is insensitive to mobile elements. None of the amphibolites are sufficiently magnesian to plot in the field of basaltic komatiite.

The trace element composition of homogeneous amphibolite (Appendix 1) is somewhat variable but generally basaltic: Cr, V and Ni are high (150–400 ppm), most lithophile elements low to moderate, and LIL elements low. Some elements like Y, Zn, V, Ga and Sc occur in very similar concentrations in most samples, whereas mobile elements like Rb, Ba and Sr show substantial variations, as noted above. Representative samples of homogeneous amphibolite have REE contents at about 10 times chondritic levels (Fig. 21a–b), with some variation in the LREE: most samples are unfractionated or weakly enriched in LREE, whereas a couple of granulite facies samples are weakly LREE depleted.

Leuco- and eastern amphibolite

Most rocks mapped as leuco-amphibolite are more felsic than the homogeneous amphibolite, with major element concentrations in the general range between basalt

and andesite (Appendix 2). Their trace element compositions are broadly similar to those of homogeneous amphibolite. However, their variations in Rb, Ba and Th are larger, they have higher concentrations of LREE (Fig. 21c), Ta and Nb, and lower concentrations of compatible elements like Cr and Ni. The most acid leuco-amphibolite samples have strong geochemical similarities with some rocks mapped as metasediment and with the most basic members of dioritic orthogneiss (see p. 24; p. 51; Appendix 5).

Two samples placed in this group (GGU 289166 and 289205, Appendix 2; GGU = Grønlands Geologiske Undersøgelse) belong to amphibolite facies amphibolite from the easternmost part of the Fiskefjord area, which at the present erosion level has escaped granulite facies metamorphic conditions (Garde, 1990). Their compositions resemble leuco-amphibolite with regard to most trace elements. Although their SiO_2 contents of *c.* 50% are comparable to that in homogeneous amphibolite, they are more aluminous (Al_2O_3 above 17% compared to *c.* 15% in homogeneous amphibolite), less magnesian, and one of them considerably more sodic (4.4% Na_2O). The concentrations of most trace elements resemble those in leuco-amphibolite. Collectively these differences from homogeneous amphibolite are unlikely to stem from their different metamorphic histories, and the two eastern amphibolites are therefore tentatively correlated with the leuco-amphibolite in spite of the higher SiO_2 contents of the latter group.

Heterogeneous amphibolite

Four analyses (Appendix 2) of heterogeneous amphibolite with calc-silicate parageneses (formerly pillow lavas?) suggest that both major and trace element concentrations are highly variable in this group. Concentrations of some elements are outside the ranges found in homogeneous and leuco-amphibolite. Total FeO and especially MgO are low (averages of 9.19% and 3.8%), and two of the samples are also distinctly aluminous with 17.8 and 21.0% Al_2O_3. The CaO contents are very high (12.8–14.7%) and interpreted as due to exchange with carbonates on the sea floor or during diagenesis. Both field observations and the available geochemical data for the heterogeneous amphibolites suggest that they have been subject to much more severe alteration of their original compositions than the other amphibolite groups; these samples are therefore omitted from the geochemical plots.

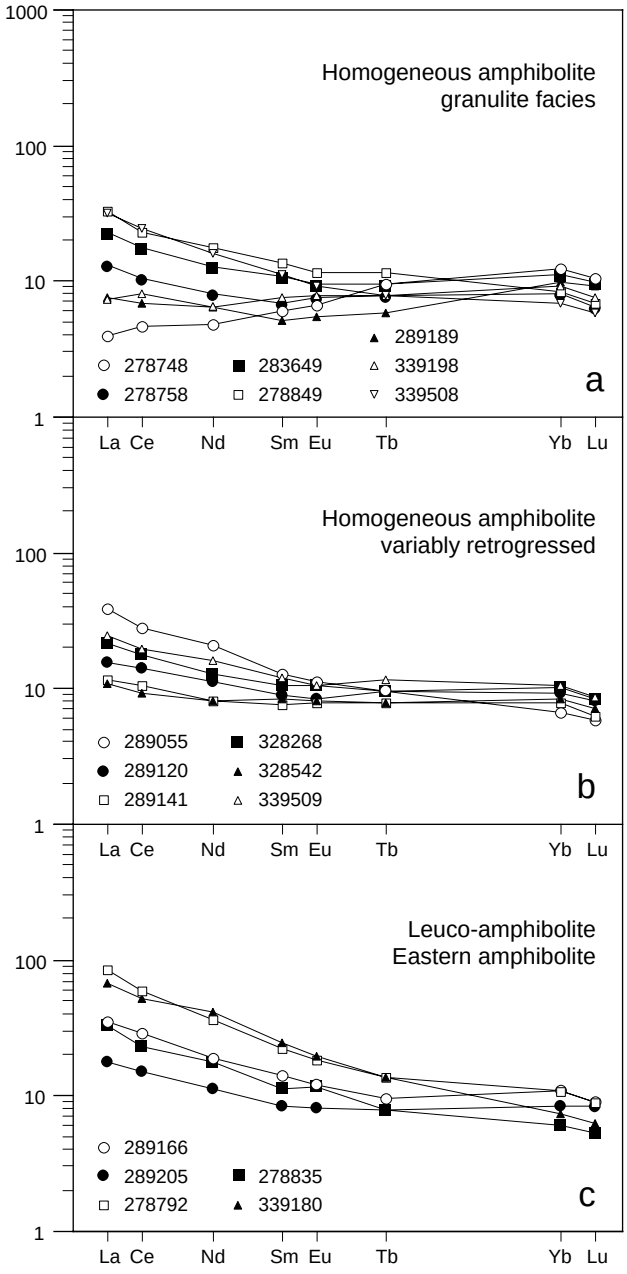

Fig. 21. Chondrite-normalised REE diagrams of three groups of amphibolites from the Fiskefjord area. Normalisation factors used for this and subsequent diagrams are from Nakamura (1974). All elements analysed by INNA; see Fig. 17 for sample localities and Appendix for analytical details.

Metasediments

The most common group of metasediments, biotite schist (± garnet, ± sillimanite) is represented by four typical samples from different parts of the Fiskefjord area (Fig. 17), which have a variable composition (Appendix 3). Two samples (GGU 289046 and 339926)

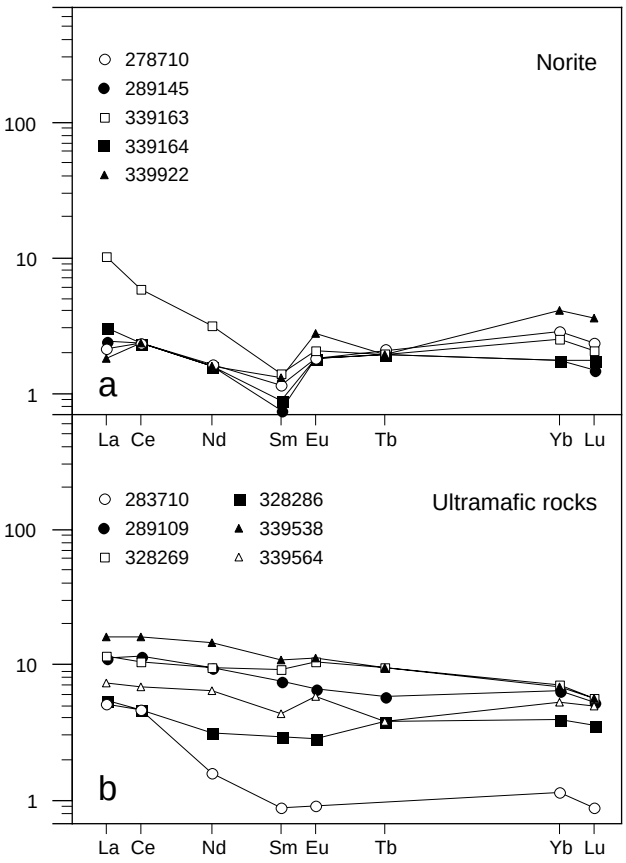

Fig. 22. Chondrite-normalised REE diagrams (Nakamura, 1974) of (**a**) norites and (**b**) ultramafic rocks from the Fiskefjord area. All elements analysed by INNA (see Appendix). See Fig. 17 for sample localities.

have FeO* concentrations above 13%, whereas two other samples are similar to leuco-amphibolite or mafic diorite. The rocks have very variable Al_2O_3 contents from *c.* 10.7 to 19.5%; none are siliceous or calcareous. Most trace elements occur in intermediate abundances; Rb, Zr, Zn, Cu and V are relatively high, and Sr, Ba, and the REE relatively low compared with mafic diorite or leuco-amphibolite.

Three of four analysed rocks in another group of supposed metasediments, fine-grained quartzo-feldspathic rocks associated with amphibolite, have a major element composition which resembles both the most felsic leuco-amphibolite and dioritic grey gneiss (compare Appendix 3 with Appendices 2 and 5). A fourth sample (283361) is more siliceous (68.1% SiO_2). The trace element composition of the quartzo-feldspathic metasediments is similar to that of leuco-amphibolite or diorite, except for lower Sr and higher Rb, Th and Zr contents. The fine-grained quartzo-feldspathic rocks are easily distinguished petrographically from dioritic orthogneiss, but their chemical compositions suggest that they may have been derived from andesitic igneous rocks without much alteration by physical or chemical surface processes, and they are therefore probably of volcanic or volcaniclastic origin.

Norite

The noritic rocks (Appendix 4; Fig. 17) contain *c.* 50% SiO_2, 17–21% Al_2O_3, and are both magnesian and calcic (*c.* 11–16% MgO and 7.5–11% CaO). Ni, V and Cr range from tens to several hundreds of parts per million. Total FeO is low, and Na_2O, K_2O and lithophile and LIL trace elements are very low (except for metasomatic? Rb in the range *c.* 10–30 ppm in three samples). A chondrite normalised REE plot (Fig. 22a) shows that REE abundances are close to chondrite or mantle values and that the patterns are generally unfractionated; the small positive Eu anomalies are interpreted as related to the large proportion of plagioclase in all norites. GGU 339163 which is enriched in LREE also has 31 ppm Rb, 9 ppm Pb and 139 ppm Ba (Appendix 4), indicative of mild metasomatism. The major and trace element compositions of the norites strongly suggest that they were formed as orthopyroxene-plagioclase cumulates which only trapped very small proportions of intercumulus melt.

Ultrabasic and ultramafic rocks

The geochemistry of units described in the field as ultrabasic rocks suggests that these are also cumulate rocks, like the norites (Appendix 4). They are calcic and highly magnesian (up to 28.3% MgO) and low in Al_2O_3 (1.2–9.9%). However, their major element geochemistry suggests some contamination or metasomatism, and some are not truly ultrabasic – SiO_2 ranges between 45.6 and 54.1% (unusually high for olivine-rich ultramafic rocks), and besides, Fe_2O_3 almost equals FeO in some samples. The Ni, V and Cr levels are high to very high, but most other trace elements occur in very low concentrations. Their REE patterns (Fig. 22b) resemble those of the norites but with slightly higher levels; the most siliceous (and metasomatised?) sample GGU 283710 has the lowest total REE content but a relative LREE enrichment.

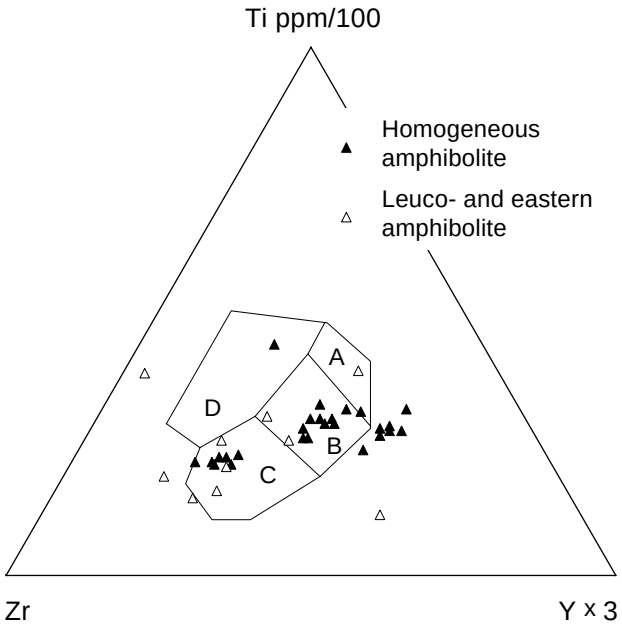

Fig. 23. Amphibolites from the Fiskefjord area plotted on the Ti–Zr–Y tectonomagmatic discrimination diagram (Pearce & Cann, 1973; A + B: low-K tholeiites, B: ocean floor basalts and island arc tholeiites, B + C: calc-alkaline basalts, D: within-plate basalts).

Anorthosite

One sample from the large leucogabbro-anorthosite association in the western part of Nordlandet, collected at the outer coast in the southern part of the Fiskefjord area (Fig. 17), was analysed (Appendix 4). Its composition, compared with a typical anorthosite from the Fiskenæsset complex, southern West Greenland (Appendix 4), shows that it clearly belongs to the calcic 'Archaean' anorthosite association (Ashwal & Myers, 1994), which occurs in most parts of the Archaean in West Greenland. Also the small occurrences of leucogabbro at Tovqussap nunâ belong to this association (Berthelsen, 1960).

Comparison of the amphibolites with modern basaltic rocks

A comparison of average homogeneous amphibolite geochemistry with compositions of modern basaltic rocks in various plate tectonic settings (using compilations of data from several sources published by Wilson, 1989) indicates that the homogeneous amphibolite most closely resembles tholeiitic ocean floor basalt or island arc tholeiite. The match with modern basalts from both settings is close for most major elements (SiO_2, Al_2O_3, total FeO, MgO and Na_2O), although the homogeneous amphibolite has lower TiO_2 and CaO and significantly higher K_2O contents. However, the latter two oxides were also shown above to be the most variable. Among the trace elements Rb, Ba and Sr (which are also very variable) are a poor match with both of the two modern basalt groups.

In terms of the Ti–Zr–Y discrimination diagram (Fig. 23) most samples of homogeneous amphibolite plot in the field of ocean floor basalts or island arc tholeiites, but a few samples plot outside any recognised field.

Spider diagrams of representative amphibolite samples normalised to normal, or N-type MORB (Fig. 24a–c) and REE diagrams (Fig. 21) can be used for a more specific comparison with modern normal, enriched and depleted MORB, island arc tholeiite, and ocean island alkali basalt (Fig. 24d). The homogeneous amphibolite plots show a clear pattern (irrespective of partial retrogression), except for the previously noted variations of mobile incompatible elements, in which they are variably enriched. Most samples are moderately depleted relative to MORB in immobile incompatible elements like P, Zr, Hf, Ti and Yb, whereas a few (represented by GGU 278849) are slightly enriched in some of the latter elements. There is no Nb anomaly, but a clear enrichment of Sc, Cr and Ni in some samples. Chondrite normalised REE diagrams of homogeneous amphibolite (Fig. 21a–b) show a general similarity to MORB with flat REE curves at *c.* 10 × chondrite values, and in some samples a weak LREE depletion as in modern N-type MORB (e.g. Schilling *et al.*, 1983).

Collectively the immobile incompatible, REE, and compatible element compositions of the homogeneous amphibolite are considered likely to reflect the original composition of their precursors to a large degree, and it may thus be argued that they have several general characteristics which resemble normal MORB (the horizontal line in Fig. 24d). In other respects they more resemble island arc tholeiites – namely in terms of their enrichment of LIL elements and depletion of immobile incompatible and moderately compatible elements, including Ti. However, these deviations from MORB are not as large as observed in modern island arc tholeiites. Besides, the homogeneous amphibolites differ noticeably from modern island arc tholeiites by their absence of a Nb anomaly and positive Cr and Ni anomalies. In addition the LIL element enrichment may be secondary as previously noted.

The composition of the homogeneous amphibolites does not preclude that they might be back-arc tholei-

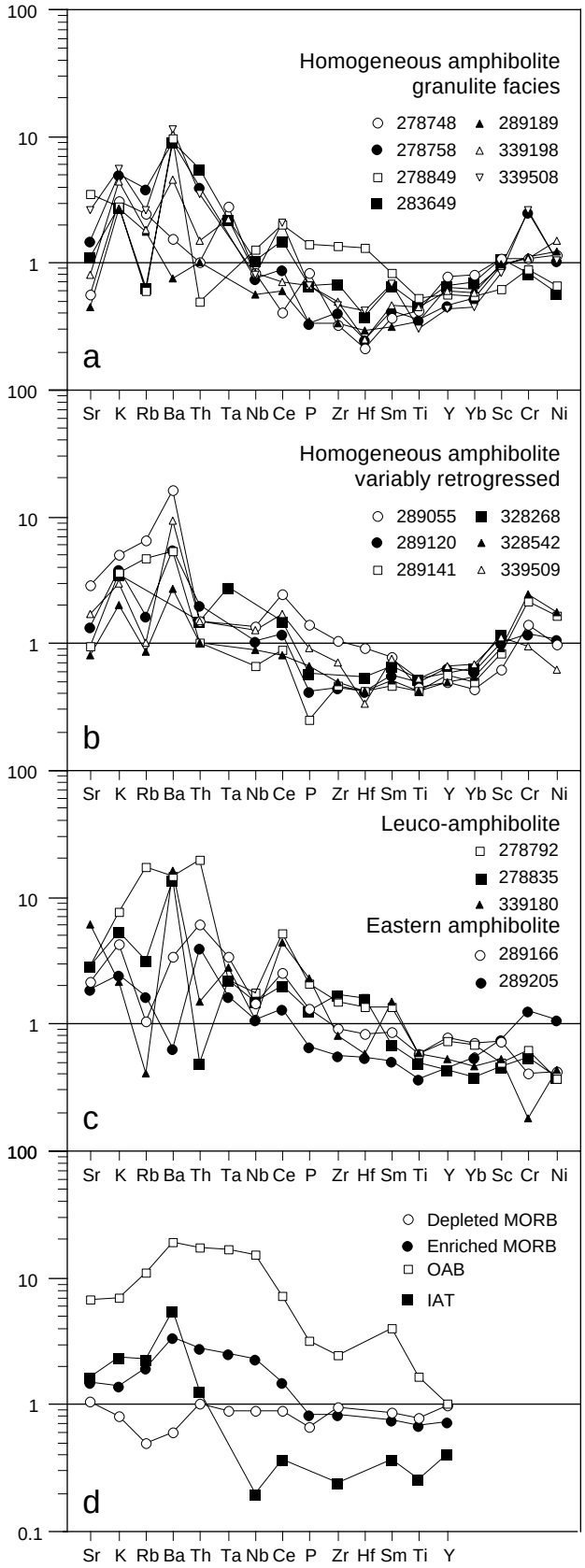

ites, a favoured interpretation of some Phanerozoic ophiolite complexes preserved within the continents (e.g. Saunders *et al.*, 1979), but this is difficult to assess on the basis of geochemistry alone; due to very variable contamination back-arc tholeiites do not possess unique geochemical signatures (e.g. Wilson, 1989). Notwithstanding geochemical considerations, modern back-arc spreading seems to occur only where the subducting oceanic lithosphere is old, dense and cold (Furlong *et al.*, 1982) – an unlikely plate-tectonic scenario in the Archaean.

The leucocratic amphibolites have geochemical affinities to more evolved and aluminous recent basaltic rocks: their compositions resemble those of basaltic andesites and andesites from modern island arc settings, although they lack a distinct negative Nb anomaly. In the Ti–Zr–Y diagram (Fig. 23) they plot in the calc-alkaline basalt field, and representative samples show more variation on the MORB-normalised spider diagram (Fig. 24c) than the homogeneous amphibolites (Fig. 24a–b). Besides, the variation in LIL elements is more pronounced than in the homogeneous amphibolite, and there is an enrichment of several incompatible immobile elements but no Cr or Ni enrichment compared to MORB. Also the REE pattern (Fig. 21c) with its weak LREE enrichment indicates a calc-alkaline affinity.

Fig. 24. MORB-normalised spider diagrams.
(**a**–**c**) Amphibolites from the Fiskefjord area. The samples have affinities both to MORB and island arc tholeiites; the large variation in LIL elements is interpreted as mainly due to metasomatism. Normalisation factors from Pearce (1983), except Sc, Cr and Ni from Taylor & McLennan (1985, p.274). Th, Ta, Ce, Hf, Sm, Yb and Sc analysed by INNA, other elements by XRF (see Appendix for details). Fig. 17 shows sample localities. (**d**) Modern volcanic rocks (Sun, 1980) for comparison with Fig. 24a–c. OAB = ocean island alkali basalt, IAT = island arc tholeiite.

Magmatic accretion of grey gneiss precursors, contemporaneous structural evolution, and late-tectonic granite domes and sheets

Outline of the main orthogneiss units and their structural and metamorphic evolution

Prior to systematic work in the Fiskefjord area in the 1980s the orthogneisses of the Akia terrane north of Godthåbsfjord were only poorly known; an overview of previous work was given in the introduction. Allaart (1982) made a general distinction between amphibolite facies and granulite facies (enderbitic) rocks, and recognised two large homogeneous tonalite complexes north and north-east of Fiskefjord, the Taserssuaq tonalite and Finnefjeld gneiss complexes. Earlier, Macdonald (1974) and especially Reed (1980) had studied dioritic and leucocratic gneisses in Nordlandet. During the subsequent systematic survey of the Fiskefjord area in the 1980s the quartzo-feldspathic rocks of intrusive magmatic origin were resolved into several groups of progressively younger and more leucocratic rocks which are described in the following sections.

The *c.* 3220 Ma Nordlandet dioritic gneiss (ion probe zircon age data shown in Fig. 25 and discussed below), which contains enclaves of an even older supracrustal association, is the earliest nucleus of continental crust that has been identified in the Akia terrane (Table 1). It forms most of Nordlandet south of the Fiskefjord area, and underlies large tracts in the southern part of the Fiskefjord area (Plate 1). The remainder of the grey gneiss is dominated by *c.* 3000 Ma old grey, K-poor, amphibolite facies tonalite-trondhjemite-granodiorite (TTG) orthogneisses and their brown granulite facies equivalents, and also comprises younger dioritic rocks. Besides there are local sheets of mesoperthite-bearing (granulite facies) granitic gneiss. The orthogneiss protoliths were emplaced into the older assemblage of supracrustal rocks and Nordlandet dioritic gneiss, and deformed and metamorphosed during a major event of continental crustal accretion at *c.* 3000 Ma.

Most orthogneiss precursors intruded as sheets of variable dimensions. Their emplacement was accompanied by regional deformation, which comprised at least two phases of isoclinal folding followed by a phase of upright folding and development of N–S trending straight zones contemporaneously with granulite facies metamorphism (see p. 41). Two large dome-like massifs were emplaced in the area. The Taserssuaq tonalite

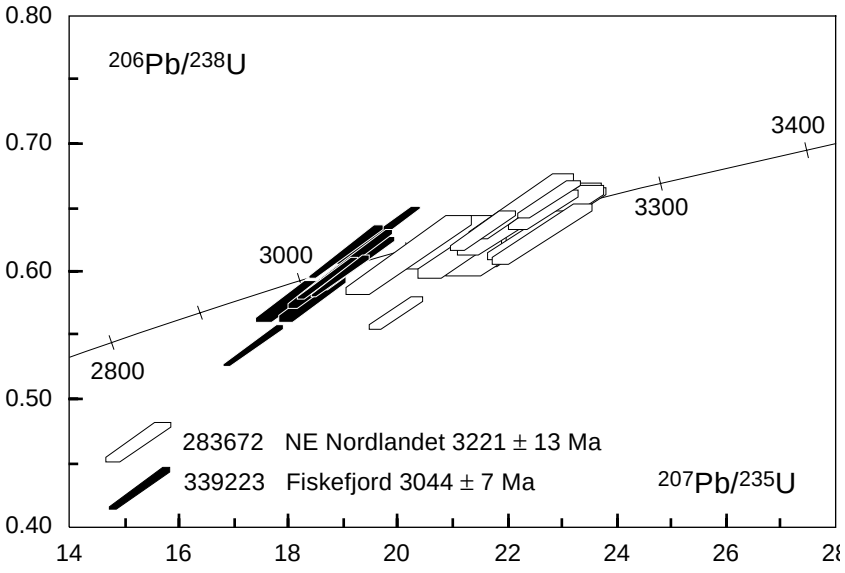

Fig. 25. SHRIMP U-Pb zircon data from Nordlandet dioritic gneiss, GGU 283672 (3221 ± 13 Ma, with a number of younger ages at *c.* 3180 Ma) and Qeqertaussaq diorite, GGU 339223 (3044 ± 7 Ma). Sample localities are shown on Fig. 52 (analyst A. P. Nutman, using Sri Lankan zircon SL13 as standard. See Compston *et al.*, 1984 and Friend & Nutman, 1994 for details of the analytical procedure). The zircons in sample 283672 have very low U contents of 15–50 ppm, but the analysed crystals were large enough that a normal count rate could be obtained with a large beam diameter (*c.* 25μ). The 3221 ± 13 Ma age is derived from a weighted mean of $^{207}Pb/^{206}Pb$ ratios, using analyses representing the least isotopically disturbed sites in the same morphological type of zircons.

complex was emplaced syn-granulite facies metamorphism, as its western parts display evidence of retrogression from granulite facies parageneses; most of the complex occurs north-east of Fiskefjord where granulite facies conditions were never reached at the exposed level. Second, the Finnefjeld gneiss complex to the north-west appears to entirely post-date granulite facies metamorphism in that area. The Igánánguit granodiorite and the Qugssuk granite (Garde *et al.*, 1986), two suites of granitic rocks in the north-eastern and eastern part of the Fiskefjord area, were formed by melts generated from older orthogneiss and emplaced after the granulite facies and main deformation events.

A brief overview of the Archaean metamorphic evolution of the Fiskefjord area, described in detail later, follows here as introduction to the field descriptions. Granulite facies metamorphism occurred at *c.* 3000 Ma over most of the Fiskefjord area, except its eastern and northernmost parts. The granulite facies metamorphism was thermal and probably caused by heat accumulated during the continuous injection of tonalitic magma into the growing continental crust (McGregor *et al.*, 1986; Garde, 1990), a mechanism that had previously been suggested by Wells (1979, 1980) for the neighbouring Buksefjorden area. The central and northern parts of the Fiskefjord area were subsequently partially or completely retrogressed from the granulite facies. Most of the orthogneiss in these areas has disequilibrium amphibolite facies mineral textures, whereas the mafic to ultramafic rocks of the supracrustal association are much less affected by the retrogression. Garde (1989a, 1990, 1991) showed that both granulite facies metamorphism and retrogression were accompanied by migration of particularly LIL elements in the orthogneisses, and suggested that much of the retrogression took place very soon after the culmination of granulite facies metamorphism. The pervasive retrogressive event was followed by younger, at least in part Proterozoic retrogression localised along narrow ductile shear zones, along brittle faults, and along the margins of mafic dykes.

Grey orthogneiss, Taserssuaq tonalite and Finnefjeld gneiss complexes

Dioritic gneiss

Dioritic, quartz-dioritic and mafic tonalitic gneiss (shown as dioritic and mafic dioritic gneiss by Garde, 1987, 1989b) constitutes most of the south-western part of the Fiskefjord area and continues southwards into the Nordlandet area (McGregor, 1993, fig. 5); in the following it is referred to as the Nordlandet dioritic gneiss.

Sensitive high-resolution ion microprobe ('SHRIMP') U-Pb analysis of very clear, pale pinkish, euhedral to slightly corroded zircons in a sample of dioritic gneiss collected in north-eastern Nordlandet (GGU 283672) gave a ^{207}Pb-^{206}Pb age of 3221 ± 13 Ma (Fig. 25); the analyses were performed by A. P. Nutman at the National University of Australia. A cluster of younger ages was also obtained from morphologically similar zircons in GGU 283672, suggesting a thermal event at *c.* 3180 Ma. A whole rock Pb-Pb isochron age of 3112 ± 40 Ma, based on samples of both Nordlandet dioritic gneiss, amphibolite facies grey gneiss and Igánánguit granodiorite, was previously published by Garde (1989a); regression of the dioritic gneiss samples alone gives a similar age with a much larger uncertainty. The *c.* 3220 Ma protolith age of the Nordlandet dioritic gneiss is supported by data from the southernmost part of the Akia terrane; A. P. Nutman and H. Baadsgaard (personal communication, 1995) obtained SHRIMP zircon ages of 3235 ± 9 Ma and 3193 ± 7 Ma from two samples of dioritic gneiss collected on the mainland 5 km north-east of Nuuk, and in southern Nordlandet *c.* 8 km north-west of Nuuk. Zircons in the latter sample contain metamorphic overgrowths dated at 3014 ± 7 Ma.

In the south-western part of the Fiskefjord area the Nordlandet dioritic gneiss appears to form three *c.* 10–15 km wide N–S trending bodies, which are separated by 1–4 km wide linear tracts of tonalitic orthogneiss and amphibolite that probably represent the cores of steep, isoclinal folds (as suggested by fold closures to the south, see McGregor, 1993, fig. 5); the latter rocks may originally have been intercalated with the dioritic gneiss along early thrusts. The northern part of the Nordlandet dioritic gneiss, south of central Fiskefjord, is intruded by, and folded together with tonalitic orthogneiss in a complex fashion (Garde *et al.*, 1987). Smaller bodies of dioritic gneiss, which may or may not be part of the *c.* 3220 Ma Nordlandet dioritic gneiss, occur in most other parts of the Fiskefjord area (an amphibolite body north-east of Sangmissup nunâ (Plate 1) was incorrectly shown as dioritic gneiss by Garde, 1989b). Where primary field relationships are preserved, the dioritic gneiss is intruded and commonly agmatised by more leucocratic gneiss. The diorite itself can locally be observed to truncate supracrustal amphibolite, but enclaves of supracrustal amphibolite in the dioritic gneiss have only locally been observed; they are difficult to distinguish on weathered outcrops of granulite facies rocks and may therefore be much more

Fig. 26. Granular, medium-grained granulite facies metadiorite with indistinct quartz-plagioclase migmatitic network. 2 km west of central Quagssûp taserssua.

Fig. 27. Partially retrogressed granulite facies dioritic gneiss with vertical schistosity and rare leucocratic veins. N–S trending dioritic unit, 2 km due north of the head of Fiskefjord. The penetrative schistosity was developed before or during granulite facies metamorphism, and subsequent growth of retrograde amphibole and biotite was not accompanied by renewed deformation. The locality lies along the northern extension of the Qugssuk–Ulamertoq zone (Fig. 44) and shows that the development of this N–S trending high strain zone preceded retrogression.

common than hitherto recognised. In certain areas trains of rounded, up to metre-sized, fragmented gabbroic and leucogabbroic enclaves (Fig. 14) are readily distinguished in the field by their specks of white calcic plagioclase. Some of these enclaves can be traced for many kilometres and outline large refolded folds (McGregor, 1993; see p. 41).

Fresh outcrops of granulite facies dioritic gneiss may locally display several intrusive phases (Garde, 1990), but it typically appears as a very homogeneous, dark, brownish weathering, medium-grained and granular rock with a weak quartzo-feldspathic network (Fig. 26). South of outer Fiskefjord the dioritic gneiss commonly possesses a weak to distinct schistosity formed by platy quartz and elongate aggregates of mafic minerals with equilibrium granulite facies textures. In this area the schistosity is in places folded on metre-scale, south-plunging, upright to overturned folds probably belonging to the Pâkitsoq phase (see p. 41). Figure 27 shows another example of dioritic gneiss with vertical (granulite facies) schistosity from the northern extension of the N–S trending Qugssuk–Ulamertoq zone, which is described below.

A geochemically distinct group of dioritic gneiss, the Qeqertaussaq diorite (see p. 51), is restricted to the peninsula Qeqertaussaq and its vicinity in central Fiskefjord, where it forms common enclaves of very variable size in tonalitic-trondhjemitic gneiss (Fig. 28; see also Plate 1 and Garde, 1989b). In the field the Qeqertaussaq diorite is indistinguishable from dioritic gneiss

Fig. 28. Enclave of dioritic gneiss (Qeqertaussaq diorite) in tonalitic orthogneiss. The rocks are retrogressed, with development of blebby texture. North-eastern end of Tasiussarssuaq. Photo: S. B. Jensen.

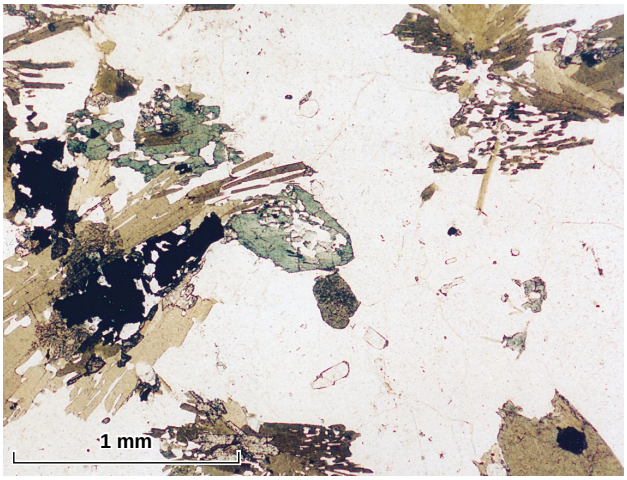

Fig. 29. Thin section of retrogressed dioritic gneiss (Qeqertaussaq diorite) with typical blebby texture: aggregates of spongy blue-green amphibole (after orthopyroxene) and sheaves of olive-brown biotite. GGU 328527, 5 km west-south-west of Kûlik.

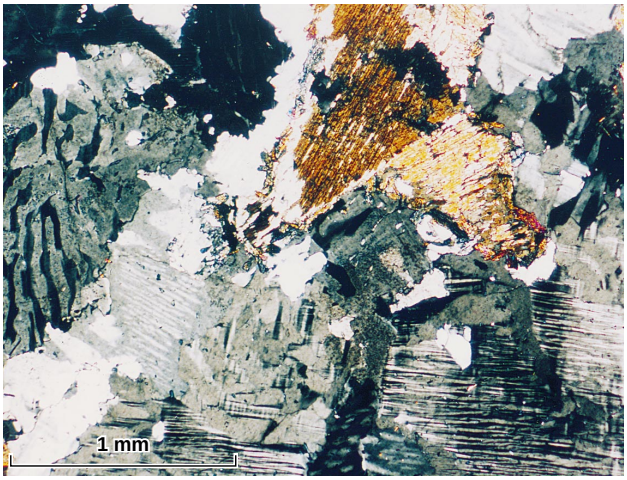

Fig. 30. Thin section of partially retrogressed dioritic gneiss (crossed polarisers), showing mesoperthite feldspar and clinopyroxene with secondary biotite overgrowths. The preservation of mesoperthite (exsolved from granulite facies intermediate alkali feldspar) shows that recrystallisation during the retrogression was incomplete. GGU 328583, east coast of island at the head of Tasiussarssuaq.

in other parts of the Fiskefjord area. The Qeqertaussaq diorite is considerably younger than the Nordlandet dioritic gneiss and is an early member of the main phase of grey gneiss; a SHRIMP Pb-Pb zircon age of 3044 ± 7 Ma was obtained from a sample (GGU 339223) collected opposite Qeqertaussaq at the south coast of Fiskefjord (Fig. 25; analyst A. P. Nutman). The zircons in this sample are light brown, euhedral or with partially rounded terminations, without obvious cores or rims, and contain 100–200 ppm U.

Granulite facies dioritic gneiss mainly consists of plagioclase, quartz, hypersthene, hornblende, iron-titanium oxides and commonly diopsidic clinopyroxene; fox-red biotite is also quite common. Textures in thin section suggest all ferromagnesian minerals to be in metamorphic equilibrium. Part of the dioritic gneiss is partially or completely retrogressed and contains irregular intergrowths of quartz and secondary blue-green amphibole, which commonly has lower contents of alkali elements and titanium than the granulite facies hornblende (Garde, 1990; see p. 59). Sheaves of secondary green or light brown biotite are likewise low in titanium. In thin section the Qeqertaussaq diorite resembles other dioritic gneiss members, except that appreciable amounts of K-feldspar may occur and accessory apatite is much more common. Figures 29 and 30 display typical disequilibrium retrogression textures in Qeqertaussaq diorite.

Fig. 31. Amphibolite facies biotite gneiss with tight folds. In spite of strong deformation, the textural details of polyphase magmatic emplacement have been preserved. Coastal outcrop at the north-eastern end of Bjørneøen.

Fig. 32. Retrogressed tonalitic gneiss with irregular quartzo-feldspathic network. Patches of secondary amphibole and biotite preferentially occur along the leucocratic segregations. Small island in inner Fiskefjord, 3 km south-east of Kûlik.

Fig. 33. Polyphase, partially retrogressed orthogneiss with blebby texture developed both in the leucocratic and more mafic parts of the rock. 7 km north-east of Ulamertoq.

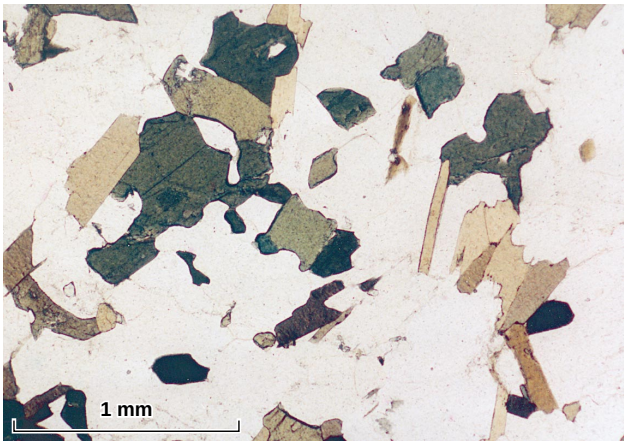

Fig. 34. Thin section of amphibolite facies hornblende-biotite orthogneiss; the ferromagnesian minerals are subhedral and in textural equilibrium, without signs of retrogression. GGU 289276, east coast of Qugssuk.

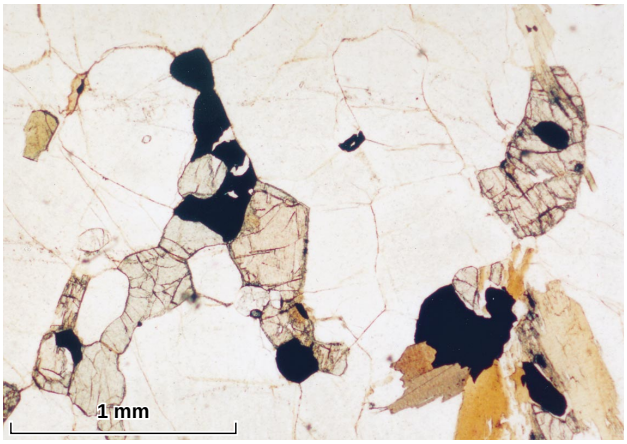

Fig. 35. Partially retrogressed granulite facies orthogneiss; ortho- and clinopyroxene are variably replaced by amphibole and biotite. GGU 278787, 8 km east of Ulamertoq.

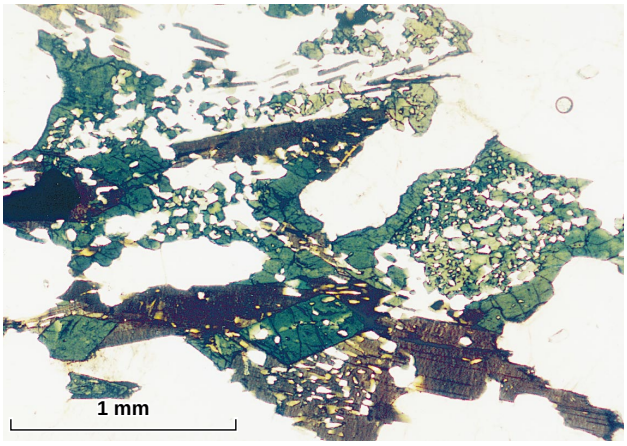

Fig. 36. Complete 'high-grade' retrogression in GGU 278787 (same thin section as in Fig. 35) with secondary, both euhedral and sieve-textured hornblende, and secondary biotite which in part also has sieve texture.

Tonalitic gneiss

The tonalitic orthogneiss which constitutes most of the Fiskefjord area typically forms tens of metres to a couple of kilometres thick composite sheets and layers in earlier supracrustal rocks and dioritic orthogneiss. Tonalitic orthogneiss in amphibolite facies (not retrogressed from granulite facies) at the east coast of Qugssuk has yielded a Rb-Sr whole-rock errorchron of 2954 ± 120 Ma and the above mentioned composite Pb-Pb whole-rock age of 3112 ± 40 Ma (see Garde, 1989a and pp. 79-81 for details). The tonalitic orthogneiss is broadly contemporaneous with the Taserssuaq tonalite complex, from which a conventional U-Pb zircon age of 2982 ± 7 Ma was reported by Garde *et al.* (1986; Table 1).

The tonalitic gneiss comprises numerous members of variable size and composition, which were successively emplaced into each other; much of the orthogneiss is polyphase even on outcrop scale. This is most easily recognised in the eastern amphibolite facies part of the area, where original boundaries between successive intrusive phases with slightly different colour indices are sharp and well preserved even where the rocks are strongly deformed (Fig. 31). Elsewhere the extensive recrystallisation accompanying first granulite facies and then retrogressive metamorphism has led to the development of blebby texture and more or less effectively destroyed such earlier lithological details (see Figs 32, 33; Garde, 1990, and discussion of blebby texture p. 81).

The tonalitic orthogneiss is generally medium-grained and composed of quartz, plagioclase (around An_{25}, commonly antiperthitic), minor interstitial K-feldspar, hornblende brown biotite or both, and accessory apatite, zircon, and magnetite-ilmenite intergrowths or pyrrhotite (Fig. 34). Granulite facies equivalents commonly contain both hornblende and hypersthene. In retrogressed gneiss hypersthene is variably replaced by fine-grained intergrowths of blue-green amphibole and quartz, and sheaves of secondary pale brown or green biotite commonly overgrow the iron-titanium oxides; large variations in the completeness of retrogression may be observed even within one thin section (Figs 35, 36). Occasionally two morphologically and compositionally different phases of biotite have been observed in retrogressed grey gneiss, typically in the form of sheaves of brown biotite a few millimetres large and much smaller interstitial flakes of greenish biotite with very low titanium contents (see section on geochemistry). The presence of two different biotite generations may

suggest that more than one episode of retrogression occurred in parts of the area.

A distinctive field type of homogeneous tonalitic gneiss, characterised by relatively coarse grain size and conspicuous clots of retrograde amphibole and biotite, occurs on Qeqertaussaq and west of Serquartup imâ around central Fiskefjord. This rock type forms a roughly equidimensional body more than 5 km in diameter, although its exact boundaries have not been delineated and are partly concealed by the fjord. In terms of texture and general field appearance it resembles retrogressed, relatively mafic parts of the Taserssuaq tonalite complex described below, and like this complex it may have been emplaced late amongst the tonalitic orthogneisses. Another variety of partially retrogressed grey gneiss, mainly of granodioritic composition, occurs around the head of Fiskefjord and north of Tovqussap nunâ (Plate 1; Garde, 1989b). This variety has characteristic purplish weathering colours and was described as 'purple gneiss' by Berthelsen (1960). It is not certain if the purple colour is related to a particular composition, a particular stage of retrogression, or both.

The tonalitic orthogneiss commonly contains metre-sized enclaves of its host rocks, especially within a few hundred metres from the margins of larger bodies of supracrustal rocks. This spatial association suggests that most enclaves were only transported over short distances within the tonalite magmas. The most common enclaves are composed of amphibolite, but in the vicinities of the previously described layered complexes and around Ulamertoq both amphibolite and ultrabasic or ultramafic enclaves occur in the gneiss. Both dioritic and tonalitic orthogneisses in the south-western part of the Fiskefjord area, and on northern Tovqussap nunâ, contain numerous enclaves of leucogabbro and anorthosite. South of Igdlutalik, an inlet of outer Fiskefjord, there are very common elongate diorite enclaves in the tonalitic host, probably derived from neighbouring dioritic bodies.

Trondhjemitic gneiss

Certain areas up to a few square kilometres are dominated by trondhjemitic, biotite-bearing orthogneiss. However, in most places this lithology could not be clearly differentiated in the field from the main phase of tonalites. One such area is located west of the head of Fiskefjord, where trondhjemite sheets up to *c.* 500 m thick were emplaced into supracrustal amphibolite and subsequently participated in repeated folding. Other, similarly deformed sheets occur at the outer coast south of Fiskefjord. Like the adjacent tonalitic gneiss these trondhjemites display distinct recrystallised, blebby textures although the mafic, mainly biotitic, clots are few and far apart. Trondhjemite emplacement, deformation and metamorphism matches that of the surrounding tonalitic gneiss, and the trondhjemites are believed to be cogenetic with the tonalitic gneiss. Other trondhjemites form the cores of late, elongate dome-like structures up to a few kilometres in size, for example north of Qôrngualik south of outer Fiskefjord.

Fig. 37. Flat-lying sheets of syn-kinematic granitic gneiss (mesoperthite granite) with discordant margins to dioritic gneiss. 1 km south of Quagssûp alánguata tasê in the central part of the Fiskefjord area.

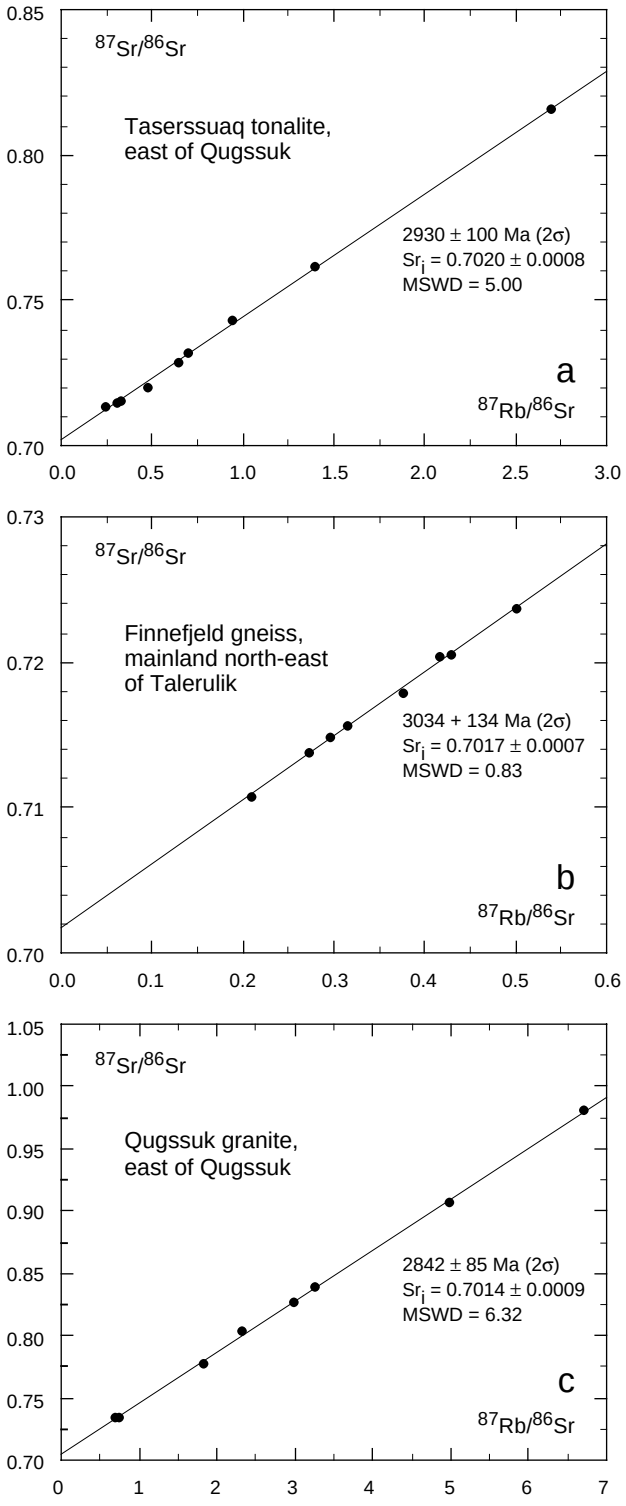

Fig. 38. Isochron diagrams of not previously published Rb-Sr data. (**a**) Taserssuaq tonalite east of Qugssuk, (**b**) Finnefjeld gneiss, and (**c**) Qugssuk granite east of Qugssuk (See also Table 1). The data set is listed in Table 2.

Trondhjemitic rocks also occur within the granulite facies dioritic gneiss in the south-western part of the Fiskefjord area, usually as thin sheets. Biotite is normally the only mafic mineral, but dark antiperthitic plagioclase and smoky blue quartz suggest pre- or syn-granulite facies emplacement. Similar rocks occur further south in Nordlandet, where they have been termed Kua granulite (Macdonald, 1974) and Imartuneq granite complex (Reed, 1980). Both the latter author and McGregor (1993) suggested that they are products of partial anatexis during granulite facies metamorphism.

Granodioritic and granitic gneiss

Small bodies of leucocratic granodiorite and granite, most of which have been emplaced before or during the granulite facies event, occur in the central and western parts of the Fiskefjord area. The granitic rocks most commonly form sheets of very variable thickness (from a few centimetres to maximum *c.* 1 km), which are locally discordant to gneissic foliation in their host rocks. They have frequently been emplaced more or less concordantly along boundaries between amphibolite and orthogneiss (e.g. on Tovqussap nunâ and south-west of Quagssûp alánguata tasê), as sheets subparallel to earlier foliation in dioritic gneiss (Fig. 37), or they form irregular bodies within tonalitic or dioritic gneiss (e.g. south of outer Fiskefjord). An elongate, *c.* 2 km long granite dome occurs at Oqúmiap taserssua. Around the sound Pâtôq north of Tovqussap nunâ granodioritic and granitic rocks constitute larger areas that may represent continuations of the largest sheets on northern Tovqussap nunâ. The granitic rocks are medium grained and biotite-bearing and have granular, equidimensional mineral textures suggesting more or less complete solid state recrystallisation. They either contain mesoperthite feldspar (indicative of crystallisation above the alkali feldspar solvus, i.e. under granulite facies conditions), or feldspar mosaics of antiperthitic plagioclase and microcline (probably also recrystallised from an intermediate alkali feldspar precursor). Biotite is concentrated in rare aggregates a few millimetres large, and magnetite is a common accessory.

Local granitic rocks within the granulite facies areas (e.g. south-west of Kingigtoq) post-date the peak metamorphic event and may be contemporaneous with syn- or post-retrogression granitic rocks in the eastern part of the Fiskefjord area (see pp. 45–48).

Taserssuaq tonalite complex

The Taserssuaq tonalite complex is a large, homogeneous, late-tectonic body akin to the grey gneiss. It was first identified during reconnaissance mapping (Allaart *et al.*, 1977) and was briefly described by Garde *et al.* (1983), Kalsbeek & Garde (1989) and Nutman & Garde (1989). The complex covers more than 1500 km^2 in the Isukasia area (Garde, 1987) and the north-eastern part of the Fiskefjord area. It forms an important element in the evolution of the Akia terrane, and a summary description is presented here. Garde *et al.* (1986) interpreted a zircon U-Pb age of 2982 ± 7 Ma (analyst R. T. Pidgeon, Western Australian Institute of Technology) as the age of intrusion. Rb-Sr data (Garde *et al.*, 1986) gave a whole rock age of 2882 ± 36 Ma (initial $^{87}Sr/^{86}Sr$ = 0.7017 ± 0.0002, MSWD = 1.57), and Rb-Sr mineral isotopic data indicated thermal events at *c.* 2500 and 1700 Ma. The Rb-Sr age was interpreted by Garde *et al.* (1986) as probably reflecting mobility of Rb associated with retrogression, as suggested by Kalsbeek & Pidgeon (1980) for orthogneisses in the Fiskenæsset area, southern West Greenland (see also pp. 79–81). A subset of samples from the Rb-Sr data set discussed above, collected from predominantly granodioritic rocks in the southernmost part of the complex east of Qugssuk, gives an age of 2930 ± 100 Ma (initial $^{87}Sr/^{86}Sr$ = 0.7020 ± 0.0008, MSWD = 5.00), see Table 2 and Fig. 38a. These samples do not appear to have been subject to retrogression.

Table 2. Rb-Sr whole rock data for Finnefjeld gneiss complex, Taserssuaq tonalite complex and Qugssuk granite

	Rb ppm	Sr ppm	$^{87}Rb/^{86}Sr$	$^{87}Sr/^{86}Sr$
Finnefjeld gneiss complex				
339638	47	323	0.415	0.7203
339644	27	381	0.209	0.7108
339645	44	459	0.272	0.7138
339647	53	354	0.430	0.7205
339648	56	323	0.500	0.7237
339650	38	360	0.315	0.7156
339652	53	414	0.376	0.7179
339655	48	466	0.295	0.7148
Taserssuaq tonalite complex				
283315	79	488	0.479	0.7200
283319	128	139	2.693	0.8157
283321	90	281	0.944	0.7433
283328	80	328	0.692	0.7318
283334	76	163	1.399	0.7612
283340	72	325	0.640	0.7286
283341	55	506	0.327	0.7155
283372	45	540	0.245	0.7131
283373	60	572	0.304	0.7145
Qugssuk granite				
283322	104	104	2.974	0.8258
283350	126	159	2.316	0.8031
283367	105	414	0.736	0.7335
283375	167	268	1.815	0.7765
283376	87	358	0.701	0.7339
283377	142	85	4.973	0.9064
283378	133	60	6.693	0.9800
283379	147	132	3.259	0.8393

Analytical methods as described by Garde *et al.* (1986); the precision of Rb/Sr measurements is within *c.* 1% (2σ), and of $^{87}Sr/^{86}Sr$ measurements better than 0.0002 (2σ). See also Fig. 38.

The Taserssuaq tonalite is locally discordant to the host grey gneiss, although most boundaries are ambiguous or transitional, and its emplacement post-dates early grey gneiss – amphibolite folds. The western boundary zone possesses a steep but commonly indistinct schistosity developed during syn-emplacement deformation (Garde *et al.*, 1983). The interior of the complex generally has a weak flat-lying S fabric and is less deformed than its margins and the surrounding gneiss. Nutman & Garde (1989) presented evidence that the Taserssuaq tonalite complex is mushroom-shaped and was emplaced in a diapiric fashion.

Most of the complex consists of homogeneous tonalitic rocks; granodioritic and granitic members occur in addition to tonalite in its southern part. This part of the complex also contains lensoid enclaves and sheets of homogeneous or indistinctly layered, medium-grained, hornblende-bearing dioritic and gabbroic rocks, which vary in length from decimetres up to *c.* 2 km. Their chemical compositions (see p. 65) suggest that most of them are cogenetic with the tonalite complex; the absence of such rocks in the neighbouring grey gneiss supports this interpretation.

A shallowly dipping compositional layering of igneous origin can locally be seen within the central part of the complex. The layering is defined by modal variations of hornblende and plagioclase and may stretch over hundreds of metres. Such layering, which is not usually found within sheeted grey gneiss of similar composition, indicates that individual batches of Taserssuaq tonalite magma had more time to differentiate during crystallisation and were therefore larger than the batches of magma that formed the earlier sheets of grey gneiss. In addition to local igneous layering the complex is characterised by subhedral, 1–2 cm large feldspar crystals set in a medium-grained quartzo-feldspathic matrix with granitic texture, and scattered, few millimetres large hornblende-biotite aggregates. A small part of the complex east of lake Taserssuaq carries granulite facies parageneses (Allaart, 1982), and some areas within the central and particularly the western parts of the com-

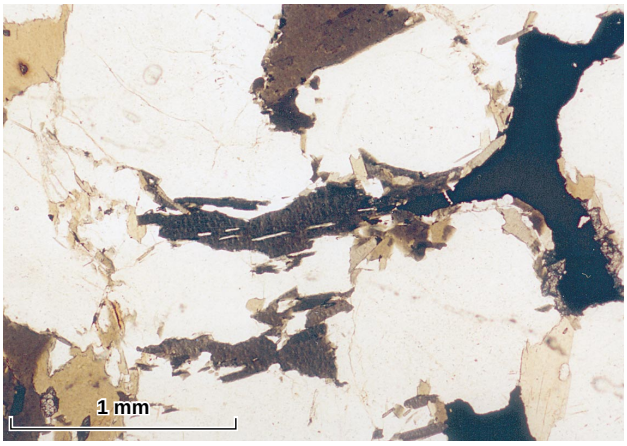

Fig. 39. Thin section of biotite-bearing Taserssuaq tonalite in amphibolite facies. Small irregular biotite grains along the margins of larger biotite grains indicate partial retrogression of the primary amphibolite facies parageneses. GGU 289287, 7 km north-east of the head of Qugssuk.

plex commonly have recrystallised, blebby textures indicative of retrogression from granulite facies. Growth of secondary biotite was also observed in some rocks with primary amphibolite facies parageneses (Fig. 39), which suggests that the effects of retrogression extended beyond the area formerly of granulite facies.

In summary, the Taserssuaq tonalite complex is in many ways similar to the surrounding grey gneiss but was intruded relatively late and in larger batches. Inclusions of supracrustal rocks are uncommon, but there are cogenetic dioritic and gabbroic enclaves.

Finnefjeld gneiss complex

The Finnefjeld complex was first described by Berthelsen (1957, 1962), who studied its north-western boundary area. The main part of the complex is located in the Maniitsoq (Sukkertoppen) district to the north, but its south-eastern margin reaches down into the Fiskefjord area (Plate 1). No precise age has so far been obtained from the Finnefjeld gneiss complex; the field evidence seems to suggest that it may be younger than the Taserssuaq tonalite complex. A conventional U-Pb zircon age of 3067 $^{+62}_{-42}$ Ma was obtained from a sample collected 3 km south-east of Sisak (GGU 339641: one concordant and two discordant size fractions of light brown, idiomorphic to slightly corroded crystals, B. T. Hansen, personal communication, 1990). A Rb-Sr whole-rock age of 3058 ± 123 Ma (initial $^{87}Sr/^{86}Sr$ = 0.7012 ± 0.0007, MSWD = 4.7), obtained by S. Moorbath, University of Oxford, from samples scattered along the mainland coast, was reported by Garde (1990). A second Rb-Sr data set from samples collected around Sisak in the southern part of the complex is very similar (3034 ± 140 Ma, initial $^{87}Sr/^{86}Sr$ = 0.7017 ± 0.0007, MSWD = 0.83), see Fig. 38b and Table 2. Pb-Pb whole rock analysis of 12 samples collected on the island Talerulik gave a best fit line of 2700 $^{+380}_{-350}$ Ma, MSWD = 20.74, model $\mu 1$ = 7.59 (P. N. Taylor, personal communication, 1987); this data set is difficult to interpret but may suggest an isotopically inhomogeneous source, contamination with unradiogenic Early Archaean lead during magma emplacement, or later Pb metasomatism, or both.

The interior parts of the Finnefjeld gneiss complex are only poorly known from helicopter reconnaissance (Allaart *et al.*, 1978) and from unpublished surveys during mineral exploration by Kryolitselskabet Øresund A/S. Its southern boundary zone on the mainland north of Tovqussap nunâ and adjacent islands along the northern boundary of the Fiskefjord map area were surveyed in detail by Marker & Garde (1988) who revised earlier interpretations of the complex.

The Finnefjeld gneiss complex resembles the Taserssuaq tonalite complex in several ways. Both complexes consist of a number of large, generally very homogeneous intrusions of predominantly tonalitic rocks which locally preserve igneous layering, and which were emplaced into already folded and metamorphosed units of supracrustal rocks and Middle Archaean grey gneiss. The main difference between the two complexes is that the Finnefjeld gneiss clearly post-dates the granulite facies event. It has indisputable intrusive contacts with grey gneiss and supracrustal rocks, and in the south-eastern border zone transects their common large-scale structures at large angles (Plate 1; Marker & Garde, 1988, fig. 2). Four intrusive phases were identified, all of which have equilibrium amphibolite facies parageneses without signs of earlier granulite facies metamorphism or pervasive retrogression; Fig. 40 shows a typical lithology. Marker & Garde (1988) noted, however, that the complex also contains local older gneissic enclaves with a more complex history. The latest intrusive phases of Finnefjeld gneiss are granodioritic to granitic in composition and constitute a hybrid border zone along the grey gneiss, which probably includes partially remobilised material derived from the latter rocks.

Whereas the south-eastern hybrid border zone itself is an area of low strain, several NNE- to NE-trending zones of strong deformation occur inside the complex,

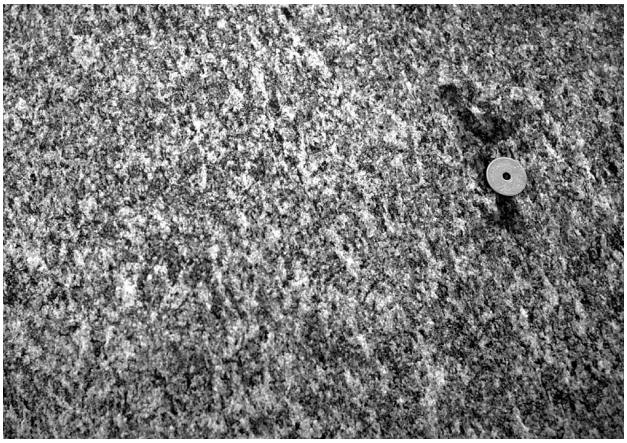

Fig. 40. Typical exposure of homogeneous, medium-grained Finnefjeld gneiss with elongate plagioclase aggregates set in a granitic matrix. 500 m north of Sisak.

e.g. on the island Talerulik and in the mainland north of Sisak (Fig. 41). These high strain zones have a distinct steep to vertical schistosity, commonly combined with tight upright small-scale and larger folds and a shallow south to south-westerly plunging mineral or intersection lineation parallel to fold axes. Marker & Garde (1998) tentatively concluded that these structures were developed in a NW–SE compressional stress field during or soon after intrusion in an overall transpressional setting. A component of transcurrent simple shear may also have been present.

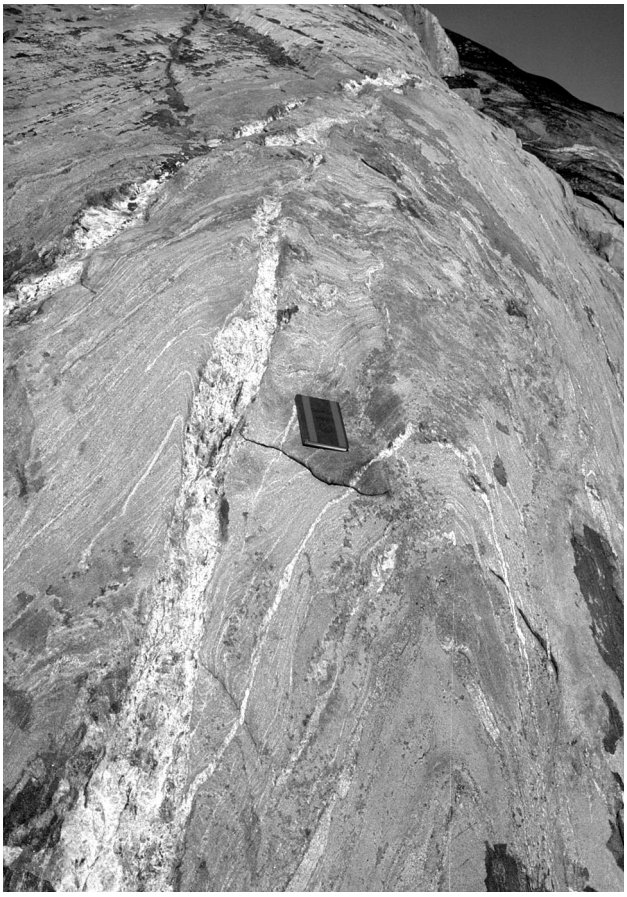

Fig. 41. NNE-trending high strain zone in Finnefjeld gneiss about 1.5 km north of Sisak with tight upright folds and axial planar pegmatite.

Emplacement mechanisms of tonalitic magma

Nutman & Garde (1989) discussed emplacement mechanisms of grey gneiss and Taserssuaq tonalite. They noted that the supracrustal rocks were intruded first by sheeted grey gneisses and then by the domal Taserssuaq tonalite complex. At early stages of magmatic accretion, the tonalitic magma would be emplaced into shallow, cool supracrustal rocks with up to about 5 wt% water, and would exploit hydraulic fractures. If the fractures were formed in an environment of extension or moderate compression, the intrusive sheets would be shallow or moderately inclined, assuming subhorizontal orientation of the maximum stress. Subsequent larger batches of magma such as those forming the dome-shaped Taserssuaq tonalite or Finnefjeld gneiss complexes would be intruded into sialic crust that was already thickened, drier (*c*. 1 wt% water), but now also much hotter and more ductile.

Structural evolution

A general picture of the deformational history that accompanied magmatic accretion of middle continental crust in the Fiskefjord area – sheets of grey gneiss, large tonalite complexes, and late granites – can be acquired by integrating observations in different parts of the area. Around central and outer Fiskefjord interleaved supracrustal rocks and grey orthogneiss outline well-exposed interference patterns between two or three sets of superimposed folds. In other parts of the area interference patterns have been modified by prominent younger, N–S trending high strain zones, and by domes with cores of younger granites. Other parts of the area, those underlain by the Taserssuaq tonalite and Finnefjeld gneiss complexes, have not been subject to strong penetrative deformation.

Interpretation is complicated because most structures in the Fiskefjord area are products of both semi-

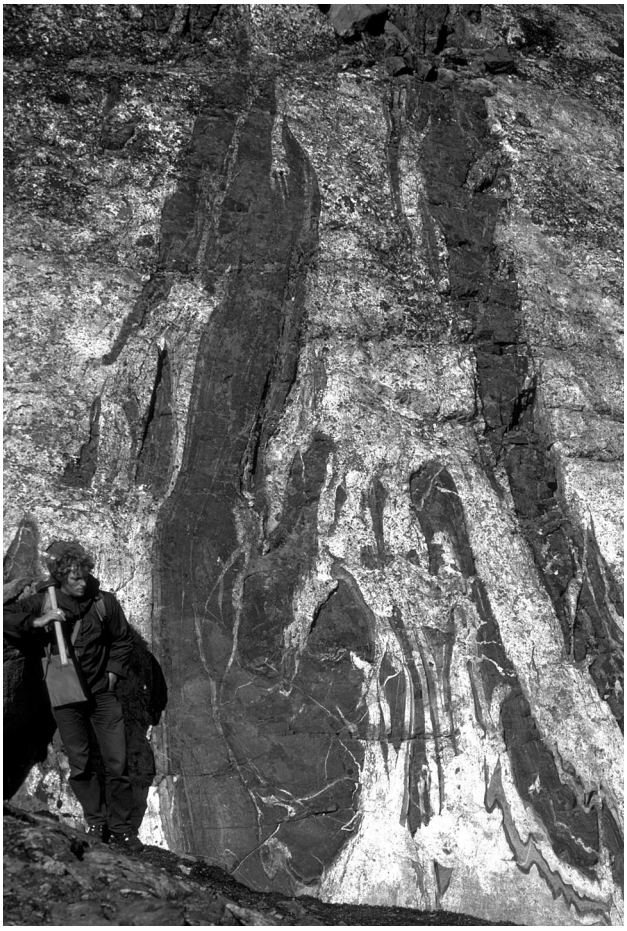

Fig. 42. Complex relationship between supracrustal amphibolite and polyphase orthogneiss, produced by both igneous processes (the splitting and interfingering nature of the intrusive leucocratic rock) and solid-state ductile deformation (isoclinally folded amphibolite screen and *s*-shaped small-folds in right part of the picture). 8 km east of Ulamertoq.

crystalline deformation during magma emplacement and subsequent solid state deformation, as can commonly be observed on outcrop scale (Fig. 42). Besides, it has been demonstrated both in the field and experimentally that several successive events of deformation are not always necessary to produce superimposed folds. For example, Ramberg (1967) and Wikström (1984) have shown by experiments and field studies that 'synchronous refolding' can occur, for instance, by diapiric movements in ductile rocks, or by interaction between gravity-induced diapiric structures and contemporaneous folding in response to a lateral stress field. However, for reasons given below it is plausible that at least three separate phases of folding involving grey gneiss have occurred in the Fiskefjord area.

Distribution of supracrustal rocks within the orthogneiss

Much of the deformation history of the Fiskefjord area is monitored by the distribution and shapes of bodies of amphibolite and related supracrustal rocks, which form structural markers in the otherwise rather monotonous orthogneiss. These patterns also reflect the primary relationships between the two groups of rocks as discussed elsewhere.

In most of the Fiskefjord area, namely where tonalitic and trondhjemitic orthogneisses predominate, older supracrustal rocks form up to about 20 per cent of the outcrop (Plate 1). In some of these areas, for instance north of Qugssuk and on Tovqussap nunâ, they form many kilometres long, multiply folded layers which are linked with each other through complex fold structures that also incorporate the intercalated intrusive orthogneiss. In other areas such as north of outer Fiskefjord, amphibolite and related rocks mostly occur as separate enclaves ranging between a few centimetres and several kilometres in length.

Supracrustal rocks are less common in the large tracts of dioritic orthogneiss that constitute most of the mainland south of Fiskefjord and Nordlandet farther south. The Taserssuaq tonalite and the Finnefjeld gneiss complexes appear to be largely without such enclaves, although their margins have in some places intruded and agmatised supracrustal units.

Outline of principal structural elements

The structural elements in various parts of the Fiskefjord area that together mark its structural evolution may well be representative of the entire Akia terrane. The north-western, north-eastern and south-eastern parts of the area are all characterised by complex, multiply folded outcrop patterns, frequent changes in the orientations of structural elements, and structures up to about 10 km in size (Berthelsen, 1960; Lauerma, 1964; Garde, 1986; Garde *et al.*, 1987). These structures appear to have been developed during the early phases of the *c.* 3000 Ma continental crustal accretion. The central and southern parts are dominated by somewhat larger structures in the lithologically very homogeneous, granulite facies areas of *c.* 3220 Ma Nordlandet dioritic gneiss. The dioritic rocks contain sporadic trains of small leucogabbroic and other inclusions, which outline large recumbent folds, e.g. north of Oqúmiap taserssua. As in the above mentioned

areas these recumbent folds are folded by smaller upright folds (see p. 41).

Several other tracts are characterised by prominent, N–S trending structure with distinct steeply dipping schistosity, subhorizontal linear elements and large isoclinal folds. Some of these N–S trending high strain zones occur along the margins of dioritic gneiss units in the southern part of the area. Another, major high strain zone follows the west coast of inner Godthåbsfjord and continues northwards through the head of Fiskefjord; this zone was established before or during the granulite facies event, with later reactivation. Still others occur in the peninsula east of Qugssuk, where they separate areas of open and variable structure. The Finnefjeld gneiss complex contains several NNE-trending high strain zones close to its south-eastern margin which may possibly be related to the above structures although they are younger (see p. 45).

Several dome-shaped structures were developed late in the structural evolution; most have cores of leucocratic tonalite, trondhjemite or granite. Lauerma (1964) described the almost 10 km large Ipernat dome west of Nãngissat, and Berthelsen (1950) mapped a smaller one around Qaersup ilua in the western part of Tovqussap nunâ. Other domes or partial domes with cores of leucocratic orthogneiss occur at Qeqertaussaq, south of Oqúmiap taserssua, at Quagsugtarssuaq, and north of Narssarssuaq. The Igánánguit granodiorite (see p. 45) forms a *c.* 20 km long, NNE-trending composite dome *c.* 10 km north-east of the head of Fiskefjord.

Early phases of deformation on Tovqussap nunâ

Berthelsen (1960) published a detailed account of the structural evolution of Tovqussap nunâ in the northwestern part of the Fiskefjord area and recognised four main phases of deformation. The first two, the Midterhøj and Smalledal phases, resulted in large recumbent isoclinal folds with NW-, and ENE- to NE-trending axes respectively. The Tovqussap dome, a prominent structure in the western part of Tovqussap nunâ, was interpreted to have formed by a combination of several factors, including both antiformal folding of earlier structures and (?diapiric) movement of material towards the top of the structure. Berthelsen placed the dome-forming episode after the two first phases of deformation. The subsequent Pâkitsoq phase resulted in a series of conspicuous upright to overturned, open to tight folds of moderate size with SE- to S-plunging axes. Their wavelengths are *c.* 2–3 km (much shorter than those of the recumbent folds), their hinge zones are more angular, and they were commonly accompanied by a new axial planar foliation and mineral or rodding lineation. The Pâkitsoq phase of deformation took place contemporaneously with the culmination of metamorphism under granulite facies conditions. Berthelsen (1960) did not discuss the possibility of 'synchronous refolding', but the above mentioned differences between the Smalledal phase of recumbent folds and the Pâkitsoq phase of upright folds suggest that this possibility is unlikely.

Berthelsen's structural analysis led him to assume that Tovqussap nunâ originally consisted of a conformable, around one kilometre thick pile of supracrustal rocks. This was a reasonable conclusion at the time, considering the prevailing conceptions about the origin of grey gneiss; it was not widely recognised until a decade later that the bulk of Archaean grey gneisses are of intrusive igneous origin (e.g. McGregor, 1973). The granitic rocks on Tovqussap nunâ were interpreted by Berthelsen (1960) as formed by *in situ* granitisation, not as (late) intrusive bodies. Berthelsen (1960, p. 212) was aware that part of his structural analysis would fall apart if some or all of the isoclinal fold closures he had described or interpreted could instead be shown to be the tips of wedge-shaped intrusions. However, the geological map (Plate 1 in Berthelsen, 1960) that forms the basis for his analysis is very accurate and mostly covers well-exposed ground. Accordingly, a substantial part of the structural evolution he proposed for Tovqussap nunâ can be recognised with appropriate modifications in much of the Fiskefjord area.

One element that warrants revision or at least commenting is Berthelsen's (1960, p. 147) earliest, Midterhøj phase of deformation. Berthelsen based the Midterhøj phase on an interpretation of one apparent isoclinal fold closure outlined by an amphibolite with a core of leucocratic gneiss, and another inferred, unexposed closure, both located in the upper flank of a later fold. The Midterhøj phase was only recognised in the eastern part of Tovqussap nunâ, and in view of the intrusive origin of the rock in the core of Berthelsen's supposed isoclinal closure, it is unlikely that the Midterhøj phase exists here. However, an early phase of deformation with isoclinal folds of similar orientation has later been documented from central Fiskefjord. These folds were refolded during two events which match Berthelsen's Smalledal and Pâkitsoq phases (see the following sections).

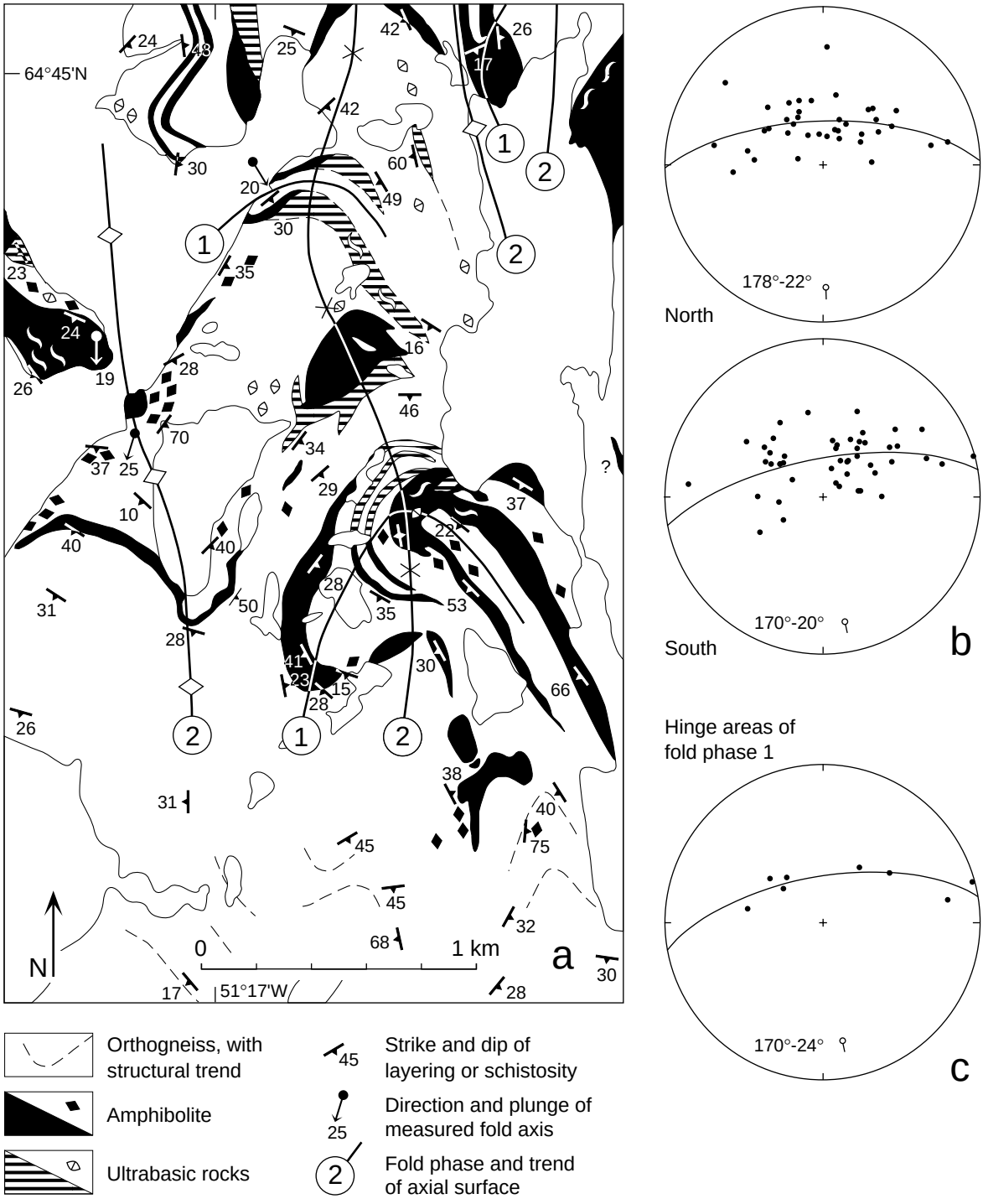

Fig. 43. (**a**) Superimposed folding north-east of Itivneraq, south of outer Fiskefjord. Axial surfaces of N–S trending folds belonging to the Pâkitsoq phase are marked as (2) and have shallow south-plunging axes. These folds are superimposed on an earlier set of overturned to recumbent isoclinal folds (1), which also have south-plunging axes but originally had E–W trending axial surfaces.
(**b**) Stereographic projections of poles to layering and schistosity from the northern and southern parts of the area. In both subareas the poles show considerable scatter relative to a constructed great circle but indicate a persistent southerly axial plunge.
(**c**) Strike and dip measurements of layering and schistosity within two hinge zones of the early folds (phase 1) suggest that also the early folds had southerly axial plunges.

Thrusting of orthogneiss and amphibolite on Angmagssiviup nunâ prior to isoclinal folding

In the western part of Angmagssiviup nunâ, M. Marker (personal communications, 1987, 1995) mapped an up to *c.* 200 m thick, compositionally banded amphibolite – grey gneiss sequence (Garde, 1989b). The banded sequence consists of tonalitic gneiss in granulite facies and retrogressed to amphibolite facies with closely spaced, parallel bands of amphibolite on a scale of centimetres to decimetres, and the composite rock has distinct schistosity. The banded sequence can be followed through isoclinal fold closures belonging to the earliest phase of folding (see below) and is interpreted by M. Marker as having resulted from tectonic mixing of orthogneiss and amphibolite units during early thrusting at a shallow crustal level. The banded sequence is thus considered to represent the earliest episode of deformation that comprises both the supracrustal association and the *c.* 3000 Ma grey gneiss.

Refolded folds around central and outer Fiskefjord

Garde *et al.* (1987) described two areas between Igdlutalik and Tasiussarssuaq north of central Fiskefjord, and south-west of Serquartup imâ south of central Fiskefjord, where early isoclinal folds with amplitudes of several kilometres are folded by a second set of large, flat-lying, E–W trending isoclinal folds. These are in turn refolded by upright, NE–SW trending open folds with smaller wavelengths (in the order of 1–2 km) and shallow NE-trending doubly plunging axes. Garde *et al.* (1987) ascribed these folds to three successive phases of deformation, which closely correspond to the Midterhøj, Smalledal and Pâkitsoq phases of Berthelsen (1960).

Other early isoclinal folds occur, for instance, in granulite facies Nordlandet dioritic gneiss west of Qôrngualik; it is possible that the earliest structures in this region predate the *c.* 3000 Ma crustal event. McGregor (1993, fig. 5) described a large synclinorium with a width of *c.* 15 km south-west of Natsigdlip tasia (in the border area between the Qôrqut and Fiskefjord map areas), the northern part of which refolds an isoclinal fold outlined by trains of leucogabbroic inclusions west of Qôrngualik. The synclinorium is refolded by a series of asymmetric south-plunging folds with wavelengths less than 1 km, which are contemporaneous with the *c.* 3000 Ma granulite facies metamorphism and can be correlated with folds of the Pâkitsoq phase further north.

The Pâkitsoq phase of upright to overturned, NE–SW to N–S trending folds with wavelengths less than *c.* 5 km is recognised in most parts of the Fiskefjord area. Figure 43 shows an example east of Itivneraq, outer Fiskefjord. Here, folds of the Pâkitsoq phase with south-plunging axes refold recumbent folds with similar fold axis orientations. Garde *et al.* (1987) described NNW-trending structures with apparent domes and basins in the north-western part of the Fiskefjord area, e.g. north-west of Tasiussarssuaq. These are now interpreted as folds belonging to the Pâkitsoq phase with axial culminations and depressions controlled by pre-existing structures.

North–south trending high strain zones

Several localised N–S and NNE-trending, steep to vertical zones of relatively late high strain occur in the central and eastern parts of the Fiskefjord area. The most prominent is the Qugssuk–Ulamertoq zone (Fig. 44). This runs along the west coast of Qugssuk, continues northwards towards Fiskefjord along the eastern shoulder of the ridge Ulamertoq, and from there follows the head of Fiskefjord further north into the Isukasia map area (with a dextral offset of *c.* 2 km along the Proterozoic Fiskefjord fault, see p. 85). The zone largely comprises orthogneiss of tonalitic and dioritic composition, several large amphibolites, and a prominent, *c.* 25 km long and up to *c.* 800 m wide layer of dioritic gneiss which crosses Fiskefjord. Some of the thickest amphibolite bodies in the Qugssuk–Ulamertoq zone outline large upright isoclinal folds with steep to vertical limbs. Their fold axes plunge *c.* 15° S, and fold axis-parallel hornblende lineation is common. In the hinge zones small scale, recumbent, shallow south-plunging isoclinal folds are outlined by amphibolite interleaved with thin orthogneiss layers. The latter folds are believed to predate the upright isoclinal folds. Besides, small, more or less symmetrical isoclinal folds with subvertical axial surfaces occur in the limbs of the regional folds; these folds could be either reorientated earlier folds or parasitic to the regional folds.

A large part of the orthogneiss within the zone is retrogressed and has an irregular quartzo-feldspathic net-veining and a diffuse, undeformed, blebby texture of secondary, centimetre-sized biotite-amphibole patches (e.g. Fig. 32). Areas of granulite facies tonalitic gneiss

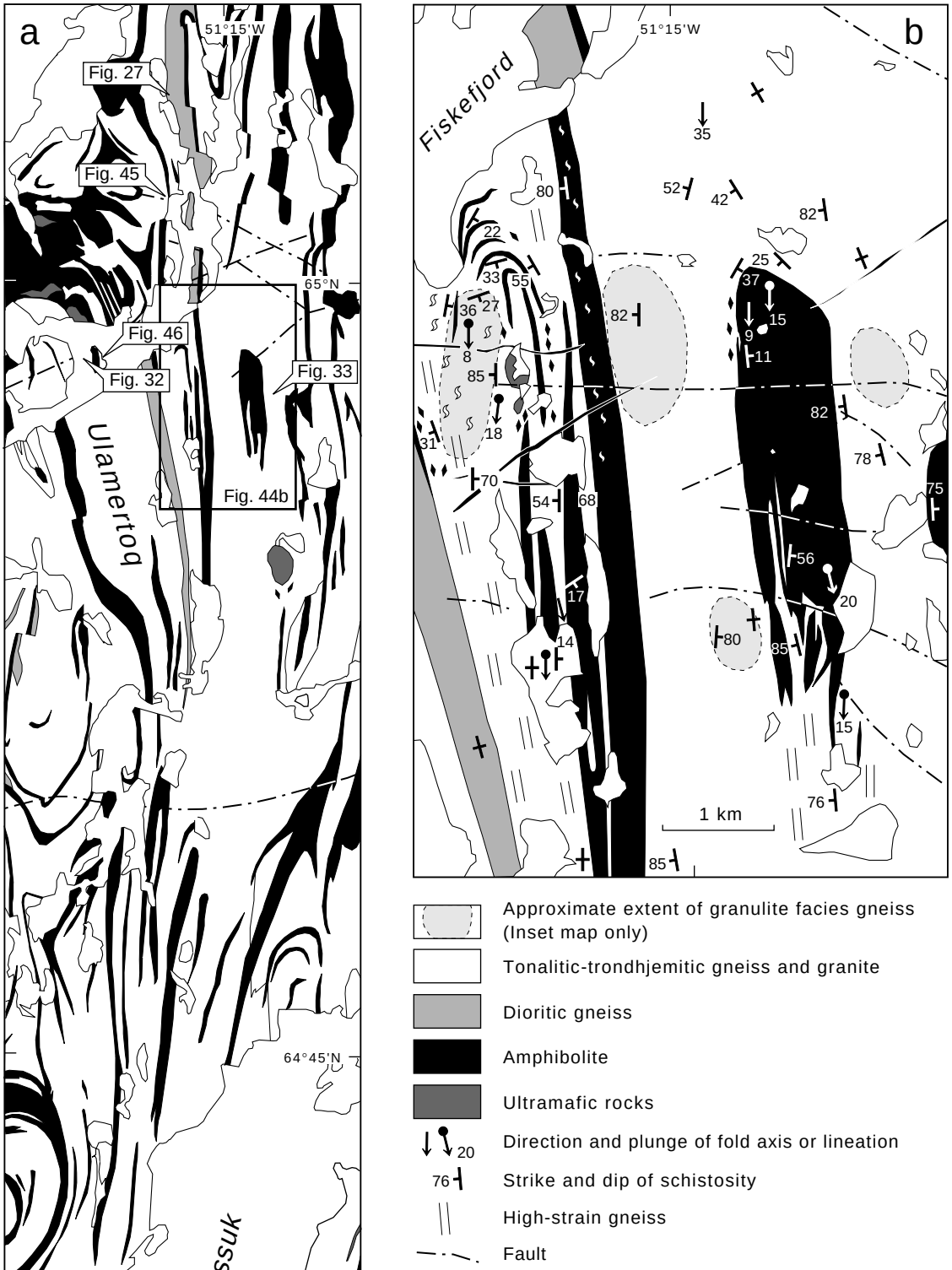

Fig. 44. (**a**) Simplified map of the Qugssuk–Ulamertoq zone, a N–S trending zone of high strain in the eastern part of the Fiskefjord area established during the *c.* 3000 Ma granulite facies event. (**b**) Inset map of the area east of Ulamertoq.

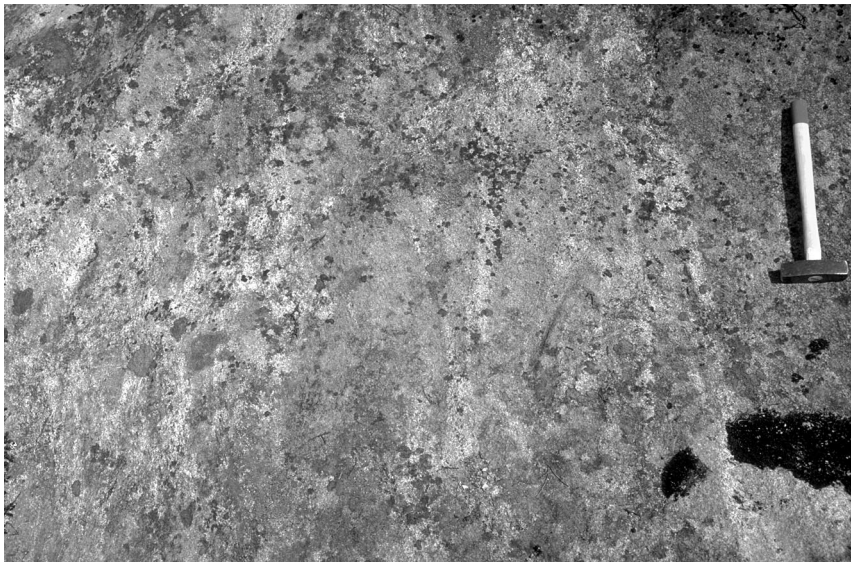

Fig. 45. Partially retrogressed grey gneiss with indistinct quartzo-feldspathic network. Qugssuk–Ulamertoq zone 200 m west of the head of Fiskefjord.

Fig. 46. Retrogressed orthogneiss with folded enclave of amphibolite. The strong planar fabric of the retrogressed orthogneiss in the central part of the picture suggests syn-retrogression deformation in this zone. East coast of island in inner Fiskefjord *c.* 5 km east of Kûlik.

with equigranular mineral textures, which have partially or completely escaped retrogression, cover irregular areas up to several square kilometres in size inside the Qugssuk–Ulamertoq zone (Fig. 44). Also, some parts of the dioritic gneiss layer that crosses the inner part of Fiskefjord have retained granulite facies parageneses and may have a distinct (granulite facies) schistosity (Fig. 27), whereas other parts (e.g. just west and south of Fiskefjord) have secondary amphibolite facies textures developed during static retrogression (Fig. 45).

The Qugssuk–Ulamertoq zone also contains local narrow tracts of retrogressed orthogneiss, a few decimetres to tens or hundreds of metres wide, with a distinct late schistosity that affects the retrograde biotite-amphibole patches (Fig. 46). In these tracts the thin quartzo-feldspathic veins commonly visible in retrogressed gneiss are reorientated and parallel to the new schistosity. Likewise, observations by V. R. McGregor (personal communication, 1995) along the western coasts of Godthåbsfjord and Qugssuk indicate that ductile deformation proceeded there after the onset of retrogression.

The relationships described above between map- and outcrop-scale structures and granulite facies and retrogressive textures in the Qugssuk–Ulamertoq zone indicate that its pervasive N–S structural grain, including the apparent transposition of earlier folds into upright isoclines, was developed while granulite facies conditions still prevailed.

The Qugssuk–Ulamertoq zone and related N–S trending structures are believed to have formed principally

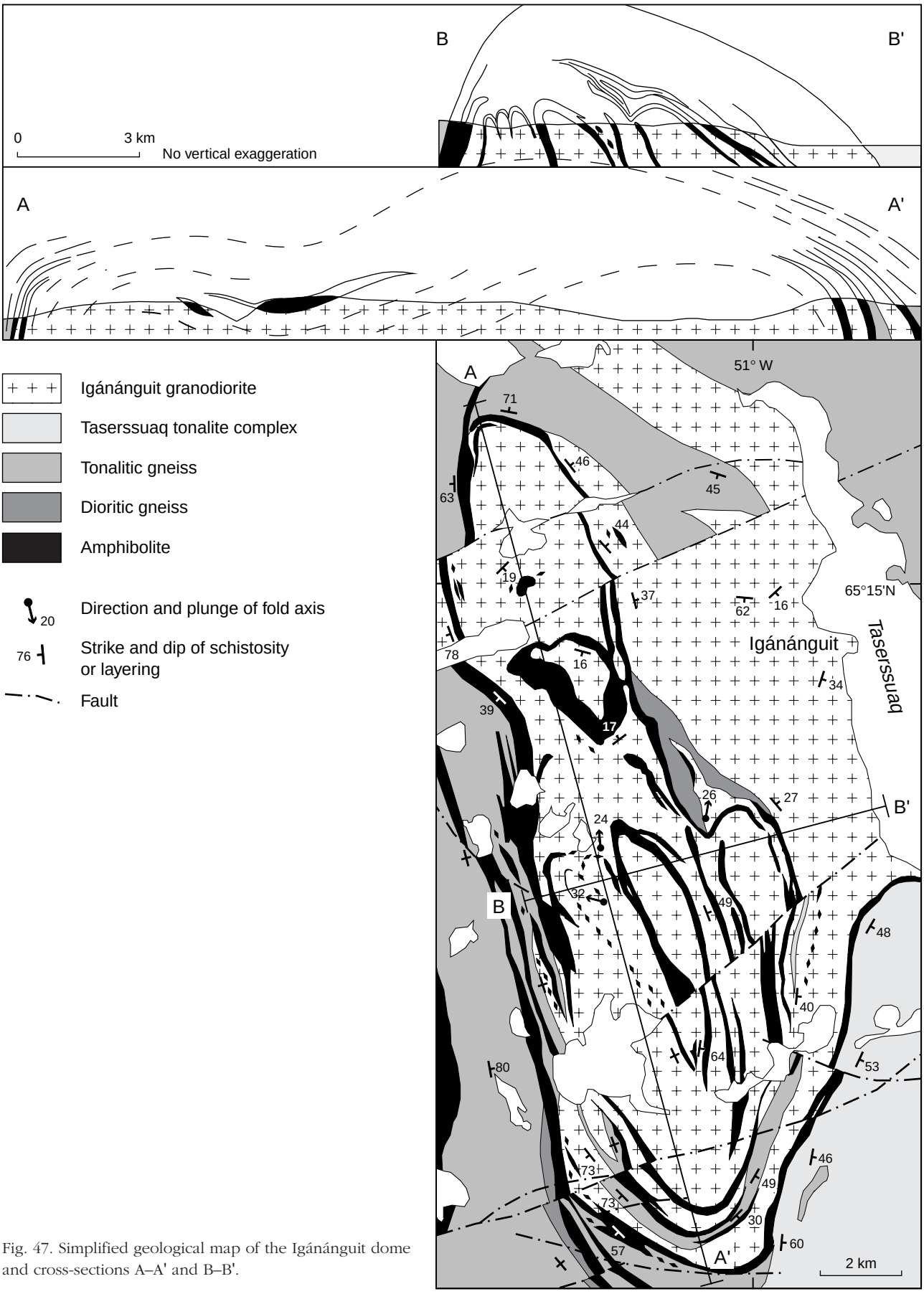

Fig. 47. Simplified geological map of the Igánánguit dome and cross-sections A–A' and B–B'.

in response to E–W compressional forces. Subhorizontal elongation is indicated by the common mineral lineation and shallow south-plunging orientations of fold axes. It is possible that this elongation was also related to a transcurrent component, but no direct evidence for this has been observed. The previously mentioned NNE-trending zone of strong deformation in the south-eastern part of the Finnefjeld gneiss complex is possibly related to the N–S trending high strain zones. Its trend is a little different and it post-dates granulite facies metamorphism, but it may overlap in time with late movements of the N–S zones and has a similar element of subhorizontal stretching.

McGregor *et al.* (1991) and McGregor (1993; personal communication, 1995) suggested that the high-strain zone along the western part of outer Godthåbsfjord and Nuuk town is continuous with the Qugssuk–Ulamertoq zone, and that both developed after the assembly of the Akia and Akulleq terranes at around 2700 Ma. While the Qugssuk–Ulamertoq zone appears to have been reactivated in connection with the terrane assembly, the available field evidence clearly suggests that it came into existence at about 3000 Ma under granulite facies metamorphic conditions.

Late granitic domes and sheets

Garde *et al.* (1986) described the Igánánguit granodiorite (formerly Igánánguit pink gneiss) and Qugssuk granite, two younger granitoids that crop out in the eastern part of the Fiskefjord area (age data follow below). Coastal outcrops of granitic rocks belonging to the Qugssuk granite were already shown on the map by Noe-Nygaard & Ramberg (1961). The Igánánguit granodiorite is confined to a composite dome west of the lake Taserssuaq. The Qugssuk granite mainly forms steep sheets conformable with the pre-existing NNE-trending regional structure on both sides of Qugssuk (Plate 1; Garde, 1989b), although there are also dome-like structures in the northern part of its outcrop area. Both the granitoids were emplaced after the peak of granulite facies metamorphism and associated partial retrogression, after the accretion of tonalitic crust had ceased at least in this part of the Akia terrane.

Granite sheets similar to the Qugssuk granite were also emplaced into an area of *c.* 5 km^2 south-east of Quagssûp taserssua, hosted by granulite facies dioritic gneiss. Like the Qugssuk granite described below, also these granite sheets are medium to fine grained and have granitic textures with dispersed biotite and two feldspars (not mesoperthite as in syn-granulite facies granites). The granite sheets are discordant to gneissic foliation in the dioritic host rock, which is bleached and recrystallised by retrogression along the granite contacts.

Garde *et al.* (1986) and Garde (1989a) presented limited geochemical data indicating that the granitoids are much more evolved than the grey tonalitic gneisses, and approach minimum melt compositions. With support from field evidence and isotopic data these authors and Garde (1990) suggested that the late granitoids were derived by partial melting of source rocks similar to the grey gneiss and Taserssuaq tonalite. Granite geochemistry is discussed on p. 72.

Igánánguit granodiorite dome

The Igánánguit granodiorite dome is a *c.* 20 by 10 km large composite dome located west of Taserssuaq in the south-western part of the Isukasia map area (Plate 1; Figs 47, 48).

The dome has a NNW-trending long axis and is asymmetric: its western flank is much steeper (dipping about 75°) than the eastern flank (dipping 20–40°, Fig. 47). The granodiorite which forms the interior of the dome was emplaced into a host consisting of interlayered and previously folded amphibolite and dioritic to tonalitic orthogneiss. The dome itself is bounded along most of its circumference by a 100–500 m thick layer of amphibolite, which also separates it in the south-east from the Taserssuaq tonalite complex; the position of the north-eastern margin of the dome is only approximately known (S. B. Jensen, personal communication, 1984).

The presence of more or less concentric horizons of amphibolite inside the Igánánguit dome suggests that the granodiorite was in part intruded as separate sheets. In the southern and western parts of the dome, screens of tonalitic gneiss flank internal amphibolite layers, and a 5 km long, bifurcated layer of dioritic gneiss occurs in its central part. The amphibolite and older gneiss horizons and trains of inclusions bring out the internal structure of the dome (Fig 47). It consists of a *c.* 5 km wide northern dome which is separated from a twice as large southern dome by a shallow depression west of Igánánguit. The southern dome itself consists of several smaller domes, which merge southwards into a single south-plunging structure (Fig. 48).

The granitoid rock in the interior of the dome is mostly undeformed but has a distinct schistosity in the immediate vicinity of the older gneiss and amphibolite

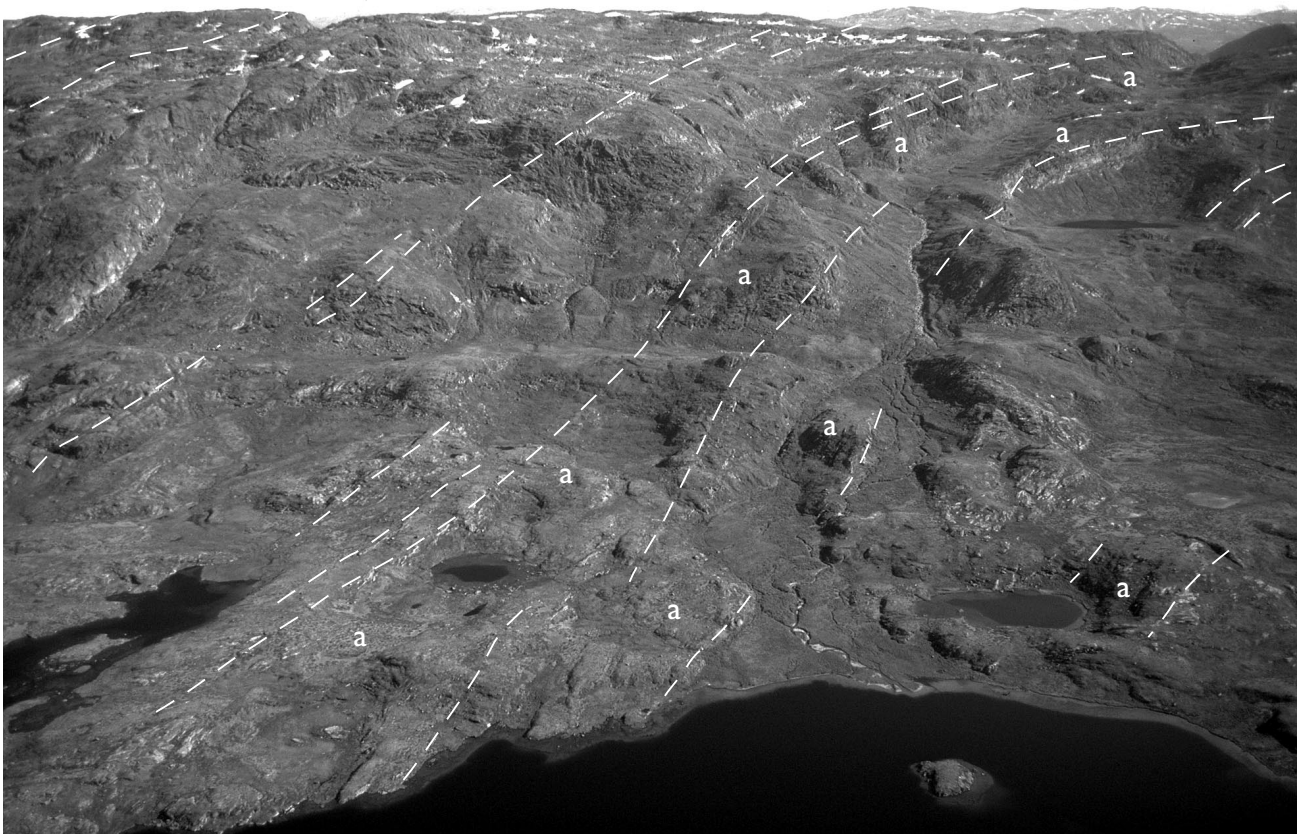

Fig. 48. North-facing slopes in the southern part of the Igánánguit dome. An interior, *c.* 200 m thick amphibolite layer in the central and right parts of the picture (labelled a), which dips away from the observer, outlines the shape of the dome. Other internal boundaries with similar orientations are also marked.

horizons. In spite of this strong foliation its intrusive character into the latter horizons is locally well exposed, and the amphibolites were already strongly deformed before they were intruded by the granite magma. Particularly in the north-western marginal part of the dome the granodiorite commonly contains rafts of amphibolite; some of these rafts are tightly folded with the granodiorite, and the orientations of these (syn-intrusion?) folds suggest shortening perpendicular to the margins of the dome. This is also apparent from Fig. 49 which displays a section perpendicular to the inclined north-western marginal zone of the dome: an amphibolite horizon is intruded by the granite, and the resulting granodiorite-amphibolite agmatite stretched out in directions parallel to the margin.

The Igánánguit granodiorite is a fine- to medium-grained, homogeneous and white to buff or pink-coloured granite to granodiorite (see section on geochemistry for composition), typically with small, evenly dispersed biotite flakes. It locally grades into coarse pegmatitic varieties and is in places cut by white or pinkish pegmatite. Under the microscope the undeformed granite has a more or less equigranular mosaic texture of *c.* 1–3 mm large subhedral grains of quartz, microcline, weakly antiperthitic plagioclase, scattered, *c.* 1 mm large euhedral biotite grains, and occasional small pockets of myrmekitic quartz-feldspar intergrowths. Apatite and zircon are common accessories. There are local signs of minor recrystallisation. The granitic texture with evenly dispersed, small biotite flakes, myrmekite, and absence of mesoperthite show that the Igánánguit granodiorite was emplaced under amphibolite facies conditions and has not been retrogressed from granulite facies. This is taken as independent textural evidence that the Igánánguit granodiorite is younger than the surrounding grey gneiss, most of which has blebby textures indicative of retrogression from granulite facies. Former granulite facies conditions in the area are also indicated by the common presence of orthopyroxene-bearing amphibolite.

As mentioned above there are several structures in the Fiskefjord area that may either be domes formed

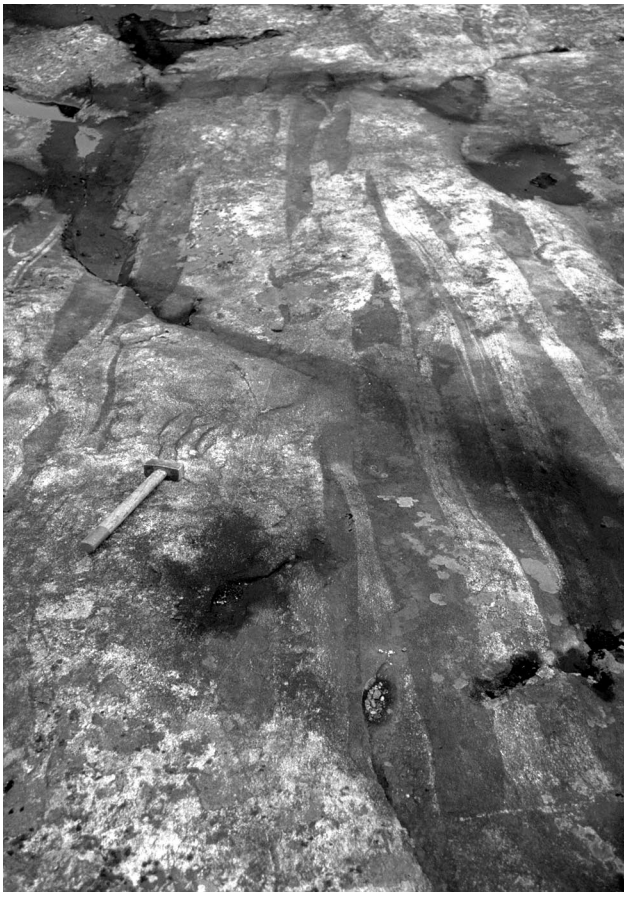

Fig. 49. Deformed marginal zone of the Igánánguit granodiorite with elongate amphibolite rafts. North-western margin of the Igánánguit dome, 9 km west of Taserssuaq.

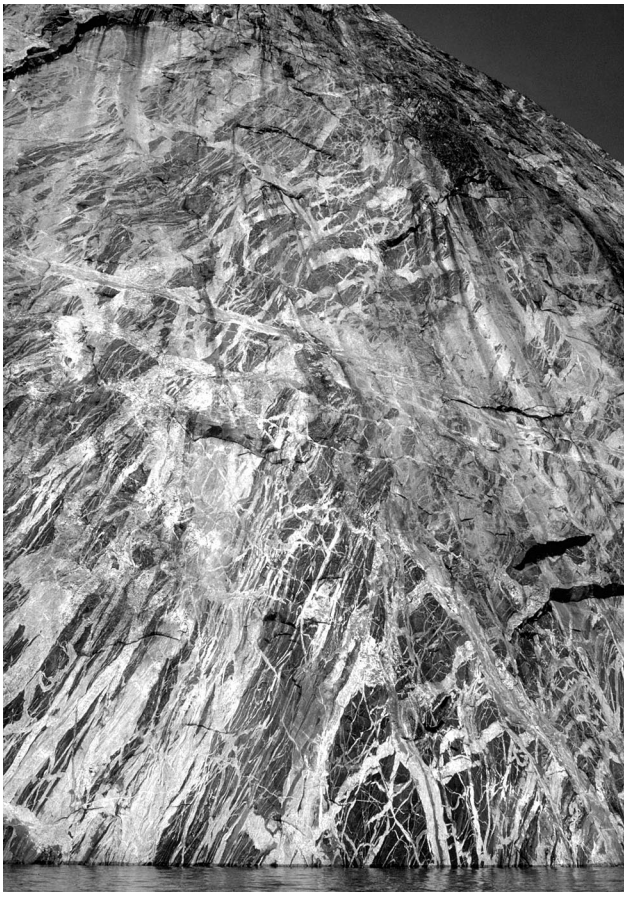

Fig. 50. Amphibolite agmatite with numerous sheets of tonalite, granite and pegmatite (predominantly Qugssuk granite). South-facing cliff opposite the north-eastern end of Bjørneøen.

by injection of magma or diapiric movement, or dome-like structures formed due to superimposed folding. The Igánánguit dome is interpreted as a magmatic or diapiric structure because it consists of a characteristic granitic lithology which is largely undeformed except at its margins, and is younger than the Taserssuaq tonalite complex and multiply deformed grey tonalitic gneiss which it intrudes.

The Igánánguit granodiorite is about 3000 Ma old. Field relationships and metamorphic textures presented here show that it is younger than the surrounding grey gneiss and Taserssuaq tonalite complex, but Rb-Sr and Pb-Pb isotopic investigations have given very imprecise results. Field observations revealed that the Igánánguit granodiorite commonly contains millimetres to centimetres thick biotite-rich wisps which most likely represent restite material from its source, and the possibility must be considered that the granodiorite is not isotopically homogeneous. Regression of 12 samples analysed for Rb-Sr gave an apparent age of 2935 ± 240 Ma (initial $^{87}Sr/^{86}Sr$ = 0.7021 ± 0.004, MSWD = 9.6). The best fit for six of these samples, collected within an area of 1 km^2, was 3013 ± 190 Ma (initial $^{87}Sr/^{86}Sr$ = 0.7013 ± 0.0008, MSWD = 1.98) (Garde *et al.*, 1986). Pb isotopic analysis (P. N. Taylor, personal communication, 1986) resulted in a well-fitted isochron of 3092 ± 48 Ma with a model μ1 value of 7.56 for 11 samples (μ1 values around 7.5 are normal for Middle Archaean orthogneisses in West Greenland). However, this result is heavily dependent on a single very radiogenic sample (GGU 278880). Omitting this sample the age is 3023^{+195}_{-227} Ma, model μ1 = 7.47. The Pb-Pb isotopic data are further discussed on p. 79.

Qugssuk granite

The Qugssuk granite (Garde, 1984; Garde *et al.*, 1986) straddles the boundary between grey gneiss retrogressed from granulite facies and the Taserssuaq tonalite

Fig. 51. Qugssuk granite (left) cutting strongly deformed, retrogressed grey gneiss with small elongate amphibolite enclaves. See discussion in the main text. North coast of Qugssuk.

pluton north and east of Qugssuk. It is a medium-grained, white to pale pinkish leucocratic biotite granite which may grade into coarse pegmatitic varieties.

A whole-rock Rb-Sr isochron age of 2969 ± 32 Ma, initial $^{87}Sr/^{86}Sr$ = 0.7020 ± 0.0003, MSWD = 1.09, was obtained by Garde *et al.* (1986). A younger but less precise Rb-Sr age was obtained from eight samples collected from granite sheets on the peninsula east of Qugssuk. These data points plot along a best-fit line with an age of 2842 ± 85 Ma, with a relatively high initial $^{87}Sr/^{86}Sr$ ratio of 0.7040 ± 0.0009, and MSWD = 6.32 (Fig. 38c; Table 2). Pb isotopic data discussed by Garde (1989a, 1990) and on p. 79 suggest open-system behaviour of lead.

Unlike the Igánánguit granodiorite, the Qugssuk granite has been emplaced mainly as anastomosing sheets up to a few metres or tens of metres thick, generally with steep or subvertical orientations roughly parallel to the orientations of the host rocks (Fig. 50). The granite also forms much thicker (up to *c.* 1 km) sheets that have been intruded into the marginal zone of the Taserssuaq tonalite complex east of Qugssuk, and into a major amphibolite unit north of Qugssuk. Particularly in the latter area there are large, homogeneous outcrops devoid of older enclaves, and here a couple of small dome-like structures occur.

Fig. 51 shows an example of the intrusive relationship between a sheet of Qugssuk granite and retrogressed grey gneiss at the north coast of Qugssuk. The interpretation by Garde (1990, p. 670) that the granite cuts pre-existing retrogressive textures in the grey gneiss may be true; alternatively the granite itself was the cause of retrogression, which was brought about by hydrous fluids liberated during solidification of the granite (see p. 77 ff.).

Terrane assembly

The Archaean crust in the Godthåbsfjord region consists of several terranes with different ages, lithologies and tectonic and metamorphic histories (Friend *et al.*, 1988a); the Akia and Akulleq terranes and their common tectonic boundary (Fig. 2) were first described by Friend *et al.* (1988b). Their assembly is the latest Archaean event known to have affected the Akia terrane. The Ivinnguit fault that forms the terrane boundary is a NE-trending, subvertical to moderately WNW-dipping, 10–15 m thick mylonite zone, which is best exposed on the coasts of south-eastern Bjørneøen and Sadelø in outer Godthåbsfjord (McGregor *et al.*, 1991). The terrane boundary straddles the south-eastern corner of the Fiskefjord map area (Fig. 2).

The timing of terrane assembly is poorly constrained but occurred in the interval between *c.* 2800 Ma (the age of Ikkatoq gneisses in the Akulleq terrane which are cut by the Ivinnguit fault) and *c.* 2720 Ma (the ages of granite sheets that cut several terrane boundaries, McGregor *et al.*, 1991; Friend *et al.*, 1996). Thus, a SHRIMP zircon U-Pb age of 2712 ± 9 Ma was reported by Friend *et al.* (1996) from a Qârusuk dyke at the type locality on Bjørneøen close to the south-eastern margin of the Akia terrane. However, no such dykes have so far been observed in the Fiskefjord area, and it is uncertain how far the effects of the terrane assembly can be traced north-west of the terrane boundary itself.

McGregor *et al.* (1991) and McGregor (1993) described a NNE–SSW zone of strong ductile deformation continuous with the Qugssuk–Ulamertoq high strain zone along western Godthåbsfjord, which according to these authors postdates the juxtaposition of the Akia and Akulleq terranes. However, as discussed above, at least the Qugssuk–Ulamertoq high strain zone itself was established prior to the assembly of the two terranes.

Geochemistry of grey gneiss, tonalite complexes and granitic rocks

The grey gneiss and granitoid rocks were originally separated into a number of mappable units based on their field relationships, mineralogical composition, colour and texture. These field divisions are largely supported by geochemical work presented here, although compositional overlaps were found especially between the dioritic and tonalitic-trondhjemitic groups. In addition, the analytical work revealed the presence of a distinct group of dioritic gneiss not recognised in the field, namely the Qeqertaussaq diorite which occurs

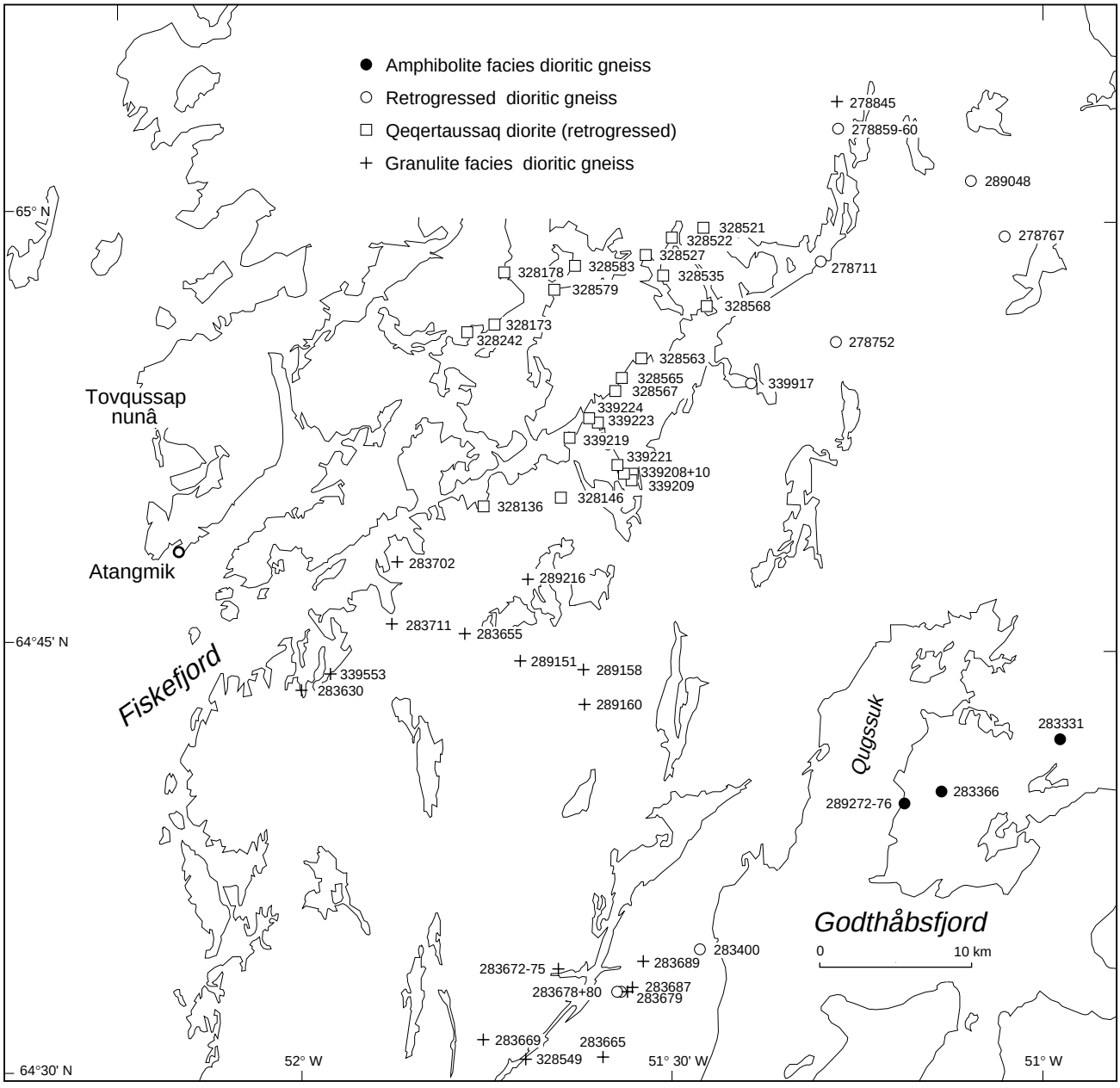

Fig. 52. Locations of analysed dioritic gneiss samples in the Fiskefjord area.

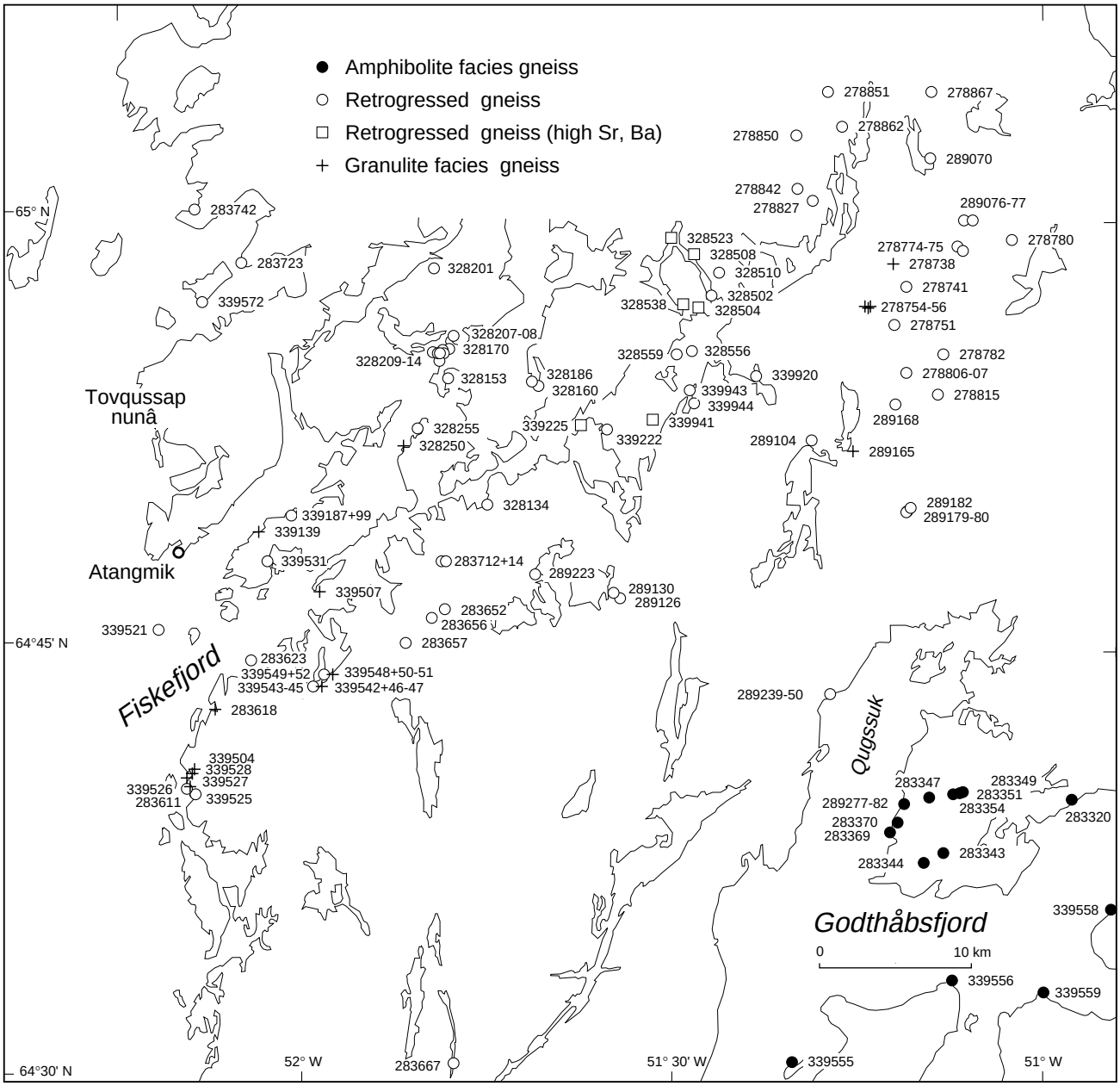

Fig. 53. Locations of analysed samples of tonalitic-trondhjemitic grey gneiss in the Fiskefjord area.

within an area of *c.* 300 km^2 around central Fiskefjord (Fig. 52).

Figures 52 and 53 show sample locations of the main groups of grey gneiss, and Fig. 54, a series of quartz–K-feldspar–plagioclase ternary diagrams (Streckeisen, 1976), gives a first overview of the range of compositions. In Fig. 54 the bulk of the grey gneiss and most samples from the Finnefjeld and Taserssuaq complexes plot in the tonalite-trondhjemite and granodiorite fields; the grey gneiss also comprises rocks in the quartz-dioritic and dioritic fields. The Igánánguit granodiorite and Qugssuk granite largely plot in the granodioritic and granitic fields, respectively.

Figure 54 is based on chemical analyses using the cation norm calculation, with the modification that biotite is introduced when hypersthene and K-feldspar appear together in the norm (6hy + 5or = 8bi + 3qz). Except for the presence of amphibole in some rocks the modified cation norm provides fair estimates of the modes, since orthopyroxene and K-feldspar only rarely occur together. This formal approach to classification gives a reasonable impression of present modal com-

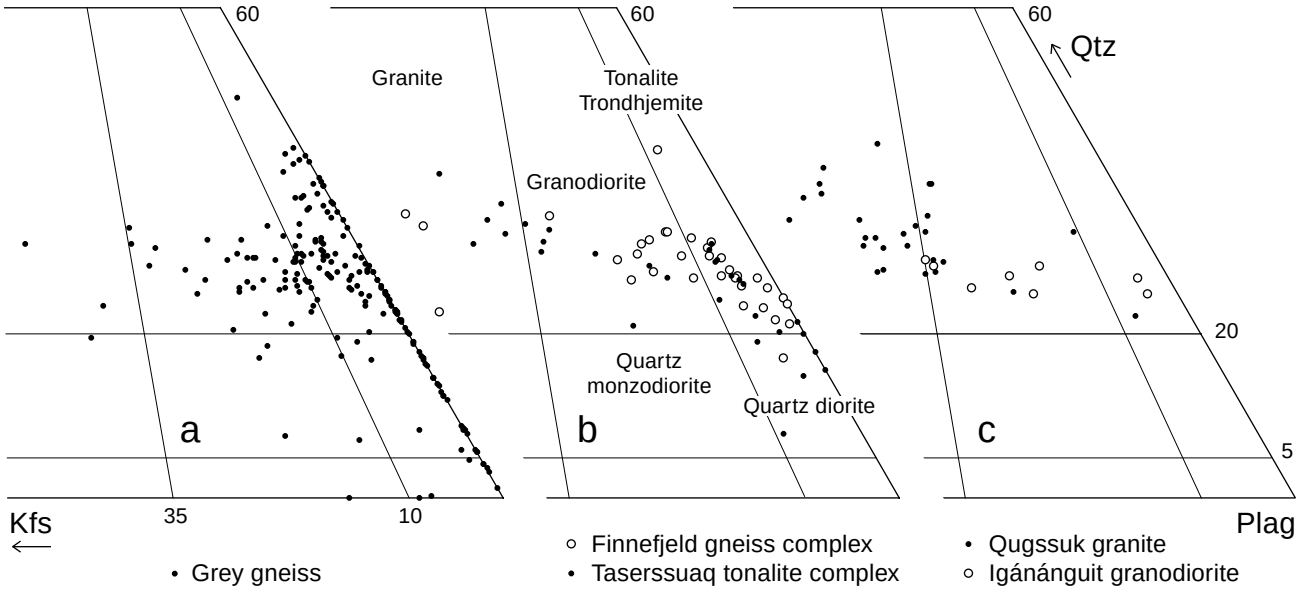

Fig. 54. Quartz–K-feldspar–plagioclase ternary diagrams (Streckeisen, 1976) for Archaean quartzo-feldspathic intrusive rocks in the Fiskefjord area, based on modified cation norm calculations from chemical analyses (see the main text for explanation). (**a**) Grey gneiss, (**b**) Finnefjeld gneiss and Taserssuaq tonalite complexes, (**c**) Igánánguit granodiorite and Qugssuk granite.

positions, but due to element mobility during metamorphic processes it does not reflect the original igneous mineral compositions of all rocks in question.

Common dioritic gneiss and Qeqertaussaq diorite

The grey gneiss covers a large range of compositions from dioritic rocks with less than 55 wt.% SiO_2 to trondhjemitic rocks with over 75% SiO_2; the presentation of geochemical data follows these two large field groups: dioritic gneiss (with less than *c.* 65% SiO_2) and tonalitic-trondhjemitic gneiss (with more than *c.* 63% SiO_2).

Fifty-eight rock samples described in the field as dioritic gneiss (sample locations in Fig. 52) range from *c.* 51 to 65% SiO_2 (Appendixes 5, 6; Fig. 55). They consist of diorite, quartz diorite and mafic tonalite, as well as a few mafic diorites which compositionally resemble andesitic leuco-amphibolites of the supracrustal rock association. The dioritic gneiss comprises two groups with distinctly different geochemical signatures (Figs 55–58): a large group of common dioritic gneiss with general geochemical characteristics similar to those of the tonalitic-trondhjemitic gneiss (which besides the *c.* 3220 Ma Nordlandet dioritic gneiss may also comprise *c.* 3000 Ma old rocks), and the Qeqertaussaq diorite characterised by very high P_2O_5, LREE, Sr and Ba contents (see below).

The common dioritic gneiss, which comprises both amphibolite facies, granulite facies and retrogressed samples, occurs over most of the Fiskefjord area (Fig. 52). Its major and trace element variations against SiO_2 are continuous with those displayed by tonalitic-trondhjemitic grey gneiss (described in detail below), if the latter are extrapolated to lower SiO_2 values (compare Figs 55 and 56 with Figs 59 and 60). Besides, amphibolite facies, granulite facies and retrogressed samples of common dioritic gneiss show some characteristic mutual differences (also found in the tonalitic-trondhjemitic gneiss, see p. 55), namely, low concentrations of LIL elements in granulite facies rocks, large variations of these elements in retrogressed rocks, and high Ba and Sr contents in some retrogressed rocks. However, the relatively small number of samples, the somewhat erratic distribution of SiO_2 contents among them, and the limited number of sample localities make it difficult to establish if there are systematic differences in major element compositions between the three subgroups, such as those demonstrated below for the tonalitic-trondhjemitic gneiss.

The second group, the *c.* 3050 Ma Qeqertaussaq diorite, consists of a group of dioritic, quartz dioritic and mafic tonalitic enclaves in tonalitic-trondhjemitic grey gneiss. These enclaves all possess the same dis-

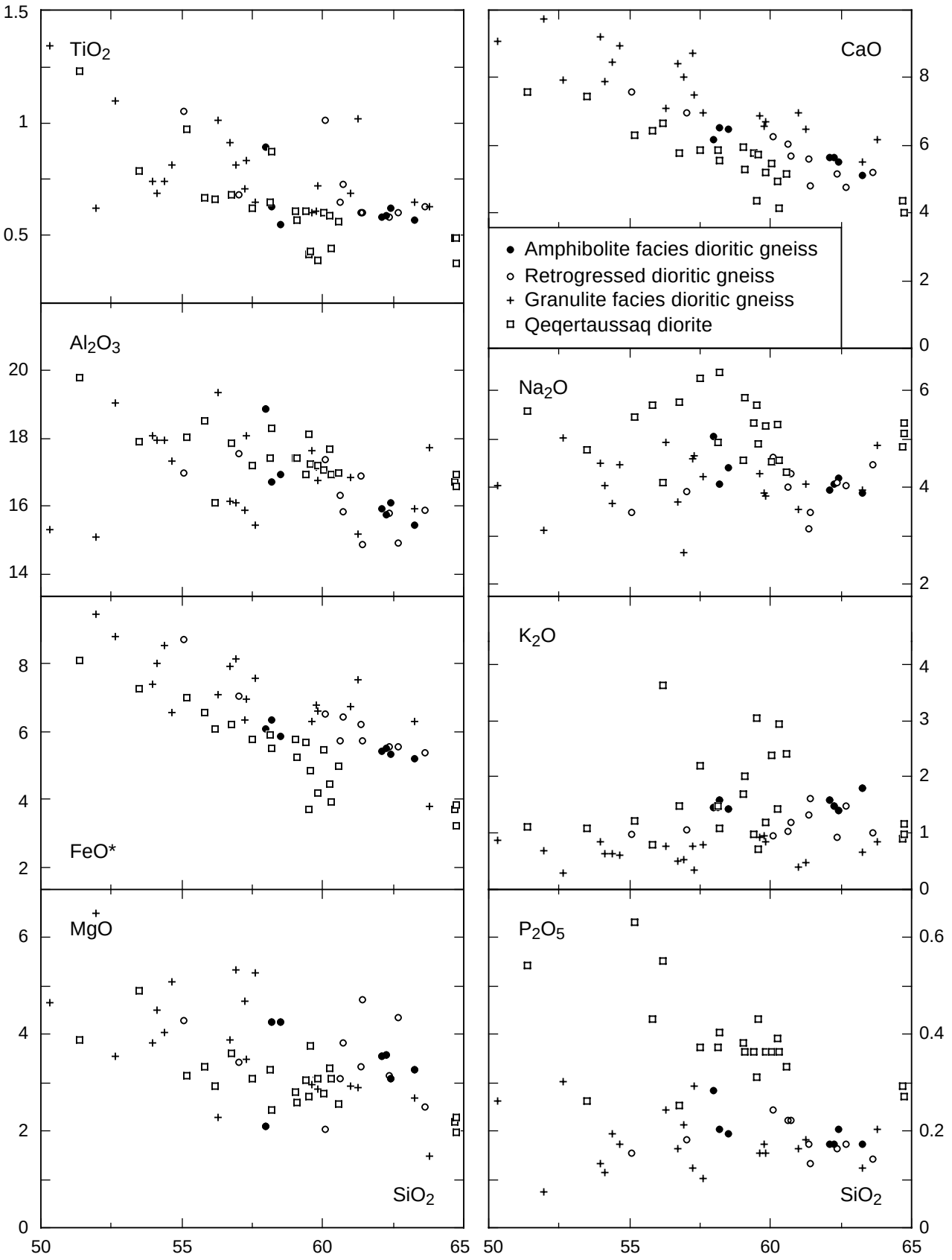

Fig. 55. Major element variation diagrams against SiO_2 (wt. %), dioritic grey gneiss. Note the differences between the main group of dioritic grey gneiss and the Qeqertaussaq diorite. Sample localities in Fig. 52.

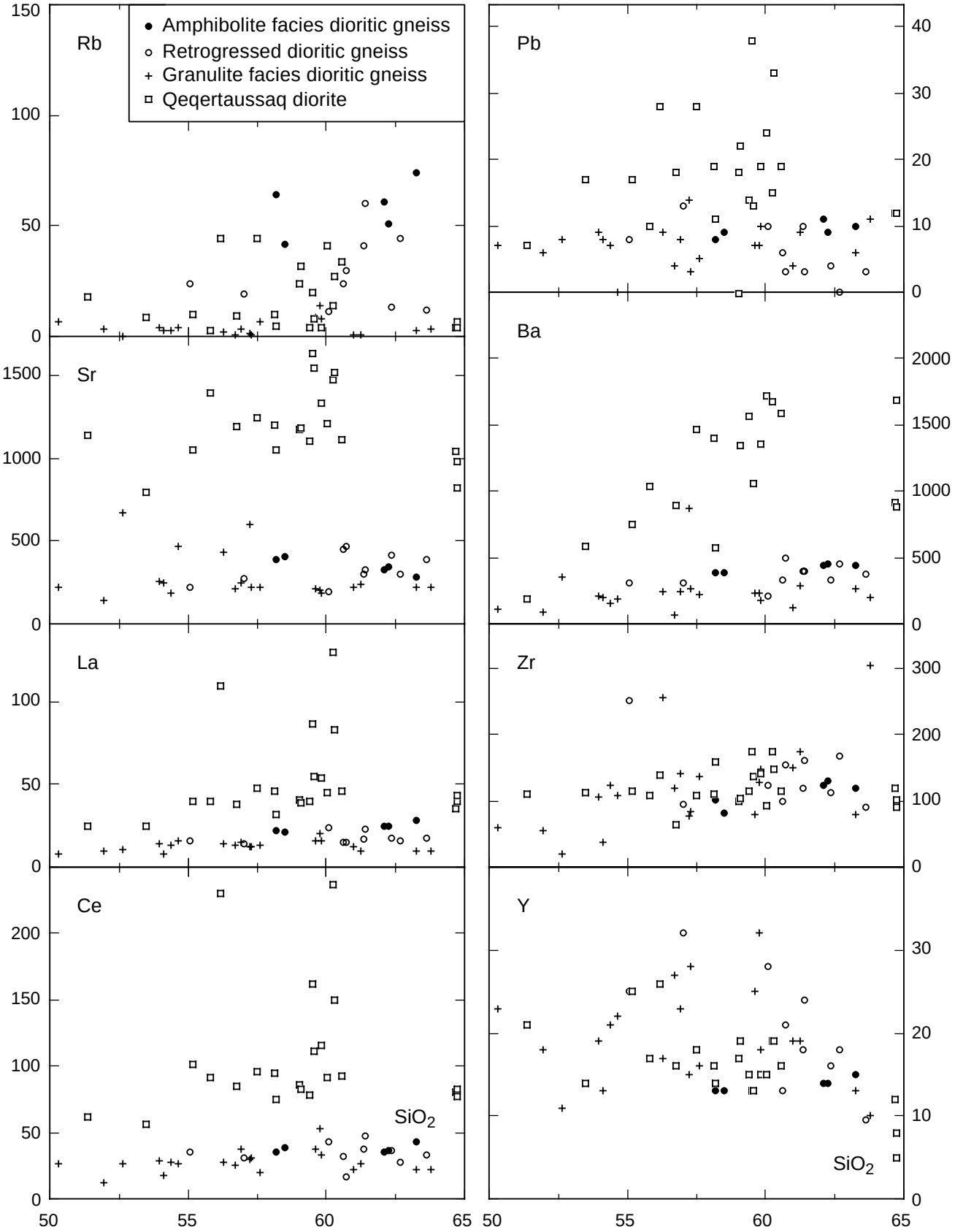

Fig. 56. Selected trace element variation diagrams against SiO_2 (in ppm and wt. %) for dioritic grey gneiss. Note the LIL element and LREE enrichment in the Qeqertaussaq diorite. All elements analysed by XRF (see Appendix for details). Sample localities shown in Fig. 52.

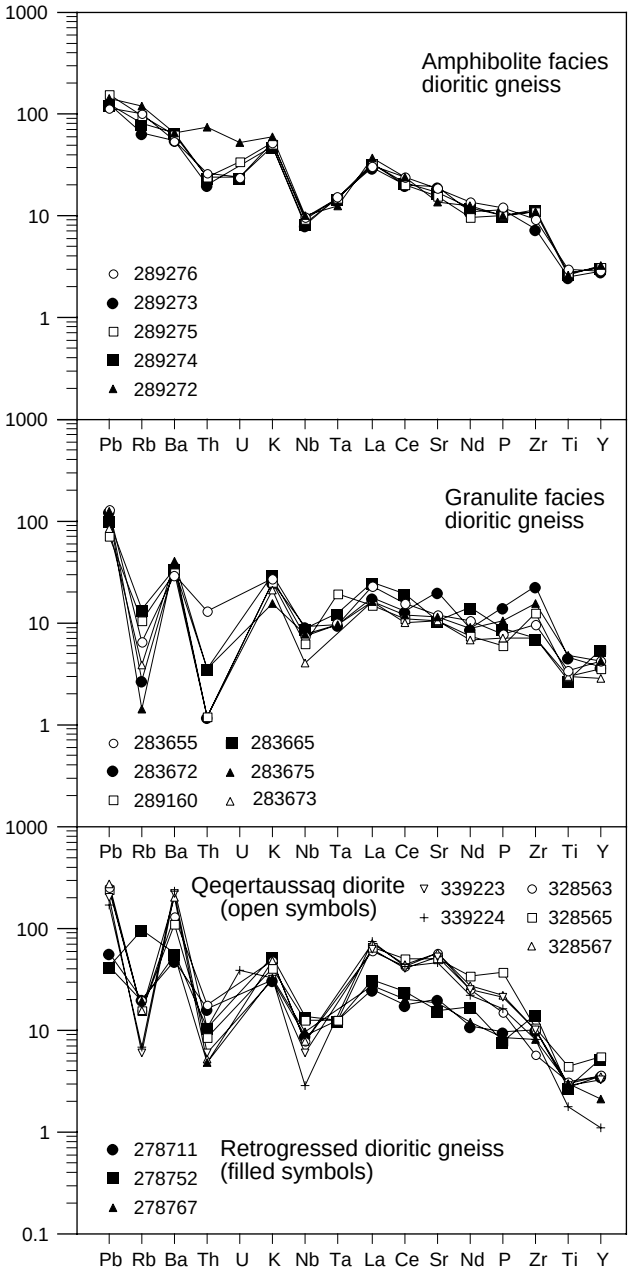

Fig. 57. Spider diagrams of dioritic grey gneiss normalised to primordial mantle, using normalisation factors from Sun & McDonough (1989). XRF and INNA analyses (Th, U, Ta, La, Ce and Nd) in this and succeeding spider diagrams as described in Appendix. Sample localities shown in Fig. 52.

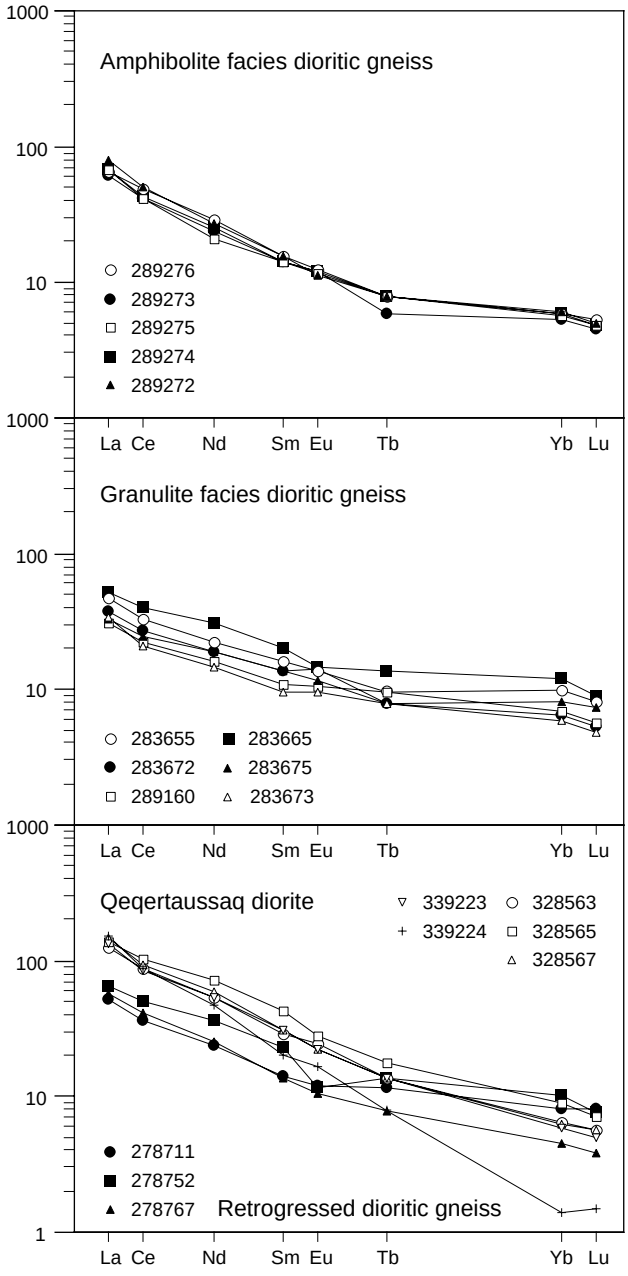

Fig. 58. Chondrite-normalised REE diagrams (Nakamura, 1974) of dioritic grey gneiss from the Fiskefjord area. Note LREE enrichment in the Qeqertaussaq diorite. All elements analysed by INNA (see Appendix). See Fig. 52 for sample localities.

tinct geochemical signature and are located around the peninsula Qeqertaussaq in central Fiskefjord (with a dextral offset of *c.* 3 km across Fiskefjord by the Proterozoic Fiskefjord fault). The Qeqertaussaq diorite is variably retrogressed but may contain partially preserved hypersthene. In the field these rocks are indistinguishable from retrogressed members of the common dioritic gneiss, and likewise form early and commonly fragmented components of the grey gneiss. However, the Qeqertaussaq diorite is clearly geochemically different from the common dioritic gneiss including its retrogressed samples, being enriched in P_2O_5, LREE and several LIL elements but depleted in HFS (high field strength) elements (Appendix 6; Figs 55–58) relative to rocks of the

former unit with similar SiO_2 content. The Qeqertaussaq diorite has low TiO_2, FeO*, MgO, CaO, Cr and Ni contents and low Mg/Fe ratios, whereas it has very high contents of especially P_2O_5, Pb, Ba, Sr and LREE, and relatively high contents of Na_2O, K_2O, Pb, Rb and other LIL trace elements. Zr and Y occur in similar concentrations as found in the common dioritic gneiss. Fig. 58 displays the strong REE fractionation of the Qeqertaussaq diorite and its distinct positive LREE anomaly compared to common dioritic gneiss. The HREE contents of both groups of dioritic gneiss are significantly higher than in the tonalitic-trondhjemitic grey gneiss (compare Figs 58 and 62).

Tonalitic-trondhjemitic grey gneiss

Major and trace element variation diagrams against SiO_2 based on 122 samples (Figs 59, 60), as well as mantle-normalised spider diagrams and chondrite-normalised REE diagrams of representative samples (Figs 61, 62), illustrate the chemical composition and variation of the tonalitic-trondhjemitic gneiss. Sample localities are shown on Fig. 53, and representative compositions and bulk averages are listed in Appendixes 7–8. The figures also highlight compositional differences between amphibolite facies (un-retrogressed) rocks, granulite facies rocks, and retrogressed rocks (also in amphibolite facies, but with disequilibrium mineral textures and compositions).

The major element compositions of the three groups of tonalitic-trondhjemitic gneiss (Appendixes 7, 8) are typical for intermediate to acid rocks of the tonalite-trondhjemite-granodiorite (TTG) suite (see e.g. reviews by Condie, 1981 and Martin, 1994), and plotted against SiO_2 (Fig. 59) most major element oxides only display moderate scatter, suggesting that the rocks may have been formed by similar magmatic processes. However, both Na_2O and K_2O and several LIL trace elements show large variations in the retrogressed gneiss (see below). Besides, Fig. 59 suggests that the granulite facies gneiss group has higher FeO*, MgO and CaO and lower Al_2O_3, Na_2O and K_2O concentrations than the two other groups, and FeO* and MgO appear to be more variable in retrogressed gneiss than in the amphibolite and granulite facies groups.

In order to investigate if these apparent differences between gneisses with different metamorphic facies are statistically significant, covariance tests between the three groups of grey gneiss were performed for all major element oxides against SiO_2 (major elements recalculated to 100%), whereby the silica content of each sample could also be taken into account. The test confirmed that the differences are all significant at the 99% confidence level (F-values above 7.50, critical F_{99} = 4.78), except for TiO_2 and P_2O_5 where there is no significant difference (F-values of 0.80 and 0.74 respectively). A linear relationship between each major element oxide and SiO_2 was assumed in the covariance tests; this is not true for K_2O, but Fig. 59 itself shows that the differences in K_2O are very large.

Amphibolite facies, granulite facies and retrogressed orthogneiss have different LIL trace element compositions, and examples of Rb and Pb are plotted against SiO_2 in Fig. 60. Amphibolite facies gneiss has normal, and granulite facies gneiss very low concentrations of these elements compared to average Archaean TTG from the literature sources quoted above. Retrogressed gneiss has lower LIL element concentrations than amphibolite facies gneiss, but there are large variations irrespective of SiO_2 content. Sr and Ba show different distributions (Fig. 60). Compared to average 'Archaean TTG' (Sr = 454 ppm, Ba = 690 ppm, Martin's, 1994, compilation), the concentrations are normal to low in both amphibolite facies gneiss and granulite facies gneiss (average amphibolite facies: Sr = 382 ppm, Ba = 691 ppm; granulite facies: Sr = 417 ppm, Ba = 430 ppm, Appendix 7). However, in retrogressed gneiss both Sr and Ba concentrations are above average Archaean TTG (average 692 and 809 ppm, respectively, Appendix 8). A few of the latter samples have Sr and Ba concentrations above *c.* 900 and 1500 ppm together with high concentrations of P_2O_5, LREE and other LIL elements (see below); these samples all occur within the area of the Qeqertaussaq diorite and are shown with open squares on Figs 59 and 60. Each of the elements La, Ce, Zr and Y (Fig. 60) is quite variable but occurs within similar limits in the three groups of grey gneiss, except in the just mentioned LREE-enriched samples of retrogressed gneiss.

In mantle-normalised spider diagrams (Fig. 61) all three groups of tonalitic-trondhjemitic gneiss show progressive enrichment from the least to the most incompatible lithophile elements relative to primordial mantle, but with negative deviations from this curve of the HFS elements Nb and to a lesser degree Ta and Ti. In addition, retrogressed and particularly granulite facies gneisses show very substantial negative Rb and Th anomalies. The overall pattern of amphibolite facies gneiss closely resembles that of average Archaean grey gneiss (Fig. 63, using Martin's, 1994, compilation), and is comparable to the patterns of some younger calc-

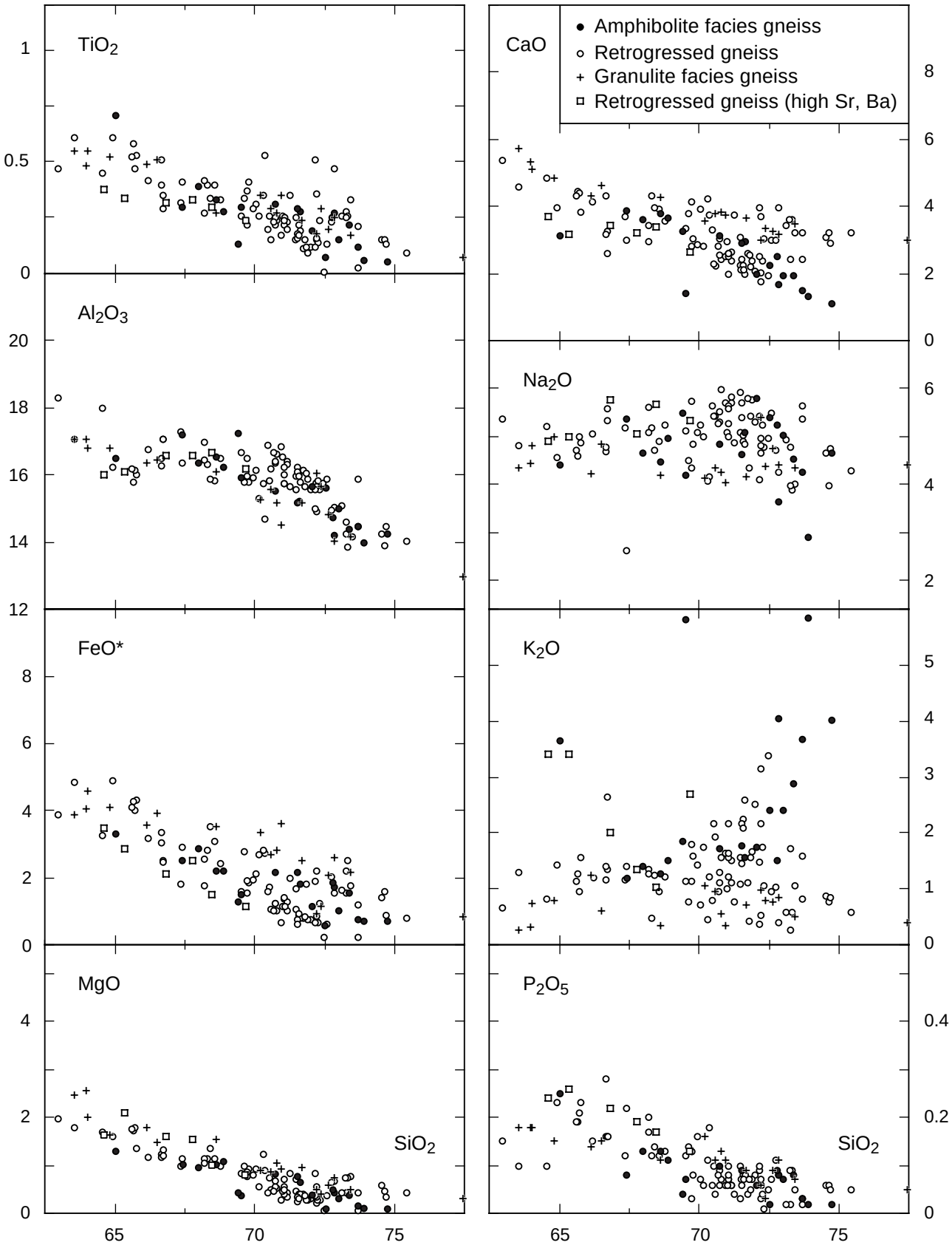

Fig. 59. Major element variation diagrams *v.* SiO_2 (wt. %), tonalitic-trondhjemitic grey gneiss. See Fig. 53 for locations of samples.

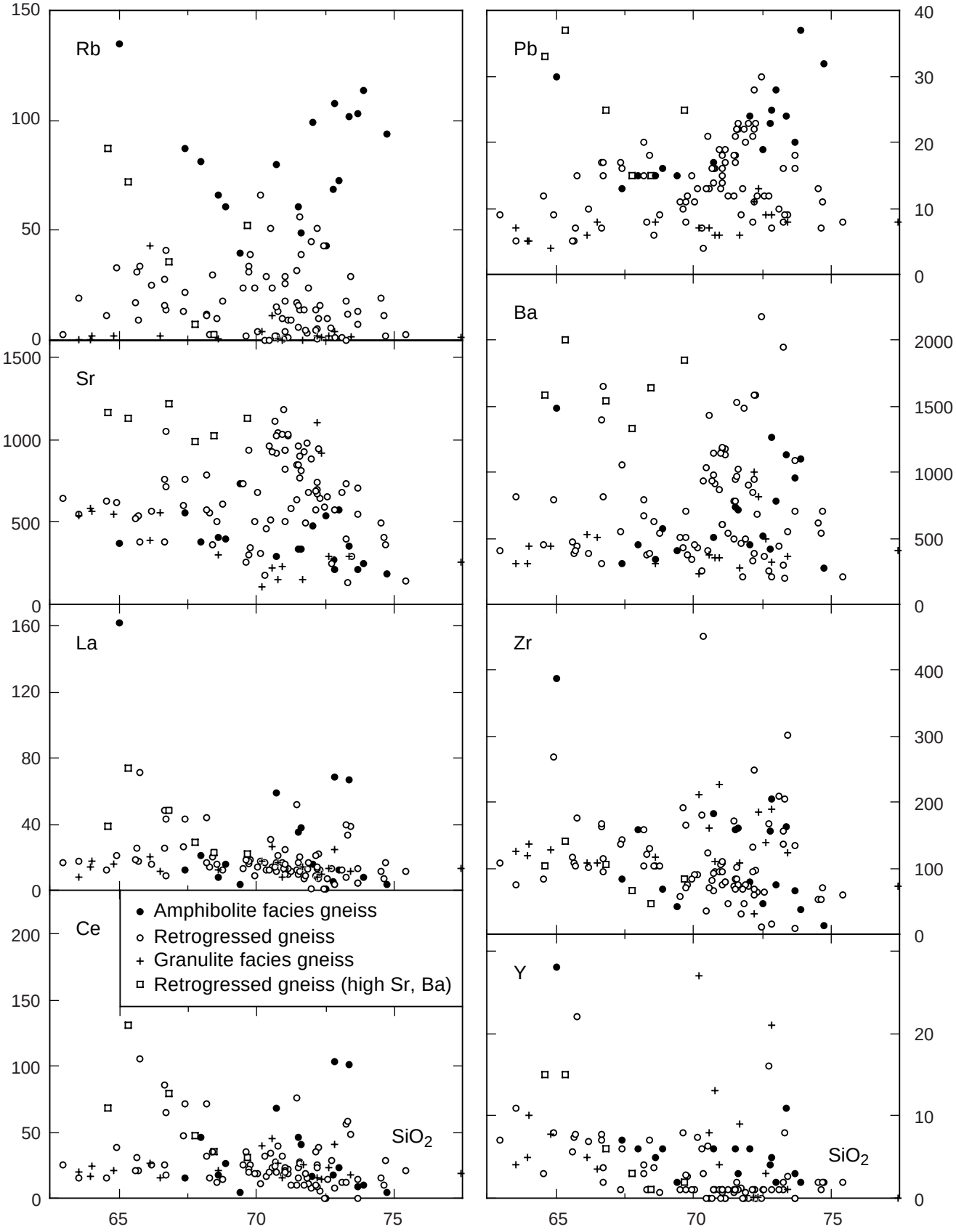

Fig. 60. Selected trace element variation diagrams against SiO_2 (in ppm and wt. %), tonalitic-trondhjemitic grey gneiss. All elements analysed by XRF (see Appendix for details). See Fig. 53 for locations of samples.

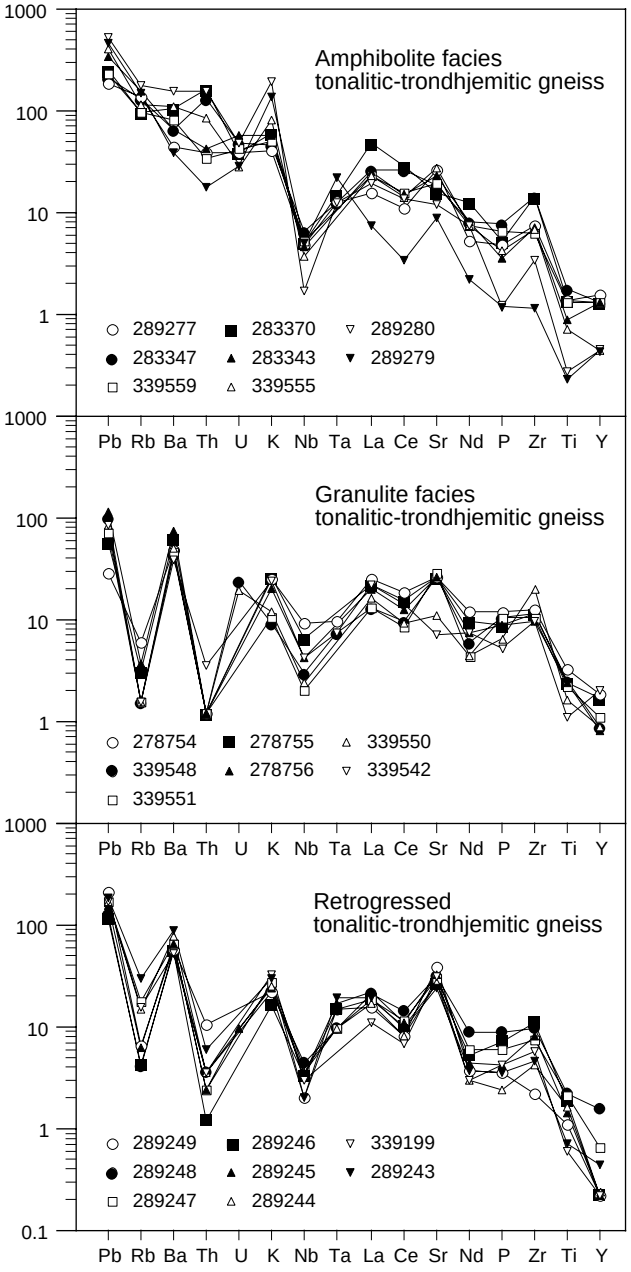

Fig. 61. Spider diagrams of tonalitic-trondhjemitic grey gneiss, Fiskefjord area, normalised to primordial mantle (normalisation factors from Sun & McDonough, 1989). XRF and INNA analyses, see Appendix. See Fig. 53 for locations of samples.

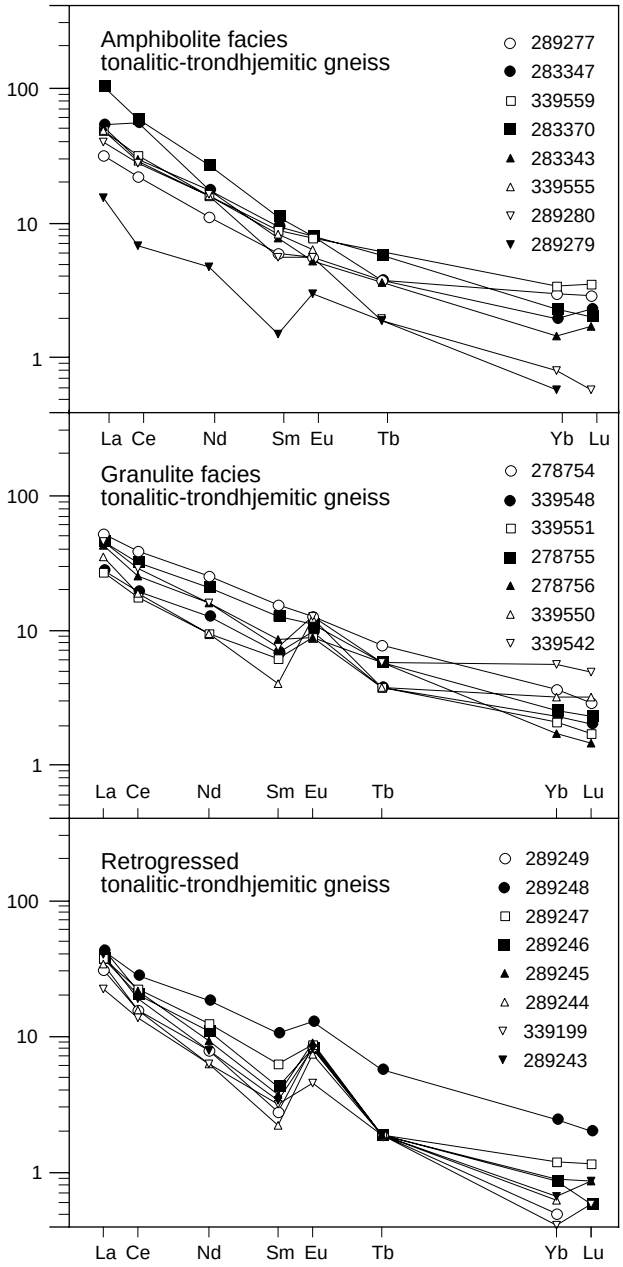

Fig. 62. Chondrite-normalised REE diagrams (Nakamura, 1974) of tonalitic-trondhjemitic grey gneiss, Fiskefjord area. All elements analysed by INNA (see Appendix). Locations of samples in Fig. 53.

alkaline suites (e.g. review by Tarney & Jones, 1994). The spider diagrams from the Fiskefjord area also bring out the low concentrations of all LIL elements in granulite facies gneiss, and show the very variable concentrations of most LIL elements and high concentrations of Sr and Ba in the retrogressed gneiss.

Chondrite-normalised REE diagrams (Fig. 62) show strong fractionation. In all three groups of tonalitic-trondhjemitic gneiss the LREE are strongly enriched, whereas HREE concentrations are close to chondrite values (average LaN/YbN values for amphibolite facies, granulite facies, and retrogressed gneiss are 27.3, 12.8 and 38.9, respectively). Y is also low (Fig. 60); this pattern is typical for most Archaean TTG suites but less common in younger calc-alkaline orogenic granitoids. All analysed samples of retrogressed gneiss have a dis-

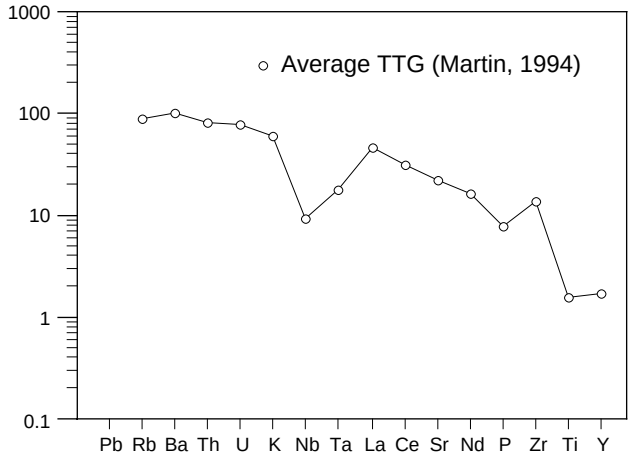

Fig. 63. Mantle-normalised spider diagram of average Archaean TTG (Martin, 1994) for comparison with grey gneiss (Fig. 61) and the Finnefjeld and Taserssuaq complexes (Fig. 71).

tinct positive Eu anomaly, which appears to be less common in the two other groups

Mineral chemistry

Representative microprobe analyses of mafic minerals and feldspars from three metamorphic groups of grey gneiss are shown in Tables 3 and 4, and Table 5 shows similar analyses from the Qugssuk granite. The granite may be considered equivalent to amphibolite facies grey gneiss in terms of the relationships between mineral compositions and metamorphic facies. Systematic variations in the compositions of amphibole and biotite, especially TiO_2, Al^{iv}, Na and K in amphibole, and TiO_2 in biotite, show that retrogression occurred under very variable (amphibolite facies) temperature and pressure

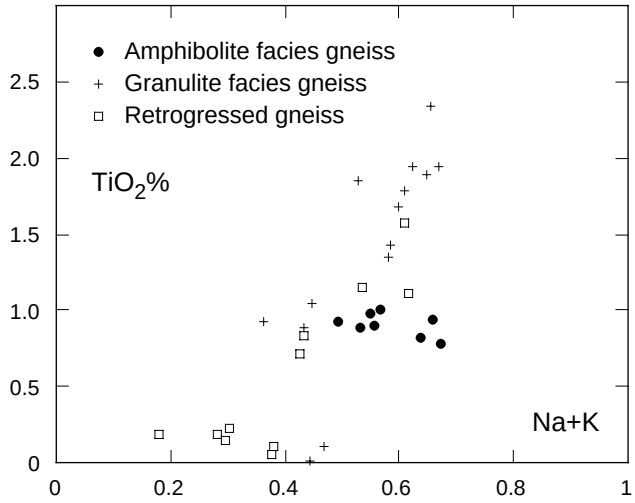

Fig. 64. TiO_2 plotted against Na + K in hornblende and actinolitic hornblende from amphibolite facies, granulite facies, and retrogressed grey gneiss. Amphiboles from retrogressed gneiss have a large range of TiO_2 and Na + K contents, which in part overlap with those of amphibolite and granulite facies hornblendes. The data may suggest two different events of retrogression. See Table 3 for analytical details.

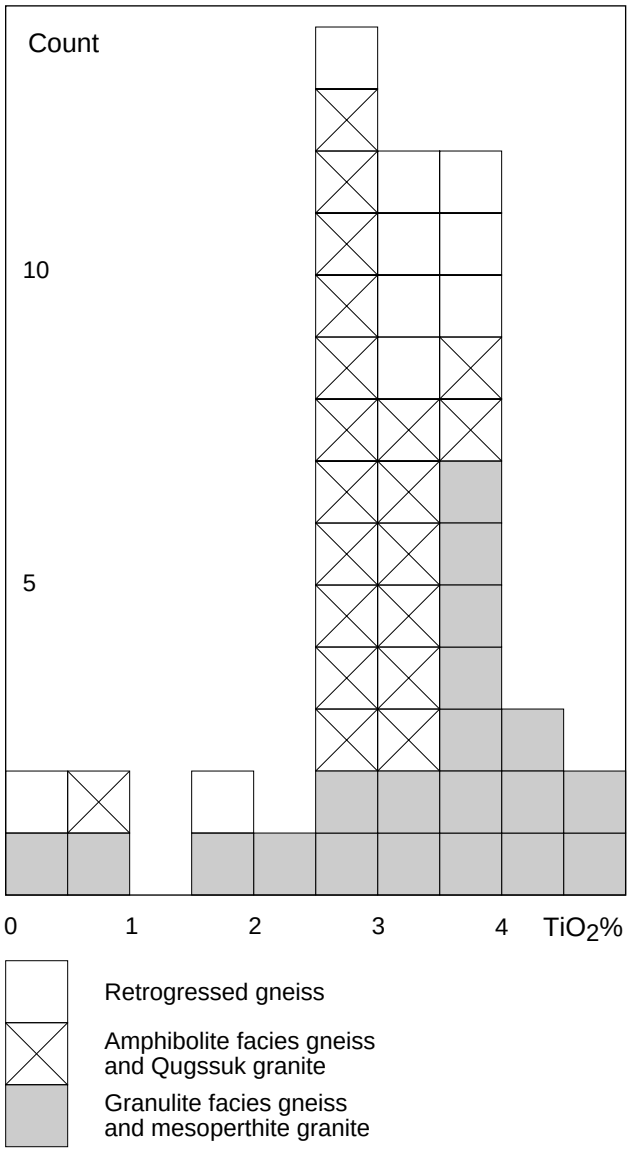

Fig. 65. Distribution of TiO_2 contents in biotites from amphibolite facies grey gneiss and granite, granulite facies grey gneiss and mesoperthite granite, and retrogressed grey gneiss. Note that many biotite grains in retrogressed gneiss have relatively high TiO_2 contents (also these grains being sheaf-like and retrograde), and that amphibolite and granulite facies gneiss may also contain a few biotite grains with very low TiO_2 contents; the latter are small secondary grains which were probably formed during late retrogression. See Table 3 for analytical details.

Table 3. Representative mineral compositions, amphibolite and granulite facies grey gneiss

GGU	Amphibolite facies							Granulite facies										
No	289272	289276	289277	289272	289276	289272	289276	278738	278738	278756	278738	278754	278756	278754	278754	278738	278754	278756
Mineral	bt 7-10	bt 28-36	bt 71-73	hbl 11-12	hbl 18-27	pl 17-18	pl 7-10	bt 25	bts 19-20	bt 11+14	hbl 58-60	hbl 35-38	hbl 19-22	opx 39-42	cpx 43-46	pl 14	pl 31-34	pl 7-10
SiO_2	36.76	36.68	36.14	44.38	44.26	60.13	59.26	35.47	36.46	37.16	43.50	43.40	43.59	52.41	51.97	59.95	60.39	60.91
TiO_2	2.60	3.25	2.67	0.89	1.00	0.01	0.01	3.78	3.01	3.24	1.95	1.89	2.34	0.07	0.19	n.d.	0.12	0.02
Al_2O_3	15.43	15.11	16.61	9.92	10.28	24.04	24.41	15.31	15.44	15.69	10.40	10.07	10.02	0.88	1.86	25.04	24.83	24.43
FeO	18.18	18.55	18.65	16.54	16.69	0.05	0.05	19.09	17.47	17.37	16.45	14.98	15.89	25.76	10.70	0.06	0.08	0.15
MnO	0.27	0.24	0.26	0.38	0.38			0.02	0.11	0.02	0.11	0.17	0.15	0.74	0.37			
MgO	11.98	11.81	10.48	10.52	10.56	0.03	0.03	11.06	13.08	12.18	10.52	11.53	11.04	19.50	12.53	n.d.	0.01	0.09
CaO	0.02	0.02	0.04	11.88	11.99	6.39	6.65	0.08	n.d.	0.08	11.47	11.91	11.76	0.65	22.11	6.36	7.06	6.44
Na_2O	0.25	0.02	0.08	1.11	1.24	8.00	7.45	0.06	0.06	0.02	1.26	1.33	1.43	n.d.	0.61	7.92	7.53	7.62
K_2O	9.39	9.64	9.53	1.08	1.10	0.23	0.23	9.55	9.73	9.35	1.34	1.36	1.27	n.d.	n.d.	0.38	0.49	0.60
Cl	0.03	0.02	0.03					n.d.	n.d.	0.05								
Sum	94.91	95.34	94.49	96.70	97.50	98.88	98.09	94.42	95.36	95.16	97.00	96.64	97.49	100.01	100.34	99.71	100.51	100.26
Ofor Cl	0.01	0.01	0.01					0.00	0.00	0.01								
FeO′				13.65	13.78						13.39	12.80	13.73	25.76	8.47			
Fe_2O_3′				3.21	3.23						3.40	2.42	2.40	0.00	2.48			
Sum′	94.90	95.33	94.48	97.02	97.82			94.42	95.36	95.15	97.34	96.88	97.73	100.01	100.59			
Ba	2000	3000		160	190	120	270	8200	2000	7400	380	340	350	60	115	580	350	590
Sr	n.d.	n.d.		n.d.	n.d.	500	650	n.d.	n.d.	n.d.	n.d.	n.d.	n.d.	n.d.	n.d.	830	630	590
Rb	790	610		n.d.	n.d.	n.d.	n.d.	n.d.	n.d.	190	n.d.	n.d.	n.d.	n.d.	n.d.	n.d.	n.d.	n.d.
Si	2.80	2.79	2.78	6.67	6.60	2.71	2.69	2.74	2.76	2.81	6.52	6.52	6.51	1.99	1.94	2.68	2.68	2.71
Al	1.39	1.36	1.50	1.76	1.81	1.28	1.31	1.39	1.38	1.40	1.84	1.78	1.76	0.04	0.08	1.32	1.30	1.28
Ti	0.15	0.19	0.15	0.10	0.11	0.00	0.00	0.22	0.17	0.18	0.22	0.21	0.26	0.00	0.01	0.00	0.00	0.00
Fe^{2+}	1.16	1.18	1.20	1.71	1.72	0.00	0.00	1.23	1.11	1.10	1.68	1.61	1.71	0.82	0.26	0.00	0.00	0.01
Fe^{3+}				0.37	0.37						0.38	0.27	0.27	0.00	0.07			
Mn	0.02	0.02	0.02	0.05	0.05			0.00	0.01	0.00	0.01	0.02	0.02	0.02	0.01			
Mg	1.36	1.34	1.20	2.35	2.35	0.00	0.00	1.27	1.48	1.37	2.35	2.58	2.46	1.10	0.70	0.00	0.00	0.01
Ca	0.00	0.00	0.00	1.91	1.92	0.31	0.32	0.01	0.00	0.01	1.84	1.92	1.88	0.03	0.88	0.30	0.34	0.31
Na	0.04	0.00	0.01	0.32	0.36	0.70	0.66	0.01	0.01	0.00	0.37	0.39	0.41	0.00	0.04	0.69	0.65	0.66
K	0.91	0.94	0.93	0.21	0.21	0.01	0.01	0.94	0.94	0.90	0.26	0.26	0.24	0.00	0.00	0.02	0.03	0.03
Cl	0.00	0.00	0.00					0.00	0.00	0.01								
Sum	7.83	7.81	7.79	15.44	15.48	5.01	4.99	7.82	7.85	7.76	15.46	15.56	15.54	4.00	4.00	5.01	5.00	5.00
Charge	2.47	2.48	2.39	23	23	8	8	2.37	2.42	2.43	23	23	23	6	6	8	8	8
A+B pos				2.44	2.48						2.46	2.56	2.54					
Or						1.27	1.31									2.14	2.74	3.41
Ab						68.53	66.13									67.79	64.08	65.85
An						30.20	32.56									30.07	33.18	30.74

n.d.=not detected

Locations of samples are shown in Fig. 53. The microprobe analyses were carried out on the Jeol 733 Superprobe at the Geological Institute, University of Copenhagen. For major elements the probe was operated at 15 kV and 15 nA with a slightly defocused beam, using crystal spectrometers for data collection. Natural silicates and oxides of end-member compositions were used as standards, and an on-line ZAF computer programme employed for data reduction. See Table 6 for analytical details regarding Ba, Sr and Rb.

Table 4. Representative mineral compositions, retrogressed grey gneiss

GGU	Retrogressed													
No	278751	278774	278815	289241	289241	278774	278815	289241	278774	289241	278751	278774	278815	289241
Mineral	bt 37	bt 10-11	bt 51-62	bt 57-64	bts 36-39	hbl 14-15	hbl 55-66	hbl 40-47	am 12-13	am 50-56	pl 35	pl 8-9	pl 47-50	pl 65-66
SiO_2	36.65	36.49	36.53	36.63	36.73	44.27	43.58	45.90	45.04	45.93	60.70	61.23	61.70	60.81
TiO_2	3.88	3.28	2.59	1.90	0.47	1.15	1.11	0.06	0.71	0.10	n.d.	n.d.	0.03	0.02
Al_2O_3	16.70	15.60	15.74	16.71	17.04	10.17	10.23	8.97	10.16	9.29	24.75	24.47	23.95	24.04
FeO	17.50	18.20	19.07	17.94	16.60	18.32	19.00	16.50	17.00	16.68	0.06	0.16	0.05	0.10
MnO	0.16	0.14	0.23	0.22	0.17	0.24	0.44	0.42	0.28	0.45				
MgO	10.89	11.56	11.19	11.56	12.73	10.56	9.51	11.54	11.07	11.27	n.d.	n.d.	0.02	0.02
CaO	n.d.	n.d.	n.d.	0.02	0.02	12.01	11.86	11.94	12.20	12.09	6.22	6.06	5.35	6.12
Na_2O	0.03	0.09	0.04	0.05	0.03	1.30	1.35	0.88	0.96	0.87	7.89	8.42	8.58	7.89
K_2O	9.69	9.50	9.65	9.47	9.29	0.87	1.17	0.66	0.81	0.70	0.22	0.54	0.19	0.19
Cl	n.d.	n.d.	0.05	0.08	0.04									
Sum	95.50	94.86	95.09	94.58	93.12	98.89	98.25	96.87	98.23	97.38	99.84	100.88	99.87	99.19
Ofor Cl	0.00	0.00	0.01	0.02	0.01									
FeO′						13.10	15.05	11.01	12.20	11.82				
Fe_2O_3′						5.81	4.40	6.10	5.33	5.40				
Sum′	95.50	94.86	95.08	94.56	93.11	99.47	98.69	97.48	98.76	97.92				
Ba	10300	7460	2800	4180	2130	290	170	140			530	250	170	300
Sr	n.d.	n.d.	n.d.	n.d.	n.d.	n.d.	n.d.	n.d.			610	780	750	1090
Rb	370	80	320	150	n.d.	n.d.	n.d.	n.d.			n.d.	n.d.	n.d.	n.d.
Si	2.76	2.78	2.80	2.79	2.82	6.51	6.52	6.79	6.62	6.78	2.70	2.71	2.74	2.72
Al	1.48	1.40	1.42	1.50	1.54	1.76	1.80	1.56	1.76	1.62	1.30	1.28	1.25	1.27
Ti	0.22	0.19	0.15	0.11	0.03	0.13	0.13	0.01	0.08	0.01	0.00	0.00	0.00	0.00
Fe^{2+}	1.10	1.16	1.22	1.15	1.07	1.61	1.88	1.36	1.50	1.46	0.00	0.01	0.00	0.00
Fe^{3+}						0.64	0.50	0.68	0.59	0.60				
Mn	0.01	0.01	0.02	0.01	0.01	0.03	0.06	0.05	0.04	0.06				
Mg	1.23	1.32	1.28	1.31	1.46	2.32	2.12	2.54	2.43	2.48	0.00	0.00	0.00	0.00
Ca	0.00	0.00	0.00	0.00	0.00	1.89	1.90	1.89	1.92	1.91	0.30	0.29	0.26	0.29
Na	0.00	0.01	0.01	0.01	0.00	0.37	0.39	0.25	0.27	0.25	0.68	0.72	0.74	0.69
K	0.93	0.92	0.94	0.92	0.91	0.16	0.22	0.13	0.15	0.13	0.01	0.03	0.01	0.01
Cl	0.00	0.00	0.01	0.01	0.01									
Sum	7.74	7.80	7.82	7.81	7.84	15.43	15.51	15.27	15.34	15.29	4.99	5.03	5.01	4.99
Charge	2.43	2.40	2.39	2.47	2.45	23	23	23	23	23	8	8	8	8
A+B pos						2.43	2.51	2.27	2.34	2.29				
Or											1.26	2.93	1.07	1.11
Ab											68.79	69.46	73.59	69.19
An											29.95	27.61	25.34	29.70

n.d.=not detected

Locations of samples are shown in Fig. 53. See Tables 3 and 6 for analytical details.

conditions. In Fig. 64 TiO_2 is plotted against Na + K (A position) in amphiboles, and TiO_2 contents of biotites are shown in Fig. 65. Biotite and hornblende in textural equilibrium with hypersthene (in granulite facies gneiss) are the most TiO_2-rich, biotite and hornblende in amphibolite facies gneiss have intermediate TiO_2 contents, and retrograde amphibole and biotite grains (in retrogressed gneiss) have variably intermediate to very low TiO_2 contents. Occasionally two successive phases of retrograde biotite were observed in the same rock, such as in sample 289241 NW of Qugssuk (Fig. 53) where a majority of brown biotite with intermediate TiO_2 contents forms large sheaves, and occasional greenish biotite almost devoid of TiO_2 forms small interstitial flakes (Table 4). A few secondary biotite grains with very low TiO_2 contents have also been found in amphibolite and granulite facies rocks (Fig. 65). Some clearly retrograde, sheaf-like biotite aggregates and spongy amphibole grains have titanium or Al^{iv}-alkali element compositions which overlap with those of biotite and amphibole in amphibolite facies gneiss not retrogressed from granulite facies, suggesting that part of the retrogression in, e.g. sample 289241, took place at intermediate to upper amphibolite facies conditions. However, the large compositional variations of retrograde biotite and amphibole in the retrogressed gneiss

Table 5. Representative mineral compositions, Qugssuk granite

GGU No	278786	278797	278797	278808	278786	278797	278808	278786	278786	278797	278808
Mineral	bt 23-27	bt 62	bts 64-67	bt 99-101	Kfs 31	Kfs 72-73	Kfs 95	pl 29	pl rim32	pl 68-69	pl 96-98
SiO_2	36.88	36.56	37.43	36.90	64.79	64.44	64.39	64.05	68.31	63.45	63.23
TiO_2	2.95	2.78	0.62	3.25	0.07	0.07	0.05	0.05	0.04	n.d.	n.d.
Al_2O_3	16.08	16.87	17.34	17.48	17.81	17.73	18.37	22.95	18.93	23.03	23.09
FeO	18.71	19.65	16.74	18.73	n.d.	0.03	0.05	0.05	n.d.	0.02	0.06
MnO	0.25	0.26	0.21	0.12							
MgO	10.50	10.37	11.87	9.98	n.d.	n.d.	n.d.	n.d.	0.02	n.d.	n.d.
CaO	n.d.	0.04	0.01	n.d.	n.d.	n.d.	n.d.	4.24	0.59	4.68	4.72
Na_2O	0.05	0.04	0.05	n.d.	0.67	0.79	0.60	9.49	11.59	9.13	9.13
K_2O	9.84	10.01	9.63	9.81	15.95	15.76	15.65	0.21	0.10	0.15	0.36
Sum	95.26	96.58	93.90	96.27	99.29	98.82	99.11	101.04	99.58	100.46	100.59
Ba	600	1010	470	1740	2920	4860	7480	n.d.	n.d.	140	120
Sr	n.d.	n.d.	n.d.	n.d.	260	340	530	210	n.d.	240	420
Rb	920	410	390	510	330	130	170	n.d.	n.d.	n.d.	n.d.
Si	2.81	2.76	2.85	2.77	3.01	3.01	3.00	2.81	3.00	2.80	2.79
Al	1.44	1.50	1.56	1.55	0.98	0.98	1.01	1.18	0.98	1.20	1.20
Ti	0.17	0.16	0.04	0.18	0.00	0.00	0.00	0.00	0.00	0.00	0.00
Fe^{2+}	1.19	1.24	1.07	1.18	0.00	0.00	0.00	0.00	0.00	0.00	0.00
Fe^{3+}											
Mn	0.02	0.02	0.01	0.01							
Mg	1.19	1.17	1.35	1.12	0.00	0.00	0.00	0.00	0.00	0.00	0.00
Ca	0.00	0.00	0.00	0.00	0.00	0.00	0.00	0.20	0.03	0.22	0.22
Na	0.01	0.01	0.01	0.00	0.06	0.07	0.05	0.81	0.99	0.78	0.78
K	0.96	0.96	0.93	0.94	0.95	0.94	0.93	0.01	0.01	0.01	0.02
Sum	7.78	7.82	7.81	7.74	5.00	5.00	4.99	5.01	5.00	5.00	5.01
Charge	2.41	2.43	2.41	2.44	8	8	8	8	8	8	8
A+B pos											
Or					94.00	92.92	94.49	1.15	0.55	0.84	1.98
Ab					6.01	7.08	5.51	79.28	96.73	77.29	76.25
An					0.00	0.00	0.00	19.56	2.72	21.88	21.77

n.d.=not detected

Sample locations shown in Fig. 68. See Tables 3 and 6 for analytical details.

may suggest prolonged retrogression during a long period of cooling, or that more than one episode of retrogression took place, as is also indicated by the presence of small biotite grains with low TiO_2 contents in amphibolite and granulite facies gneiss.

Table 6 summarises microprobe analyses of Ba, Sr and Rb and TiO_2 in various minerals from the three metamorphic groups of grey gneiss and a sample of Qugssuk granite. Insofar as Ba, Sr and Rb do not form their own mineral phases in the grey gneiss or granite, their absolute concentrations in the analysed minerals are obviously related to whole rock compositions. More importantly the analyses provide information about Ba, Sr and Rb distributions between coexisting minerals and the different metamorphic groups. Ba preferentially occurs in K-feldspar (*c.* 3000–12000 ppm), but also in biotite (*c.* 2000–8000 ppm); amphibole and plagioclase may contain up to *c.* 600 ppm Ba. Sr is located in feldspars (300–1100 ppm); the Sr content of plagioclase is approximately similar in the three facies groups. Rb preferentially occurs in biotite (up to *c.* 900 ppm in amphibolite facies biotite of grey gneiss and Qugssuk granite, 150 ppm in retrograde biotite), but is notably below the detection limit of 70 ppm in granulite facies, high-titanium biotite, and also low in late secondary biotite grains (sample 289241).

Mineral reactions and movement of granitic melts or fluids during prograde and retrograde metamorphic events are prone to have affected the distributions of Ba, Sr and Rb in different ways. As shown above Ba and Rb are especially accommodated in biotite and K-feldspar (although in different proportions). Prograde

Table 6. Ba, Sr, Rb and TiO_2 contents of minerals from orthogneisses in different metamorphic facies and Qugssuk granite

		Ba ppm	Sr ppm	Rb ppm	TiO_2%
Detection limit (microprobe)		45	100	70	0.01
Amphibolite facies orthogneiss					
289272	Whole rock	444	286	74	0.57
	Biotite	2000	n.d.	790	2.60
	K-feldspar	12100	440	175	
	Plagioclase	120	500	n.d.	
	Hornblende	160	n.d.	n.d.	0.89
Granulite facies orthogneiss					
278738	Whole rock	444	568	2	0.55
	Biotite	8200	n.d.	n.d.	3.78
	Biotite (late)	2000	n.d.	n.d.	3.01
	Plagioclase	580	830	n.d.	
	Hornblende	380	n.d.	n.d.	1.95
Retrogressed orthogneiss					
278774	Whole rock	811	549	19	0.61
	Biotite	7300	n.d.	80	3.28
	Plagioclase	250	780	n.d.	
	Hornblende	290	n.d.	n.d.	1.15
289241	Whole rock	383	668	1	0.36
	Biotite	4180	n.d.	150	1.90
	Biotite (late)	2130	n.d.	n.d.	0.47
	Plagioclase	300	1090	n.d.	
	Hornblende	140	n.d.	n.d.	0.06
Qugssuk granite					
278786	Whole rock	777	146	135	0.10
	Biotite	600	n.d.	920	2.95
	K-feldspar	2920	260	330	
	Plagioclase	n.d.	210	n.d.	

n.d.=not detected

See discussion in the main text.
Analytical procedure: Ba, Sr and Rb were analysed with the instrument described in the text to Table 3, operated at 25 kV with a beam current of 300 nA, beam diameter *c.* 40 µ. In order to minimise volatilisation due to the high beam current and long counting times necessary for sufficient signal intensity, an automatic step procedure was employed during the measurement. Each figure quoted for Ba, Sr or Rb is averaged from one or a few groups of six measurements, each consisting of four adjacent points, and representing total counting times of 240 and 480 seconds at peak and background positions. Under these analytical conditions the calculated lower limits of detection were 45, 100, and 70 ppm (2σ) for Ba, Sr and Rb, respectively. Baryte, strontianite, and rubidium chloride were used as standards, with ZAF corrections as above. A silica glass standard was used as blank for Sr and Rb. Ba contents were empirically corrected for interference by Ti-Kα, where 1% TiO_2 gave an apparent concentration of 40 ppm BaO. Microprobe measurements on leucite and sanidine from Italy using similar analytical conditions agree well with PIXE measurements using separates of the same minerals (J. Rønsbo, personal communication, 1989).

granulite facies metamorphism with partial melting, consumption of K-feldspar and removal of a melt fraction can therefore be expected to have strongly influenced the Ba and Rb contents of remaining biotite (see p. 79). Plagioclase accommodates most of the Sr; mobility of Sr during prograde and retrograde metamorphism must therefore have been linked with recrystallisation of plagioclase.

Element distribution within retrogressed tonalitic-trondhjemitic gneiss in the central and northern parts of the Fiskefjord area

The observations that (a) the major element compositions of amphibolite facies, granulite facies, and retrogressed tonalitic-trondhjemitic gneiss are statistically different, (b) the dioritic grey gneiss comprises a geochemically and geographically distinct group with (amongst other characteristics) very high Sr and Ba contents around the peninsula Qeqertaussaq in central Fiskefjord, and (c) both Sr and Ba are among the most variable elements in the retrogressed tonalitic-trondhjemitic gneiss, together raise the questions as to whether the latter group was originally a geochemically homogeneous population, and hence which elements were actually affected by metasomatism during granulite facies and retrogressive metamorphic events.

The retrogressed gneiss is located in a wide intermediate zone between granulite facies and amphibolite facies areas and might therefore be expected to show geochemical variation of mobile elements that are related to sample location. This problem is difficult to handle with statistical methods alone, but can be addressed with element distribution maps; however, the stream sediment survey from this region undertaken by Steenfelt (1988) was not applicable due to low sample density and because the stream sediments include all rock types within their catchment areas.

Distribution maps of selected elements, based on rock samples of retrogressed gneiss from the northern part of the Fiskefjord area, are presented in Figs 66 and 67. Although the samples are not evenly distributed they provide a visual estimate of variations in the concentrations of the chosen elements. For each element three levels of concentration are shown, each comprising approximately one third of the samples (oxide concentrations of major elements have been retained to facilitate comparison with tables and variation diagrams).

Figure 66 shows geographical distributions of elements in the retrogressed tonalitic-trondhjemitic gneiss,

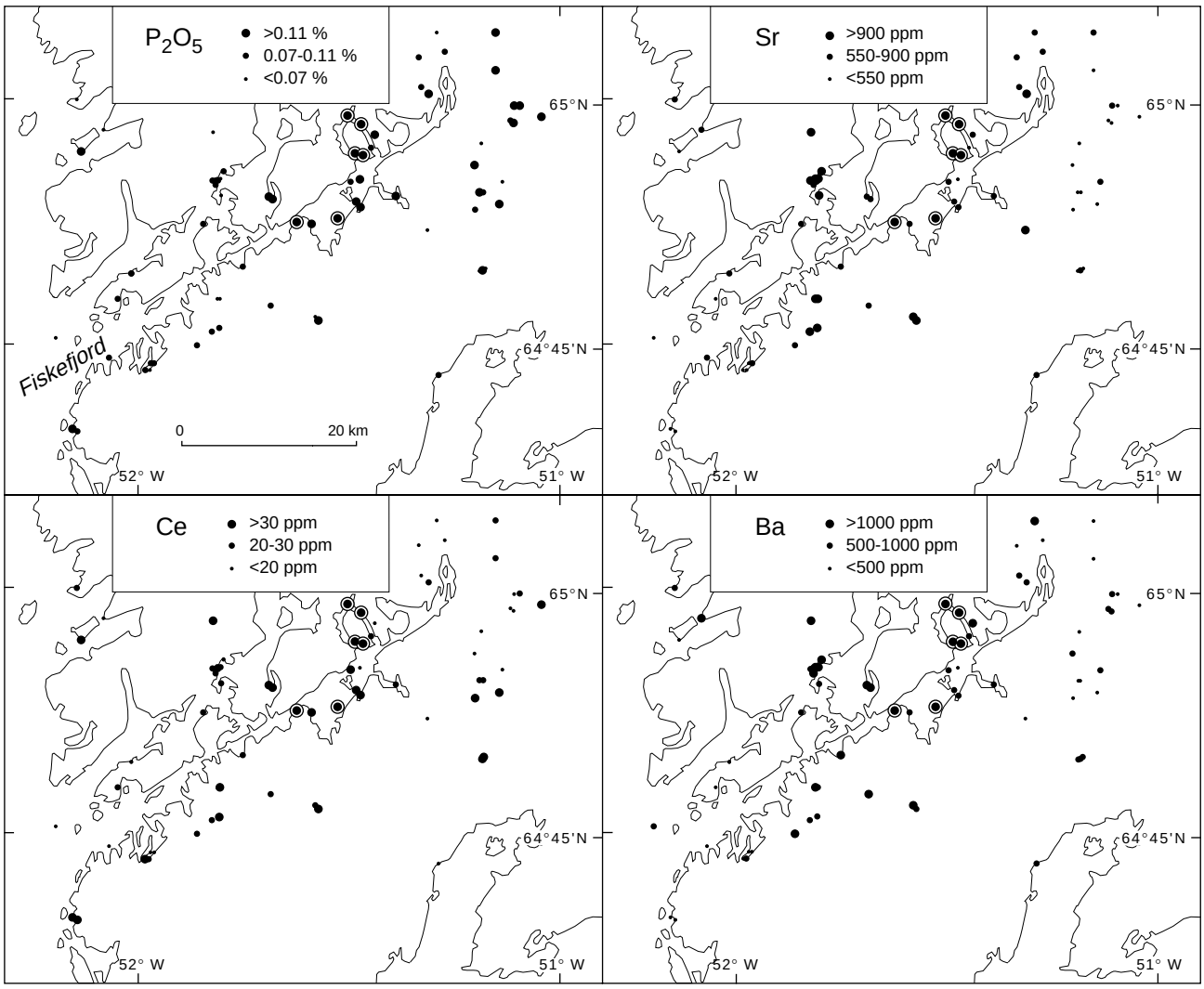

Fig. 66. Distributions of P_2O_5, Sr, Ba and Ce in rock samples of retrogressed tonalitic-trondhjemitic gneiss in the central and northern parts of the Fiskefjord area (oxide concentrations of major elements have been retained to facilitate comparison with tables and other figures). Enrichment of all four elements only occurs within the area of the Qeqertaussaq diorite (ringed samples), suggesting a genetic relationship rather than metamorphic effects in this area; see the main text for further discussion.

which are all strongly enriched in the Qeqertaussaq diorite. Only a few samples have high contents of all four elements (ringed, Fig. 66), all of which occur in the Qeqertaussaq area. Several high values of Sr and Ba also occur south of central Fiskefjord. Figure 67 shows the distributions of LIL elements which are all strongly depleted in granulite facies grey gneiss and very variable in retrogressed grey gneiss – although mostly significantly lower than in the adjacent amphibolite facies gneiss to the east (Appendixes 7, 8). Also these elements are relatively enriched in the samples correlated with the Qeqertaussaq diorite (ringed, Fig. 67). K and Rb, which display fairly similar patterns, are also high in the eastern part of the area, whereas Th has an erratic distribution. The Pb distribution resembles those of Sr and Ba (Fig. 66).

In summary, element distributions in retrogressed tonalitic-trondhjemitic gneiss around Fiskefjord suggest that a few samples in the Qeqertaussaq area, and only there, are geochemically related to the Qeqertaussaq diorite by virtue of a combination of high P, LREE, Sr, Ba, Pb, Rb and K. Moreover, Sr, Ba and Pb (and to some extent K) are concentrated in the central part of the area where retrogression is mostly pervasive. Rb and to some extent K increase eastward towards the area of amphibolite facies gneiss not affected by retrogression, whereas Th is erratic.

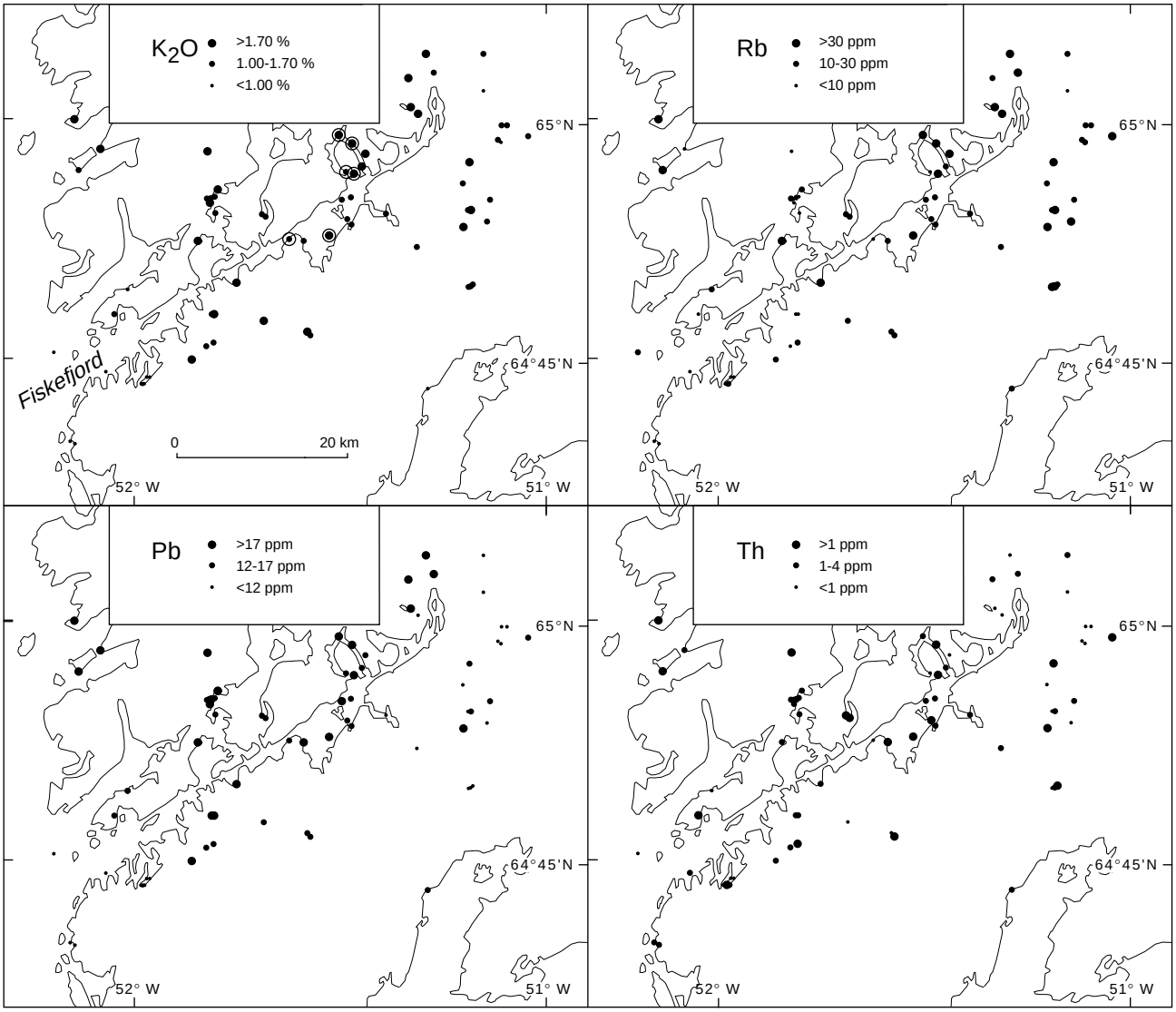

Fig. 67. Distributions of K_2O, Rb, Pb and Th in rock samples of retrogressed tonalitic-trondhjemitic gneiss in the central and northern parts of the Fiskefjord area. See discussion in the main text.

Finnefjeld gneiss and Taserssuaq tonalite complexes

The compositions of available samples from the southeastern parts of the Finnefjeld and Taserssuaq complexes, respectively (sample localities shown on Fig. 68), both largely resemble those of amphibolite facies grey gneiss (Appendix 9; Figs 69, 70). However, the compositions of available samples indicate some general differences between the two complexes. The variation trends of TiO_2, MgO and FeO against SiO_2 appear to be steeper for the Finnefjeld gneiss than for the Taserssuaq tonalite complex, whereas the opposite is the case for Al_2O_3 and CaO. In addition, the Taserssuaq tonalite complex comprises a relatively large granodioritic to granitic group and only a few trondhjemites, whereas the Finnefjeld gneiss complex mainly shows a trondhjemitic trend above 70% SiO_2. These features indicate that partial melting or crystal fractionation processes in the source regions of the two complexes were not identical; a possible interpretation is that plagioclase fractionation was more important in the evolution of the Taserssuaq tonalite than in in the case of the Finnefjeld gneiss complex (see p. 73).

Both complexes have somewhat variable trace element compositions, with increasing LIL element concentrations in the most acid rocks. The concentrations of LIL elements are never as low as in granulite facies

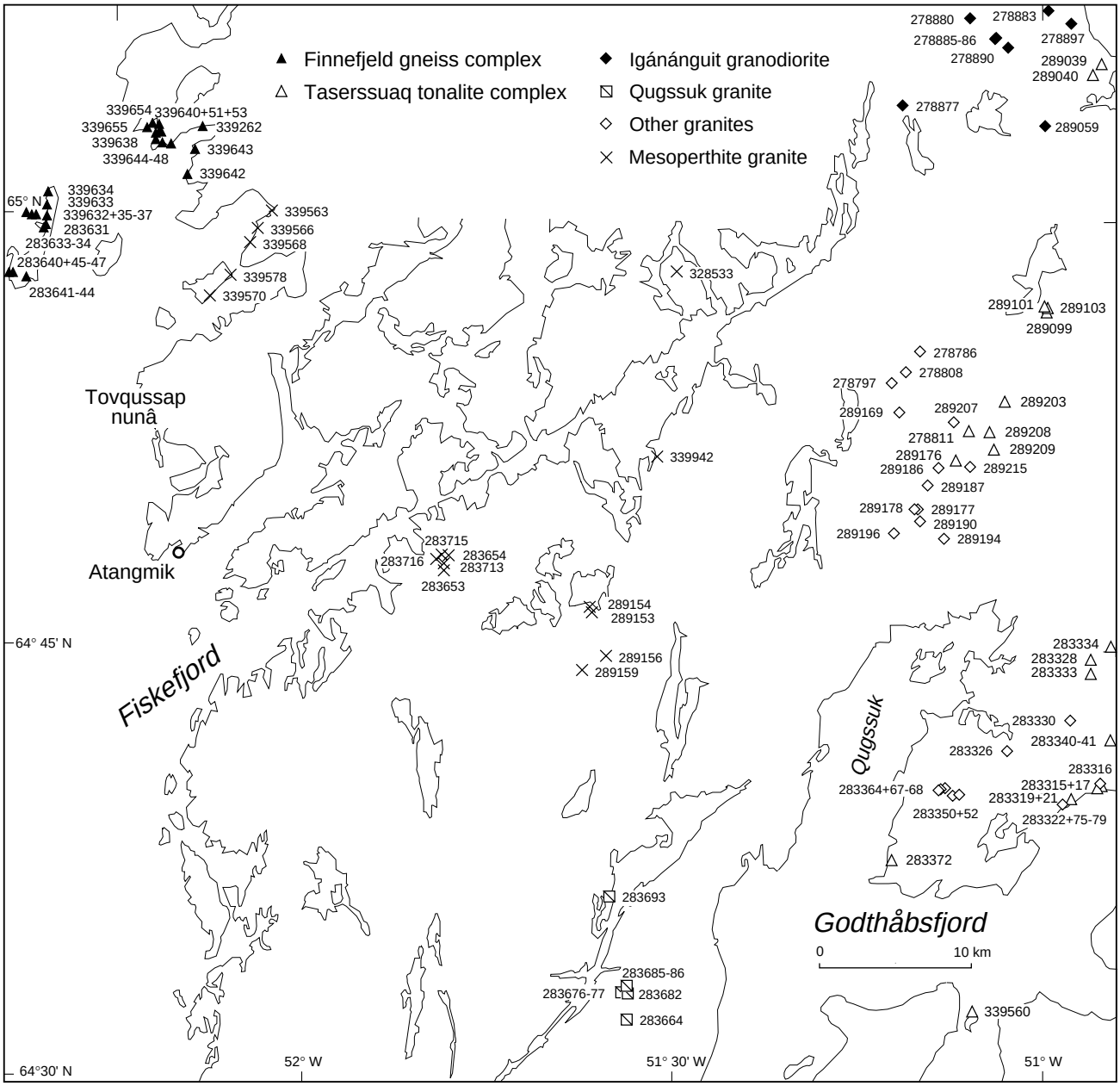

Fig. 68. Locations of analysed samples, Finnefjeld gneiss complex, Taserssuaq tonalite complex and granitic rocks. Five additional samples from the Taserssuaq tonalite complex were collected east of the map area.

grey gneiss, and the very high concentrations of e.g. Sr and Ba encountered in the retrogressed grey gneiss are only approached in a few samples.

Plotted on mantle-normalised spider diagrams (Fig. 71), representative samples from both complexes define clear patterns which are similar to 'average Archaean TTG' (Fig. 63) in general, and to Fiskefjord amphibolite facies grey gneiss in particular (Fig. 61). The patterns are fairly smooth, with high proportions and relatively small variations of the mobile incompatible (LIL) elements, and with clear negative Nb, Ta and Ti anomalies; however, Th and U are depleted in the Finnefjeld gneiss. Sample no. 289208 of Taserssuaq tonalite has very erratic concentrations of incompatible immobile elements and is very high in LIL elements, presumably due to metasomatism.

Also the REE patterns (Fig. 72) are comparable to those of amphibolite facies grey gneiss, with LREE enrichment, strongly fractionated curves, and some samples showing a positive Eu anomaly. Figs 71 and

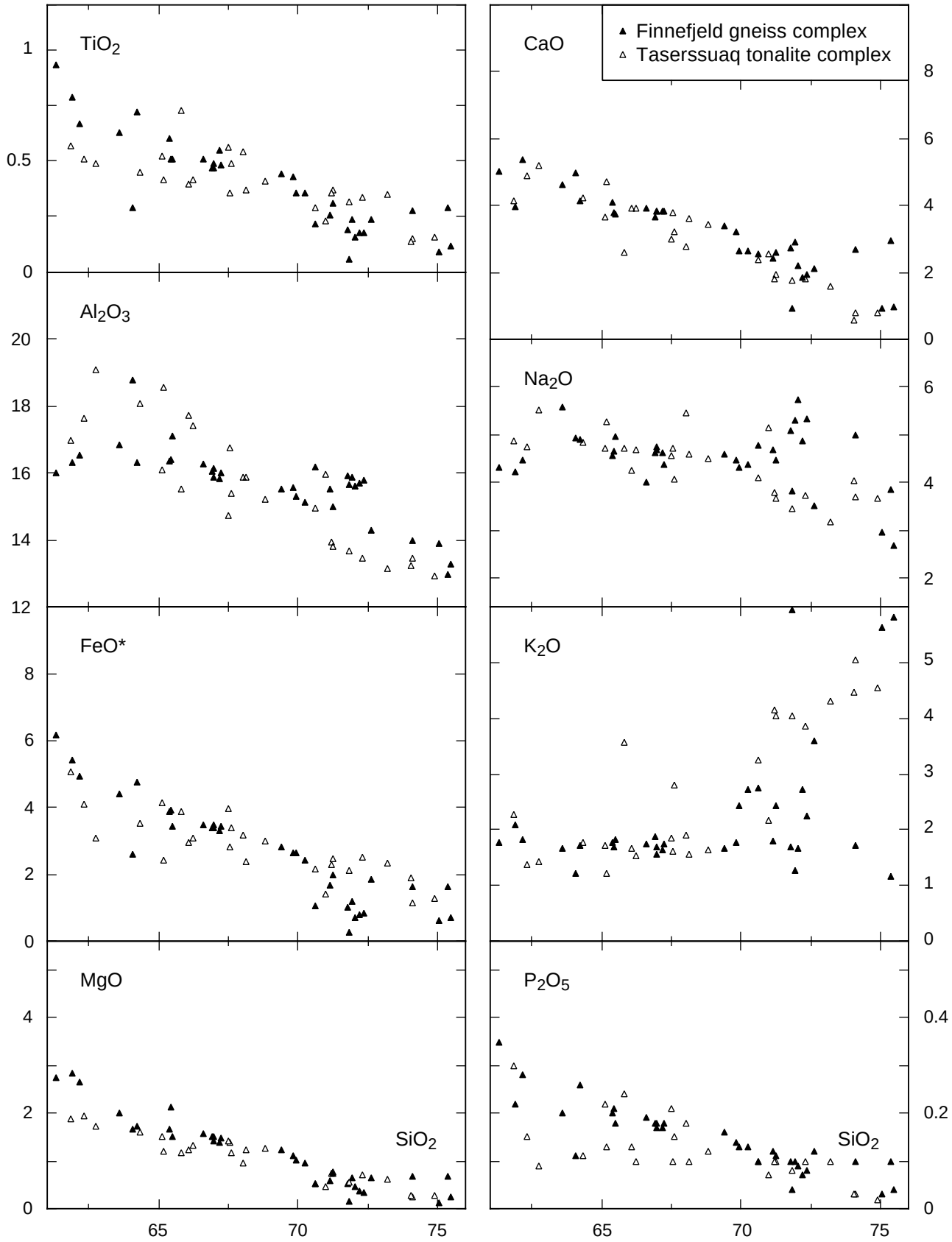

Fig. 69. Major element variation diagrams against SiO_2 (wt. %), Finnefjeld gneiss and Taserssuaq tonalite complexes, Fiskefjord area. See Appendix for analytical details. Sample localities shown in Fig. 68.

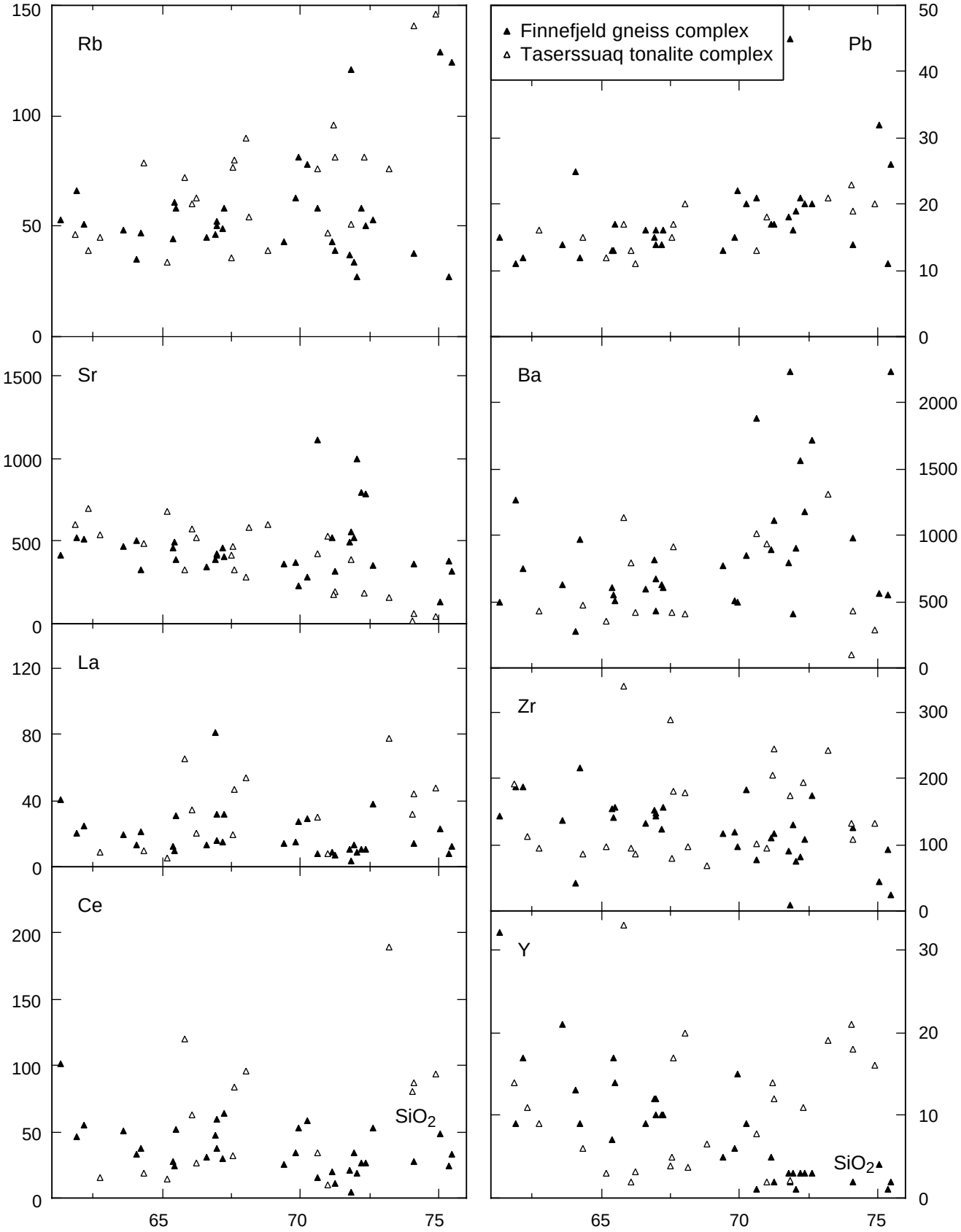

Fig. 70. Selected trace element variation diagrams against SiO_2 (in ppm and wt. %), Finnefjeld gneiss and Taserssuaq tonalite complexes. Analytical details in Appendix. Sample localities shown in Fig. 68.

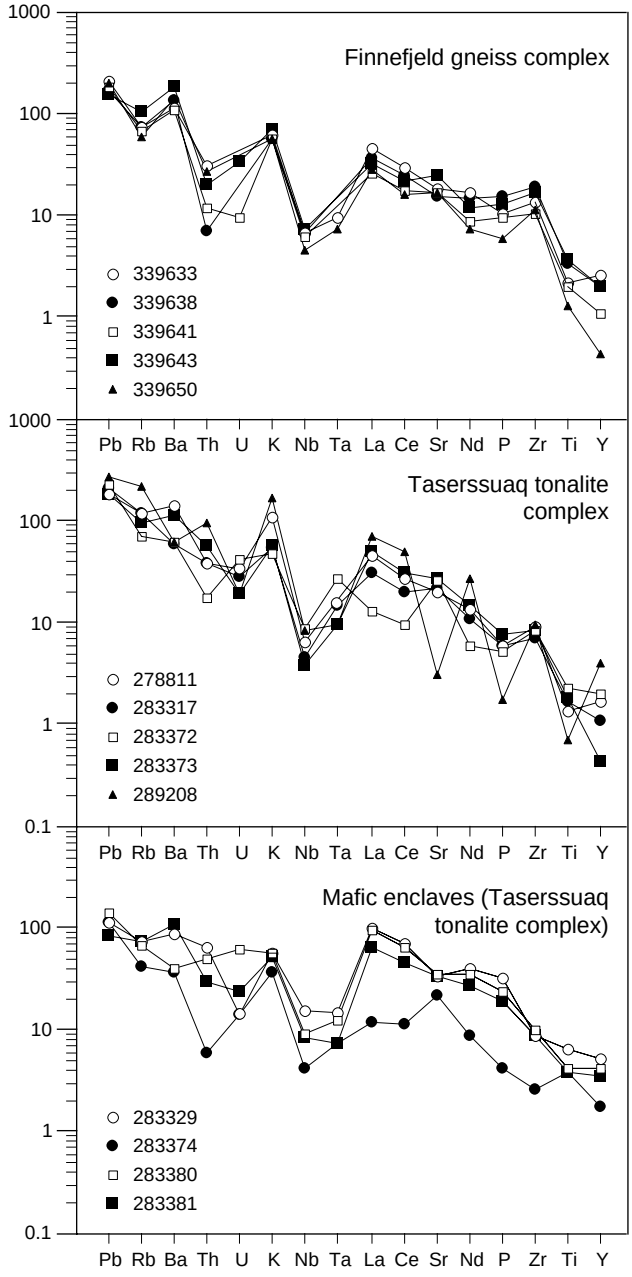

Fig. 71. Spider diagrams of Finnefjeld gneiss and Taserssuaq tonalite complexes, Fiskefjord area, normalised to primordial mantle (Sun & McDonough, 1989). XRF and INNA analyses, see Appendix. Sample localities shown in Fig. 68.

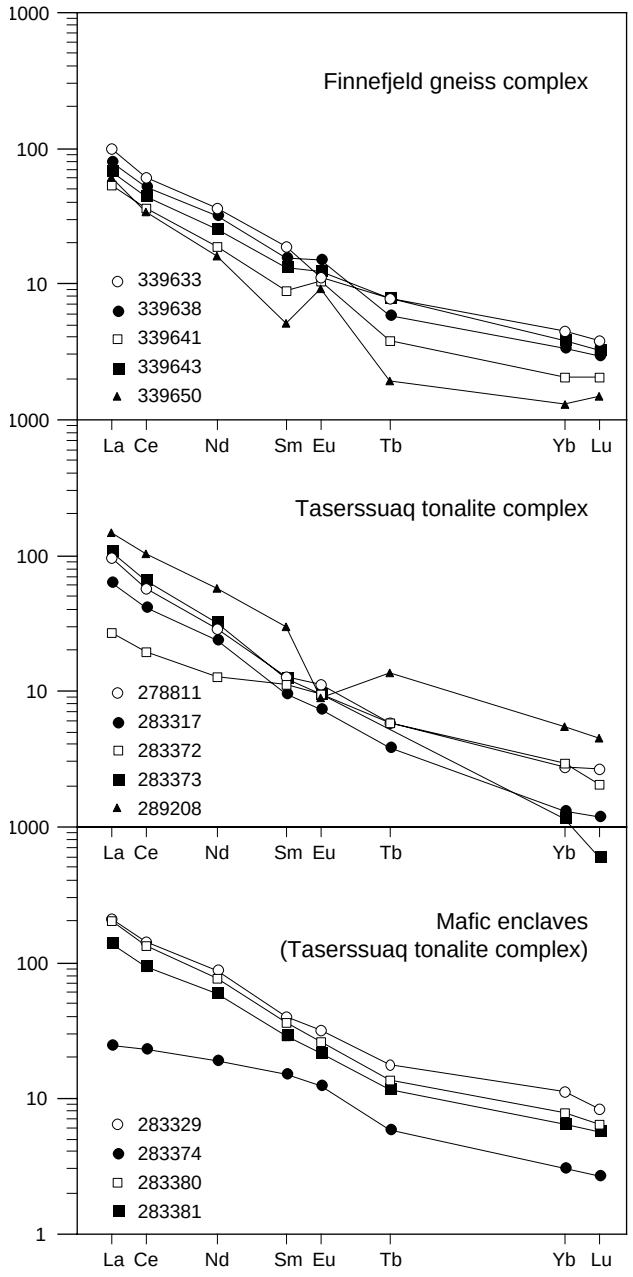

Fig. 72. Chondrite-normalised REE diagrams (Nakamura, 1974) of Finnefjeld gneiss and Taserssuaq tonalite complexes, Fiskefjord area. All elements analysed by INNA (see Appendix). Sample localities shown in Fig. 68.

72 include four hornblende- and plagioclase-rich dioritic to gabbroic enclaves collected in the southern part of the Taserssuaq tonalite complex (analyses in Appendix 9). The multi-element patterns of three of these samples resemble those of the Taserssuaq tonalite complex, except that they have higher REE and Y contents and slightly less fractionated REE spectra than the tonalite complex itself. Sample 283374 has an altogether different composition and lower REE contents combined with weak REE fractionation; it therefore appears not to be related to the complex and could be of supracrustal origin.

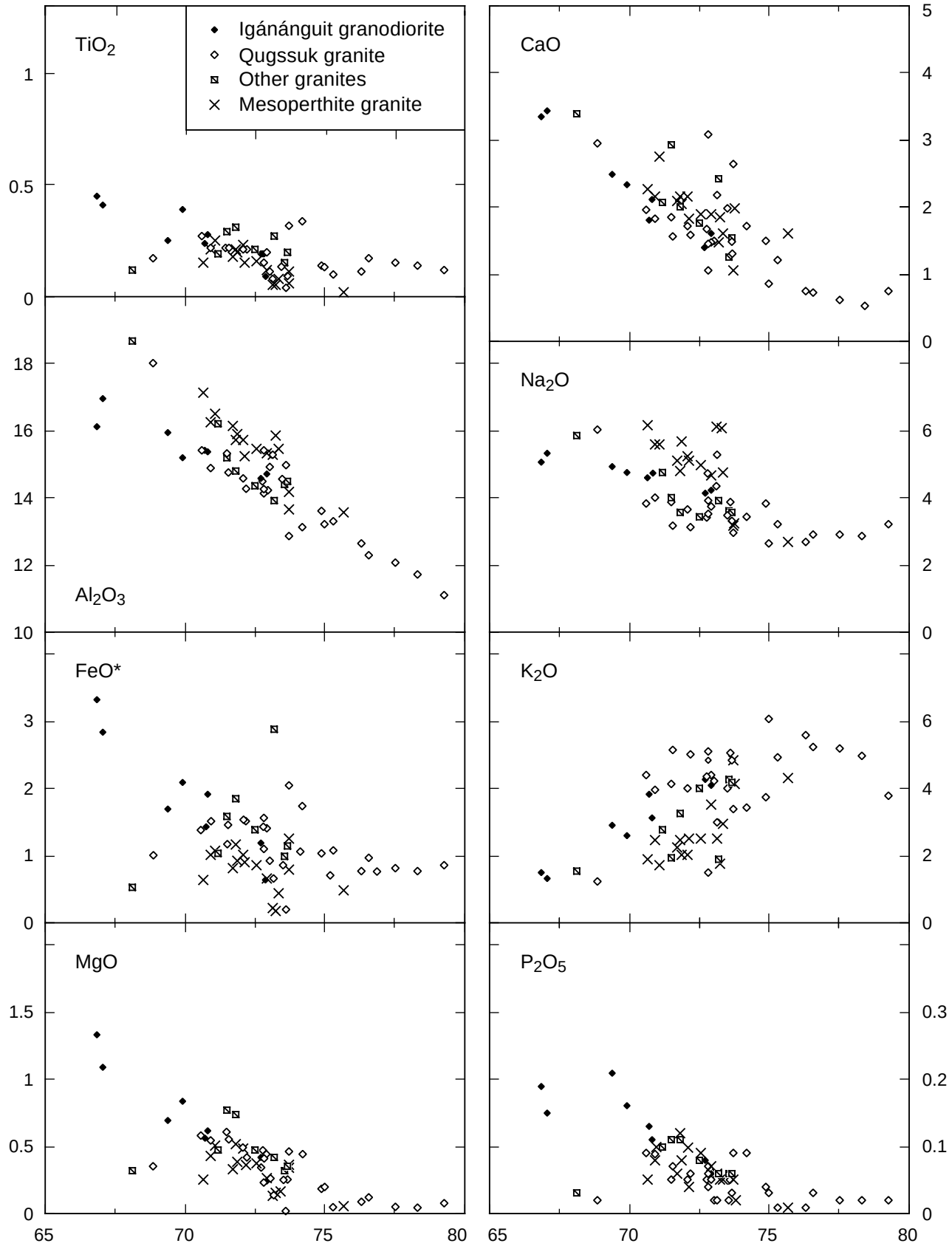

Fig. 73. Major element variation diagrams against SiO_2 (wt. %), granitic rocks, Fiskefjord area. See Appendix for analytical details. Sample localities shown in Fig. 68.

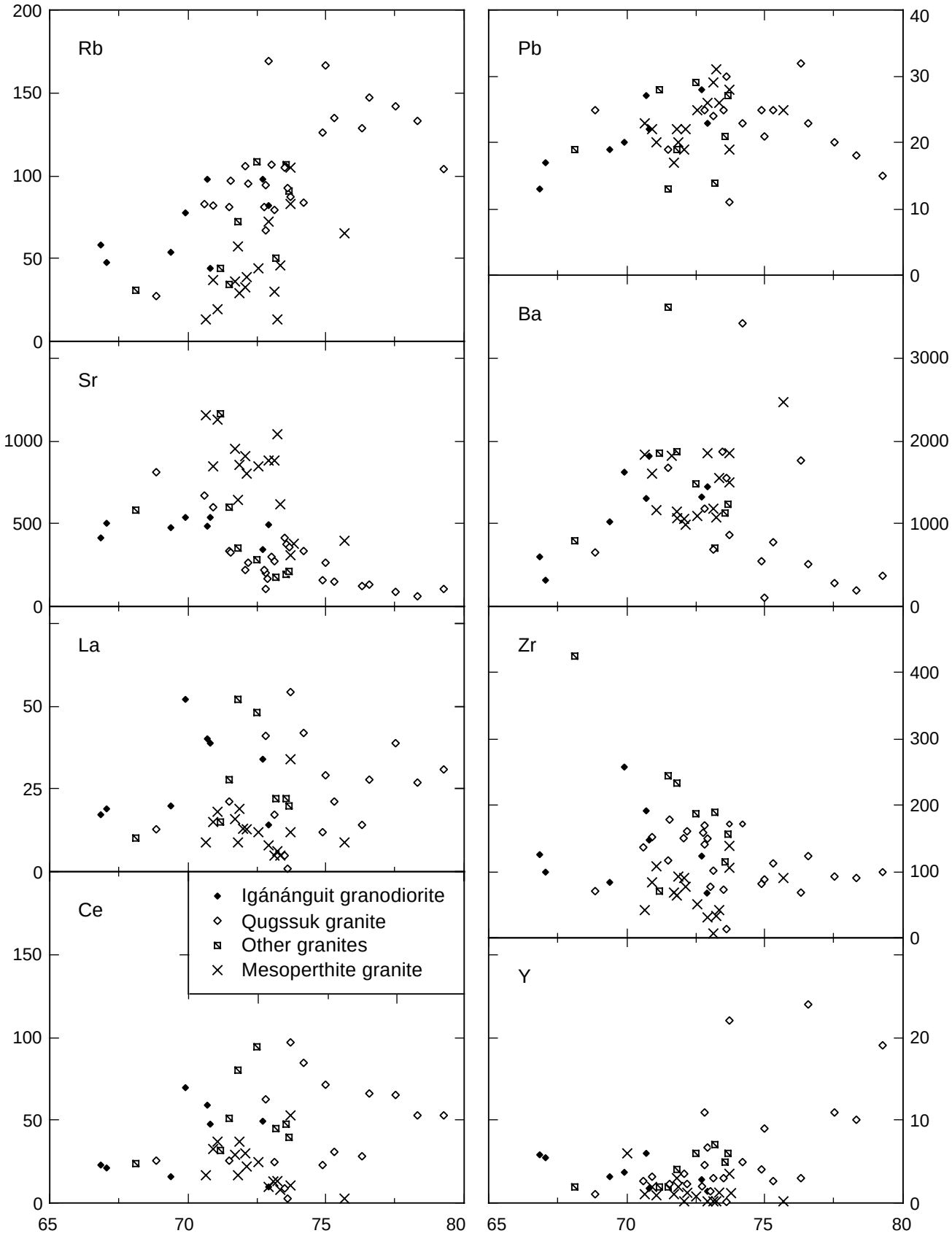

Fig. 74. Selected trace element variation diagrams against SiO_2 (in ppm and wt. %), granitic rocks, Fiskefjord area. See Appendix for analytical details. Sample localities shown in Fig. 68.

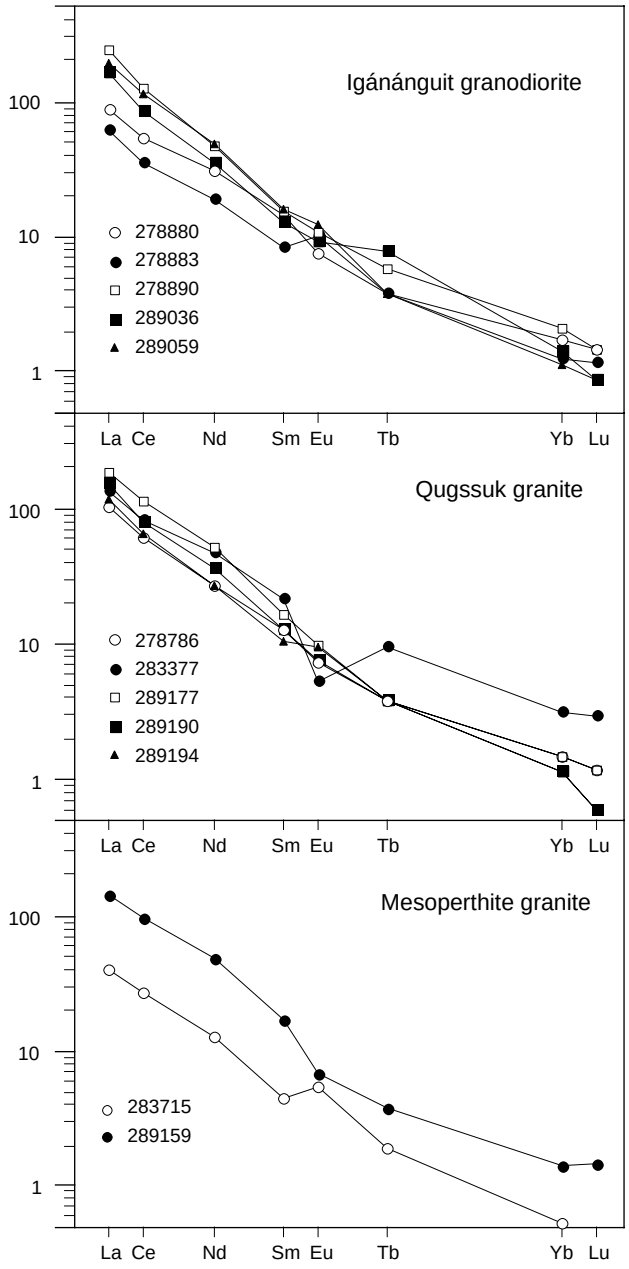

Fig. 75. Chondrite-normalised REE diagrams (Nakamura, 1974) of granitic rocks, Fiskefjord area. All elements analysed by INNA (see Appendix). Sample localities shown in Fig. 68.

Granodiorite and granite

Four different groups of granitoid rocks have been studied (sample locations shown on Fig. 68), namely the late-kinematic (a) Igánánguit granodiorite and (b) Qugssuk granite bodies, (c) a group of contemporaneous amphibolite facies granite sheets emplaced into granulite facies dioritic gneiss in north-eastern Nordlandet (referred to as 'other granites' on Fig. 68 and subsequent figures), and (d) synkinematic mesoperthite (granulite facies) granite sheets in the central and western parts of the Fiskefjord area. Representative and average chemical compositions of the four groups of granitoid rocks are presented in Appendixes 10–11.

Variation diagrams of major and trace elements against SiO_2 (Figs 73, 74) show that groups a–c outline more or less continuous compositional fields. Collectively they are comparable to the most K_2O-rich end members of Taserssuaq tonalite, but clearly different from the most acid members of the TTG suite of grey gneiss (lower MgO, FeO* and CaO, similar or lower TiO_2 and P_2O_5 contents, higher LIL trace element contents and higher K_2O/Na_2O ratios). Their chondrite-normalised REE patterns (Fig. 75) are highly fractionated and LREE-enriched – even more so than in tonalitic-trondhjemitic gneiss, with La >100 × chondrite and normalised La/Yb ratios of *c.* 100. Sample 283377 of Qugssuk granite has a different REE pattern and a large negative Eu anomaly, resembling the altered sample 289208 of Taserssuaq tonalite.

As previously noted the mesoperthite granite has a very felsic modal composition, almost entirely consisting of quartz and variably exsolved ternary feldspar. It has remarkably homogeneous major and trace element compositions which only partially overlap with those of the other granitoids (Figs 73, 74), and its relatively small internal variations are interpreted as solely reflecting variable modal proportions of quartz and feldspar. Most elements show distinct correlations with silica, which has a narrow range between *c.* 71 and 76 wt. % SiO_2 (Figs 73, 74). The rocks are very low in MgO and FeO* and high in Al_2O_3, and display a granitic trend despite relatively low K_2O/Na_2O ratios. Sr contents are very high, up to *c.* 1200 ppm, whereas Pb and Ba contents (*c.* 20–30 and 1000–2000 ppm, respectively) are comparable to those in groups a–c. Rb is low, rarely exceeding 50 ppm, and also the Zr, Y and REE contents (Figs 74, 75) are lower than in groups a–c. As in the other granitoid rocks the two available REE spectra from the mesoperthite granite are strongly fractionated (Fig. 75); they display both positive and negative Eu anomalies.

In terms of their major and trace element compositions all four groups of granite are comparable to Archaean I-type calc-alkaline orogenic granites, generally assumed to represent partial melts of crustal igneous precursors (e.g. Sylvester, 1994).

Discussion

Origin of tonalitic, trondhjemitic and granodioritic magmas

Field observations, petrography and geochemistry suggest that the amphibolite facies tonalitic-trondhjemitic grey gneisses and the late-tectonic, mainly amphibolite facies Finnefjeld and Taserssuaq complexes are the least altered members of grey gneiss *s.l.* in the Fiskefjord area. In the preceding sections it was shown that the compositions of these units strongly resemble average Archaean TTG *sensu* Condie (1981) or Martin (1994), specifically with respect to their low K_2O/Na_2O ratios, low FeO* + MgO + TiO_2 and comparatively high Al_2O_3 contents, relative depletions in mantle-normalised Nb, Ta and Ti compared to other elements, and highly fractionated REE spectra. In addition the low initial $^{87}Sr/^{86}Sr$ ratio of grey gneisses (*c.* 0.7020, Table 1) implies a short crustal residence before emplacement of their igneous precursors. These geochemical features, taken together, are now assumed by most authors to indicate an origin by partial melting of an amphibolite source with residual hornblende ± garnet. Several experiments (e.g. Winther & Newton, 1991; Rapp *et al.*, 1991) have shown that partial melting of a tholeiitic source at moderate pressures can produce large amounts of TTG melts – provided that the source is hydrated; besides, hornblende ± garnet ± titanite are capable of retaining HREE, Y, Nb, Ta and Ti in appropriate proportions to account for their observed concentrations in the TTG rocks (Saunders *et al.*, 1980; Green & Pearson, 1987).

The wide range of major element compositions in the TTG rocks indicate that the source magmas underwent significant modification by crystal fractionation before final emplacement. Dioritic and gabbroic plagioclase-hornblende enclaves in both the Finnefjeld gneiss and Taserssuaq tonalite complexes support this; it was shown above that (at least) the latter are likely to be cogenetic with the complex in which they are found. Besides, the two distinct sample populations from the Taserssuaq tonalite and Finnefjeld gneiss complexes show different major element variation trends against SiO_2, which are compatible with different degrees of plagioclase and hornblende fractionation in the two complexes.

Origin of common dioritic gneiss

The large proportion of mafic tonalite, quartz diorite and diorite in the grey gneiss of the Fiskefjord area is unusual compared with other parts of the Archaean block of West Greenland and with most other Archaean cratons, where dioritic or andesitic components are uncommon. Part of the dioritic gneiss is significantly older than the main TTG suite (Table 1). The less fractionated REE patterns and moderate Nb, Ta and Ti anomalies of the common dioritic gneiss compared to the tonalitic-trondhjemitic gneiss might indicate that the diorite melts were formed by unusually large degrees of partial melting of the supposed amphibolitic TTG source during an embryonic stage of continent formation. However, experiments have shown that bulk melting of amphibolite is not approached under realistic lower crust or upper mantle temperature and pressure conditions (e.g. Rapp *et al.*, 1991; Winther & Newton, 1991). It is therefore more likely that the magmatic precursor to the common dioritic gneiss was generated in a more complicated process, and that a significant component of mantle was involved; the compositional overlap between the diorite and the most leucocratic amphibolites of the supracrustal association might actually suggest this. Experiments e.g. by Green (1976) have shown that quartz-saturated diorites can be produced by *c.* 25% hydrous melting of peridotite, and as noted by Stern *et al.* (1989) natural diorite melts would probably be somewhat less mafic than the experimental melts, due to dissolved silica and LIL elements in the natural hydrous fluids. Assuming that plate tectonic processes were active in the Archaean (see p. 89), magmatic accretion of diorite could have taken place in a convergent plate-tectonic scenario similar to that suggested for modern island arc environments, with participation of a mantle wedge which was fluxed by hydrous fluids originating from the subducted slab. Also this model would require a residue containing hornblende ± garnet ± titanite in order to account for the observed Y, HREE and HFS element depletion in the dioritic gneiss.

Origin of the Qeqertaussaq diorite

As already shown the Qeqertaussaq diorite and immediately adjacent tonalitic gneiss have low TiO_2, MgO, FeO*, CaO, Nb, Cr, Ni and V contents, high to very high Na_2O, K_2O, P_2O_5, Pb, Ba, Sr and LREE contents, and relatively high K/Rb ratios compared with the common grey gneiss or average TTG suites. Some of these characteristics, notably enrichment of Sr and Ba, are also known from other, more leucocratic basement rocks elsewhere in West Greenland, namely from certain

Archaean granitoids in the Disko Bugt region (A. Steenfelt, personal communication, 1995) and from Proterozoic orthogneiss units in the central part of the Nagssugtoqidian orogen (F. Kalsbeek, personal communication, 1995). In terms of LIL element compositions, but not with regard to compatible elements such as Mg, Cr and Ni, the Qeqertaussaq diorite also resembles some modern high-Mg andesites (sanukitoids, Tatsumi & Ishizaka, 1982; bajaites, Saunders *et al.*, 1987), certain Caledonian lavas and granitoids of West Scotland (Stephens & Halliday, 1984; Tarney & Jones, 1994), and Archaean sanukitoids and associated granitoids described by Stern *et al.* (1989) from the Superior Province in Canada. There are also clear similarities with LIL element and P_2O_5-enriched, HFS element-depleted (e.g. Nb, Ti) dioritic members of the Late Archaean Skjoldungen alkaline igneous province in southern East Greenland (Blichert-Toft *et al.*, 1995). Contrary to the Qeqertaussaq diorite, most of the latter suites of rocks are late tectonic, interpreted by the respective authors as having had a large component of primitive or fluid-enriched mantle in their sources, and hornblende fractionation is commonly supposed to have taken place at some stage in their formation. Blichert-Toft *et al.* (1995) argued that the Skjoldungen province has a chondritic mantle signature rather than having been derived from recycled older sediments.

Due to the low Mg/Fe ratios and low concentrations of MgO, Cr, Ni and related trace elements in the Qeqertaussaq diorite, an interpretation which implies a large component of enriched mantle in the end product, is not viable. Amphibolite melting is ruled out because it is not supported by experimental data and furthermore could not produce sufficiently high concentrations of, e.g. Sr and Ba, in the diorite. A purely metamorphic origin of the anomalous composition of the Qeqertaussaq diorite is also not favoured.

The Qeqertaussaq diorite probably had a multistage origin, in which localised mantle metasomatism may have played an important role prior to the formation of a diorite melt. Assuming that the source of the Qeqertaussaq diorite comprised a large mantle component, it would have to be strongly enriched in P_2O_5, Sr, Ba, other LIL elements and LREE. It is considered unlikely that this enrichment could have been achieved during partial melting of the upper mantle, solely by hydrous fluids released into the mantle from recycled crustal sediments or amphibolites; a process of this type might also be expected to have a more regional influence than observed. However, more intense and more localised mantle metasomatism may take place if the mantle comes into contact with carbonatite melts. Experiments with dolomitic melts at upper mantle temperatures and pressures (Green & Wallace, 1988) and studies of carbonated mantle peridotite xenoliths in volcanic rocks (e.g. Ionov *et al.*, 1993) have shown that ephemeral carbonatite melts in the upper mantle can produce very effective LIL element and LREE enrichment and HFS element depletion in spinel peridotite, whereby enstatite is transformed to magnesian diopside or pargasite but Mg/Fe ratios remain largely unchanged. Dolomitic carbonatite melts can coexist with pargasite-bearing lherzolite at *c.* 25 kbar, 1000°C, whereby extensive trace element exchange can take place between carbonate and silicate phases, and new LREE-enriched apatite can be formed. The HFS elements Ti, Nb and Ta are retained in the amphibole. Subsequent decarbonation (without carbonatite magma eruption) may occur from the metasomatised mantle under pressures less than 21 kbar at 950–1050°C, and could conceivably have taken place prior to partial hydrous melting of the enriched mantle.

In support of the proposed localised mantle metasomatism prior to diorite formation it can be noted that two carbonatites (one Late Archaean, one Late Proterozoic) and a number of Late Proterozoic kimberlite dykes are known from the northern part of the Archaean block in southern West Greenland adjacent to the Fiskefjord area (Larsen & Rex, 1992). However, it has not been established if this 'carbonatite-kimberlite province' can be extended back to the earliest history of the region.

Origin of the granitic rocks

It has been shown that the Igánánguit granodiorite, Qugssuk granite and also the mesoperthite granite sheets geochemically belong to the I-type of calc-alkaline granites which are generally assumed to represent late orogenic partial melts of crustal igneous precursors.

In his recent compilation of Archaean granites, Sylvester (1994) subdivided Archaean calc-alkaline granites from eight cratons worldwide into two subgroups, CA_1 and CA_2, the former with higher mean Y, TiO_2, FeO, MgO, CaO, P_2O_5, Sc, V, Zr, REE and Ta, and lower mean Na_2O and Cr concentrations. He argued that the quoted compositional differences are mainly due to different crustal depths of the source areas (viz. pressures of *c.* 6 and 10 kbar), where garnet and hornblende would only occur as restite phases to the group CA_2. He also argued that the CA_2 group, potentially

having had a greater distance available to rise in the crust, would generally be more effectively separated from restite minerals (and hence have the more felsic composition of the two groups).

Except for Cr contents which are always very low (1–20 ppm) all granite groups in the Fiskefjord area would chemically belong to group CA_2 of Sylvester (1994), with the mesoperthite granite providing the best fit. It seems reasonable from granite field relationships and *P-T* estimates of the granulite facies metamorphism in the southern part of the Akia terrane (Reed, 1980; Pillar, 1985; Riciputi *et al.*, 1990) that the granites could have been melted from sources at pressures up to *c.* 10 kbar. In addition, the fact that the granites have more fractionated REE patterns than the grey gneiss supports the idea that hornblende ± garnet were important restite phases, assuming that the granitic melts were indeed separated from a source of grey gneiss.

Granulite facies metamorphism, retrogression and element mobility in grey gneiss

Granulite facies metamorphism

Granulite facies metamorphism extends over the south-western part of the Akia terrane, including Nordlandet and a large part of the Fiskefjord area, whereas the easternmost part of the Fiskefjord area (and of the Akia terrane) consists of upper amphibolite facies rocks that have not experienced granulite facies metamorphism. Large tracts between these two areas are variably retrogressed (Fig. 76). Whole-rock Pb-Pb ages of 3000 ± 70 Ma (Taylor *et al.*, 1980) and 3112 ± 40 Ma (Garde, 1989a) obtained from orthogneiss in Nordlandet and the eastern part of the Fiskefjord area have been interpreted to date the granulite facies metamorphism; a 2999 ± 4 Ma SHRIMP age of metamorphic zircon overgrowth in a garnet-sillimanite-bearing metasediment from Nordlandet just south of the Fiskefjord area (Friend & Nutman, 1994) firmly establishes that the peak of granulite facies metamorphism occurred at *c.* 3000 Ma, i.e., it culminated during or just after emplacement of the main phase of grey tonalitic-trondhjemitic gneiss. SHRIMP zircon data from Nordlandet dioritic gneiss reported in Table 1 and Fig. 25 suggest that this unit also experienced an earlier thermal event at *c.* 3180 Ma. The *c.* 3000 Ma granulite facies metamorphism outlasted two phases of isoclinal folding and a phase of upright, more open folding (the Pâkitsoq phase, Berthelsen, 1960) in the western and central parts of the Fiskefjord area. Granulite facies metamorphism appears to have overlapped with doming, and was succeeded by localised ductile deformation and emplacement of small granodiorite and granite plutons and granite sheets in the northern and eastern parts of the area.

Physical conditions of metamorphism

In Nordlandet the peak of metamorphism occurred under *P-T* conditions of *c.* 850°C, 8 kbar (Reed, 1980; Riciputi *et al.*, 1990), and at Langø, a small island west of Tovqussap nunâ, *c.* 825°C and 8.3 kbar were reported by Dymek (1984). Titanium-rich hornblende and biotite appear to have been stable throughout the granulite facies event in suitable rock types (Garde, 1990 and this paper), indicating that complete dehydration did not take place. According to Pillar (1985) and Riciputi *et al.* (1990) granulite facies metamorphism took place without free fluids, and fluid inclusion data from grey gneiss in the Fiskefjord area seem to support this (Garde, 1990). However, some aspects of the granulite facies rocks may be ascribed to fluid activity during the granulite facies event, for instance hornblende-bearing mafic pegmatites on Nordlandet in which 'high-grade' hornblende partially replaces orthopyroxene (McGregor *et al.*, 1986; McGregor, 1993); also the geochemistry of granulite facies biotite (p. 63) may suggest the former presence of metamorphic fluids (see p. 78).

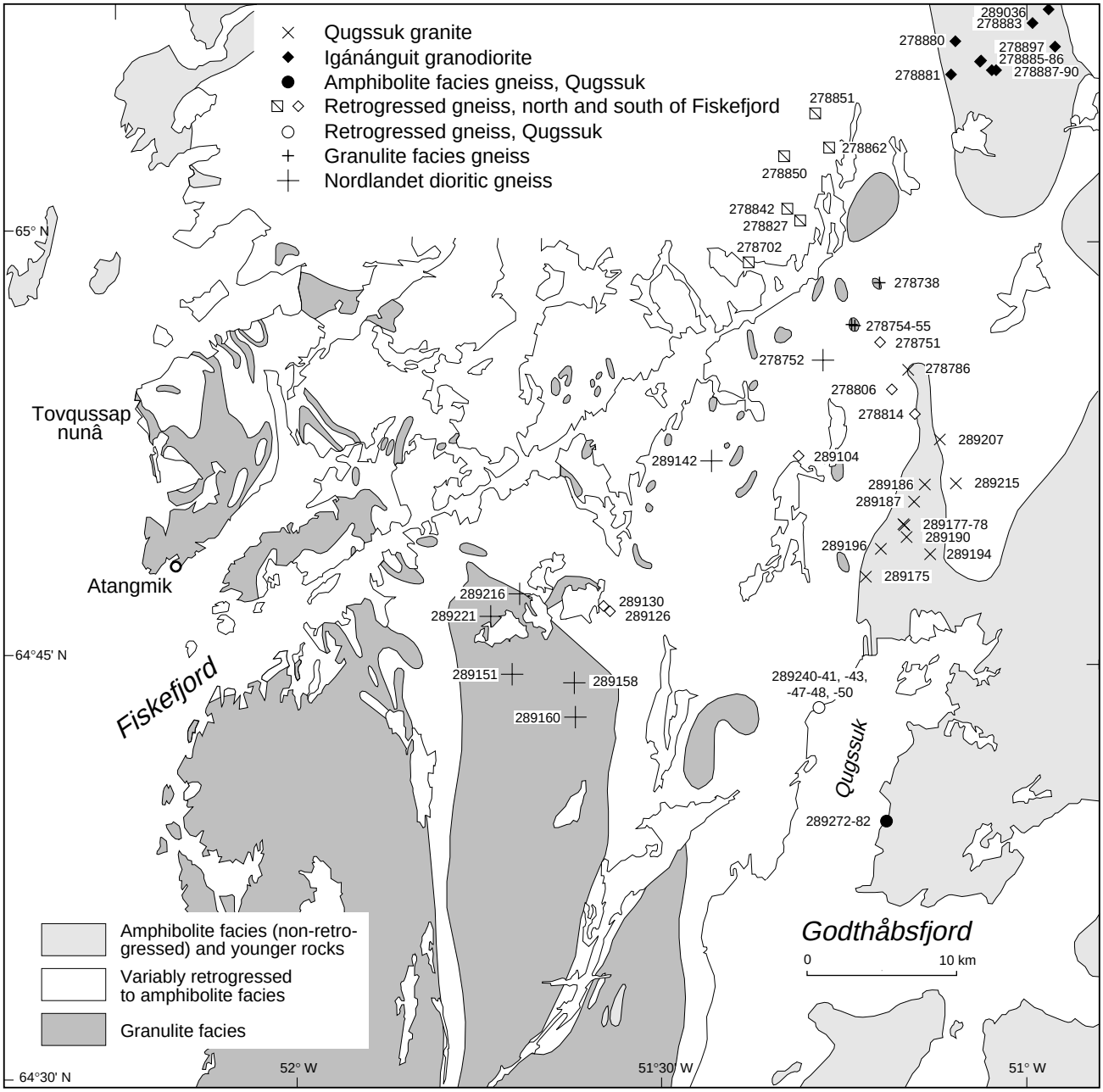

Fig. 76. Distributions of granulite facies, amphibolite facies (not retrogressed from granulite facies), and variably retrogressed grey gneiss in the Fiskefjord area modified from Garde, 1990, fig. 2, and locations of samples used for Pb-Pb and Rb-Sr isotope geochemical study. The amphibolite facies areas comprise both grey gneiss east of Qugssuk, the Finnefjeld gneiss complex in the north-west, the Igánánguit granodiorite in the north-east, and the Taserssuaq tonalite complex and Qugssuk granite north and east of Qugssuk. Samples used for Pb-Pb isotope geochemistry (Fig. 78) are: Qugssuk granite, Igánánguit granodiorite, amphibolite facies and retrogressed gneiss at Qugssuk, and Nordlandet dioritic gneiss (including GGU 289142 and 278752 north-east of the main outcrop). Samples used for Rb-Sr isotope geochemistry and shown in Fig. 79 are: amphibolite facies and retrogressed gneiss from all localities, and Qugssuk granite. Rb-Sr geochronology of the Igánánguit granodiorite is discussed on p. 47.

Phases of metamorphism

Dymek (1978, 1984), who studied metamorphism of supracrustal rocks from several parts of the Godthåbsfjord region (within the Fiskefjord area including rocks from Langø – Tovqussap nunâ and Qugssuk), described a regional upper amphibolite to hornblende granulite facies metamorphic event *M1* and a regional retro-

gressive event *M2*, the latter within the stability field of kyanite. Although his study was carried out before it was realised that the Godthåbsfjord region consists of several terranes with different magmatic, tectonic and metamorphic histories, his observations regarding the *M2* metamorphic phase are pertinent to the Fiskefjord area. Dymek (1978, 1984) noted that the *M2* event was very variably developed within a given outcrop or even within a single thin section. When Dymek (1978) first described the *M2* event, no source for the thermal input or water necessary for hydration was proposed. In a subsequent paper Dymek (1984) suggested a possible correlation of the *M2* event with shear heating and hydration along predominantly subvertical high-grade shear zones of local and regional extent.

Cause of granulite facies metamorphism

Garde (1990) discussed several possible mechanisms of the *c.* 3000 Ma granulite facies metamorphism in the Fiskefjord area (emplacement of originally dry magma; dehydration by CO_2 streaming; thermal metamorphism) and in agreement with other workers cited above concluded that the *c.* 3000 Ma granulite facies metamorphism was probably caused by heat accumulated during continuous injection of tonalitic magma into the growing continental crust. This mechanism of thermal metamorphism by over-accretion had previously been described in detail by Wells (1979, 1980) and applied to *c.* 2800 Ma granulite facies metamorphism in the Buksefjorden area south of Godthåbsfjord (see also Garde, 1990, p. 679).

Retrogression and element mobility

Garde (1989a, 1990, this paper) described progressive changes on outcrop and microscopic scale during prograde and retrograde metamorphism of grey gneiss and presented evidence of element mobility during metamorphism. He showed that in the northern and central parts of the Fiskefjord area most of the grey gneiss (and to a lesser extent mafic and ultramafic supracrustal rocks) has been partially or completely retrogressed from granulite facies, mainly under static conditions, has disequilibrium mineral assemblages and textures, and contains amphibole and biotite which formed over a wide range of amphibolite facies *P-T* conditions – in places two secondary generations of biotite. Only the eastern and northernmost parts of the Fiskefjord area escaped granulite facies metamorphism. Here the orthogneiss contains upper amphibolite facies metamorphic parageneses with equilibrium mineral textures. The original prograde amphibolite to granulite facies boundary in grey gneiss is not preserved in the Fiskefjord area, having been overprinted by retrogression. In West Greenland, outcrops of prograde amphibolite to granulite facies transitions in grey gneiss (resembling those in e.g. the Kabbaldurga quarry, South India, Pichamuthu, 1960) have so far only been described from the southern part of the Fiskenæsset region south of Nuuk, within the Tasiusarsuaq terrane (McGregor & Friend, 1992).

Timing and significance of retrogression, and mechanisms of element transport

Field observations, conventional and isotope geochemistry, mineral chemistry, and a *c.* 3000 Ma U-Pb zircon age obtained from a post-kinematic diorite plug emplaced during or after retrogression suggested to Garde (1990, 1991) that much of the retrogression took place very soon after the culmination of granulite facies metamorphism. Garde (1990) proposed a mechanism of retrogression whereby continuous dehydration and partial melting under granulite facies *P-T* conditions at depth were accompanied by penecontemporaneous retrogression slightly higher in the crust. Liberation of aqueous fluids from the hydrous anatectic melts, as they moved into the upper levels of granulite facies orthogneiss and solidified, would lead to partial or complete retrogression of previously dehydrated rocks, as part of the same thermal event. Figure 77 schematically shows several stages of this development, whereby dehydration and development of a diffuse anatectic network were followed by local mobilisation of leucocratic melts and recrystallisation with secondary amphibole and biotite. Leucocratic veins only centimetres thick may not have travelled far from their source, but a similar process may have operated at a scale of metres to a few tens of metres, as evidenced by retrogression of dioritic gneiss immediately adjacent to granite sheets south-east of Quagssûp taserssua. In the case of the Qugssuk granite, which was emplaced not long after granulite facies metamorphism and is likely to have been derived by coalescing anatectic melts formed during the 3000 Ma granulite facies metamorphism (Rb-Sr whole-rock ages 2969 ± 32 Ma and 2842 ± 85 Ma, Tables 1, 2; Fig. 38), no such halo of ret-

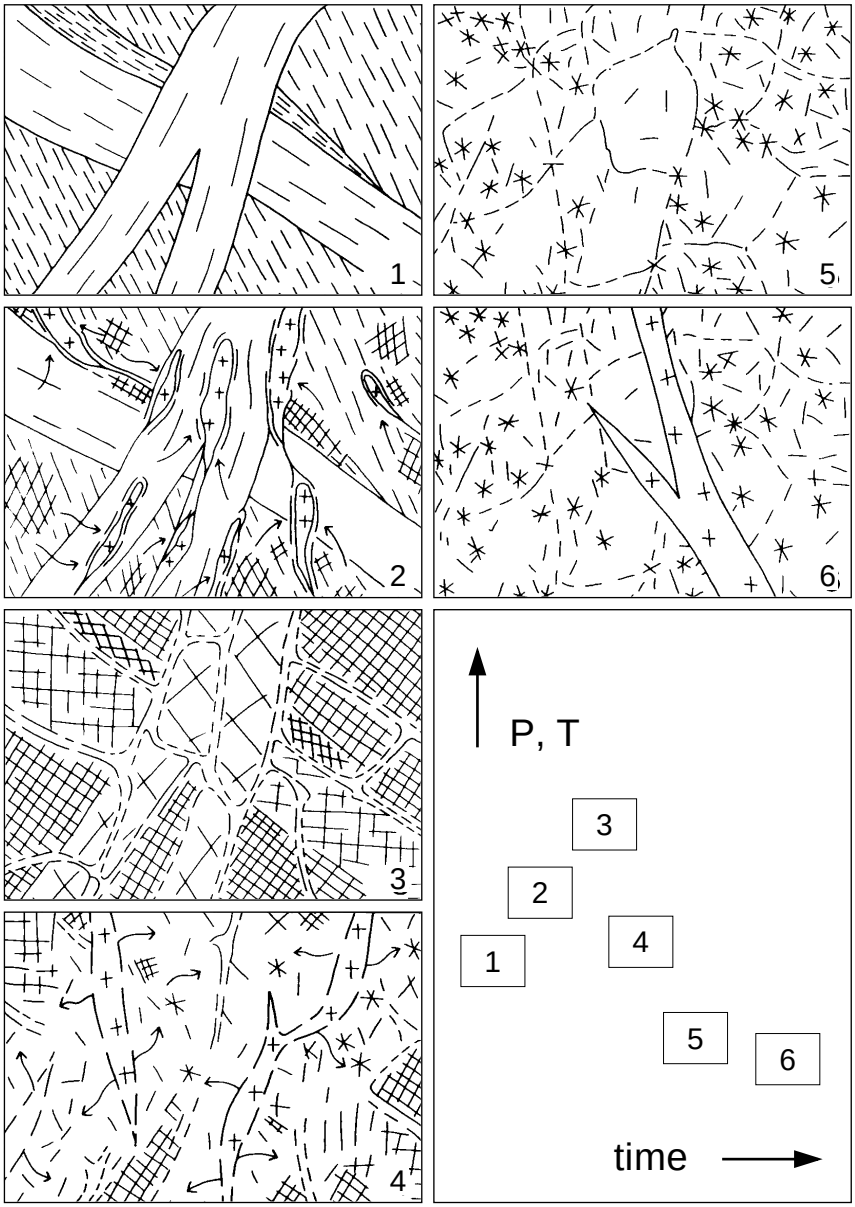

Fig. 77. Schematic stages of grey gneiss development in the Fiskefjord area during granulite facies metamorphism and 'high-grade' retrogression (modified from Garde, 1990, fig. 16). (**1**) Polyphase amphibolite facies gneiss, as shown in Fig. 31. (**2**) Early stage of dehydration and growth of orthopyroxene in cross-hatched areas, and beginning of partial melting (++). (**3**) Granulite facies stage with diffuse quartz-plagioclase anatectic network. Compare Figs 26 (undeformed) and 27 (deformed). (**4**) Early stage of retrogression; former orthopyroxene grains become visible as secondary amphibole-biotite blebs (stars) (compare Figs 32 and 45). (**5**) Fully retrogressed and recrystallised gneiss with blebby texture, compare Fig. 33. (**6**) Retrogressed gneiss intruded by syn- or post-retrogression granite (compare Fig. 51). For reasons unknown, the orthopyroxene crystals (viz. blebby texture) may preferentially be located in the quartzo-feldspathic veins (Fig. 32), in the surrounding rock (Fig. 27), or in both positions (Fig. 33).

rogression can be identified. The granite sheets are bounded to the west and north by retrogressed grey gneiss which, except for islands of granulite facies gneiss, extend many kilometres to the west, north and north-east. Garde (1990) argued that the Qugssuk granite cuts, and is hence younger than, the blebby textures in grey gneiss north of Qugssuk; alternatively V. R. McGregor suggested (personal communication, 1995) that the retrogression in the adjacent tonalitic-trondhjemitic gneiss could have been caused by fluids emanating from the granite during its solidification. This is further discussed below.

It was demonstrated in previous sections that both granulite facies metamorphism and retrogression appear to have been accompanied by very significant migration of LIL elements in the orthogneisses. The migrating elements may have been transported both in anatectic quartzo-feldspathic melts as suggested by field observations and bulk geochemistry, in concentrated fluids (perhaps coexisting with the melts) as suggested by low Rb contents of granulite facies biotite, and in aqueous fluids released from the crystallising quartzo-feldspathic melts. It was also shown that retrogression took place under a large range of upper to lower amphibolite facies *P-T* conditions, as evidenced by disequilibrium mineral textures and the compositions of retrograde amphibole and biotite (Garde, 1990).

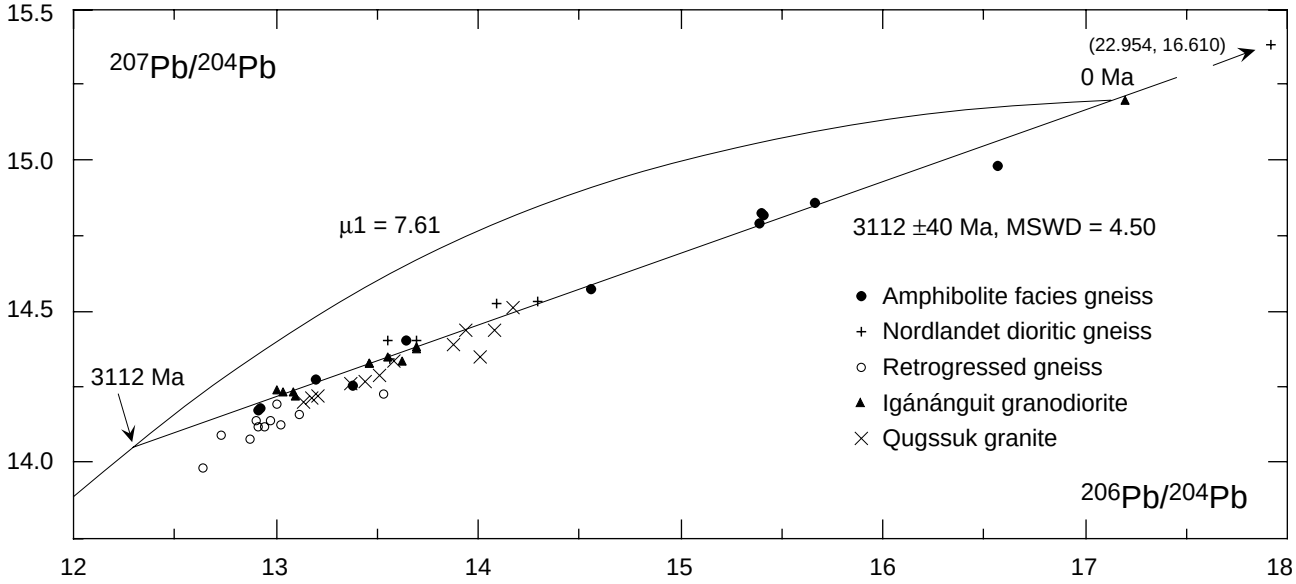

Fig. 78. Pb-Pb isochron diagram of grey gneiss and granitoid rocks from the Fiskefjord area (modified from Garde, 1990, fig. 13). The 3112 Ma age is calculated from samples of amphibolite facies grey gneiss at Qugssuk, Igánánguit granodiorite and Nordlandet dioritic gneiss (see also p. 28). The retrogressed grey gneiss and the Qugssuk granite both plot below the 3114 Ma line and have been contaminated with less radiogenic lead. Sample locations are shown in Fig. 76 (all samples of retrogressed gneiss were collected on the north-west coast of Qugssuk). Analyst: P. N. Taylor.

In the Rb-depleted granulite facies samples from which minerals were analysed, titanium-rich high-grade (granulite facies) biotite with low Rb contents occurs in equilibrium with hornblende and hypersthene (Tables 3, 6). Morphologically (and presumably compositionally) similar high-grade biotite is common in many other granulite facies samples. In theory, this refractory biotite, like phlogopite, should retain Rb in preference to a granitic melt, and the observed Rb distribution is therefore not well explained by granitic melt extraction. Hansen & Newton (1995) described a similar pattern of inverse correlation between Rb and TiO_2 in biotite from an area of prograde amphibolite to granulite facies transition in southern Karnataka, India. They interpreted the low Rb content of granulite facies biotite as due to Rb extraction by a pervasive fluid with high partitioning of Rb relative to biotite under granulite facies *P-T* conditions – perhaps a concentrated, immiscible chloride-carbonate brine coexisting with a quartzofeldspathic melt.

Pb and Rb-Sr isotope data: further evidence of mechanisms and timing of retrogression

Pb and Rb-Sr isotopic data from grey gneiss, Igánánguit granodiorite and Qugssuk granite in the eastern part of the Fiskefjord area were reported by Garde (1989a, 1990). Isotopic ages were discussed in the section on magmatic accretion, and additional Rb-Sr data are presented here. Regarding the U-Pb system, Garde (1990) presented Pb-Pb whole rock data from grey gneiss and granite (P. N. Taylor, personal communication, 1990) showing that the lead isotopic compositions of retrogressed gneiss and Qugssuk granite are less radiogenic than those of the other groups (Fig. 78; locations of samples Fig. 76). This pattern is evidence of open-system behaviour of lead and also suggests contamination with (?Early Archaean) unradiogenic lead during retrogression. The data also show that the lead source of the Qugssuk granite was not isotopically homogenised.

As regards the Rb-Sr system, 10 samples of amphibolite facies gneiss (not retrogressed from granulite facies) define an errorchron of 2954 ± 120 Ma (initial $^{87}Sr/^{86}Sr$ = 0.7014 ± 0.0004, MSWD = 6.85) (Fig. 79a and Garde, 1989a; sample locations Fig. 76). Retrogressed samples from the north-western coast of Qugssuk plot along this line but very near its origin (Fig. 79b). Other granulite facies and retrogressed samples of grey gneiss from the north-eastern part of the Fiskefjord area (Table 7) plot a little above the 2954 Ma reference line but parallel to it, despite some scatter in the data points (Fig. 79c). A regression of these points gives an apparent age of 3137 ± 172 Ma, initial $^{87}Sr/^{86}Sr$ = 0.7017 ± 0.0001, and

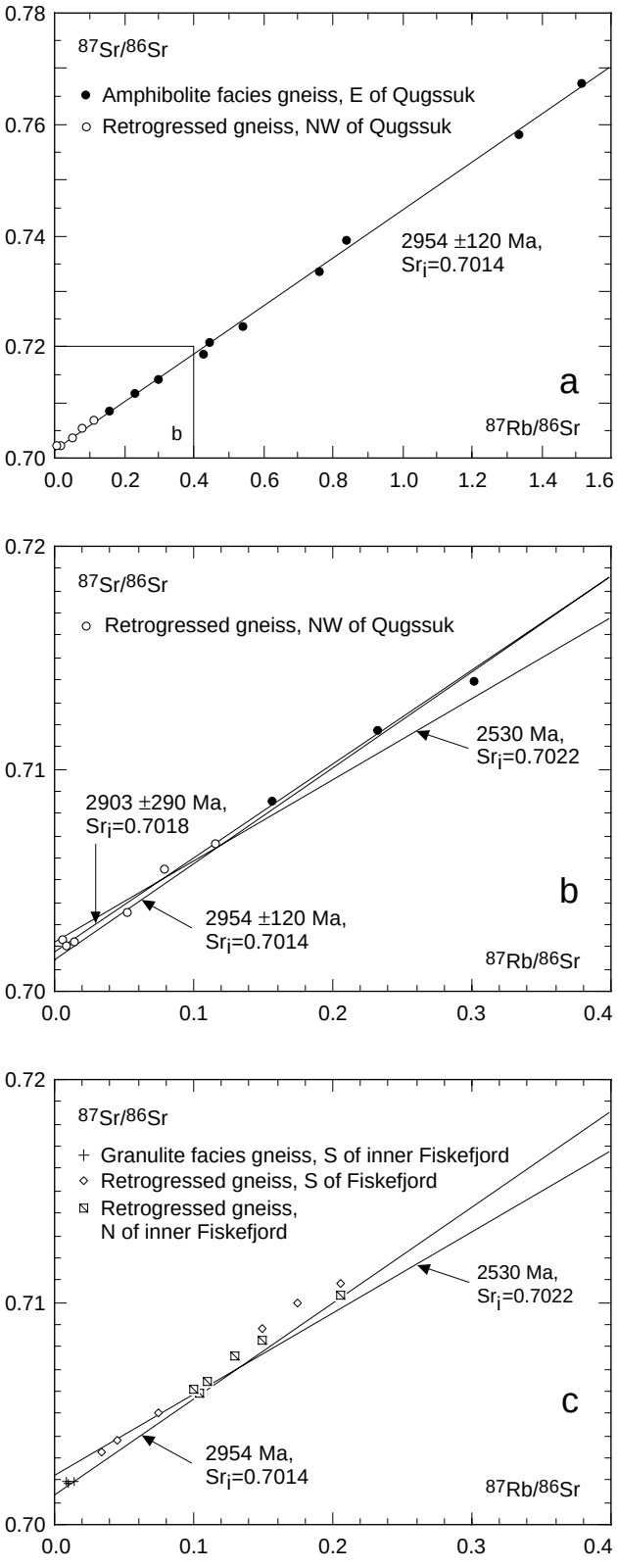

Fig. 79. Rb-Sr isochron diagrams for grey gneiss around Qugssuk and inner Fiskefjord. Sample locations are shown on Fig. 76. (**a**) Amphibolite facies gneiss 289272–289282 from the eastern side of Qugssuk with a regression line (2954 ± 120 Ma (2σ), Sr_i = 0.7014 ± 0.0003, MSWD = 6.85 for these points. Retrogressed gneiss from the western side of Qugssuk (open circles) plots on the same line but near its origin (error magnification is used in the calculation of all 2σ values; modified from Garde, 1990, fig. 12). (**b**) Enlarged portion of (a) with an errorchron of 2903 ± 290 Ma (2σ), Sr_i = 0.7018 ± 0.0004 for the retrogressed gneiss samples NW of Qugssuk, and two reference lines of 2954 Ma and 2530 Ma (estimated Sr_i = 0.7022) for comparison (see the main text). (**c**) Rb-Sr isochron diagram for granulite facies and retrogressed grey gneiss located around inner Fiskefjord. The diagram shows data points from three groups of samples (Table 7): granulite facies and retrogressed grey gneiss from the area south of Fiskefjord, and a group of retrogressed, very leucocratic gneiss occurring north of inner Fiskefjord; several samples lie within the Qugssuk–Ulamertoq zone. The data points from both granulite facies and retrogressed gneiss clearly show that their Rb-Sr isotope systems were closed quickly after 3000 Ma ago. In spite of some disturbance due to granulite facies metamorphism and retrogression (and perhaps minor initial isotopic inhomogeneity) their initial $^{87}Sr/^{86}Sr$ ratio remains low, and their apparent age is not lowered; regression of the data points shown in Table 7 and Fig. 79c gives an apparent age of 3137 ± 192 Ma, initial $^{87}Sr/^{86}Sr$ = 0.7016 ± 0.0001, and MSWD = 2.20.

MSWD = 2.20. If significant migration of Rb and Sr took place during retrogression (as is strongly suggested by Rb and Sr concentration data, petrography and mineral compositions reported in previous sections), this must have happened soon after closure of the Rb-Sr system in its igneous precursor.

McGregor (1993) suggested that much of the retrogression in the eastern part of the Fiskefjord area was related to major Late Archaean (*c.* 2530 Ma?) deformation along the north-western coast of Qugssuk and the Qugssuk–Ulamertoq zone (see p. 82), with potential disturbance of the Rb-Sr system which would have affected most or all of retrogressed gneiss samples referred to above.

Field observations by the author in the Qugssuk–Ulamertoq zone itself only suggest limited Late Archaean deformation. Besides, disturbance of an isotopically homogeneous Rb-Sr system significantly later than 3000 Ma would have resulted in a decrease of the apparent age of the retrogressed gneiss, and would also have increased the apparent initial $^{87}Rb/^{86}Sr$ ratio in the cases of later isotopic homogenisation, or later addition of Rb or crustal Sr. Such changes would be difficult to detect in the retrogressed gneiss on the north-west coast of Qugssuk due to their low Rb/Sr ratios, but they would be apparent in the other groups south and north of inner Fiskefjord. For instance, if isotopic homogenisation of

these retrogressed gneisses took place in a closed system at 2530 Ma, an initial $^{87}Sr/^{86}Sr$ ratio of 0.7014 at 2954 Ma would have increased to *c.* 0.7022 at 2530 Ma (using an average $^{87}Rb/^{86}Sr = 0.123$). On Fig. 79c the data points of granulite facies and (mainly) retrogressed gneiss from the two latter areas are shown together with two reference lines of 2954 and 2530 Ma. The initial $^{87}Sr/^{86}Sr$ ratio of the retrogressed gneiss (calculated value 0.7017 ± 0.0001) actually does appear to be slightly higher than that of amphibolite facies gneiss (initial ratio 0.7014 ± 0.0004), but the apparent difference is very small and within analytical error. In addition, the age is not reset; an age older than 2954 Ma is actually indicated, as noted above.

Significance of blebby texture

The two alternative interpretations of the field relationship between Qugssuk granite and retrogressed gneiss presented above prompt a discussion of the significance of blebby texture, commonly observed in retrogressed gneiss whatever the cause of its retrogression. V. R. McGregor (personal communication, 1995) pointed out that a major part of the textural modification observable in outcrops of retrogressed grey gneiss is likely to have formed during the preceding granulite facies metamorphic event, whereby iron and magnesium derived from the evenly distributed hornblende or biotite characteristic of not previously retrogressed amphibolite facies gneiss are concentrated in fewer and larger orthopyroxene crystals or crystal aggregates (or garnet in rocks of appropriate composition). This (granulite facies) textural coarsening of mafic components only becomes apparent in the field in the form of blebby texture if and when the rocks are rehydrated, and felsic and mafic minerals again become easily recognisable by colour. It may therefore be difficult to establish the relative timing of granite emplacement and retrogression of an adjacent body of older rocks on textural grounds alone (Fig. 51). However, in the case of the Qugssuk granite, the age of granite emplacement would provide a minimum age of retrogression, irrespective of whether retrogression was caused by the granite or had already taken place.

Causes of retrogression

Retrogression of high-grade terrains is conventionally explained by later geological events which are unrelated to granulite facies metamorphism, for instance along major thrusts or shear zones, whereby water is introduced at a higher crustal level from underthrust hydrated rocks. This was, e.g. suggested for the northern boundary of the Tasiusarsuaq terrane in the Godthåbsfjord region (Friend *et al.*, 1988b).

Was retrogression in the Fiskefjord area mainly related to granulite facies metamorphism as suggested by Garde (1990) and outlined above, or was it mainly caused by various younger unrelated events? In the Fiskefjord area later retrogression of country rock gneiss might be surmised to happen during emplacement of post-granulite facies Archaean plutons such as the Finnefjeld gneiss complex, adjacent to faults at the time of juxtaposition of the Akia and Akulleq terranes, during Late Archaean ductile 'straight belt' deformation, and related to Early Proterozoic dykes and faults (McGregor, 1993; V. R. McGregor, personal communication, 1995; McGregor *et al.*, 1991). A fully satisfactory answer to these questions is difficult to obtain, although the very variable nature of retrogression as displayed by mineral assemblages, mineral chemistry and microscopic textures may point to high-grade and low-grade retrogression operating successively and with variable intensity in the same areas.

Table 7. Rb-Sr whole rock data for grey gneiss around inner Fiskefjord

	Rb ppm	Sr ppm	$^{87}Rb/^{86}Sr$	$^{87}Sr/^{86}Sr$
Granulite facies gneiss, south of inner Fiskefjord				
278738	1.7	568	0.009	0.7019
278754	3.8	540	0.014	0.7020
278755	2.0	543	0.010	0.7018
Retrogressed gneiss, south of Fiskefjord				
278751	29	456	0.175	0.7100
278806	28	381	0.206	0.7109
278814	32	581	0.149	0.7089
289104	14	923	0.046	0.7038
289126	14	1050	0.034	0.7033
289130	24	922	0.075	0.7050
Retrogressed gneiss, north of inner Fiskefjord				
278702	52	1110	0.130	0.7076
278827	34	937	0.105	0.7059
278842	45	883	0.150	0.7083
278850	24	681	0.100	0.7061
278851	43	590	0.205	0.7103
278862	32	843	0.110	0.7065
283379	147	132	3.259	0.8393

See discussion in the main text and Fig. 79. Analytical methods as described by Garde *et al.* (1986); the precision of Rb/Sr measurements is within *c.* 1% (2σ) for samples with more than *c.* 5 ppm Rb, and of $^{87}Sr/^{86}Sr$ measurements better than 0.0002 (2σ).

The south-eastern boundary zone of the Finnefjeld gneiss complex adjacent to grey and purple gneiss was studied by Marker & Garde (1988); contact relationships are complicated, with several different intrusive phases; in places, granulite facies gneiss occurs quite close to the margin of the complex. The northern and interior boundary zones of the complex are not well known, but earlier reconnaissance mapping indicates that granulite facies gneiss occurs at or close to the margins of the complex in these areas (Allaart, 1982). In the view of the author, known field relationships do not suggest that the emplacement of the Finnefjeld gneiss complex caused widespread retrogression of the surrounding grey gneiss – at least not at the exposed level.

Retrogression along Late Archaean 'straight belts' of ductile deformation was observed by McGregor *et al.* (1991) and McGregor (1993) in a number of places in the Godthåbsfjord region, a possibility also mentioned by Dymek (1984). One of these belts, supposed to be *c.* 2530 Ma old (McGregor, 1993), occurs along the west coast of outer Godthåbsfjord and continues into the Qugssuk–Ulamertoq zone. Along with other 'straight belts' in the Qugssuk area McGregor envisaged it to be a major cause of lateral fluid movement at a scale of kilometres and concomitant retrogression of grey gneiss in the eastern part of the Fiskefjord area. Contrary to McGregor's interpretation, it was shown above that disturbance of Rb-Sr isotopic systems of this retrogressed grey gneiss must have happened close to 3000 Ma ago. It was also shown above that the pervasive N–S structural grain of the Qugssuk–Ulamertoq zone, including the transposition of earlier folds into upright isoclines, was acquired while granulite facies conditions still prevailed. Far from precluding localised Late Archaean ductile deformation and fluid movement along the Qugssuk–Ulamertoq zone, this observation merely shows that late reactivation was not regionally important in this area. Besides, notwithstanding that pro- and retrograde granulite facies transitions are to some extent lithologically controlled (see e.g. discussion in Garde, 1990 p. 670), substantial parts of the more leucocratic (tonalitic-trondhjemitic) tracts in eastern Nordlandet south of the Fiskefjord area would supposedly also have been affected by retrogression, if Late Archaean lateral fluid infiltration at a scale of many kilometres had taken place along this zone. This is not the case.

Effects of Proterozoic retrogression can be observed in the field along mafic dykes and faults, but the retrogression is restricted to narrow subvertical zones a few metres wide, or at the most a few hundred metres wide along the Fiskefjord fault (a narrow fjord-parallel zone of retrogression occurs in granulite facies gneiss where the fault comes closest to the shores in outer Fiskefjord). However, the Sr isotopic composition of retrogressed gneiss shows that Proterozoic retrogression did not have regional significance.

Conclusions

The widespread retrogression in the central and eastern parts of the Fiskefjord area had several causes. Some Late Archaean and Proterozoic retrogression unrelated to granulite facies metamorphism is readily visible at small scale along late shear zones, faults, and at the margins of Proterozoic dykes. However, the author contends that much of the retrogression is best explained as related to *c.* 3000 Ma granulite facies thermal metamorphism. In spite of difficulty in assessing the precise compositions of magmatic precursors to grey gneiss there is strong geochemical evidence that both granulite facies metamorphism and retrogression were accompanied by mobility of LIL elements. The presence of granulite facies quartzo-feldspathic veins and syn- and post-granulite facies I-type granites suggest that dehydration melting of grey gneiss took place. Fluid activity at granulite facies conditions is indicated from Rb geochemistry of biotite. Petrography and mineral chemistry suggest that retrogression took place under a range of upper to lower amphibolite facies *P-T* conditions, and that there were perhaps two or more episodes of retrogression in some areas. Field relationships between the Qugssuk granite and adjacent grey gneiss may be equivocal in terms of the age of retrogression, but Rb-Sr isotope geochemistry of grey gneiss in this part of the Fiskefjord area independently indicates that a large part of the retrogression took place not later than *c.* 2950 Ma ago. There is field evidence that also Late Archaean and Proterozoic retrogression not related to granulite facies metamorphism took place, but the author has not found evidence of *widespread, Late* Archaean deformation along the Qugssuk–Ulamertoq zone or other zones of high strain in the Fiskefjord area, or of accompanying fluid activity and retrogression with regional importance.

Post-kinematic diorites

Field and petrographic observations

About twenty individual bodies of post-kinematic diorite range in outcrop size from a few square metres to *c.* 1 km^2 (Garde, 1991, fig. 1), but more may be present; they are not easily recognised in areas of granulite facies tonalitic or dioritic gneiss. Post-kinematic diorites on Tovqussap nunâ were first described by Berthelsen (1960) who considered that they had formed by replacement of their host rocks. Pillar (1985) interpreted small sheets and segregations of plagioclase-rich rocks in the Nordlandet area as being contemporaneous with granulite facies metamorphism; some or all of these may also belong to the post-kinematic diorites. The post-kinematic diorites are undeformed and unmigmatised and intrude all other Archaean lithologies, except that they are cut by very rare *c.* 5 cm thick pegmatite veins of presumed Late Archaean age. They are also cut by Proterozoic mafic dykes. They form steep or inclined bodies of brown, crumbling, homogeneous rocks (Garde, 1991, fig. 2); their boundaries are up to a few metres wide and gradational with the orthogneiss host rocks, and the marginal parts of their interiors commonly contain partially resorbed country rock xenoliths.

The post-kinematic diorites have very variable modal compositions and mineral textures, but individual bodies appear to be fairly homogeneous. They consist of hypersthene, diopsidic clinopyroxene, hornblende and intermediate plagioclase in variable proportions, besides local coarse-grained biotite (Berthelsen, 1960; Garde, 1991). The rocks typically consist of *c.* 0.5–0.8 cm large, equidimensional hornblende crystals with inclusions of pyroxene and plagioclase, set in a medium-grained plagioclase matrix. Also granular, medium-grained plagioclase-rich rocks occur, and rocks consisting of randomly orientated, subhedral hornblende and pyroxene or biotite, surrounded by plagioclase. A few of the diorites have proto-orbicular textures (*sensu* Leveson, 1966) or contain single (rarely multiple) shelled orbicules (e.g. Berthelsen, 1960). The orbicular textures may indicate crystallisation from a superheated magma (Vernon, 1985). Pyroxene and hornblende in some bodies are mantled by up to *c.* 1 mm thick rims of homogeneous, blue-green ?auto-metamorphic amphibole. However, the post-kinematic diorites do not display retrograde blebby textures of spongy amphibole-quartz intergrowths or sheaves of secondary biotite, such as commonly found in the host grey gneiss. Textures of the post-kinematic diorites are thus partially magmatic, partially ?auto-metamorphic, suggesting that they were emplaced during or after the main retrogressive event.

Age

Garde (1991) reported a conventional U-Pb zircon age of 3017 $^{+10}_{-12}$ Ma (B. T. Hansen, personal communication, 1990) from a diorite plug 3 km east-south-east of Tartorssuaq. The zircon material in the analysed sample 339512 mostly consists of highly irregular crystals and crystal fragments, but there are no signs of partial resorption although the diorite magma was probably superheated when it was emplaced (see below), and the zircon age is practically concordant. The zircons are therefore interpreted as having crystallised from the diorite magma. It might be argued that this *c.* 3000 Ma U-Pb zircon age represents the age of zircons inherited from wall rock orthogneiss, and that the post-kinematic diorites themselves are much younger, perhaps contemporaneous with the Nain plutonic suite (M. Smith, personal communication, 1995) which intruded the Archaean Nain province in Labrador at *c.* 1400 Ma. However, the post-kinematic diorites cannot be young, because Early Proterozoic dykes cut (some of) them.

Also, Rb-Sr isotopic data point to an Archaean age. Strontium isotopic compositions were determined in three samples of post-kinematic diorite (Table 8), likewise collected east-south-east of Tartorssuaq. Figure 80 shows the data plotted in a Rb-Sr isochron diagram together with retrogressed gneiss from the north-western coast of Qugssuk (from Fig. 79b) and a 2954 Ma reference line (the Rb-Sr age of amphibolite facies gneiss at Qugssuk). The post-kinematic diorites plot close to this line, and in spite of their low Rb contents an Archaean age is indicated.

Geochemistry and interpretation

Garde (1991) described the unusual and very variable chemical compositions of the post-kinematic diorites.

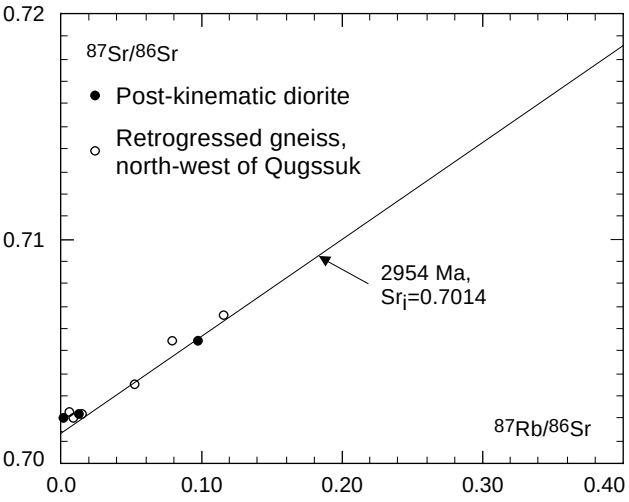

Fig. 80. Rb-Sr diagram showing three samples of post-kinematic diorite, a reference line of 2954 Ma, and samples of retrogressed grey gneiss from the north-west coast of Qugssuk for comparison (see Fig. 79). The samples of post-kinematic diorite are indistinguishable from the grey gneiss, indicating an Archaean age of the diorites.

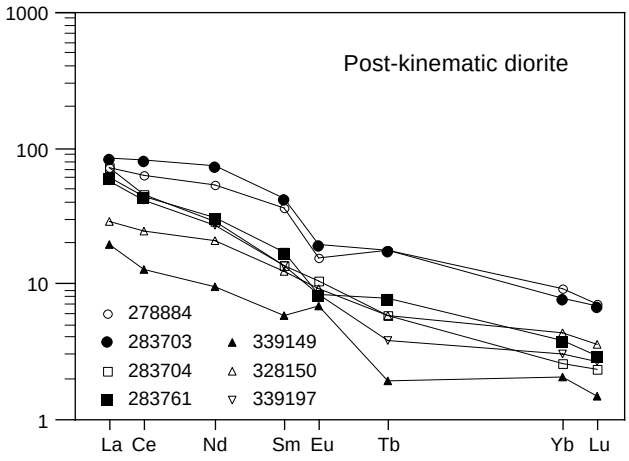

Fig. 81. Chondrite-normalised REE diagram (using normalisation constants by Nakamura, 1974) of post-kinematic diorites from the western part of the Fiskefjord area. Note the extremely variable REE compositions.

The overall intermediate composition of the intrusives is expressed by their silica contents in the range 52.5–58% SiO_2 (Garde, 1991, table 1). They have high contents of compatible and mostly very low contents of incompatible elements, and in several samples the concentrations of, e.g. MgO, TiO_2, P_2O_5, Cr and Ni (high contents) and Rb, Nb and Zr (low contents) are comparable to those normally found in ultramafic rocks. REE contents are very variable. Individual samples have widely different REE patterns normalised to chondrite (Fig. 81); collectively the REE contents are higher than in ultramafic rocks, and lower than in (most) dioritic and tonalitic-trondhjemitic grey gneiss in the Fiskefjord area (compare with Figs 22, 58, 62). On the whole, the chemical compositions of the post-kinematic diorites strongly suggest that they were derived from ultrabasic magma with variable contamination or assimilation of continental crustal material.

Garde (1991) noted a general similarity with a group of post-kinematic noritic intrusions some 50 km north of Fiskefjord, with which the post-kinematic diorites may be genetically related. He also noted that the most plagioclase-rich of the post-kinematic diorites are similar in composition to leuconorite and anorthosite dykes in the Nain province, Labrador, described by Wiebe (1979, 1990) to have been intruded as hot liquids above the clinopyroxene-plagioclase cotectic, not as crystal mushes. Garde (1991) concluded that the field relationships, modal mineralogy, textures and chemical compositions of the post-kinematic diorites suggest or are compatible with crystallisation from superheated dioritic magmas. These magmas most likely formed by contamination of hot ultrabasic melts, either with more felsic magma, or by injection of water and assimilation of felsic wall rocks as indicated by field observations and geochemical data reported above.

Table 8. Rb-Sr whole rock data for post-kinematic diorite

	Rb ppm	Sr ppm	$^{87}Rb/^{86}Sr$	$^{87}Sr/^{86}Sr$	Locality
Post-kinematic diorite					
283703	13.8	409	0.098	0.7055	51°48′17″W, 64°47′38″N
283706	3.6	863	0.012	0.7022	51°47′45″W, 64°47′51″N
283746	0.6	839	0.002	0.7020	51°47′45″W, 64°47′51″N

The samples were collected south-east of Tartorssuaq. See also Fig. 80. Analytical methods as described by Garde *et al.* (1986); the precision of Rb/Sr measurements is within c. 1% (2σ) for samples with more than c. 5 ppm Rb, and of $^{87}Sr/^{86}Sr$ measurements better than 0.0002 (2σ).

Early Proterozoic events

The Early Proterozoic geological events in the Fiskefjord area may be cratonic expressions of the contemporary Nagssugtoqidian, Ammassalikian and Ketilidian orogenic events at the northern and southern margins of the Archaean block (e.g. Watterson, 1978; Kalsbeek *et al.*, 1987, 1990; Chadwick & Garde, 1996). These events are peripheral to the general topic of the present paper and only an outline is presented.

Proterozoic igneous, structural and metamorphic modification of the Archaean crust at the exposed level was very limited. As elsewhere in the Archaean block of southern West Greenland several generations of mafic dykes were emplaced in the Fiskefjord area, and a contemporaneous system of wrench faults was developed. A weak regional thermal event caused resetting of epidote and biotite Rb-Sr and biotite K-Ar ages in this and other parts of the Archaean craton (Garde *et al.*, 1986 and references therein). Besides, intrusion of a few metres thick granitic dykes of continental crustal origin at Qugssuk and Isukasia north-east of the Fiskefjord area (Kalsbeek *et al.*, 1980; Kalsbeek & Taylor. 1983) indicate that stronger localised heating also occurred.

Faults

The Fiskefjord area contains a number of prominent dextral, NE- to ENE-trending faults and a few conjugate sinistral, WNW-trending faults which are best developed in the eastern part of the area (Fig. 82). The faults are Early Proterozoic in age; they are younger than the earliest, *c.* 2200 Ma old, N–S trending high-Mg and related dykes (Bridgwater *et al.*, 1995; Nutman *et al.*, 1995) which they offset, approximately contemporaneous with NE-trending MD dykes, and apparently older than the *c.* 2085 Ma old granitic dyke at Qugssuk (see p. 87).

The largest fault is the NE-trending Fiskefjord fault with a dextral displacement of *c.* 5 km in the outer part of Fiskefjord. The displacement diminishes towards north-east, and at the head of the fjord the fault dissolves into a conjugate system of smaller NE- and WNW-trending dextral and sinistral faults (Garde, 1987); their senses of displacement indicate that the maximum stress vector had an approximately E–W orientation. Towards Taserssuaq a new dextral fault reappears along the line of the Fiskefjord fault and probably continues under the lake and the glacier Sermeq north-east of the Fiskefjord area (Garde, 1987). At outer Fiskefjord the Fiskefjord fault is accompanied by several smaller faults north of the fjord with maximum displacements of about 1–2 km (Berthelsen & Bridgwater, 1960; Garde, 1989b). Along these faults and a similar fault south of the fjord ductile deformation has locally taken place with the development of a few metres thick zones of flaggy, variably chloritised rocks. Other NE-trending faults occur, e.g. north of Tovqussap nunâ and east of Qugssuk; also in these areas lateral displacement of mafic marker horizons in the country rocks suggest dextral fault movement in the order of 1 km.

Most of the Proterozoic faults are bounded by narrow zones up to a few tens of metres wide, where movement of hydrous fluids has caused low-temperature retrogression with growth of chlorite and muscovite, oxidation of iron sulphides and reddening of feldspar.

Mafic dykes

Berthelsen & Bridgwater (1960), Bridgwater *et al.* (1985, 1995), Hall *et al.* (1985) and Hall & Hughes (1986, 1987) have published detailed field and geochemical accounts of mafic dykes in the southern Sukkertoppen, Isukasia and Fiskefjord areas. The dykes comprise several groups. An older N–S trending group of high-Mg and related dykes (Appendix 12) predates the main period of faulting (this group apparently also includes some NE-trending dykes listed in Appendix 13; Hall & Hughes, 1987). Two younger tholeiitic groups trending *c.* 050° and 085° (Appendix 13) are contemporary with, or postdate faulting and belong to the tholeiitic 'MD' dykes of southern West Greenland ('MD' for metadolerite, Rivalenti, 1975; Bridgwater *et al.*, 1976). One of the earliest dykes, the N–S trending Pâkitsoq dyke through Tovqussap nunâ (Berthelsen & Bridgwater, 1960), has been dated at 2110 ± 85 Ma by the whole-rock Rb-Sr method (Bridgwater *et al.*, 1995), and an early, likewise N–S trending high-Mg dyke from the adjacent Isukasia area has yielded a SHRIMP zircon U-Pb age of 2214 ± 10 Ma (Nutman *et al.*, 1995).

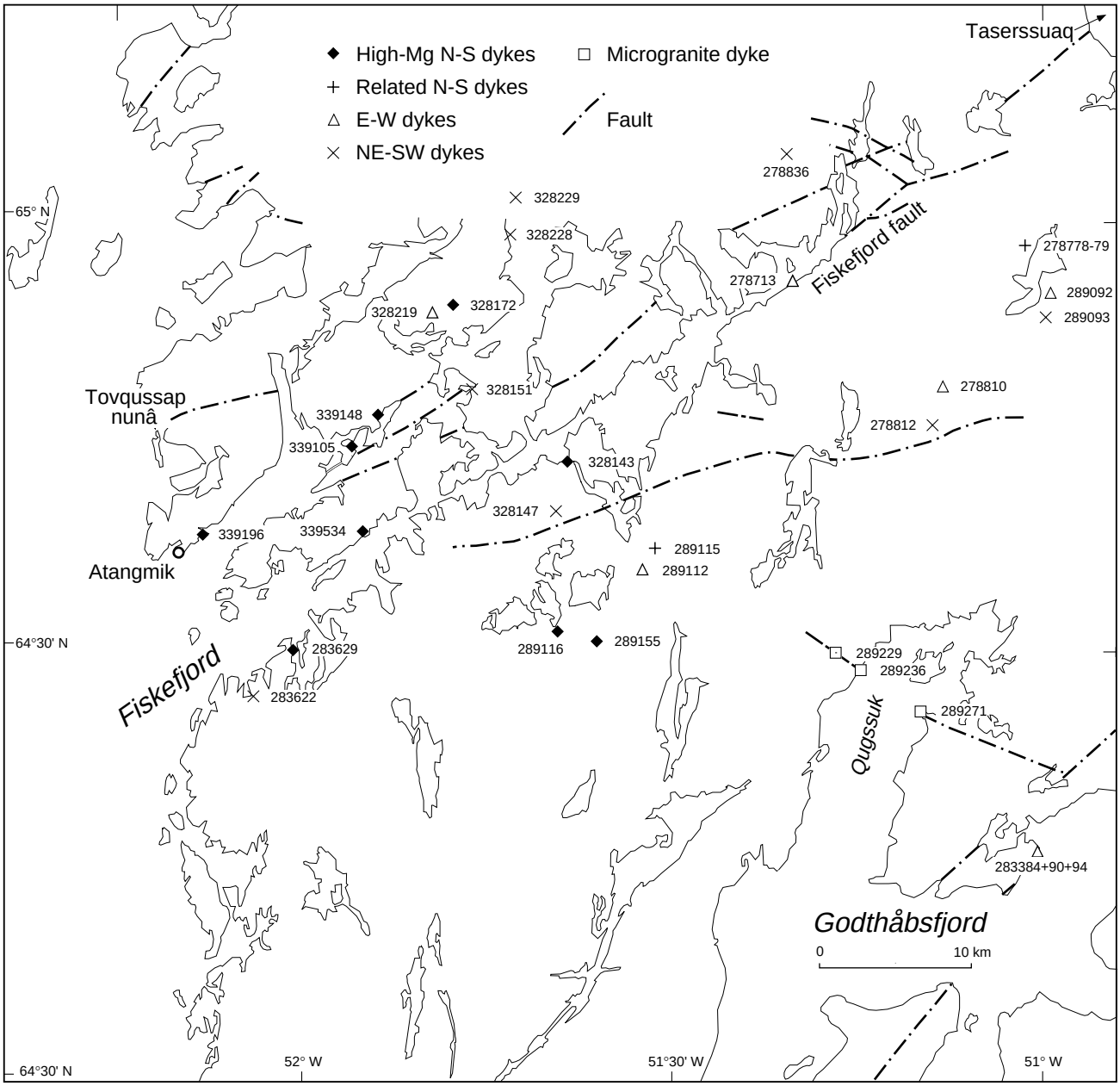

Fig. 82. Proterozoic faults in the Fiskefjord area, and locations of analysed samples of Proterozoic dykes.

The high-Mg dykes were first described by Berthelsen & Bridgwater (1960). Geochemical, mineral-chemical and isotopic data from these dykes have been published by Bridgwater *et al.* (1985, 1995), Hall *et al.* (1985) and Hall & Hughes (1986, 1987). Additional, previously unpublished major and trace element analyses of high-Mg and tholeiitic dykes in the Fiskefjord area are listed in Appendix 12 with accompanying sample localities in Fig. 82; the dykes themselves are shown on the Isukasia and Fiskefjord 1:100 000 scale maps (Garde, 1987, 1989b). Several of the new analyses come from new sample localities of dykes described in previous contributions, or they were collected from presumed continuations *en echelon* of previously described dykes.

Most of the dykes consist of variably altered pyroxene and plagioclase and have doleritic textures and tholeiitic compositions, but several of the N–S trending ones are olivine- or orthopyroxene-bearing or both and boninitic to noritic in composition, with up to 21% MgO, high Cr and Ni, high Mg/Fe ratios, and also rela-

tively high silica contents (Appendix 12; Hall & Hughes, 1987; Bridgwater *et al.*, 1995). In addition to several high-Mg N–S trending dykes Appendix 12 also contains analyses of two N–S dykes from the central and eastern parts of the Fiskefjord area with SiO_2 contents of *c.* 56.5 % and MgO contents of only *c.* 5–6 %. In spite of their low MgO contents both of these dykes probably belong to the high-Mg series. The dyke sampled north-west of Usuk, which probably represents a southern continuation of the Aornit dyke (Berthelsen & Bridgwater, 1960; Hall & Hughes, 1987) has 1–2 mm grains of composite pigeonite-augite primocrysts (like those previously described from the high-Mg group of dykes) and strongly zoned plagioclase laths with albitic overgrowths, from which microcline has been exsolved. The other sample is very fine grained but likewise mainly consists of primary pigeonite-augite and plagioclase. Compared with the tholeiitic E–W dykes both dykes have higher K_2O, Na_2O, Ba, Sr and Rb contents, and lower TiO_2 and FeO* contents, like the high-Mg dykes themselves.

The high-Mg dykes only rarely show evidence of interaction with their local wall rock, and for this and other reasons Hall & Hughes (1987) argued that they represent a distinct boninitic magma type and were derived from depleted harzburgitic mantle which had been metasomatised in the Late Archaean prior to melt extraction. Contrary to this interpretation Bridgwater *et al.* (1985, 1995) suggested that the high-Mg dykes were derived from a primitive high-magnesium magma, which was contaminated shortly before dyke emplacement with components selectively extracted from the lower crust. In this context it is interesting to note that post-kinematic Archaean diorites south of outer Fiskefjord have most likely obtained their apparent boninitic character by strong contamination with wall rock orthogneiss (see previous section and Garde, 1991), which may lend support to the second of the above interpretations of the origin of the high-Mg dykes by Bridgwater *et al.* (1985, 1995).

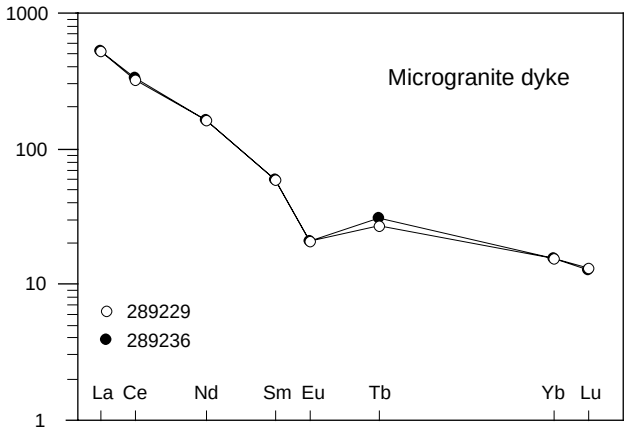

Fig. 83. Chondrite-normalised REE diagram (using normalisation constants by Nakamura, 1974) of microgranite dyke north-west of Qugssuk. The LREE enrichment is interpreted as inherited from a source of Archaean grey gneiss; note the negative Eu anomaly, which suggests retention of plagioclase in the source.

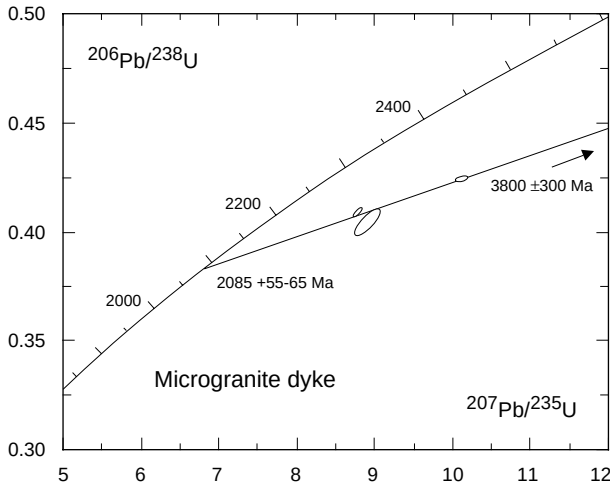

Fig. 84. U-Pb concordia diagram, microgranite dyke north-west of Qugssuk. Analyst: B. T. Hansen. See discussion in the main text.

Microgranite dyke at Qugssuk

An up to *c.* 5 m thick and apparently *c.* 8 km long microgranite dyke occurs in the Qugssuk area with outcrops on both sides of the fjord; the dyke is homogeneous and fine grained, with a pale greenish grey colour. It was emplaced along a WNW-trending Proterozoic fault which has a maximum sinistral displacement of *c.* 800 m (Garde, 1989b) and is probably related to the above mentioned conjugate fault system. The dyke itself is not visibly affected by faulting and is probably younger, having exploited the weak zone of the fault during its emplacement. It consists of microporphyritic biotite, plagioclase, microcline and pseudo-hexagonal quartz set in a very fine-grained matrix of the same minerals and abundant accessory sphene and epidote, besides apatite, zircon and iron oxide. The *c.* 0.5 mm large pseudo-hexagonal quartz crystals commonly contain euhedral plagioclase and apatite inclusions; microcline forms subhedral, partially resorbed laths 0.5–3 mm long with inclusions of small euhedral quartz and plagioclase grains.

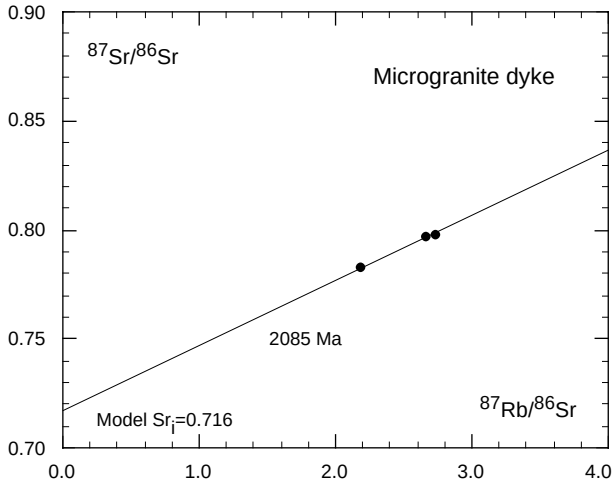

Fig. 85. Rb-Sr isochron diagram, microgranite dyke north-west of Qugssuk. The three samples, which all have high $^{87}Sr/^{86}Sr$ and $^{87}Rb/^{86}Sr$ ratios, plot along a reference line of 2085 Ma (zircon age, Fig. 84); the model initial $^{87}Sr/^{86}Sr$ ratio of *c.* 0.716 indicates an Archaean continental crustal source (the grey gneiss).

Chemical compositions of three samples collected on either side of Qugssuk (Appendix 12) are very similar. The samples are true granites strongly enriched in both LIL trace elements and REE; compared to the nearby Archaean Qugssuk granite (Appendix 10) their concentrations of several of these elements are much higher. A REE spectrum from the dyke (Fig. 83) shows that the REE are strongly fractionated; in this respect the microgranite resembles the Archaean country rock grey gneiss and adjacent granitoid rocks (Figs 62, 75), but it has a strong negative Eu anomaly (see below).

A conventional U-Pb zircon discordia age with a lower intercept of 2085 $^{+55}_{-65}$ Ma (B. T. Hansen, personal communication, 1990; Fig. 84) was obtained from euhedral, less than 100 μm long zircon crystals, which were extracted from several small samples collected at two adjacent outcrops of the dyke north-west of Qugssuk.

Table 9. Rb-Sr whole rock data, microgranite dyke at Qugssuk

	Rb ppm	Sr ppm	$^{87}Rb/^{86}Sr$	$^{87}Sr/^{86}Sr$
Microgranite dyke				
289231	256	275	2.7367	0.7979
289237	255	280	2.6633	0.7968
289271	217	291	2.1822	0.7833

See also Fig. 85. Analytical methods as described by Garde *et al.* (1986); the precision of Rb/Sr measurements is within *c.* 1% (2σ), and of $^{87}Sr/^{86}Sr$ measurements better than 0.0002 (2σ).

The age is not very precise and the upper intercept of the discordia line at 3800 ± 300 Ma may not have geological significance; the data points might also support a line with an upper intercept of *c.* 3000 Ma.

Three samples collected at both sides of the fjord were analysed to determine the Sr isotopic composition of the dyke (Table 9). The three samples all have high $^{87}Sr/^{86}Sr$ and $^{87}Sr/^{86}Sr$ ratios (Fig. 85), and a model initial $^{87}Sr/^{86}Sr$ isotopic composition of *c.* 0.716 at 2085 Ma was estimated using the zircon age as reference. This relatively high initial $^{87}Sr/^{86}Sr$ ratio indicates that the dyke probably originated as a partial anatectic melt from a source of Middle Archaean orthogneiss. The enrichment of LIL and REE elements, as well as the strong negative Eu anomaly, furthermore suggest that only a small degree of partial melting took place; the strong fractionation between LREE and HREE (Fig. 83) is interpreted as inherited from the Archaean source. Within error the zircon age indicates that the microgranite dyke was intruded contemporaneously with the regional episode of MD dyke emplacement. It is considered likely that the local heat source necessary to achieve the crustal melting was a mafic or picritic magma related to this episode.

Summary, discussion and conclusions

Recent developments in research of Archaean crustal processes increasingly favour that 'plate tectonics' was the principal geotectonic framework by the Middle Archaean and possibly even before (e.g. Condie, 1994), and this view forms a starting point for a discussion of the origin and setting of the Fiskefjord supracrustal association and orthogneisses. The two most important recent advances towards a general acceptance of plate tectonics in the Archaean are (a) a better understanding of the architecture of orthogneiss complexes by precise zircon dating supported by modern structural analysis, and (b) the realisation based on geochemical data and laboratory experiments that partial melting of wet ocean floor basalts may have produced voluminous Archaean tonalites and trondhjemites during subduction, if the subducted ocean floor was hotter than it is at present (see p. 93). In contrast, the locus of origin for more recent calc-alkaline magmas in convergent plate settings is the mantle wedge above the subducted oceanic plate.

Distinctive features of orthogneiss and the supracrustal association in the Fiskefjord area

The orthogneiss terrain of the Fiskefjord area, taken as a whole, resembles many other Archaean high-grade orthogneiss complexes in various parts of the world (e.g. compilation by Martin, 1994). There is substantial field evidence that the orthogneisses are younger than the supracrustal rocks. Most of them form a typical tonalite-trondhjemite-granodiorite (TTG) suite with felsic, predominantly sodic end members and only small volumes of younger granites. Dioritic and mafic tonalitic rocks, which are *c.* 200 Ma older than the main tonalites, represent an early continental nucleus (see Table 1). Geochemically the tonalites and trondhjemites are characterised by a fairly large range of major element compositions, negative Nb and Ta anomalies in spider diagrams normalised to mantle abundances, and steep chondrite normalised REE patterns with strongly depleted HREE. The Qeqertaussaq diorite with its unusual pattern of geochemical enrichment (much weaker than, but reminiscent of lamproitic rocks) forms a separate unit.

The early tonalitic orthogneiss precursors were intruded into the supracrustal rocks as sheets, which were subsequently multiply folded together with their supracrustal host rocks in a tectonic regime dominated by lateral forces. Subsequent tonalite-trondhjemite and tonalite-granodiorite intrusions into the folded orthogneiss–amphibolite associations formed large, composite, dome-shaped plutons, which only rarely contain supracrustal enclaves but in places carry fragments of cogenetic hornblende-plagioclase cumulate rocks. In addition, much smaller domes with cores of trondhjemitic compositions were formed. The accretion of orthogneisses culminated with thermal granulite facies metamorphism, and both this and subsequent widespread retrogression severely disturbed the LIL element contents of the orthogneisses. After the culmination of deformation and metamorphism the orthogneisses were partially remobilised, giving rise to localised sheets and small domes of granodioritic and granitic rocks that are contemporaneous with or postdate the retrogression.

It was shown above that homogeneous amphibolite is the most common member of the supracrustal association in the Fiskefjord area – notwithstanding the notion that the association may comprise more than one originally independent sequences intruded by *c.* 3220 and, in turn, 3000 Ma orthogneiss precursors. The chemical composition of the homogeneous amphibolite resembles that of modern ocean floor basalt except for a variable enrichment of mobile incompatible elements (illustrated by Sr, K, Rb, Ba, and Th on Fig. 24) and a lower TiO_2 content. The enrichment of mobile LIL elements in homogeneous amphibolite relative to modern MORB is likely to have been caused by contamination after emplacement and is probably not a primary feature. The supracrustal association contains fragments of large layered complexes which include cumulate noritic and ultrabasic rocks, but whereas ultrabasic lava is known from other parts of the Archaean craton of West Greenland (see next section), komatiitic rocks or high-magnesium basalts have not been recognised in the Fiskefjord area. Sheeted dyke complexes have likewise not been found; they may however be present but not recognised due to deformation and metamorphism. Metasediments are very insignificant, and quartz-rich clastic rocks are almost absent; furthermore, no basement to the supracrustal rocks has

been identified. In spite of their poor and fragmented state of preservation the supracrustal rocks thus possess some similarities with ophiolite complexes.

Middle to Late Archaean supracrustal rocks in adjacent terranes within the Archaean block of southern West Greenland

Only a relatively small part of the Middle to Late Archaean supracrustal rocks in southern West Greenland have been investigated in detail, especially with regard to their geochemistry. Summaries of such studies have been presented by Rivalenti (1976) and Hall *et al.* (1990); see also references in Kalsbeek & Garde (1989). The supracrustal sequences are all dominated by tholeiitic amphibolites, but they occur within terranes of different ages (magmatic accretion of their orthogneiss hosts spans from *c.* 3050 to 2800 Ma) and some contain significant components of metasedimentary rocks. They are thus not directly comparable. The thickest and most complete sequences comprise both pillowed ultrabasic metavolcanic rocks and tholeiitic metabasalts besides other supracrustal rocks. In the Tasiusarsuaq terrane they occur at Ravn Storø and Bjørnesund (Fiskenæsset region), and in the Akulleq terrane at Ivisârtoq northeast of Godthåbsfjord (Andersen & Friend, 1973; Hall, 1980; Friend *et al.*, 1981; Chadwick, 1986, 1990; Hall *et al.*, 1987). Isortuarssup tasia, a thinner and geographically more restricted sequence in the Fiskenæsset region, was studied by Stecher (1981). The geochemical study by Weaver *et al.* (1982) at Qeqertarssuatsiaq in the same region mostly comprised amphibolites of gabbroic origin associated with anorthositic rocks. The Fiskenæsset region also contains small volumes of andesitic and more leucocratic metavolcanic rocks ('grey amphibolite'), which may have formed in an island arc setting (Wilf, 1982). Along the south-eastern margin of the Akia terrane a *c.* 2 km thick sequence dominated by amphibolites and possibly including komatiitic supracrustal rocks occurs on the Nuuk peninsula, Sadelø and Bjørneøen in outer Godthåbsfjord (Bridgwater *et al.*, 1976; Olsen, 1986; Appel & Garde, 1987; McGregor, 1993). Primary structures such as pillow lavas are fairly common in all these supracrustal rocks, the metamorphic grade is lower (middle to upper amphibolite facies), and most of them are more complete and less deformed than those preserved in the Fiskefjord area. However, a gradual transition from a coherent 'greenstone belt' sequence into fragmented supracrustal rocks in a 'high-grade grey gneiss – amphibolite' setting can be observed at Bjørnesund (Andersen & Friend, 1973; Garde *et al.*, 1991).

As in the Fiskefjord area, a basement to the supracrustal rocks has not been identified anywhere in the above mentioned areas. The supracrustal rocks in the Fiskenæsset region are intruded by Middle to Late Archaean orthogneisses and also tectonically interleaved with them, and the Ivisârtoq supracrustal rocks have been tectonically juxtaposed against early Archaean Amîtsoq gneisses (Hall & Friend, 1979; Chadwick, 1985, 1986). It was furthermore shown by Hall (1982) on chemical grounds that the Ivisârtoq metabasalts are unrelated to the Ameralik dykes, a major mafic Archaean dyke swarm that has intruded the nearby Early Archaean Amîtsoq gneiss.

The chemical compositions of the tholeiitic metabasalts at Ivisârtoq and in the Fiskenæsset region resemble that of the homogeneous amphibolite in the Fiskefjord area with respect to most major and trace elements, and it may be significant that they also have relatively low TiO_2 contents (see Hall *et al.*, 1990, p. 256). The main difference is the much lower LIL element content (e.g. K_2O < 0.30% and Rb <15 ppm) in most of the former rocks (Weaver *et al.*, 1982; Hall *et al.*, 1990), which is regarded by the author to reflect a more pristine state of preservation than in the Fiskefjord area. Friend *et al.* (1981) and Hall *et al.* (1990) discussed possible chemical affinities of the basic metavolcanic suites at Ivisârtoq, Ravn Storø and Isortuarssup tasia to modern tholeiitic basalts in various settings. They concluded that the metabasalts all have similar tholeiitic compositions, and although their chemistry alone does not indicate a direct affinity to any particular modern tholeiite setting, their field settings suggest an origin as ocean floor basalts. Regarding the amphibolites at Qeqertarssuatsiaq, Weaver *et al.* (1982) concluded on the basis of trace element data that an ocean floor setting is the most likely of several possible tectonic environments.

Discussion

Archaean upper mantle and oceanic crust

Both the field setting of the Fiskefjord amphibolites and their geochemical similarity with modern MORB – with the above mentioned qualifications – are compatible with an origin as ocean floor basalts. The same is true for other amphibolite-dominated supracrustal

sequences in West Greenland. However, despite the recent trend towards a general acceptance of plate tectonics in the Archaean, unquestionable ocean floor sequences of Archaean age have not yet been identified (see p. 92), and it has not been settled if Archaean MORB had a composition similar to that of modern MORB. It is also still debated how important plate tectonics were in the Archaean, and if Archaean plate-tectonic processes were identical to those that are generally accepted to have operated since the Early Proterozoic. In as much as any interpretation of the supracrustal rocks in the Fiskefjord area must in the first place be evaluated against their poor state of preservation, it is not appropriate to introduce a lengthy discussion of each of these problems. However, a few central points are relevant in the present context.

One such point, which refers to the role of plate tectonics in general, is how the elevated interior heat production by radioactive decay in the Archaean earth was expressed in crustal processes. The fact that the metamorphic zonation of most Archaean continental crust suggests a moderate geothermal gradient implies that the excess heat from the mantle was channelled to the surface elsewhere. Komatiites provide unequivocal evidence of formerly superheated ultrabasic magma (probably from a deep mantle source), and are indicative of localised ambient mantle temperatures at least *c.* 200° and perhaps up to 400°C hotter than in post-Archaean times (e.g. Sleep & Windley, 1982; Jarvis & Campbell, 1983; Campbell & Jarvis, 1984; McKenzie, 1984). It has also been assumed that the Archaean oceanic crust was both hotter and thicker than at present (Sleep & Windley, 1982; Bickle, 1986) due to a steep geothermal gradient in the oceanic regions. The common assumption that the Archaean oceanic crust was on the average much more short lived than today (due to vigorous production of mantle-derived basaltic rocks) implies that it was also generally hotter, simply because cooling of the ocean floor is known to be a very slow process (see e.g. Martin, 1986, 1993; Drummond & Defant, 1990; Tarney & Jones, 1994). Some authors have taken this view even further, suggesting that the heat flow was so high that the uppermost part of the Archaean mantle was not sufficiently rigid to support plate-tectonic processes, and that the formation of continental crust – at least in the Early Archaean – took place by vertical sagging from oceanic plateaus much like those supposed to exist on Venus (Hamilton, 1993). However, komatiites, with their direct evidence of elevated Archaean mantle temperature, only make up a small proportion of surviving Archaean supracrustal rocks and are by no means ubiquitous in Archaean supracrustal terrains. Campbell *et al.* (1989), Campbell & Griffiths (1992) and others have suggested that while hot plumes produced localised komatiites, much more voluminous ocean floor basalts with MgO contents of less than 12% were produced by passive upwelling from mantle sources with 'normal' temperatures around 1300°C, located under mid-ocean ridges. In other words, the high mantle temperatures related to komatiite production need not have been characteristic for the Archaean upper mantle as a whole, were not necessarily reflected in elevated crustal geothermal gradients worldwide, and do not preclude the operation of plate tectonics in the Archaean.

Also the chemical evolution of the upper mantle in the early part of the Earth's history is uncertain (e.g. review by Bickle, 1990). Early to Late Archaean komatiites from several parts of the world are variably depleted in LREE and other incompatible elements and have positive εNd values (e.g. Collerson *et al.*, 1991; Bennett *et al.*, 1993), and a similar but less marked depletion occurs in associated tholeiitic basalts (e.g. Sun & Nesbitt, 1978; Campbell *et al.*, 1989). Although some of these rocks may have experienced later geochemical disturbance, this indicates that MORB-like, moderately depleted mantle had formed already by the Early and Middle Archaean, and is considered by some authors to have been a common source of mafic and ultramafic rocks. However, as pointed out, e.g. by Arndt (1994), komatiitic rocks are probably not an adequate sample medium for contemporaneous upper mantle. Besides, some komatiites and basalts in Archaean greenstone belts show evidence of crustal contamination, commonly in the form of high-MgO rocks which also have high contents of SiO_2 and incompatible elements and negative Nb anomalies, or they contain xenocrystic zircons of continental crustal origin. The evidence of contamination impedes estimates of the compositions of both the Archaean mantle itself and its direct melt products. The matter is further complicated by widely differing estimates of (a) the growth rate of the early continental crust (reviewed by Taylor & McLennan, 1985) and hence the net amount of overall mantle depletion during the Archaean, and (b) the patterns of Archaean mantle convection. The latter has an important bearing on the effectiveness of its contemporaneous chemical homogenisation (e.g. Bickle, 1990; Campbell & Griffiths, 1992) and (as stated above) whether komatiites can be used at all for estimates of upper mantle composition (Arndt, 1994). In conclu-

sion, the composition of Archaean MORB may not in all respects have been close to that of modern MORB.

Controversy about the recognition of ancient oceanic crust in Archaean cratons adds to the uncertainty about Archaean crustal evolution in general and the role and nature of plate tectonics in particular, and is illustrated by a recent paper by Bickle *et al.* (1994). These authors examined a number of extensively studied Archaean greenstone belts in the world: the Belingwe greenstone belt in the Zimbabwe craton, the Barberton greenstone belt in the Kaapvaal craton, the Kambalda and other greenstone belts in the Yilgarn and eastern Pilbara cratons of Western Australia, and various greenstone belts in the southern Slave and Superior provinces of Canada including the Abitibi belt. All of these greenstone belts have been or are currently interpreted as (containing) remnants of oceanic crust, but for various reasons they were all rejected as such by the above cited authors. Several of the examined greenstone successions have (arguably) been laid down on a continental basement (some contain basal conglomerates), others show signs of contamination by continental crust during their ascent or emplacement, others again contain thick sequences of shallow-water sedimentary rocks, and none contain complete ophiolite sequences (as defined by the Geological Society of America, Anonymous, 1972). Bickle *et al.* (1994) concluded that although no indisputable fragments of Archaean oceanic crust have yet been found, it probably did exist. This conclusion is probably fairly representative for the current state of the debate, although there are also strong proponents that some Archaean greenstone belts do indeed represent ocean floor sequences (e.g. de Wit *et al.*, 1987; Kusky & Kidd, 1992). Bickle *et al.* (1994) suggest that the search for Archaean ophiolite complexes should continue in other tectonic environments such as for instance the Fiskenæsset region in the high-grade Archaean block of West Greenland. However, it has been shown above that an inherent problem with this suggestion is the progressively more fragmentary preservation and likelihood of chemical alteration associated with the most high-grade supracrustal sequences.

Generation of Archaean continental crust

Contrary to the situation in those Archaean greenstone belts where komatiites attest to very high mantle temperatures of their source areas, most Middle Archaean high-grade cratons do not provide evidence of elevated geothermal gradients, neither in the continental crust itself nor in its underlying mantle. This is true for the regions of Early Archaean Amîtsoq gneiss within the Akulleq terrane immediately adjacent to the Akia terrane (e.g. McGregor *et al.*, 1991) and is also well documented in other, younger parts of the Archaean block of southern West Greenland (see Kalsbeek, 1976, references to general descriptions in Kalsbeek & Garde, 1989, and thermal modelling by Wells, 1979, 1980).

It has long been known that some orthogneiss terrains in Archaean continental cratons have chemical compositions that differ in several important respects from those of their Proterozoic and younger counterparts. Most, but not all intermediate and felsic plutonic rocks in Archaean cratons are characterised by calcic to sodic TTG suites and a relative scarcity of true granites (e.g. in Scotland, Weaver & Tarney, 1981, and eastern Finland, Martin, 1987), whereas younger orthogneiss suites are calc-alkaline with common granitic end members. Another example of these general differences has recently been beautifully displayed by Steenfelt (1994) in her compilation of regional stream sediment data from West and South Greenland: the major boundary between the orthogneisses in the Archaean craton of southern West Greenland and the Lower Proterozoic Ketilidian orogen to the south with its large calc-alkaline Julianehåb batholith stands out on the regional K and Ca plots of stream sediment compositions. The Ketilidian batholith has distinctly higher K_2O and lower CaO than the adjacent Archaean orthogneiss – at least at the crustal levels now exposed north and south of the boundary. Steenfelt's data (1994 and personal communication, 1995), however, also show that there are exceptions to this pattern; some members of the Archaean orthogneisses in the Disko Bugt region and in the Nagssugtoqidian orogen have high K_2O/Na_2O ratios and are relatively low in Ca, whereas the opposite is the case for juvenile Proterozoic rocks in the Nagssugtoqidian orogen.

In addition to their characteristic major element compositions, Archaean orthogneisses generally have steep REE patterns with a strong depletion of HREE, upward curving HREE ends and absent or weak Eu anomalies (e.g. Taylor & McLennan, 1985; Martin, 1994). This is also true for the West Greenland Archaean (e.g. O'Nions & Pankhurst, 1974; Compton, 1978) and, as already shown, the Fiskefjord area in particular – except that retrogressed grey gneiss members have distinct positive Eu anomalies. The generally favoured interpretation of these REE patterns is that the TTG magmas left a residuum rich in hornblende and garnet, which retained the HREE.

The different compositions of Archaean and younger granitoids have suggested to many authors (e.g. Martin, 1987, 1993, 1994; Arkani-Hamed & Jolly, 1989; Drummond & Defant, 1990) that they were formed by different processes: Proterozoic and younger magmas of calc-alkaline affinity are produced at destructive plate margins by a multistage process that begins with partial fusion of the mantle wedge above the subducted (or underplated) ocean floor. The fluids necessary to sufficiently lower the mantle solidus are liberated from the cold subducting slab by solid state dehydration. Typical Archaean TTG suites were not formed by this process, because the ultimate partial melt products from the mantle are too potassic and have different trace element characteristics, e.g. flat REE curves. Conversely, recent experiments by Rapp *et al.* (1991) and Winther & Newton (1991) have convincingly demonstrated that partial melting of hydrous low-K tholeiitic basalt can produce tonalites and trondhjemites in one stage with major element compositions closely comparable to those of real rocks, while leaving a hornblende- and garnet-bearing residuum (see also van der Laan & Wyllie, 1992). Winther & Newton (1991) showed that this is possible at temperatures and pressures that can be realistically reached in a hot subducted slab of ocean floor (Arkani-Hamed & Jolly, 1989); it is an important prerequisite for the production of TTG melts that the basalt source being subducted is sufficiently hydrated, as otherwise smaller amounts of granitic melts are produced at higher temperature and pressure. Alternatively the appropriate physical conditions for partial melting could be met in the lower part of a tectonically thickened pile of hydrated (ocean floor) basalt. The former of these two alternatives seems to be the most attractive one, both in the light of the common speculation that the Archaean oceanic crust was young and hot (e.g. Drummond & Defant, 1990), and when compared with modern analogues. Thus Martin (1993) drew attention to the situation in south Chile where subduction of very young ocean floor is spatially related to the production of andesitic lavas with HREE depletion similar to that found in Archaean TTG suites (Stern *et al.*, 1984a, b).

Isotopic and tectonic evidence of Middle to Late Archaean plate tectonics in southern West Greenland

Two decades ago Bridgwater *et al.* (1974) emphasized the role of horizontal tectonics in Archaean crustal thickening and juxtaposition of different lithologies. The paper was mainly based on observations from the Godthåbsfjord and Fiskenæsset regions. These authors also suggested as a working hypothesis that the underlying driving force was horizontal movements in the mantle, perhaps related to plate-tectonic processes. Nevertheless, in order to account for observed radiometric ages within a given geographical region it was then commonly assumed that in the Archaean, crustal processes might last well over 200 million years in so-called crustal accretion and differentiation superevents (CADS, Moorbath, 1976) which had no direct modern analogues.

Between 1985 and 1988 it was realised with the aid of precise zircon age determinations and modern structural analysis (Friend *et al.*, 1987, 1988a; Nutman *et al.*, 1989) that the region south of Godthåbsfjord contains several Archaean blocks or tectono-stratigraphic terranes (*sensu* Coney, Jones & Monger, 1980) which have different ages, consist of different lithologies, and have different magmatic, structural and metamorphic histories which each took place during relatively short periods of time. Studies elsewhere in southern West Greenland (Nutman *et al.*, 1993; Friend & Nutman, 1994; Nutman & Kalsbeek, 1994) and in other Archaean cratons (e.g. Nutman, 1991; de Wit *et al.*, 1992; Williams *et al.*, 1992; Myers, 1995) have subsequently indicated that the prior existence of many individual terranes in Archaean cratons is probably the rule rather than the exception. The accretion and differentiation of Archaean continental crust is now envisaged to have taken place in individual, relatively quickly developed terranes or microcontinents, with the implication that 'plate tectonics' in some form was active and important at least from the Middle Archaean.

Archaean geotectonics

Some aspects of Archaean crustal igneous and tectonic processes are now well understood. As just outlined, the terrane concept provides strong evidence of Archaean plate tectonics, although only small volumes of new crust were formed during the juxtaposition itself. There is also substantial, and in the view of the present author convincing experimental evidence, supported by geochemical modelling and compatible with field observations, that new Archaean continental crust (tonalites, trondhjemites and granodiorites) was generated by subduction and partial melting of wet tholeiitic ocean floor basalts; the process differs from modern accretion of calc-alkaline island

arcs and continental batholiths, which form by mantle melting.

Other important facets of Archaean geotectonics are still not resolved. There is disagreement about the composition and thermal structure of both the Archaean upper mantle and oceanic crust, first of all because no indisputable sample of Archaean oceanic crust has yet been identified anywhere in the world, and because it is not known if komatiites were natural products of the major processes that formed the oceanic crust, or exceptions created by localised hot mantle plume activity. In addition, the very high production of new continental crust in most Archaean cratons in the short interval between approximately 3000 and 2750 Ma requires an explanation.

Plate-tectonic scenario of the Fiskefjord area

The field relationships, compositions, ages and structural evolution of most orthogneiss and related rock units in the Fiskefjord area are compatible with and suggestive of a convergent plate-tectonic environment. These rocks (tonalitic-trondhjemitic grey gneiss and tonalite complexes) have compositions which are consistent with an origin from subducted oceanic crust by melting of hydrated basaltic rocks and modified by subsequent crystal fractionation in the lower crust; mantle components are only likely to have been directly involved in the genesis of the Nordlandet dioritic gneiss and the Qeqertaussaq diorite precursors, but in different ways.

The early structures in the grey gneiss, subhorizontal(?) thrusts and two or several phases of recumbent isoclinal folds, would comply with conditions formed by lateral stress fields which might be expected in progressively deeper levels of a convergent plate margin. Possible directions of plate motion and subduction would be broadly east–west during the main, Smalledal and Pâkitsoq phases of deformation. The succeeding emplacement of large dome-shaped plutonic complexes and development of vertical structures, broadly contemporaneously with and succeeding the peak of metamorphism, may have been achieved at a stage when subduction was ceasing, the production of new continental crust had culminated, and the accumulation of heat in the middle part of the new crust reached its maximum and declined.

Remobilisation of part of the earlier formed orthogneisses and emplacement of localised granitic rocks then took place, perhaps associated with contemporary redistribution of mobile elements in the deeper part of the crust. The narrow linear high-strain zones with horizontal structures, which form a long-lived structural element in the evolution of the Fiskefjord area, may have developed in response to a gradual change from convergence of the inferred plates to transcurrent motion along an approximately north–south path, where the crust was still sufficiently ductile.

The intrusion of post-kinematic diorite plugs is not interpreted as directly related to plate-tectonic processes but was more likely due to subsequent underplating by ultramafic magma and apparently linked to the formation of the norite belt in the adjacent area to the north.

While the plate-tectonic scenario outlined above for the orthogneisses in the Fiskefjord area and their structural evolution is in part based on positive evidence (especially referring to the geochemistry of the TTG suites), the origin of the supracrustal association is much more speculative. The heterogeneous and homogeneous amphibolites, partially preserved layered mafic-noritic-ultrabasic rocks, and sporadic metasediments may represent fragments of one or more ophiolite sequences, but remnants of a sheeted dyke complex have not been identified, and cherty layers are so far not known. There may have been more than one group, separated in time by the accretion of the Nordlandet dioritic gneiss. Further, it has not been firmly established how much of the homogeneous amphibolite has been derived from extrusive volcanic rocks, subvolcanic sills, sheeted dyke complexes, layered complexes, or combinations of these possibilities.

The homogeneous amphibolite was probably chemically altered during or after its emplacement, but important geochemical similarities with better preserved Archaean tholeiitic metabasalts from neighbouring regions can still be recognised. However, even the origin of the latter rocks has not been proven – partly because of their likely contamination and metasomatic alteration, and partly because the detailed composition of a hypothetical Archaean MORB is not known. Nevertheless, the author favours the opinion that the supracrustal rocks in the Fiskefjord area represent relict oceanic crust, due to (1) the fact that no basement of continental crust has been identified (coupled with widespread evidence that the supracrustal rocks have been intruded by the orthogneiss precursors), and (2) the nature and in particular great scarcity of metasediments.

The simple plate-tectonic model presented above requires that early intrusions of orthogneiss precursors

would have to be emplaced into oceanic crust. Xenoliths and fragments of mafic supracrustal rocks are actually present both in dioritic and tonalitic grey gneiss, but the picture is complicated by the fact that some of the dioritic gneiss represents an earlier continental nucleus. Furthermore, in the absence of age determinations of the supracrustal units, still more complicated tectonic scenarios could easily be advanced.

Acknowledgements

This study would not have been possible without help from many persons in various phases of the work. I thank colleagues and assistants during field work, especially Mogens Marker and the late Stig Bak Jensen, and I am grateful to Vic McGregor for his excellent introduction to the field geology of the Godthåbsfjord region. I would also like to thank the staff at the geochemical and isotope laboratories in Copenhagen and abroad, in particular John Bailey, Jørgen Christensen, John Fløng, Ole Larsen, Svend Pedersen and Jørn Rønsbo, University of Copenhagen, the staff at the former Geological Survey of Greenland laboratories, Allen Nutman, Australian National University, and Paul Taylor, Oxford University. I am also very grateful to the former Geological Survey of Greenland and in particular Hans Kristian Schønwandt for encouragement and support, and to Feiko Kalsbeek for always very precise and constructive discussions and comments. Several other present and former colleagues at the Survey have contributed with valuable comments at various stages of the study, especially Lotte Melchior Larsen, Mogens Marker, Flemming Mengel, Agnete Steenfelt and Cees Swager. Thanks also to David Bridgwater, University of Copenhagen, and Clark Friend, Oxford Brookes University, who performed very constructive reviews of the text. The Danish Natural Science Research Council is thanked for financing a very substantial part of the publication.

References

Allaart, J. H. 1982: Geological map of Greenland, 1:500 000, Frederikshåb Isblink – Søndre Strømfjord, sheet 2. Copenhagen: Geological Survey of Greenland.

Allaart, J. H., Jensen, S. B., McGregor, V. R. & Walton, B. J. 1977: Reconnaissance mapping for the 1:500 000 map sheet in the Godthåb–Isua region, southern West Greenland. *Rapport Grønlands Geologiske Undersøgelse* **85**, 50–54.

Allaart, J. H., Friend, C. R. L., Hall, R. P., Jensen, S. B. & Roberts, I. W. N. 1978: Continued 1:500 000 reconnaissance mapping in the Precambrian of the Sukkertoppen region, southern West Greenland. *Rapport Grønlands Geologiske Undersøgelse* **90**, 50–54.

Andersen, L. S. & Friend, C. [R. L.] 1973: Structure of the Ravns Storø amphibolite belt in the Fiskenæsset region. *Rapport Grønlands Geologiske Undersøgelse* **51**, 37–40.

Anonymous 1972: Ophiolites. *Geotimes* **17**, 24–25.

Appel, P. W. U. & Garde, A. A. 1987: Stratabound scheelite and stratiform tourmalinites in the Archaean Malene supracrustal rocks, southern West Greenland. *Bulletin Grønlands Geologiske Undersøgelse* **156**, 26 pp.

Arkani-Hamed, J. & Jolly, W. T. 1989: Generation of Archean tonalites. *Geology* **17**, 307–310.

Arndt, N. T. 1994: Archaean komatiites. *In* Condie, K. C. (ed.) *Archaean crustal evolution*, 11–44. Amsterdam: Elsevier.

Ashwal, L. D. & Myers, J. S. 1994: Archaean anorthosites. *In* Condie, K. C. (ed.) *Archaean crustal evolution*, 315–355. Amsterdam: Elsevier.

Beech, E. M. & Chadwick, B. 1980: The Malene supracrustal gneisses of north-west Buksefjorden: their origin and significance in the Archaean crustal evolution of southern West Greenland. *Precambrian Research* **11**, 329–355.

Bengaard, H.-J. 1988: Basic rocks of the inner Fiskefjord area, southern West Greenland. *Rapport Grønlands Geologiske Undersøgelse* **140**, 55–56.

Bennett, V. C., Nutman, A. P. & McCulloch, M. T. 1993: Nd isotopic evidence for transient, highly depleted mantle reservoirs in the early history of the Earth. *Earth and Planetary Science Letters* **119**, 299–317.

Berthelsen, A. 1950: A Pre-Cambrian dome structure at Tovqussaq, West Greenland. *Meddelelser fra Dansk Geologisk Forening* **11**, 558–572.

Berthelsen, A. 1957: The structural evolution of an ultra- and polymetamorphic gneiss-complex, West Greenland. *Geologische Rundschau* **46**, 173–185.

Berthelsen, A. 1960: Structural studies in the pre-Cambrian of western Greenland. II. Geology of Tovqussap nunâ. *Bulletin Grønlands Geologiske Undersøgelse* **25**, 223 pp. (Also *Meddelelser om Grønland* **135**(6)).

Berthelsen, A. 1962: Structural studies in the pre-Cambrian of western Greenland. III. Southern Sukkertoppen district. *Bulletin Grønlands Geologiske Undersøgelse* **31**, 47 pp. (Also *Meddelelser om Grønland* **123**(2)).

Berthelsen, A. & Bridgwater, D. 1960: On the field occurrence and petrography of some basic dykes of supposed pre-Cambrian age from the southern Sukkertoppen District, western Greenland. *Bulletin Grønlands Geologiske Undersøgelse* **24**, 43 pp. (Also *Meddelelser om Grønland* **123**(3)).

Bickle, M. J. 1986: Implications of melting for stabilization of the lithosphere and heat loss in the Archaean. *Earth and Planetary Science Letters* **80**, 314–324.

Bickle, M. J. 1990: Mantle evolution. *In* Hall, R. P. & Hughes, D. J. (ed.) *Early Precambrian basic magmatism*, 111–135. Glasgow: Blackie.

Bickle, M. J., Nisbet, E. G. & Martin, A. 1994: Archaean greenstone belts are not oceanic crust. *Journal of Geology* **102**, 121–138.

Blichert-Toft, J., Rosing, M. T., Lesher, C. E. & Chauvel, C. 1995: Geochemical constraints on the origin of the Late Archaean Skjoldungen alkaline igneous province, SE Greenland. *Journal of Petrology* **36**, 515–561.

Bridgwater, D., McGregor, V. R. & Myers, J. S. 1974: A horizontal tectonic regime in the Archaean of Greenland and its implications for early crustal thickening. *Precambrian Research* **1**, 179–197.

Bridgwater, D., Keto, L., McGregor, V. R. & Myers, J. S. 1976: Archaean gneiss complex of Greenland. *In* Escher, A. & Watt, W. S. (ed.) *Geology of Greenland*, 18–75. Copenhagen: Geological Survey of Greenland.

Bridgwater, D., Fryer, B. & Gorman, B. E. 1985: Proterozoic basic dykes in southern Greenland and the coast of Labrador: tectonic setting, intrusion forms and chemistry. *Proceedings International Conference on Mafic Dyke Swarms*, 15–21. Toronto: University of Toronto Press.

Bridgwater, D., Mengel, F., Fryer, B., Wagner, P. & Hansen, S. C. 1995: Early Proterozoic mafic dykes in the North Atlantic and Baltic cratons: field setting and chemistry of distinctive dyke swarms. *In* Coward, M. P. & Ries, A. C. (ed.) Early Precambrian processes. *Geological Society Special Publication* (London) **95**, 193–210.

Campbell, I. H. & Griffiths, R. W. 1992: The changing nature of mantle hotspots through time: implications for the chemical evolution of the mantle. *Journal of Geology* **100**, 497–523.

Campbell, I. H. & Jarvis, G. T. 1984: Mantle convection and early crustal evolution. *Precambrian Research* **26**, 15–57.

Campbell, I. H., Griffiths, R. W. & Hill, R. I. 1989: Melting in Archaean mantle plume: heads it's basalts, tails it's komatiites. *Nature* **339**, 697–689.

Chadwick, B. 1985: Contrasting styles of tectonism and magmatism in the late Archaean crustal evolution of the north-eastern part of the Ivisârtoq region, inner Godthåbsfjord, southern West Greenland. *Precambrian Research* **27**, 215–238.

Chadwick, B. 1986: Malene stratigraphy and late Archaean structure: new data from Ivisârtoq, inner Godthåbsfjord, southern West Greenland. *Rapport Grønlands Geologiske Undersøgelse* **130**, 74–85.

Chadwick, B. 1990: The stratigraphy of a sheet of supracrustal rocks within high-grade orthogneisses and its bearing on Late Archaean structure in southern West Greenland. *Journal of the Geological Society* (London) **147**, 639–652.

Chadwick, B. & Garde, A. A. 1996: Palaeoproterozoic oblique plate convergence in South Greenland: a re-appraisal of the Ketilidian orogen. *In* Brewer, T. S. (ed.) Precambrian crustal evolution in the North Atlantic region. *Geological Society Special Publication* (London) **112**, 179–196.

Collerson, K. D., Campbell, L. M., Weaver, B. L. & Palacz, Z. A. 1991: Evidence for extreme fractionation in early Archaean ultramafic rocks from northern Labrador. *Nature* **349**, 209–214.

Compston, W., Williams, I. S. & Myer, C. 1984: U-Pb geochronology of zircon from lunar breccia 73217 using a sensitive high mass-resolution ion microprobe. *Journal of Geophysical Research (Supplement)* **89**, B525–B534.

Compton, P. 1978: Rare earth evidence for the origin of the Nûk gneisses, Buksefjorden region, southern West Greenland. *Contributions to Mineralogy and Petrology* **66**, 283–293.

Condie, K. C. 1981: *Archaean greenstone belts*. Amsterdam: Elsevier, 434 pp.

Condie, K. C. 1994: Introduction. *In* Condie, K. C. (ed.) *Archaean crustal evolution*, 1–9. Amsterdam: Elsevier.

Coney, P. J., Jones, D. L. & Monger, J. W. H. 1980: Cordilleran suspect terranes. *Nature* **288**, 329–333.

de Wit, M. & Ashwal, L. D. 1995: Greenstone belts: what are they? *In* Percival, J. & Ludden, J. (ed.) *Precambrian '95. Tectonics and metallogeny of Early/Mid Precambrian orogenic belts*, 310 only. Montreal: Université du Québec à Montréal.

de Wit, M., Hart, R. A. & Hart, R. J. 1987: The Jamestown ophiolite complex, Barberton Mountain belt: a section through 3.5 Ga oceanic crust. *Journal of African Earth Science* **5**, 681–730.

de Wit, M., Roering, M., Hart, R. J., Armstrong, R. A., de Ronde, C. E. J., Green, R. W. E., Tredoux, M., Peberdy, E. & Hart, R. A. 1992: Formation of an Archaean continent. *Nature* **357**, 553–562.

Drummond, M. S. & Defant, M. J. 1990: A model for tonalite-trondhjemite-dacite genesis and crustal growth via slab melting: Archean to modern comparisons. *Journal of Geophysical Research* **95**, 21503–21521.

Dymek, R. F. 1978: Metamorphism of Archaean Malene supracrustals, Godthåb district, West Greenland. *In* Smith, I. E. M. & Williams, J. G. (ed.) *Proceedings of the 1978 Archaean geochemistry field conference*, 339–342. Toronto: University of Toronto Press.

Dymek, R. F. 1984: Supracrustal rocks, polymetamorphism, and evolution of the SW Greenland Archaean gneiss complex. *In* Holland, H. D. & Trendall, A. F. (ed.) *Patterns of change in Earth evolution*, 313–343. Berlin: Springer-Verlag.

Dymek, R. F. & Smith, M. S. 1990: Geochemistry and origin of Archaean quartz-cordierite gneisses from the Godthåbsfjord region, West Greenland. *Contributions to Mineralogy and Petrology* **105**, 715–730.

Friend, C. R. L. & Nutman, A. P. 1994: Two Archaean granulite-facies metamorphic events in the Nuuk–Maniitsoq region, southern West Greenland: correlation with the Saglek block, Labrador. *Journal of the Geological Society* (London) **151**, 421–424.

Friend, C. R. L., Hall, R. P. & Hughes, D. J. 1981: The geochemistry of the Malene (mid-Archaean) mafic-ultramafic amphibolite suite, southern West Greenland. *In* Glover, J. E. & Groves, D. I. (ed.) *Archaean geology. Geological Society of Australia Special Publication* **7**, 301–312.

Friend, C. R. L., Nutman, A. P. & McGregor, V. R. 1987: Late Archaean tectonics in the Færingehavn–Tre Brødre area, south of Buksefjorden, southern West Greenland. *Journal of the Geological Society* (London) **144**, 369–376.

Friend, C. R. L., Nutman, A. P. & McGregor, V. R. 1988a: Late Archaean terrane accretion in the Godthåb region, southern West Greenland. *Nature* **355**, 535–538.

Friend, C. R. L., Nutman, A. P. & McGregor, V. R. 1988b: Significance of the late Archaean granulite facies terrain boundaries, southern West Greenland. *In* Ashwal, L. D. (ed.) Workshop on the deep continental crust of South India. *Lunar and Planetary Institute Technical Report* **88-06**, 46–48.

Friend, C. R. L., Nutman, A. P., Baadsgaard, H., Kinny, P. D. & McGregor, V. R. 1996: Timing of late Archaean terrane assembly, crustal thickening and granite emplacement in the Nuuk region, southern West Greenland. *Earth and Planetary Science Letters* **142**, 353–365.

Furlong, K. P. D., Chapman, D. S. & Alfeld, P. W. 1982: Thermal modelling of the geometry of subduction with implications for the tectonics of the overriding plate. *Journal of Geophysical Research* **87**, 1786–1802.

Garde, A. A. 1984: Field work between Fiskefjord and Godthåbsfjord, southern West Greenland. *Rapport Grønlands Geologiske Undersøgelse* **120**, 45–50.

Garde, A. A. 1986: Field observations around northern Godthåbsfjord, southern West Greenland. *Rapport Grønlands Geologiske Undersøgelse* **130**, 63–68.

Garde, A. A. 1987: Geological map of Greenland, 1:100 000, Isukasia 65 V.2 Syd. Copenhagen: Geological Survey of Greenland.

Garde, A. A. 1989a: Retrogression and fluid movement across a granulite-amphibolite facies boundary in middle Archaean Nuk gneisses, Fiskefjord, southern West Greenland. *In* Bridgwater, D. (ed.) *Fluid movements – element transport and the composition of the deep crust*, 125–137. Dordrecht: Kluwer.

Garde, A. A. 1989b: Geological map of Greenland, 1:100 000, Fiskefjord 64 V.1 Nord. Copenhagen: Geological Survey of Greenland.

Garde, A. A. 1990: Thermal granulite-facies metamorphism with diffuse retrogression in Archaean orthogneisses, Fiskefjord, southern West Greenland. *Journal of Metamorphic Geology* **8**, 663–682.

Garde, A. A. 1991: Post-kinematic diorite intrusions in Archaean basement rocks around outer Fiskefjord, southern West Greenland. *Bulletin of the Geological Society of Denmark* **39**, 167–177.

Garde, A. A. & McGregor, V. R. 1982: Mapping in the Fiskefjord area, southern West Greenland. *Rapport Grønlands Geologiske Undersøgelse* **110**, 55–57.

Garde, A. A., Hall, R. P., Hughes, D. J., Jensen, S. B., Nutman, A. P. & Stecher, O. 1983: Mapping of the Isukasia sheet, southern West Greenland. *Rapport Grønlands Geologiske Undersøgelse* **115**, 20–29.

Garde, A. A., Larsen, O. & Nutman, A. P. 1986: Dating of late Archaean crustal mobilisation north of Qugssuk, Godthåbsfjord, southern West Greenland. *Rapport Grønlands Geologiske Undersøgelse* **128**, 23–36.

Garde, A. A., Jensen, S. B. & Marker, M. 1987: Field work in the Fiskefjord area, southern West Greenland. *Rapport Grønlands Geologiske Undersøgelse* **135**, 36–42.

Garde, A. A., Kalsbeek, F., Marker, M. & Schønwandt, H. K. 1991: Archaean supracrustal rocks at different crustal levels in West Greenland, and their metallogeny. *Terra Abstracts* **3**, 194 only.

Green, D. H. 1976: Experimental testing of "equilibrium" partial melting of peridotite under water-saturated, high pressure conditions. *Canadian Mineralogist* **14**, 255–268.

Green, D. H. & Wallace, M. E. 1988: Mantle metasomatism by ephemeral carbonatite melts. *Nature* **336**, 459–462.

Green, T. H. & Pearson, N. J. 1987: An experimental study of Nb and Ta partitioning between Ti-rich minerals and silicate liquids at high pressure and temperature. *Geochimica et Cosmochimica Acta* **51**, 55–62.

Hall, R. P. 1980: The tholeiitic and komatiitic affinities of the Malene metavolcanic amphibolites from Ivisârtoq, southern West Greenland. *Rapport Grønlands Geologiske Undersøgelse* **97**, 20 pp.

Hall, R. P. 1982: Geochemistry of the Malene metavolcanic amphibolites from Ivisârtoq, southern West Greenland. *Rapport Grønlands Geologiske Undersøgelse* **110**, 68–72.

Hall, R. P. & Friend, C. R. L. 1979: Structural evolution of the Archaean rocks in Ivisârtoq and the neighbouring inner Godthåbsfjord region, southern West Greenland. *Geology* **7**, 311–315.

Hall, R. P. & Hughes, D. J. 1982: Transitional amphibolite-granulite facies granites, diorites and metavolcanic amphibolites in the Isukasia map sheet, southern West Greenland. *Rapport Grønlands Geologiske Undersøgelse* **110**, 46–49.

Hall, R. P. & Hughes, D. J. 1986: A boninitic dyke in the eastern Sukkertoppen region: geochemistry of the boninitic-noritic dyke swarm of southern West Greenland. *Rapport Grønlands Geologiske Undersøgelse* **130**, 44–52.

Hall, R. P. & Hughes, D. J. 1987: Noritic dykes of southern West Greenland: early Proterozoic boninitic magmatism. *Contributions to Mineralogy and Petrology* **97**, 169–182.

Hall, R. P., Hughes, D. J. & Friend, C. R. L. 1985: Geochemical evolution and unusual pyroxene chemistry of the MD tholeiite dyke swarm from the Archaean craton of southern West Greenland. *Journal of Petrology* **26**, 253–282.

Hall, R. P., Hughes, D. J. & Friend, C. R. L. 1987: Mid-Archaean basic magmatism of southern West Greenland. *In* Park, R. G. & Tarney, J. (ed.) Evolution of the Lewisian and comparable Precambrian high grade terrains. *Geological Society Special Publication* (London) **27**, 261–175.

Hall, R. P., Hughes, D. J. & Tarney, J. 1990: Early Precambrian basic rocks of Greenland and Scotland. *In* Hall, R. P. & Hughes, D. J. (ed.) *Early Precambrian basic magmatism*, 248–272. Glasgow: Blackie.

Hamilton, P. J., O'Nions, R. K., Bridgwater, D. & Nutman, A. P. 1983: Sm-Nd studies of Archaean metasediments and metavolcanics from West Greenland and their implications for the Earth's early history. *Earth and Planetary Science Letters* **62**, 263–272.

Hamilton, W. B. 1993: Evolution of Archaean mantle and crust. *In* Reed, J. C., Bickford, M. E., Houston, R. S., Link, P. K., Rankin, D. W., Sims, P. K. & Van Schmus, W. R. (ed.) Precambrian. *The geology of North America* **C.2**, 597–614. Boulder, Colorado: Geological Society of America.

Hansen, E. C. & Newton, R. C. 1995: Rb depletion in Archaean deep-crust metamorphism, South India. *In* Percival, J. & Ludden, J. (ed.) *Precambrian '95. Tectonics and metallogeny of Early/Mid Precambrian orogenic belts*, 282 only. Montreal: Université du Québec à Montréal.

Hill, R. E. T., Barnes, S. J., Gole, M. J. & Dowling, S. E. 1990: *Excursion guide book No. 1. Physical volcanology of komatiites*. Perth: Geological Survey of Western Australia, 100 pp.

Ionov, D. A., Dupuy, C., O'Reilly, S. Y., Kopylova, M. G. & Genshaft, Y. S. 1993: Carbonated peridotite xenoliths from Spitsbergen: implications for trace element signature of mantle carbonate metasomatism. *Earth and Planetary Science Letters* **119**, 283–297.

Jarvis, G. & Campbell, I. H. 1983: Archaean komatiites and geotherms: solutions to an apparent contradiction. *Geophysical Research Letters* **10**, 1133–1136.

Jensen, L. S. 1976: A new cation plot for classifying subalkalic volcanic rocks. *Ontario Division of Mines Miscellaneous Papers* **66**, 22 pp.

Kalsbeek, F. 1976: Metamorphism in the Fiskenæsset region. *Rapport Grønlands Geologiske Undersøgelse* **73**, 34–41.

Kalsbeek, F. & Garde, A. A. 1989: Geological map of Greenland 1:500 000, Frederikshåb Isblink – Søndre Strømfjord, sheet 2. Descriptive text. Copenhagen: Geological Survey of Greenland, 36 pp.

Kalsbeek, F. & Pidgeon, R. T. 1980: The geological significance of Rb-Sr whole-rock isochrons of polymetamorphic Archaean gneisses, Fiskenæsset area, southern West Greenland. *Earth and Planetary Science Letters* **50**, 225–237.

Kalsbeek, F. & Taylor, P. N. 1983: Anatectic origin of mid-Proterozoic granite dyke in the Isukasia area, West Greenland. Pb-Pb and Rb-Sr isotopic evidence. *Rapport Grønlands Geologiske Undersøgelse* **115**, 38–42.

Kalsbeek, F., Bridgwater, D. & Boak, J. 1980: Evidence of mid-Proterozoic granite formation in the Isua area. *Rapport Grønlands Geologiske Undersøgelse* **100**, 73–75.

Kalsbeek, F., Pidgeon, R. T. & Taylor, P. N. 1987: Nagssugtoqidian mobile belt of West Greenland: a cryptic 1850 Ma suture between two Archaean continents – chemical and isotopic evidence. *Earth and Planetary Science Letters* **85**, 365–385.

Kalsbeek, F., Larsen, L. M. & Bondam, J. 1990: Geological map of Greenland 1:500 000, Sydgrønland, sheet 1. Descriptive text. Copenhagen: Geological Survey of Greenland, 36 pp.

Kusky, T, M. & Kidd, W. S. F. 1992: Remnants of an Archean oceanic plateau, Belingwe greenstone belt, Zimbabwe. *Geology* **20**, 43–46.

Larsen, L. M. & Rex, D. C. 1992: A review of the 2500 Ma span of alkaline-ultramafic, potassic and carbonatitic magmatism in West Greenland. *Lithos* **28**, 367–402.

Lauerma, R. 1964: On the structure and petrography of the Ipernat dome, western Greenland. *Bulletin de la Commission géologique de la Finlande* **215**, 1–88 (Also *Bulletin Grønlands Geologiske Undersøgelse* **46**, 88 pp).

Leveson, D. J. 1966: Orbicular rocks: a review. *Geological Society of America Bulletin* **77**, 409–426.

Macdonald, R. 1974: Investigations on the granulites of southern Nordland, Godthåbsfjord, central West Greenland. *Rapport Grønlands Geologiske Undersøgelse* **65**, 44–49.

Marker, M. & Garde, A. A. 1988: Border relations between the amphibolite facies Finnefjeld gneiss complex and granulite facies grey gneisses in the Fiskefjord area, southern West Greenland. *Rapport Grønlands Geologiske Undersøgelse* **140**, 49–54.

Martin, H. 1986: Effect of steeper Archaean geothermal gradient on geochemistry of subduction-zone magmas. *Geology* **14**, 753–756.

Martin, H. 1987: Petrogenesis of Archaean trondhjemites, tonalites and granodiorites from eastern Finland: major and trace element geochemistry. *Journal of Petrology* **28**, 921–953.

Martin, H. 1993: The mechanisms of petrogenesis of the Archaean continental crust – comparison with modern processes. *Lithos* **30**, 373–388.

Martin, H. 1994: The Archaean grey gneisses and the genesis of Archaean crust. *In* Condie, K. C. (ed.) *Archaean crustal evolution*, 205–259. Amsterdam: Elsevier.

McGregor, V. R. 1969: Early Precambrian geology of the Godthåb area. *Rapport Grønlands Geologiske Undersøgelse* **19**, 28–30.

McGregor, V. R. 1973: The early Precambrian gneisses of the Godthåb district, West Greenland. *Philosophical Transactions of the Royal Society of London* **A 273**, 343–358.

McGregor, V. R. 1993: Geological map of Greenland, 1:100 000, Qôrqut 64 V. 1 Syd. Descriptive text. Copenhagen: Geological Survey of Greenland, 40 pp.

McGregor, V. R. & Friend, C. R. L. 1992: Late Archaean prograde amphibolite- to granulite-facies relations in the Fiskenæsset region, southern West Greenland. *Journal of Geology* **100**, 207–219.

McGregor, V. R., Nutman, A. P. & Friend, C. R. L. 1986: The Archaean geology of the Godthåbsfjord region, southern West Greenland. *In* Ashwal, L. D. (ed.) Workshop on early crustal genesis: *The World's oldest rocks. Lunar and Planetary Institute Technical Report* **86-04**, 113–169.

McGregor, V. R., Friend, C. R. L. & Nutman, A. P. 1991: The late Archaean mobile belt through Godthåbsfjord, southern West Greenland: a continent-continent collision zone? *Bulletin of the Geological Society of Denmark* **39**, 179–197.

McKenzie, D. P. 1984: The generation and compaction of partially molten rock. *Journal of Petrology* **23**, 713–765.

Middlemost, E. A. K. 1975: The basalt clan. *Earth-Science Reviews* **11**, 337–364.

Moorbath, S. 1976: Age and isotope constraints for the evolution of Archaean crust. *In* Windley, B. F. (ed.) *The early history of the Earth*, 351–360. London: Wiley.

Myers, J. S. 1985: Stratigraphy and structure of the Fiskenæsset complex, West Greenland. *Bulletin Grønlands Geologiske Undersøgelse* **150**, 72 pp.

Myers, J. S. 1995: The generation and assembly of an Archaean supercontinent: evidence from the Yilgarn craton, Western Australia. *In* Coward, M. P. & Ries, A. C. (ed.) Early Precambrian processes. *Geological Society Special Publication* (London) **95**, 143–154.

Nakamura, N. 1974: Determination of REE, Ba, Mg, Na and K in carbonaceous and ordinary chondrites. *Geochimica et Cosmochimica Acta* **38**, 757–75.

Noe-Nygaard, A. & Ramberg, H. 1961: Geological reconnaissance map of the country between latitudes 69°N and 63°45′N, West Greenland. *Grønlands Geologiske Undersøgelse Geological Map* **1**, 9 pp. (Also *Meddelelser om Grønland* **123**(5)).

Nutman, A. P. 1991: Tectonostratigraphic terranes within Archaean gneiss complexes: examples from Western Australia and southern West Greenland. *Bulletin of the Geological Society of Denmark* **39**, 199–211.

Nutman, A. P. & Garde, A. A. 1989: Fluid control on emplacement of sialic magmas during Archaean crustal accretion. *In* Bridgwater, D. (ed.) *Fluid movements – element transport and the composition of the deep crust*, 235–243. Dordrecht: Kluwer.

Nutman, A. P. & Kalsbeek, F. 1994: A minimum age of 2944 ± 7 Ma for the Tartoq Group, South-West Greenland. *Rapport Grønlands Geologiske Undersøgelse* **161**, 35–38.

Nutman, A. P., Friend, C. R. L., Baadsgaard, H. & McGregor, V. R. 1989: Evolution and assembly of Archaean gneiss terranes in the Godthåbsfjord region, southern West Greenland: structural, metamorphic, and isotopic evidence. *Tectonics* **8**, 573–589.

Nutman, A. P., Friend, C. R. L., Kinny, P. D. & McGregor, V. R. 1993: Anatomy of an early Archaean gneiss complex: 3900 to 3600 Ma crustal evolution in southern West Greenland. *Geology* **21**, 415–418.

Nutman, A. P., Hagiya, H. & Maruyama, S. 1995: SHRIMP U-Pb single zircon geochronology of a Proterozoic mafic dyke, Isukasia, southern West Greenland. *Bulletin of the Geological Society of Denmark* **42**, 17–22.

Olsen, H. K. 1986: Tungsten mineralisation in Archaean supracrustal rocks at Sermitsiaq, southern West Greenland. *Rapport Grønlands Geologiske Undersøgelse* **130**, 60–63.

O'Nions, R. K. & Pankhurst, R. J. 1974: Rare earth element distribution in Archaean gneisses and anorthosites, Godthåb area, West Greenland. *Earth and Planetary Science Letters* **22**, 328–338.

O'Nions, R. K., Evensen, N. M. & Hamilton, P. J. 1980: Differentiation and evolution of the mantle. *Philosophical Transactions of the Royal Society of London* **A 297**, 479–493.

Passchier, C. 1995: Precambrian orogenesis: was it really different? *Geologie en Mijnbouw* **74**, 141–150.

Pearce, J. A. 1983: Role of the sub-continental lithosphere in magma genesis at active continental margins. *In* Hawkesworth, C. J. & Norry, M. J. (ed.) *Continental basalts and mantle xenoliths*, 230–249. Nantwich (UK): Shiva.

Pearce, J. A. & Cann, J. R. 1973: Tectonic setting of basic volcanic rocks determined using trace element analysis. *Earth and Planetary Science Letters* **19**, 290–300.

Pichamuthu, C. S. 1960: Charnockite in the making. *Nature* **188**, 135 only.

Pillar, J. E. 1985: Geochemistry of high grade gneisses with examples from West Greenland and British Columbia. Unpublished Ph.D. thesis, University of Leicester, U.K.

Ramberg, H. 1967: *Gravity, deformation and the Earth's crust as studied by centrifuged models*. New York: Academic Press, 241 pp.

Rapp, R. P., Watson, E. B. & Miller, C. F. 1991: Partial melting of amphibolite/eclogite and the origin of Archaean trondhjemites and tonalites. *Precambrian Research* **51**, 1–25.

Reed, S. J. 1980: The petrology of the high grade Archaean rocks from Nordlandet, southern West Greenland. Unpublished Ph.D. thesis, University of Exeter, U.K., 467 pp.

Riciputi, L. R., Valley, J. W. & McGregor, V. R. 1990: Conditions of Archean granulite metamorphism in the Godthaab–Fiskenaesset region, southern West Greenland. *Journal of Metamorphic Geology* **8**, 171–190.

Rivalenti, G. 1975: Chemistry and differentiation of mafic dykes in an area near Fiskenaesset, West Greenland. *Canadian Journal of Earth Sciences* **12**, 721–730.

Rivalenti, G. 1976: Geochemistry of metavolcanic amphibolites from South-West Greenland. *In* Windley, B. F. (ed.) *The early history of the Earth*, 213–223. London: Wiley.

Saunders, A. D., Tarney, J., Stern, C. & Dalziel, I. W. D. 1979: Geochemistry of Mesozoic marginal basin floor igneous rocks from southern Chile. *Geological Society of America Bulletin* **90**, 237–258.

Saunders, A. D., Tarney, J. & Weaver, S. D. 1980: Transverse geochemical variations across the Antarctic Peninsula: implications for the genesis of calc-alkaline magmas. *Earth and Planetary Science Letters* **46**, 344–360.

Saunders, A. D., Rogers, D., Marriner, G. F., Terrell, D. J. & Verma, S. P. 1987: Geochemistry of Cenozoic volcanic rocks, Baja California, Mexico: implications for the petrogenesis of post-subduction magmas. *Journal of Volcanology and Geothermal Resources* **32**, 223–246.

Schilling, J.-G., Zajac, M., Evans, R., Johnston, T., White, W., Devine, J. D. & Kingsley, R. 1983: Petrologic and geochemical variations along the Mid-Atlantic Ridge from 27°N to 73°N. *American Journal of Science* **283**, 510–586.

Schiøtte, L., Compston, W. & Bridgwater, D. 1988: Late Archaean ages for the deposition of clastic sediments belonging to the Malene supracrustals, southern West Greenland: evidence from an ion probe U-Pb zircon study. *Earth and Planetary*

Science Letters **87**, 45–58.

Shackleton, R. M. 1995: Tectonic evolution of greenstone belts. *In* Coward, M. P. & Ries, A. C. (ed.) Early Precambrian processes. *Geological Society Special Publication* (London) **95**, 53–65.

Sleep, N. H. & Windley, B. F. 1982: Archaean plate tectonics: constraints and inferences. *Journal of Geology* **90**, 363–379.

Sørensen, H. 1953: The ultrabasic rocks at Tovqussaq, West Greenland. *Bulletin Grønlands Geologiske Undersøgelse* **4**, 86 pp. (Also *Meddelelser om Grønland* **136**(4)).

Stecher, O. 1981: Geokemien af et Arkæisk amfibolit bælte fra Kangerdluarssungup Taserssua–Iortuarssup Tasia området, Vestgrønland. Unpublished thesis, Aarhus Universitet, Denmark, 128 pp.

Steenfelt, A. 1988: Progress in geochemical mapping of West Greenland. *Rapport Grønlands Geologiske Undersøgelse* **140**, 17–24.

Steenfelt, A. 1994: Crustal structure in West and South Greenland reflected by regional distribution patterns of calcium and potassium in stream sediment. *Rapport Grønlands Geologiske Undersøgelse* **161**, 11–20.

Stephens, W. E. & Halliday, A. N. 1984: Geochemical contrasts between late Caledonian granitoid plutons of northern, central and southern Scotland. *Transactions of the Royal Society of Edinburgh Earth Science* **72**, 259–273.

Stern C. R., Futa, K. & Muehlenbachs, K. 1984a: Isotopic and trace element data for orogenic andesites from the austral Andes. *In* Harmon, R. S. & Barreiro, B. A. (ed.) *Andean magmatism, chemical and isotopic constraints*, 1–46. Nantwich (UK): Shiva.

Stern C. R., Futa, K., Muehlenbachs, K., Dobbs, M., Munoz, J., Godoy, E. & Charrier, R. 1984b: Sr, Nd, Pb, O isotope composition of late Cenozoic volcanics; northernmost SVZ (33–34°S). *In* Harmon, R. S. & Barreiro, B. A. (ed.) *Andean magmatism, chemical and isotopic constraints*, 96–105. Nantwich (UK): Shiva.

Stern, R. A., Hanson, G. N. & Shirey, S. B. 1989: Petrogenesis of mantle-derived, LILE-enriched Archean monzodiorites and trachyandesites (sanukitoids) in southwestern Superior Province. *Canadian Journal of Earth Sciences* **26**, 1688–1712.

Streckeisen, A. L. 1976: To each plutonic rock a proper name. *Earth-Science Reviews* **12**, 1–33.

Sun, S.-S. 1980: Lead isotope study of young volcanic rocks from mid-ocean ridges, ocean islands and island arcs. *Philosophical Transactions of the Royal Society of London* **A**, **297**, 409–445.

Sun, S.-S. & McDonough, W. F. 1989: Chemical and isotopic systematics of oceanic basalts; implication for mantle composition and processes. *In* Saunders, A. D. & Norry, M. J. (ed.) Magmatism in the ocean basins. *Geological Society Special Publication* (London) **42**, 313–345.

Sun, S.-S. & Nesbitt, R. W. 1978: Petrogenesis of Archaean ultrabasic and basic volcanic rocks: evidence from rare earth elements. *Contributions to Mineralogy and Petrology* **65**, 301–325.

Sylvester, P. J. 1994: Archaean granite plutons. *In* Condie, K. C. (ed.) *Archaean crustal evolution*, 261–314. Amsterdam: Elsevier.

Tarney, J. & Jones, C. E. 1994: Trace element geochemistry of orogenic igneous rocks and crustal growth models. *Journal of the Geological Society* (London) **151**, 855–868.

Tatsumi, Y. & Ishizaka, K. 1982: Origin of high-magnesian andesites in the Setouchi volcanic belt, southwest Japan, I. Petrological and chemical characteristics. *Earth and Planetary Science Letters* **60**, 293–304.

Taylor, P. N., Moorbath, S., Goodwin, R. & Petrykowski, A. C. 1980: Crustal contamination as an indication of the extent of early Archaean continental crust: Pb isotopic evidence from the late Archaean gneisses of West Greenland. *Geochimica et Cosmochimica Acta* **44**, 1437–1453.

Taylor, S. R. & McLennan, S. M. 1985: *The continental crust: its composition and evolution*. Oxford: Blackwell, 312 pp.

van der Laan, S. & Wyllie, P. J. 1992: Constraints on Archaean trondhjemite genesis from hydrous crystallisation experiments on Nûk gneiss at 10–17 kbar. *Journal of Geology* **100**, 57–68.

Vernon, R. H. 1985: Possible role of superheated magma in the formation of orbicular granitoids. *Geology* **13**, 843–845.

Watterson, J. 1978: Proterozoic intraplate deformation in the light of south-east Asian neotectonics. *Nature* **273**, 636–640.

Weaver, B. L. & Tarney, J. 1981: Lewisian gneiss geochemistry and Archaean crustal development models. *Earth and Planetary Science Letters* **55**, 171–180.

Weaver, B. L., Tarney, J., Windley, B. F. & Leake, B. E. 1982: Geochemistry and petrogenesis of Archaean metavolcanic amphibolites from Fiskenaesset, S. W. Greenland. *Geochimica et Cosmochimica Acta* **46**, 2203–2215.

Wells, P. R. A. 1979: Chemical and thermal evolution of Archaean sialic crust, southern West Greenland. *Journal of Petrology* **20**, 187–226.

Wells, P. R. A. 1980: Thermal models for the magmatic accretion and subsequent metamorphism of continental crust. *Earth and Planetary Science Letters* **46**, 253–265.

Wiebe, R. A. 1979: Anorthositic dikes, southern Nain complex, Labrador. *American Journal of Science* **279**, 394–410.

Wiebe, R. A. 1990: Evidence for unusually feldspathic liquids in the Nain complex. *American Mineralogist* **75**, 1–12.

Wilf, C. I. Z. 1982: Geokemien af de grå amfiboliter, en del af en suprakrustal bjergartsenhed, ved Grædefjorden, nord for bygden Qeqertarsuatsiaat (Fiskenæsset) i den centrale del af Sydvestgrønland. Unpublished thesis, Aarhus Universitet, Denmark, 145 pp.

Wikström, A. 1984: A possible relationship between augen gneisses and postorogenic granites in S. E. Sweden. *Journal of Structural Geology* **6**, 409–415.

Williams, H. R., Stott, G. M., Thurston, P. C., Sutcliffe, R. H., Bennett, G., Easton, R. M. & Armstrong, D. K. 1992: Tectonic evolution of Ontario: summary and synthesis. *In* Thurston, P. C., Williams, H. R. Sutcliffe, R. H. & Stott, G. M. (ed.) Geology of Ontario. *Ontario Geological Survey Special Volume* **4**,(2), 1255–1324.

Wilson, M. 1989: *Igneous petrogenesis*. London: Unwin Hyman, 466 pp.

Windley, B. F. 1984: *The evolving continents*. London: Wiley, 399 pp.

Winther, T. K. & Newton, R. C. 1991: Experimental melting of hydrous low-K tholeiite: evidence on the origin of Archaean cratons. *Bulletin of the Geological Society of Denmark* **39**, 213–228.

Appendixes

All samples listed in Appendixes 1–13 are GGU samples (GGU = Grønlands Geologiske Undersøgelse).

Analytical procedures. Major element analysis at the Geological Survey of Greenland; most elements by XRF on fused glass disks, except Fe_2O_3 by titration and Na_2O by atomic absorption spectrometry. Trace elements analysed by XRF on pressed powder pellets at the Geological Institute, University of Copenhagen (analysts J. C. Bailey and J. Christensen). Further details concerning the analytical methods, and information about detection limits and precision of the XRF methods at these laboratories can be found in Blichert-Toft *et al.* (1995).

†: INNA at Activation Laboratories Ltd., Canada ('research grade' analyses). In some samples Th, La, Ce and Nd were analysed by both INNA and XRF on pressed powders. For these elements the INNA method has lower detection limits and a better precision at low concentrations. Otherwise agreement between the two sets of analyses is good (generally within 10%), and no corrections to the results obtained by either method have been made. Where these elements appear in figures displaying geochemical data, the accompanying text to the first figure indicates which analytical method was used.

Appendix 1. Chemical compositions of homogeneous amphibolites from the Fiskefjord area

GGU	Retrogressed		Granulite facies			all samples		granulite facies		retrogressed	
No	289141	289120	278758	339508	278849	average (*n=31*)	s.d.	average (*n=22*)	s.d.	average (*n=9*)	s.d.
SiO_2	47.64	49.45	50.74	51.34	55.66	50.43	2.62	50.88	2.72	49.33	2.09
TiO_2	0.62	0.73	0.54	0.46	0.78	0.67	0.15	0.64	0.11	0.76	0.20
Al_2O_3	15.06	14.61	14.19	15.58	17.09	15.17	1.04	15.44	1.11	14.53	0.43
Fe_2O_3	3.44	4.32	2.82	2.41	2.33	3.14	0.95	2.84	0.78	3.87	0.98
FeO	7.32	7.34	7.36	5.61	5.36	7.59	1.31	7.63	1.48	7.51	0.82
FeO*	10.42	11.23	9.90	7.78	7.46	10.42	1.61	10.19	1.65	10.99	1.44
MnO	0.18	0.20	0.15	0.15	0.11	0.17	0.03	0.17	0.03	0.19	0.02
MgO	10.42	7.71	10.16	9.42	6.65	8.39	0.89	8.35	0.75	8.50	1.23
CaO	10.88	10.57	9.36	9.31	7.15	9.94	1.92	9.72	2.10	10.48	1.35
Na_2O	2.15	2.75	2.98	3.51	3.77	2.67	0.59	2.74	0.63	2.49	0.45
K_2O	0.54	0.58	0.76	0.83	0.42	0.57	0.32	0.60	0.35	0.48	0.19
P_2O_5	0.03	0.05	0.04	0.08	0.17	0.09	0.05	0.09	0.05	0.09	0.05
l.o.i.	1.61	1.34	0.98	0.91	0.35	1.12	0.38	0.97	0.34	1.49	0.15
Sum	99.89	99.65	100.08	99.61	99.84	99.96 (*n=26*)	0.37	100.06 (*n=19*)	0.35	99.71 (*n=7*)	0.29
Rb	9	3.3	7.7	5	1	9	14	10	16	5	4
Ba	108	111	178	29	193	150	115	157	122	130	99
Pb	1	1	3	9	4	3	3	3	3	3	2
Sr	113	161	182	311	417	177	106	182	113	163	90
La	9	5		11	8	6	5	6	5	7	4
Ce	9	10		23	11	10	9	10	10	11	4
Nd	7	8	3	11	11	8	5	8	5	8	2
Y	17	19	14	13	17	18	4	18	3	17	6
Th	<1	<1	<1	<1	<1	<1			<1	<1	
Zr	41	40	37	42	123	59	35	60	39	56	23
Nb	2	3.7	3	3	4	3	1	3	2	3	1
Zn	83	104	59	82	69	91	16	88	14	98	19
Cu	25	57	11	9	41	44	57	34	44	70	82
Co	75	62	74	57	48	68	8	68	9	67	8
Ni	219	148	142	143	90	146	50	145	49	150	58
V	214	260	229	177	161	232	52	225	50	252	57
Cr	571	317	690	697	236	409	182	405	196	419	149
Ga	14	17	14	16	22	18 (*n=13*)	5	18	2	20	10
Cs †	0.2	0.2	0.2	0.2	0.2	0.3	0.1				
Hf †	1.0	1.0	0.6	1.0	3.2	1.1	0.8				
Sc †	31.1	37.8	36.3	31.2	23.5	35.4	6.7				
Ta †	<0.3	<0.3	<0.3	<0.3	<0.3						
Th †	0.2	0.4	0.8	0.7	0.1	0.4	0.3				
U †	0.1	0.1	0.1	0.1	0.1	0.1	0.1				
La †	3.8	5.0	4.3	10.4	10.6	6.1	3.6				
Ce †	9	12	9	21	20	12.8	6.3				
Nd †	5	7	5	10	11	7.2	3.1				
Sm †	1.51	1.83	1.37	2.23	2.75	1.89	0.55				
Eu †	0.60	0.64	0.58	0.7	0.88	0.68	0.14				
Tb †	0.4	0.5	0.4	0.4	0.6	0.5	0.1				
Yb †	1.7	2.02	1.78	1.51	1.84	2.00	0.36				
Lu †	0.21	0.27	0.22	0.20	0.23	0.26	0.05				

Representative analyses, grand average, and averages of 22 amphibolites with granulite facies parageneses, and of nine amphibolites with textural evidence of partial rehydration. Sample localities are shown in Fig. 17.

Appendix 2. Chemical compositions of various amphibolites from the Fiskefjord area

GGU	Leuco-amphibolite						Eastern amphibolite		Heterogeneous amphibolite			
No	339180	278792	278835	289199	average (*n*=8)	s.d.	289205	289166	278848	278744	278788	289204
SiO_2	53.05	55.92	59.19	63.80	57.23	4.80	48.60	50.24	47.17	49.57	51.43	53.40
TiO_2	0.86	0.87	0.73	0.50	0.77	0.26	0.55	0.87	0.30	1.11	0.62	0.85
Al_2O_3	18.39	16.78	17.40	17.09	16.96	1.56	18.78	17.33	20.98	14.59	15.41	17.80
Fe_2O_3	2.67	1.97	1.28	1.21	2.49	1.34	1.94	3.59	4.02	5.22	2.26	1.45
FeO	5.24	6.43	6.24	3.22	4.83	1.22	6.74	6.91	4.96	8.75	6.03	5.28
FeO*	7.64	8.20	7.39	4.31	7.07	1.85	8.49	10.14	8.58	13.45	8.06	6.59
MnO	0.12	0.11	0.11	0.06	0.12	0.03	0.15	0.18	0.18	0.22	0.16	0.13
MgO	4.69	3.89	3.66	2.24	3.67	0.82	7.56	5.39	3.67	3.55	4.87	3.09
CaO	8.34	7.22	4.94	5.18	7.30	2.13	11.50	9.79	14.52	12.80	14.62	14.67
Na_2O	2.05	4.02	4.50	4.31	3.78	0.95	2.55	3.98	2.20	3.04	2.70	1.92
K_2O	0.32	1.13	0.81	1.06	0.83	0.38	0.36	0.63	0.72	0.42	0.33	0.13
P_2O_5	0.27	0.25	0.15	0.13	0.24	0.15	0.08	0.16	0.22	0.07	0.13	0.07
l.o.i.	1.44	0.92	0.54	0.62	1.02	0.47	1.24	1.18	0.93	1.06	1.52	1.52
Sum	97.44	99.51	99.55	99.42	99.21	0.72	100.05	100.25	99.87	100.40	100.08	100.31
Rb	1	34	6	42	25	26	3	2	20	2	2	2
Ba	322	291	275	352	327	160	13	68	221	57	179	16
Pb	7	6	<1	6	6	3	2	<1	<1	4	7	5
Sr	726	340	340	490	478	225	226	259	204	123	583	191
La	20	31	11	16	30	21	13	16	26	<1	12	7
Ce	53	32	21	29	48	35	11	25	26	8	30	16
Nd	31	43	11	12	27	17	6	14	15	7	17	10
Y	16	22	13	50	22	12	1	23	16	33	16	180
Th	<1	<1	<1	<1	<1		<1		<1	<1	<1	<1
Zr	73	136	152	89	111	44	50	83	42	65	53	83
Nb	4	6	5	4	6	2	4	5	2	3	4	4
Zn	97	81	56	57	83	25	70	121	78	165	73	80
Cu	51	5	<1	11	18	16	8	<1	6	35	15	36
Co	42	11	63	40	48	20	57	68	52	88	55	69
Ni	58	49	52	17	52	24	144	57	21	65	151	94
V	159	133	122	58	129	44	157	168	190	323	181	158
Cr	49	166	145	39	115	102	346	110	32	148	488	194
Ga	22	20	20	21	20	3	18	18	15	19	12	19
Cs †	0.4	1.4	0.2				0.2	0.2				
Hf †	1.4	3.3	3.8				1.3	2.0				
Sc †	19.8	18.6	17.6				28.3	27.7				
Ta †	0.5	0.4	0.4				0.3	0.6				
Th †	0.3	3.9	0.1				0.8	1.2				
U †	0.1	0.8	0.1				0.1	0.3				
La †	21.8	28.1	10.8				5.7	11.6				
Ce †	44	51	20				13	25				
Nd †	26	23	11				7	12				
Sm †	4.88	4.49	2.24				1.7	2.82				
Eu †	1.47	1.42	0.88				0.62	0.91				
Tb †	0.7	0.7	0.4				0.4	0.5				
Yb †	1.59	2.36	1.3				1.83	2.39				
Lu †	0.21	0.3	0.18				0.28	0.3				

Representative samples and average of leuco-amphibolite, and examples of eastern amphibolite and heterogeneous amphibolite. Sample localities are shown in Fig. 17.

Appendix 3. Chemical compositions of metasediments from the Fiskefjord area

GGU	Quartzo-feldspathic metasediment				Biotite schist			
No	289161	289191	289163	283361	289046	339573	283718	339926
SiO_2	61.04	61.35	62.03	68.08	50.08	57.16	61.53	62.37
TiO_2	0.54	1.24	0.55	0.36	1.28	0.79	0.44	1.34
Al_2O_3	15.89	15.66	15.62	16.68	15.30	19.52	16.71	10.68
Fe_2O_3	1.38	3.05	1.36	0.38	8.50	5.45	1.70	4.69
FeO	3.87	4.72	4.51	2.21	8.91	5.69	4.17	9.20
FeO*	5.11	7.47	5.73	2.55	16.56	10.60	5.70	13.42
MnO	0.10	0.11	0.10	0.05	0.19	0.13	0.08	0.10
MgO	3.56	2.35	3.90	1.06	4.12	4.30	4.07	7.92
CaO	6.54	4.69	5.63	3.29	3.62	2.27	6.30	1.38
Na_2O	3.76	3.95	3.73	4.52	2.60	2.05	3.03	1.64
K_2O	1.61	1.70	1.02	2.70	1.97	1.46	0.47	0.21
P_2O_5	0.15	0.18	0.14	0.13	0.24	0.06	0.15	0.07
l.o.i.	0.66	0.73	0.64	0.25	3.20	1.54	1.06	0.86
Sum	99.10	99.73	99.23	99.72	100.01	100.41	99.70	100.46
Rb	58	94	22	83	72	44		2.4
Ba	518	245	544	589	226	536		67
Pb	10	10	9	25	22	5		6
Sr	215	191	235	279	60	208		22
La	25	18	23	31	7	5		7
Ce	40	39	30	58	29	11		12
Nd	17	22	15	25	17	3		9
Y	14	34	12	6	31	14		58
Th	4	7	2	8	<1	1		4
Zr	137	188	119	113	134	63		97
Nb	6.7	8.6	5	4.1	7.9	3		4.3
Zn	72	101	81	63	384	165		98
Cu	8	19	<1	13	115	95		<1
Co	51	49	59	18	82	155		112
Ni	70	34	58	7	7	302		64
V	91	184	95	33	249	342		185
Cr	146	14	161	11	28	643		0
Ga	17	21	19	19	21	25		28
Sc	12	19	13	5		46		92

Sample localities are shown in Fig. 17.

Appendix 4. Chemical compositions of norite, ultramafic rocks and anorthosite from the Fiskefjord area

GGU	Norite							Ultramafic rocks								Anorthosite	
No	339922	289145	339163	278710	339164	average (n=5)	s.d.	328286	339564	328269	339538	289109	283710	average (n=6)	s.d.	339501	125763 Fiskenæsset
SiO_2	49.09	49.43	49.62	49.81	50.41	49.67	0.49	45.63	47.25	47.47	49.47	50.50	54.09	49.07	17.29	47.13	48.97
TiO_2	0.19	0.07	0.11	0.11	0.12	0.12	0.04	0.29	0.39	0.67	0.53	0.51	0.09	0.41	3.04	0.21	0.12
Al_2O_3	19.36	20.76	20.24	17.74	16.75	18.97	1.69	7.17	9.91	6.42	6.08	7.18	1.24	6.33	2.60	29.74	31.41
Fe_2O_3	1.76	1.51	2.01	0.89	2.80	1.79	0.70	6.00	5.07	4.27	4.36	3.11	0.80	3.94	2.47	0.00	0.25
FeO	7.25	4.10	4.10	6.76	4.60	5.36	1.52	6.71	6.29	9.05	7.80	8.45	3.86	7.03	2.55	2.73	0.75
FeO*	8.83	5.46	5.91	7.56	7.12	6.98	1.34	12.11	10.85	12.89	11.72	11.25	4.58	10.57	3.97	2.73	0.97
MnO	0.18	0.12	0.15	0.15	0.15	0.15	0.02	0.21	0.20	0.26	0.22	0.22	0.16	0.21	3.12	0.06	0.03
MgO	11.81	11.43	10.76	13.97	15.94	12.78	2.14	28.28	18.52	13.83	18.50	13.71	19.79	18.77	7.17	2.21	0.90
CaO	9.82	10.75	10.05	9.29	7.45	9.47	1.25	5.22	10.03	14.90	10.80	13.44	16.82	11.87	4.77	15.31	14.63
Na_2O	0.96	1.09	1.69	0.80	1.16	1.14	0.34	0.12	0.95	1.41	0.96	1.41	0.51	0.89	2.88	1.88	1.79
K_2O	0.04	0.29	0.65	0.09	0.54	0.32	0.27	0.07	0.16	0.43	0.54	0.23	0.02	0.24	3.11	0.29	0.46
P_2O_5	0.05	0.01	0.05	0.00	0.05	0.03	0.02	0.04	0.07	0.09	0.05	0.04	0.02	0.05	3.18	0.05	0.10
l.o.i.	0.74	0.59	0.87	0.82	0.75	0.75	0.11	0.76	1.25	1.30	0.78	1.35	2.02	1.24	2.74	0.58	0.44
Sum	101.25	100.15	100.29	100.43	100.71	100.57	0.43	100.49	100.09	100.09	100.10	100.15	99.42	100.06	0.35	100.19	99.85
Rb	1	16	31	1	13	12	13		3		6	4				3.5	26
Ba	23	27	139	23	47	52	50		39		70	30				93	33
Pb	2	1	9	<1	<1	2	4		2		2	1				5	5
Sr	54	64	63	43	61	57	9		42		31	71				149	83
La																<2	11
Ce																5	18
Nd	<2	<2	2	<2	<2	<2			5		8	6				1	6
Y	5	2	3	4	3	3	1		10		16	15				4	2
Th	<1	<1	<1	<1	<1	<1			<1		<1	<1				1	3
Zr	10	5	12	4	11	8	4		31		52	34				12	6
Nb	1	1	1	1	1	1	0		2		5	3				2.1	<1
Zn	60	40	47	47	62	51	9		87		117	92				34	8
Cu	<2	9	<2	<2	<2	2	4		47		20	22				5	17
Co	78	65	53	74	71	68	10		90		109	83				55	13
Ni	134	203	102	192	247	176	58		655		981	237				57	25
V	153	89	113	152	142	130	28		188		180	252				70	28
Cr	109	399	173	263	949	379	337		2340		1860	1170				101	232
Ga	4	11	12	13	9	10	4		13		14	11				18	21
Cs †	<0.2	0.5	1.5	<0.2	1.0			<0.2	<0.2	<0.2	0.6	<0.2	<0.2	<0.2			
Hf †	<0.2	<0.2	0.4	0.2	0.2	0.3	0.1	0.4	0.6	1.1	0.6	0.9	<0.2	0.6	0.4		
Sc †	38.8	21.1	27.0	33.3	31.6	30.4	6.7	22.6	30.9	49.1	21.5	45.4	41.4	35.2	11.8		
Ta †	<0.3	<0.3	<0.3	<0.3	0.3	<0.3		<0.3	<0.3	<0.3	0.3	<0.3	<0.3	<0.3			
Th †	<0.1	0.1	0.9	0.1	<0.1			0.2	0.4	<0.1	0.2	0.1	0.2	0.2	0.1		
U †	<0.1	<0.1	0.3	<0.1	<0.1	<0.1		<0.1	<0.1	<0.1	<0.1	<0.1	<0.1	<0.1			
La †	0.6	0.8	3.3	0.7	1.0	1.3	1.1	1.8	2.4	3.8	5.3	3.7	1.7	3.1	1.4		
Ce †	2	2	5	2	2	3	1.3	4	6	9	14	10	4	8	4		
Nd †	1	1	2	<1	1	1	0.7	2	4	6	9	6	1	5	3		
Sm †	0.26	0.15	0.28	0.23	0.18	0.22	0.05	0.6	0.87	1.84	2.2	1.54	0.18	1.21	0.78		
Eu †	0.21	0.14	0.16	0.14	0.14	0.16	0.03	0.22	0.45	0.8	0.87	0.51	0.07	0.49	0.31		
Tb †	0.1	0.1	0.1	<0.1	0.1	0.1	0.1	0.2	0.2	0.5	0.5	0.3	0.0	0.3	0.2		
Yb †	0.90	0.38	0.54	0.62	0.38	0.56	0.21	0.86	1.16	1.54	1.52	1.40	0.25	1.12	0.50		
Lu †	0.12	0.05	0.07	0.08	0.06	0.08	0.03	0.12	0.17	0.19	0.19	0.18	0.03	0.15	0.06		

Sample localities shown in Fig. 17. Anorthosite sample GGU 125763 from the Fiskenæsset complex, southern West Greenland (Ashwal & Myers, 1994) shown for comparison.

Appendix 5. Chemical compositions of dioritic grey gneiss, Fiskefjord area

GGU	Amphibolite facies						Granulite facies						Retrogressed					
No	283366	289273	283331	289272	average (*n=7*)	s.d.	283630	283672	289160	283673	average (*n=20*)	s.d	283680	278752	278711	278767	average (*n=10*)	s.d
SiO_2	57.98	58.50	62.40	63.25	60.67	2.32	52.63	56.29	57.63	63.26	57.13	3.71	55.06	61.39	62.36	63.63	60.49	2.61
TiO_2	0.89	0.55	0.62	0.57	0.63	0.12	1.10	1.01	0.65	0.65	0.79	0.19	1.05	0.60	0.58	0.63	0.71	0.17
Al_2O_3	18.89	16.92	16.09	15.43	16.53	1.17	19.07	19.35	15.42	15.92	16.95	1.29	16.97	14.86	15.77	15.86	16.24	0.95
Fe_2O_3	2.35	1.42	1.42	1.33	1.54	0.39	4.06	3.69	2.60	2.30	3.13	1.02	3.19	1.78	1.67	1.89	2.10	0.49
FeO	3.96	4.58	4.04	3.99	4.29	0.38	5.14	3.78	5.25	4.22	4.63	0.92	5.87	4.12	4.04	3.69	4.40	0.64
FeO*	6.08	5.86	5.32	5.19	5.67	0.43	8.79	7.10	7.59	6.29	7.46	1.64	8.74	5.72	5.54	5.39	6.29	1.01
MnO	0.09	0.11	0.10	0.10	0.10	0.01	0.13	0.12	0.14	0.12	0.14	0.03	0.15	0.09	0.09	0.08	0.11	0.02
MgO	2.07	4.23	3.07	3.23	3.42	0.75	3.53	2.26	5.25	2.64	3.78	1.22	4.26	4.70	3.13	2.46	3.44	0.85
CaO	6.16	6.47	5.53	5.12	5.87	0.52	7.95	7.11	6.96	5.53	7.66	1.15	7.56	4.79	5.15	5.19	5.80	0.90
Na_2O	5.05	4.40	4.19	3.88	4.23	0.40	5.02	4.93	4.22	3.96	4.10	0.60	3.49	3.50	4.10	4.48	3.96	0.46
K_2O	1.43	1.41	1.38	1.78	1.51	0.14	0.27	0.75	0.76	0.63	0.64	0.20	0.96	1.59	0.91	0.97	1.13	0.24
P_2O_5	0.28	0.19	0.20	0.17	0.20	0.04	0.30	0.24	0.10	0.12	0.17	0.06	0.15	0.13	0.16	0.14	0.18	0.04
l.o.i.	0.44	0.51	0.45	0.44	0.48	0.04	1.05	0.33	0.50	0.39	0.59	0.38	1.03	1.33	1.06	0.54	0.87	0.37
Sum	99.59	99.30	99.49	99.29	99.47 (*n=5*)	0.18	100.25	99.86	99.48	99.73	99.72	0.24	99.73	98.88	99.02	99.56	99.42	0.30
Rb		42		74	58	12	<1	2	7	2	4	3	24	60	13	12	28	16
Ba		384		444	420	33	349	243	218	263	237	163	304	397	335	377	361	84
Pb		9		10	9	1	8	9	5	6	7	3	8	3	4	3	6	4
Sr		409		286	351	48	669	428	217	220	283	143	220	326	415	390	335	94
La		21		28	24	3	11	14	13	10	13	3	16	23	18	18	18	3
Ce		39		43	38	3	27	28	20	22	28	8	35	47	36	33	34	8
Nd		19		21	17	5	18	16	13	11	16	4	22	26	17	19	19	4
Y		13		15	14	1	11	17	16	13	19	6	25	24	16	10	20	7
Th		5		7	4	2	2	1	<1	<1	2	1	3	1	1	<1	1	1
Zr		82		120	111	20	19	256	137	80	119	68	251	161	112	91	137	49
Nb		5.7		7.2	6.4	0.6	3.1	6.5	4.4	2.9	5.8	2.0	9.7	9.5	6.2	6.8	7.5	1.3
Zn		74		65	71	7	103	75	84	67	89	19	116	67	67	81	78	16
Cu		6		<1	4	3	102	31	0	44	21	23	26	10	10	<1	13	8
Co		37		31	33	2	41	41	64	56	55	12	47	42	45	70	49	13
Ni		82		56	67	10	25	17	124	40	55	27	53	85	50	26	52	22
V		112		90	103	12	188	93	127	104	138	42	236	98	86	71	109	47
Cr		195		160	175	18	13	12	172	42	81	55	87	253	110	65	123	78
Ga		18		15	17	1	22	22	18	17	20	2	21	19	16	18	19	2
Sc		15		14	15 (*n=5*)	1	17	13	19	14	21 (*n=6*)	7	25	16	12		19 (*n=3*)	6
Cs †		2.2		2.0	2.3	0.2		<0.1	<0.1	<0.1	0.1	0.1		<0.1	<0.1	<0.1	<0.1	<0.1
Hf †		2.8		2.3	2.8	0.5		4.6	2.6	2.0	3.0	0.9		4.8	3.6	2.2	3.5	1.3
Sc †		14.6		12.6	14.0	1.1		14.4	18.7	13.7	18.0	3.8		15.9	12.6	10.4	13.0	2.8
Ta †		0.0		0.5	0.5	0.3		0.4	0.8	<0.3	0.4	0.3		0.5	0.5	<0.3	0.3	0.3
Th †		1.7		6.3	2.8	1.9		0.0	0.0	0.1	0.3	0.4		0.9	1.4	0.4	0.9	0.5
U †		0.0		1.1	0.6	0.4		<0.1	<0.1	<0.1	<0.1	<0.1		<0.1	<0.1	<0.1	<0.1	<0.1
La †		20.2		25.5	22.1	2.0		12.2	10.1	11.2	12.8	2.8		21.5	17.2	18.5	19.1	2.2
Ce †		35		43	38	4		23	19	18	24	6		43	31	35	36	6
Nd †		15		17	16	2		12	10	9	13	4		23	15	16	18	4
Sm †		2.84		3.11	2.95	0.15		2.77	2.18	1.92	2.84	0.78		4.64	2.87	2.76	3.42	1.06
Eu †		0.93		0.86	0.91	0.04		1.09	0.80	0.74	0.94	0.15		0.90	0.91	0.81	0.87	0.06
Tb †		0.3		0.4	0.4	<0.3		0.4	0.5	0.4	0.5	0.1		0.7	0.6	0.4	0.6	0.2
Yb †		1.17		1.31	1.25	0.05		1.39	1.51	1.28	1.78	0.50		2.22	1.77	0.97	1.65	0.63
Lu †		0.15		0.17	0.16	0.01		0.18	0.19	0.16	0.23	0.06		0.26	0.27	0.13	0.22	0.08

Representative samples and averages of all analyses (amphibolite facies, granulite facies and retrogressed). Sample locations in Fig. 52.

Appendix 6. Chemical compositions, Qeqertaussaq diorite, Fiskefjord area

GGU	(Variably retrogressed)						
No	328565	328563	328567	339223	339224	average (*n*=22)	s.d.
SiO_2	55.16	56.77	58.14	59.40	64.75	58.84	3.35
TiO_2	0.97	0.68	0.65	0.61	0.38	0.62	0.20
Al_2O_3	18.05	17.84	17.41	16.94	16.95	17.47	0.79
Fe_2O_3	3.80	3.19	2.91	2.60	0.90	2.39	0.83
FeO	3.57	3.35	3.29	3.34	2.41	3.19	0.73
FeO*	6.99	6.22	5.91	5.68	3.22	5.34	1.28
MnO	0.11	0.12	0.12	0.12	0.07	0.10	0.02
MgO	3.12	3.59	3.24	3.02	1.96	3.01	0.64
CaO	6.29	5.77	5.87	5.76	4.02	5.54	0.99
Na_2O	5.45	5.76	4.94	5.34	5.34	5.21	0.61
K_2O	1.19	1.45	1.46	0.94	0.95	1.61	0.81
P_2O_5	0.63	0.25	0.37	0.36	0.27	0.38	0.10
l.o.i.	1.02	0.91	0.72	0.82	1.02	0.86	0.26
Sum	99.35	99.67	99.12	99.25	99.01	99.21	0.60
Rb	10	10	10	4	4	17	14
Ba	755	896	1400	1560	1690	1465	811
Pb	17	18	19	14	12	18	8
Sr	1050	1190	1200	1100	980	1240	290
La	40	38	46	40	43	52	27
Ce	101	85	95	78	83	106	48
Nd	59	40	47	40	34	51	20
Y	25	16	16	15	5	16	5
Th	2	2	2	<1	2	5	8
Zr	115	65	110	114	91	120	27
Nb	9.0	5.4	5.4	4.3	2.0	4.9	1.7
Zn	115	100	94	88	71	90	13
Cu	51	13	33	15	27	26	16
Co	34	40	35	41	42	39	8
Ni	30	42	18	20	17	31	16
V	123	128	124	115	50	103	29
Cr	17	39	29	25	18	40	26
Ga	25	21	22	20	19	21	2
Sc	14	15	17	14	23	14 (*n=5*)	4
Cs †	<0.1	<0.1	<0.1	<0.1	0.5	0.1	0.2
Hf †	3.1	1.7	3.5	2.0	2.0	2.5	0.8
Sc †	12.4	15.2	14.2	13.2	13.9	13.8	1.1
Ta †	0.5	<0.3	<0.3	<0.3	<0.3	<0.3	<0.3
Th †	0.7	1.5	0.4	0.5	0.9	0.8	0.4
U †	<0.1	<0.1	<0.1	<0.1	<0.1	0.2	0.4
La †	45.0	41.5	48.2	43.4	50.5	45.7	3.6
Ce †	87	75	79	72	74	77	6
Nd †	45	34	37	34	29	36	6
Sm †	8.66	5.78	6.24	6.18	4.08	6.19	1.64
Eu †	2.11	1.90	1.72	1.69	1.28	1.74	0.31
Tb †	0.9	0.7	0.7	0.7	0.4	0.7	0.2
Yb †	1.93	1.41	1.35	1.29	0.30	1.26	0.59
Lu †	0.24	0.19	0.19	0.17	0.05	0.17	0.07

Representative samples and average of all analyses. The Qeqertaussaq diorite is enriched in P_2O_5, LREE and several LIL elements but depleted in high field strength elements relative to dioritic grey gneiss. Sample locations in Fig. 52.

Appendix 7. Chemical compositions of amphibolite and granulite facies tonalitic-trondhjemitic grey gneiss, Fiskefjord area

GGU	Amphibolite facies								Granulite facies							
No	339558	283347	289278	283343	289280	289279	average (*n=19*)	s.d.	278754	339551	278756	339550	328250	339528	average (*n=19*)	s.d.
SiO_2	65.06	67.99	69.41	72.07	73.92	74.73	71.04	2.61	62.19	63.99	66.53	70.93	72.36	73.45	69.22	4.20
TiO_2	0.71	0.39	0.13	0.19	0.06	0.05	0.25	0.15	0.71	0.48	0.51	0.35	0.29	0.17	0.35	0.17
Al_2O_3	16.49	16.36	17.24	15.68	13.98	14.24	15.48	1.01	17.03	17.07	16.47	14.52	15.67	14.17	15.64	1.17
Fe_2O_3	0.30	0.82	0.36	0.21	0.17	0.15	0.36	0.22	1.74	1.21	1.25	1.80	0.33	1.19	1.07	0.50
FeO	3.05	2.12	0.97	0.96	0.55	0.56	1.37	0.68	3.99	2.97	2.82	1.99	0.84	1.09	2.09	0.91
FeO*	3.32	2.86	1.29	1.15	0.70	0.70	1.69	0.77	5.56	4.06	3.95	3.61	1.14	2.16	2.91	1.26
MnO	0.04	0.05	0.03	0.04	0.01	0.02	0.03	0.01	0.08	0.08	0.05	0.06	0.03	0.03	0.06	0.02
MgO	1.29	0.97	0.44	0.38	0.08	0.08	0.57	0.37	2.34	2.56	1.47	0.93	0.41	0.49	1.24	0.73
CaO	3.12	3.60	3.27	2.00	1.32	1.09	2.52	0.91	5.66	5.35	4.65	3.75	3.36	3.48	4.10	0.89
Na_2O	4.40	4.66	5.48	5.80	2.89	4.67	4.71	0.68	4.78	4.45	4.83	4.05	4.38	4.35	4.49	0.35
K_2O	3.66	1.40	1.84	1.74	5.83	4.03	2.65	1.47	0.74	0.31	0.61	0.35	0.79	0.51	0.68	0.27
P_2O_5	0.25	0.13	0.04	0.06	0.02	0.02	0.08	0.05	0.20	0.18	0.15	0.11	0.03	0.07	0.12	0.05
l.o.i.	0.88	0.24	0.11	0.11	0.06	0.06	0.24	0.24	0.33	0.52	0.41	0.30	0.21	0.18	0.36	0.16
Sum	99.26	98.73	99.32	99.25	98.89	99.70	99.27 (n=18)	0.35	99.79	99.16	99.75	99.15	98.69	99.19	99.41	0.33
Rb	135	81	40	99	114	94	81	26	4	<1	2	<1	2	1	4	10
Ba	1490	449	411	453	1100	273	691	361	328	313	512	355	816	364	430	189
Pb	30	15	15	24	37	32	22	7	2	5	8	6	13	8	7	2
Sr	371	381	728	475	250	183	382	146	540	586	559	227	921	287	417	266
La	146	19	3	14	7	3	27	36	13	13	10	7	9	10	13	5
Ce	290	46	4	17	10	5	47	68	37	17	15	16	14	18	24	9
Nd	99	14	3	8	7	3	17	23	23	8	10	6	4	7	11	5
Y	28	6	2	6	2	2	6	6	9	5	4	4	<1	1	7	7
Th	35	16	1	6	16	4	12	9	<1	<1	<1	<1	3	2	1	2
Zr	387	159	42	80	37	13	122	88	141	119	109	228	185	124	134	46
Nb	12.0	4.6	2.5	3.3	1.2	3.6	4.0	2.6	6.5	1.4	3.0	1.7	0.9	1.0	3.1	2.1
Zn	65	66	23	49	5	12	39	17	79	68	60	52	19	41	53	17
Cu	38	8	3	<1	<1	3	6	8	18	4	11	4	10	5	12	14
Co	47	11	21	16	23	30	31	24	58	69	72	152	56	143	91	43
Ni	8	7	4	5	4	2	6	3	27	35	11	6	5	3	14	12
V	50	32	12	11	2	0	17	13	73	66	43	36	29	14	36	20
Cr	18	11	11	8	4	4	10	7	53	54	26	9	4	6	21	18
Ga	22	19	17	22	13	14	17	3	21	21	18	14	14	12	17	3
Sc	1	5	<1	1	<1	<1	2 (*n=9*)	2		10		6	2	1	5 (*n=7*)	3
Cs †		1.7	0.6	2.0	0.7	0.4	1.6	1.6	<0.2	<0.2	<0.2	<0.2			<0.2	0.1
Hf †		3.8	1.6	3.0	1.4	0.9	2.6	1.2	2.1	2.0	1.8	4.1			2.3	0.8
Sc †		4.1	2.4	1.9	0.8	1.6	2.8	1.5	9.3	8.2	5.5	4.4			7.3	2.5
Ta †		0.5	0.3	<0.3	0.5	0.9	0.4	0.3	0.4	<0.3	<0.3	<0.3			<0.3	<0.3
Th †		11.0	0.3	3.6	12.9	1.5	6.3	5.2	<0.2	<0.2	<0.2	<0.2			0.0	0.1
U †		1.0	<0.1	1.2	1.0	0.6	0.6	0.5	<0.1	<0.1	<0.1	0.4			0.1	0.2
La †		17.6	4.1	17.0	13.1	5.0	14.7	8.5	17.0	8.8	13.9	11.3			12.8	3.1
Ce †		47	6	26	24	6	26	15	33	15	22	16			22	7
Nd †		11	3	11	10	3	9	4	16	6	10	6			10	4
Sm †		1.91	0.52	1.60	1.14	0.31	1.39	0.65	3.10	1.24	1.77	0.83			1.78	0.80
Eu †		0.61	0.34	0.40	0.43	0.23	0.46	0.13	0.98	0.68	0.69	0.95			0.84	0.13
Tb †		0.2	0.1	<0.1	0.1	0.1	0.1	0.1	0.4	0.2	0.3	0.2			0.3	0.1
Yb †		0.44	0.18	0.33	0.18	0.13	0.36	0.26	0.80	0.47	0.38	0.71			0.67	0.29
Lu †		0.08	0.03	0.06	0.02	0.00	0.05	0.04	0.10	0.06	0.05	0.11			0.09	0.04

Representative samples and averages of all analyses. See Fig. 53 for sample localities.

Appendix 8. Chemical composition of retrogressed tonalitic-trondhjemitic grey gneiss, Fiskefjord area

GGU	Retrogressed									High P_2O_5, Sr, Ba, LREE								All retrogressed	
No	289247	289126	289246	289245	289130	339199	289243	average (n=82)	s.d.	328508	339941	328504	328538	339225	328523	average (*n=6*)	s.d.	average (*n=88*)	s.d.
SiO_2	64.58	66.71	68.33	70.04	70.59	72.57	74.52	70.26	2.87	64.62	65.36	66.84	67.80	68.49	69.67	67.13	1.91	70.05	2.91
TiO_2	0.45	0.29	0.40	0.31	0.15	0.13	0.15	0.28	0.14	0.38	0.34	0.32	0.33	0.30	0.24	0.32	0.05	0.28	0.13
Al_2O_3	17.99	17.07	16.31	16.15	16.18	15.86	14.24	15.97	1.05	16.03	16.11	16.57	16.58	16.67	16.19	16.36	0.28	15.99	1.02
Fe_2O_3	0.89	0.97	1.03	0.53	0.47	0.00	0.27	0.63	0.56	1.67	0.98	0.91	1.04	0.10	0.24	0.82	0.58	0.64	0.56
FeO	2.45	1.63	1.89	1.64	0.63	0.61	1.15	1.30	0.72	1.99	2.00	1.29	1.57	1.43	0.92	1.53	0.42	1.32	0.71
FeO*	3.25	2.50	2.82	2.12	1.05	0.61	1.39	1.87	1.09	3.49	2.88	2.11	2.51	1.52	1.14	2.27	0.87	1.90	1.08
MnO	0.05	0.03	0.05	0.04	0.01	0.02	0.03	0.03	0.02	0.09	0.08	0.04	0.05	0.03	0.03	0.05	0.03	0.03	0.02
MgO	1.71	1.32	1.13	0.94	0.50	0.38	0.58	0.75	0.45	1.63	2.10	1.62	1.53	1.02	0.81	1.45	0.47	0.80	0.48
CaO	4.83	3.25	4.31	3.93	2.26	2.99	3.08	3.16	0.84	3.69	3.18	3.42	3.23	3.38	2.63	3.26	0.35	3.17	0.81
Na_2O	5.21	5.59	5.17	5.24	5.43	5.49	4.66	5.03	0.59	4.92	5.00	5.77	5.06	5.68	5.35	5.30	0.36	5.05	0.58
K_2O	0.83	1.35	0.48	0.71	1.92	0.95	0.88	1.31	0.61	3.42	3.41	2.01	1.36	1.02	2.71	2.32	1.03	1.38	0.69
P_2O_5	0.10	0.16	0.12	0.07	0.04	0.07	0.06	0.10	0.06	0.24	0.26	0.22	0.19	0.17	0.13	0.20	0.05	0.10	0.06
l.o.i.	0.27	0.51	0.21	0.18	0.40	0.47	0.13	0.38	0.20	0.62	0.45	0.47	0.57	0.79	0.40	0.55	0.14	0.39	0.20
Sum	99.37	98.88	99.42	99.78	98.58	99.55	99.75	99.19	0.54	99.30	99.27	99.48	99.31	99.07	99.32	99.29	0.13	99.19	0.53
Rb	11	14	3	4	24	10	19	17	15	87	72	36	7	3	52	43	34	19	18
Ba	457	818	375	454	1430	369	616	747	424	1590	2000	1540	1330	1640	1850	1658	237	809	474
Pb	12	15	8	11	13	12	13	14	6	33	37	25	15	15	25	25	9	15	6
Sr	630	1050	558	683	922	654	496	662	244	1160	1130	1220	988	1020	1130	1108	88	692	262
La	11	39	13	13	13	6	10	16	11	35	67	44	26	21	20	36	18	17	12
Ce	15	65	16	19	23	14	16	26	19	68	131	79	47	35	31	65	37	29	23
Nd	8	25	6	8	9	5	5	11	7	32	54	33	22	14	11	28	16	12	9
Y	3	4	1	1	<1	1	2	3	4	15	15	6	3	1	2	7	6	3	4
Th	5	5	2	2	<1	1	1	3	3	8	16	7	1	<1	4	6	6	3	3
Zr	84	114	121	91	71	63	52	108	67	103	141	105	67	47	84	91	33	107	65
Nb	2.7	2.0	2.3	2.4	1.3	2.1	1.4	2.2	1.8	4.6	6.2	2.9	2.2	1.5	2.2	3.3	1.8	2.3	1.8
Zn	58	56	53	39	27	24	32	39	17	75	59	48	55	36	28	50	17	40	18
Cu	15	18	8	3	<1	8	9	8	8	16	21	15	15	17	23	18	3	9	8
Co	31	39	28	28	31	72	29	66	33	91	55	68	55	53	86	68	17	66	32
Ni	18	10	10	9	<1	3	2	6	5	11	28	27	17	7	9	17	9	6	6
V	51	30	33	21	12	7	13	23	14	67	48	36	44	30	21	41	16	24	15
Cr	19	8	16	7	4	12	5	9	8	14	40	31	27	8	13	22	12	9	9
Ga	19	21	17	18	20	15	15	18	2	24	21	19	20	16	18	20	3	18	2
Sc	5	3	3	2	<1	2	1	2	2	9	7	4	8	8	2	6	3	2	2
								(*n=8*)											
Cs †	0.5		<0.2	<0.2		<0.2	0.3	0.1	0.2										
Hf †	2.0		2.6	2.3		1.8	1.4	1.8	0.5										
Sc †	4.9		3.2	2.2		1.1	1.4	3.1	2.3										
Ta †	0.4		0.6	0.7		<0.3	0.8	0.5	0.3										
Th †	0.2		0.0	0.2		0.3	0.5	0.3	0.3										
U †	<0.1		<0.1	0.2		<0.1	<0.1	<0.1	0.1										
La †	12.7		12.7	14.7		7.6	13.4	12.2	2.3										
Ce †	20		18	19		12	17	17	4										
Nd †	8		7	6		4	5	6	3										
Sm †	1.30		0.87	0.77		0.66	0.69	0.94	0.57										
Eu †	0.68		0.64	0.71		0.36	0.64	0.66	0.18										
Tb †	0.1		0.1	0.1		0.1	0.1	0.1	0.1										
Yb †	0.27		0.19	0.20		0.09	0.15	0.21	0.14										
Lu †	0.04		0.02	0.03		0.02	0.03	0.03	0.02										

Representative samples and averages of ordinary retrogressed tonalitic-trondhjemitic grey gneiss and a group with high P_2O_5, Sr, Ba, LREE, etc. at central Fiskefjord, related to the Qeqertaussaq diorite (see the main text and Appendix 6). Sample localities shown in Fig. 53.

Appendix 9. Chemical compositions of Finnefjeld gneiss and Taserssuaq tonalite complexes, Fiskefjord area

GGU	Finnefjeld gneiss complex							Taserssuaq tonalite complex								Mafic enclaves (Taserssuaq)			
No	339643	339638	339633	339641	339650	average (n=34)	s.d.	288616	283372	283317	278811	289103	289208	average (*n=30*)	s.d.	283329	283381	average (n=5)	s.d.
SiO_2	61.89	64.20	66.89	69.40	74.12	68.63	4.22	57.96	62.74	67.53	70.62	72.30	74.08	67.53	5.17	49.95	54.62	52.87	2.12
TiO_2	0.79	0.72	0.47	0.44	0.28	0.40	0.21	0.30	0.49	0.36	0.29	0.34	0.15	0.43	0.20	1.39	0.85	0.88	0.35
Al_2O_3	16.30	16.33	16.07	15.52	13.99	15.68	1.10	15.97	19.11	16.77	14.94	13.45	13.45	15.69	1.99	16.59	17.69	15.41	4.26
Fe_2O_3	1.50	1.38	1.00	0.88	0.19	0.76	0.50	1.48	0.86	0.69	0.84	1.05	0.28	1.18	0.63	3.80	2.25	2.60	0.70
FeO	4.08	3.53	2.48	2.05	1.48	2.05	1.23	4.49	2.33	2.19	1.41	1.57	0.90	2.07	0.96	6.94	5.45	6.02	0.61
FeO*	5.43	4.77	3.38	2.84	1.65	2.73	1.65	5.82	3.10	2.81	2.17	2.52	1.15	3.13	1.41	10.36	7.48	8.36	1.19
MnO	0.09	0.08	0.06	0.05	0.03	0.05	0.03	0.12	0.05	0.05	0.03	0.05	0.04	0.06	0.03	0.16	0.13	0.14	0.02
MgO	2.84	1.74	1.52	1.23	0.69	1.29	0.96	6.03	1.72	1.39	0.54	0.71	0.26	1.31	1.09	4.72	4.08	6.25	3.42
CaO	3.98	4.14	3.68	3.38	2.69	3.24	1.20	6.14	5.18	3.80	2.40	1.83	0.80	3.17	1.54	8.27	7.40	8.85	1.86
Na_2O	4.23	4.90	4.63	4.59	4.99	4.51	0.65	3.90	5.53	4.72	4.11	3.73	3.69	4.39	0.70	3.72	4.20	3.36	1.34
K_2O	2.09	1.73	1.89	1.68	1.72	2.27	1.24	1.59	1.42	1.61	3.25	3.85	5.04	2.64	1.29	1.74	1.54	1.40	0.42
P_2O_5	0.22	0.26	0.18	0.16	0.10	0.15	0.07	0.04	0.09	0.10	0.10	0.10	0.03	0.14	0.09	0.54	0.33	0.33	0.17
l.o.i.	0.81	0.64	0.72	0.32	0.32	0.51	0.23	1.15	0.26	0.24	0.54	0.35	0.36	0.51	0.33	0.77	0.61	0.67	0.07
Sum	98.82	99.65	99.60	99.70	100.61	99.53	0.41	99.17	99.78	99.45	99.07	99.33	99.08	99.10	0.28	98.58	99.14	98.77	0.38
														(*n=17; Rb, Sr, Y, Zr, Nb: n=29*)					
Rb	66	47	46	43	38	57	25	62	45	77	76	81	141	73	40	47	46	37	12
Ba	1270	967	811	775	976	876	511		428	414	1010		427	677	387	624	770	463	238
Pb	11	12	15	13	14	18	7		16	15	13		19	17	4	8	6	8	2
Sr	519	323	388	359	360	462	199	437	540	466	420	187	65	396	202	721	704	597	240
La	20	21	81	14	14	20	14		9	19	30		44	39	30	63	43	45	19
Ce	46	38	47	25	28	39	20		15	32	34		87	74	62	113	81	82	37
Nd	24	18	23	10	11	18	10		9	17	17		35	29	21	49	38	39	15
Y	9	9	12	5	2	9	8	19	9	5	8	11	18	12	8	24	16	17	4
Th	2	<1	5	1	4	5	4		6	5	3		9	9	6	6	<1	4	3
Zr	187	217	153	116	126	121	47	62	94	79	102	195	108	154	98	100	99	90	23
Nb	5.2	4.9	4.8	4.5	3.3	4.3	2.6	5.9	6.2	3.2	4.6	7.6	5.9	5.8	3.4	11.0	5.9	6.3	3.2
Zn	90	82	70	59	38	53	26		47	57	39		39	59	23	121	88	93	20
Cu	20	22	14	7	7	13	8		3	11	10		5	11	8	62	15	70	71
Co	48	41	50	56	80	64	24		14	15	95		78	40	42	40	31	40	11
Ni	28	8	13	12	6	11	13		15	15	5		8	7	4	42	44	159	239
V	104	69	53	43	26	43	30		50	40	18		7	31	19	235	158	183	32
Cr	37	8	25	13	8	21	40		12	15	10		<1	7	4	19	24	152	264
Ga	22	19	21	18	15	18	3		23	18	17		16	19	4	20	21	18	5
Sc	11	20	13	5	2	7	7		5	4			5	6	4	21	17	26	13
						(*n=5*)								(*n=5*)				(*n=3*)	
Cs †	0.6	0.4	0.7	0.6	0.7	0.6	0.1		0.9	2.0	0.6		0.3	0.9	0.6	1.1	1.0	1.1	0.1
Hf †	5.1	5.3	4.5	2.9	2.2	4.0	1.4		3.0	2.4	2.0		3.3	2.7	0.5	3.0	2.9	3.0	0.2
Sc †	9.2	18.7	12.5	4.6	1.7	9.3	6.7		6.3	5.2	2.9		4.0	4.4	1.4	21.6	17.5	20.1	2.3
Ta †	<0.3	<0.3	0.4	<0.3	0.3	0.1	0.2		1.1	0.6	<0.3		0.4	0.5	0.4	0.6	0.3	0.5	0.2
Th †	1.7	0.6	2.6	1.0	2.3	1.6	0.8		1.5	3.3	3.2		8.1	4.2	2.5	5.5	2.5	4.1	1.5
U †	0.7	<0.1	<0.1	0.2	<0.1	0.2	0.3		0.9	0.6	0.7		0.4	0.6	0.2	0.3	0.5	0.7	0.5
La †	22.1	25.5	32.1	17.5	19.9	23.4	5.7		8.8	20.9	31.7		47.9	28.7	14.7	67.8	44.8	59.5	12.7
Ce †	38	44	53	31	29	39	10		17	36	49		89	49	27	124	81	107	23
Nd †	16	20	23	12	10	16	5		8	15	18		36	19	10	54	37	46	9
Sm †	2.66	3.09	3.83	1.80	1.04	2.48	1.09		2.25	1.95	2.62		6.01	3.06	1.67	8.08	5.87	7.11	1.13
Eu †	0.94	1.16	0.87	0.80	0.71	0.90	0.17		0.73	0.57	0.85		0.68	0.71	0.10	2.41	1.63	2.02	0.39
Tb †	0.4	0.3	0.4	0.2	0.1	0.3	0.1		0.3	0.2	0.3		0.7	0.3	0.3	0.9	0.6	0.7	0.2
Yb †	0.85	0.74	0.99	0.45	0.29	0.66	0.29		0.65	0.29	0.60		1.21	0.60	0.39	2.44	1.42	1.86	0.53
Lu †	0.11	0.10	0.13	0.07	0.05	0.09	0.03		0.07	0.04	0.09		0.15	0.07	0.05	0.28	0.19	0.23	0.05

Representative samples and averages of all analyses. See Fig. 68 for sample localities.

Appendix 10. Chemical compositions of Igánánguit granodiorite and Qugssuk granite, Fiskefjord area

GGU	Igánánguit granodiorite						Qugssuk granite					
No	278880	278883	278890	289059	average (*n=8*)	s. d.	289194	278786	283377	283378	average (*n=27*)	s. d.
SiO_2	67.04	69.40	69.89	70.83	70.04	2.27	70.58	75.30	77.50	78.29	73.69	2.38
TiO_2	0.41	0.25	0.39	0.28	0.29	0.12	0.27	0.10	0.15	0.14	0.17	0.07
Al_2O_3	16.98	15.97	15.21	15.36	15.54	0.79	15.43	13.30	12.08	11.73	14.08	1.43
Fe_2O_3	0.73	0.62	0.76	0.83	0.65	0.29	0.21	0.23	0.33	0.51	0.35	0.25
FeO	2.18	1.13	1.41	1.17	1.31	0.64	1.20	0.88	0.53	0.32	0.83	0.32
FeO*	2.84	1.69	2.09	1.92	1.89	0.87	1.39	1.09	0.83	0.78	1.41	0.39
MnO	0.04	0.03	0.03	0.02	0.03	0.01	0.01	0.01	0.02	0.02	0.02	0.01
MgO	1.09	0.70	0.84	0.62	0.73	0.35	0.58	0.05	0.05	0.05	0.30	0.19
CaO	3.44	2.49	2.33	2.12	2.32	0.75	1.97	1.22	0.61	0.58	1.56	0.66
Na_2O	5.34	4.93	4.78	4.71	4.73	0.40	3.85	3.24	2.91	2.86	3.64	0.77
K_2O	1.33	2.92	2.61	3.15	2.96	1.12	4.40	4.92	5.18	4.97	4.28	1.11
P_2O_5	0.15	0.21	0.16	0.11	0.14	0.05	0.09	0.01	0.02	0.02	0.04	0.03
l.o.i.	0.46	0.49	0.47	0.26	0.43	0.24	0.33	0.08	0.06	0.04	0.22	0.21
Sum	99.19	99.14	98.88	99.46	99.15	0.21	98.92	99.34	99.45	99.53	99.18	0.28
												(*n=16; Rb, Sr, Y, Th, Zr, Nb: n=25*)
Rb	48	54	78	44	70	22	83	135	142	133	105	32
Ba	317	1030	1630	1810	1183	507		777	287	197	1032	858
Pb	17	19	20	22	21	5		25	20	18	23	5
Sr	507	475	538	537	474	66	667	146	85	60	282	185
La	19	20	52	39	29	14		21	39	27	25	14
Ce	21	16	70	48	37	22		31	65	53	45	28
Nd	13	8	22	16	14	5		12	30	20	17	10
Y	5	3	4	2	4	2	3	3	11	10	6	7
Th	7	<1	15	12	9	6		12	12	14	12	6
Zr	99	84	258	148	138	62	136	113	93	90	118	43
Nb	4.9	1.8	3.9	1.9	3.2	1.6	2.0	1.4	3.5	4.3	3.4	2.5
Zn	60	30	45	33	36	17		16	11	10	20	10
Cu	37	8	9	8	10	11		3	7	<1	8	11
Co	92	106	71	95	97	21		233	22	17	42	59
Ni	3	4	5	4	4	2		4	4	<1	4	2
V	37	20	21	20	20	13		8	3	3	7	5
Cr	17	6	13	10	8	5		5	4	3	6	4
Ga	21	17	17	17	7	3		13	14	14	14	2
					(*n=6*)						(*n=5*)	
Cs †	0.8	0.2	0.4	<0.2	0.4	0.3	0.3	0.3	0.8		0.4	0.2
Hf †	2.7	1.5	5.6	3.6	3.2	1.5	2.8	2.3	3.5		3.0	0.8
Sc †	5.0	1.8	2.8	2.0	2.6	1.4	2.0	1.2	1.2		1.5	0.5
Ta †	0.6	0.4	<0.3	<0.3	0.3	0.3	<0.3	<0.3	0.6		0.1	0.3
Th †	9.6	0.7	14.2	14.0	11.2	6.5	9.1	13.4	9.2		12.3	3.3
U †	0.8	<0.1	0.8	<0.1	0.3	0.4	0.5	0.5	0.5		0.6	0.1
La †	28.4	20.1	77.4	62.9	48.4	23.8	38.6	33.9	43.3		45.2	10.2
Ce †	46	30	106	96	70	32	56	52	70		69	18
Nd †	19	12	29	30	22	7	17	17	29		24	7
Sm †	2.92	1.67	3.17	3.29	2.72	0.65	2.09	2.59	4.41		2.99	0.90
Eu †	0.59	0.79	0.84	0.96	0.78	0.14	0.74	0.56	0.40		0.61	0.14
Tb †	0.2	0.2	0.3	0.2	0.3	0.1	0.2	0.2	0.5		0.3	0.1
Yb †	0.38	0.28	0.47	0.25	0.34	0.09	0.25	0.33	0.69		0.37	0.18
Lu †	0.05	0.04	0.05	0.03	0.04	0.01	0.02	0.04	0.10		0.04	0.03

Representative samples and averages of all analyses belonging to Igánánguit granodiorite and Qugssuk granite (groups a and b in the main text). See Fig. 68 for sample localities.

Appendix 11. Chemical compositions of various granitic rocks, Fiskefjord area

GGU	Other granites (amphibolite facies)						Mesoperthite granite					
No	283664	283682	283686	283683	average (n=8)	s. d.	283715	289156	289159	289153	average (n=16)	s. d.
SiO_2	68.14	71.49	72.49	73.56	71.94	1.80	70.67	72.15	73.70	75.68	72.53	1.28
TiO_2	0.12	0.29	0.21	0.15	0.22	0.07	0.15	0.15	0.11	0.02	0.14	0.07
Al_2O_3	18.68	15.20	14.38	14.43	15.27	1.54	17.14	15.24	13.66	13.55	15.46	0.96
Fe_2O_3	0.15	0.24	0.34	0.38	0.43	0.44	0.00	0.48	0.41	0.15	0.21	0.19
FeO	0.40	1.37	1.08	0.66	1.05	0.41	0.65	0.48	0.88	0.34	0.59	0.27
FeO*	0.54	1.59	1.39	1.00	1.43	0.71	0.65	0.91	1.25	0.48	0.78	0.32
MnO	0.02	0.03	0.03	0.03	0.03	0.01	0.02	0.01	0.01	<0.01	0.02	0.01
MgO	0.32	0.77	0.47	0.32	0.48	0.18	0.25	0.37	0.36	0.06	0.32	0.14
CaO	3.39	2.92	1.77	1.26	2.17	0.71	2.27	1.83	1.06	1.62	1.93	0.38
Na_2O	5.88	4.00	3.42	3.62	4.09	0.84	6.17	5.13	3.16	2.71	4.94	1.07
K_2O	1.56	1.95	4.01	4.28	3.00	1.11	1.88	2.50	4.85	4.33	2.75	0.96
P_2O_5	0.03	0.11	0.08	0.06	0.08	0.03	0.05	0.04	0.05	0.01	0.06	0.03
l.o.i.	0.19	0.34	0.68	0.60	0.36	0.20	0.11	0.28	0.51	0.31	0.24	0.12
Sum	98.89	98.70	98.96	99.35	99.12	0.28	99.36	98.66	98.76	98.78	99.18	0.32
Rb	31	34	108	107	67	32	13	39	105	65	45	26
Ba	796	3620	1490	1130	1587	929	1830	980	1500	2470	1455	425
Pb	19	13	29	21	21	6	23	22	28	25	23	4
Sr	578	603	280	196	445	333	1151	800	381	396	792	253
La	10	28	48	22	27	15	9	13	34	9	13	7
Ce	24	51	94	48	52	24	17	22	53	3	22	13
Nd	8	17	33	17	19	8	7	9	21	4	9	5
Y	2	2	6	5	4	2	1	1	4	<1	1	1
Th	7	11	29	20	16	9	3	4	14	1	4	3
Zr	426	244	188	115	203	107	43	77	139	90	70	35
Nb	0.8	<0.8	3.3	2.2	2.0	1.4	0.8	1.0	1.3	0.8	1.0	0.7
Zn	15	28	36	19	28	8	18	32	26	3	27	14
Cu	8	21	5	8	9	6	14	2	4	<1	9	6
Co	41	40	77	43	61	24	101	51	74	134	94	29
Ni	6	8	4	4	5	2	2	5	7	5	4	2
V	7	26	14	9	15	6	7	8	15	9	9	4
Cr	3	12	14	8	10	5	8	4	4	<1	4	4
Ga	22	13	14	15	15	3	15	17	14	13	17	2
Sc	2	2	3	3	3	1	2	<1	<1	<1	1 (*n*=2)	1
Cs †							<0.2		<0.2			
Hf †							1.5		3.9		5.4	
Sc †							0.4		1.1		1.5	
Ta †							<0.3		<0.3			
Th †							0.2		14.9		15.1	
U †							<0.1		0.6			
La †							12.9		46.3		59.2	
Ce †							23		84		107	
Nd †							8		30		38	
Sm †							0.92		3.42		4.34	
Eu †							0.42		0.53		0.9	
Tb †							0.1		0.2		0.3	
Yb †							0.12		0.32		0.44	
Lu †							<0.03		0.05		0.05	

Representative samples and averages of all analyses belonging to amphibolite facies granite sheets in north-eastern Nordlandet (group c in the main text) and mesoperthite (granulite facies) granite sheets (group d). See Fig. 68 for sample localities.

Appendix 12. Chemical analyses of High-Mg and other dykes in the Fiskefjord area

GGU	High-Mg N-S dykes									Related N-S dykes			Microgranite dyke			
No	339196	339105	283629	339534	339148	328172	289116	328143	289155	289115	278778	278779	289229	289236	289271	average
	Pâkitsoq	Feeder	E Feeder	E Feeder	E Feeder	E Feeder	W Sister	W Sister	E Sister	NW of Usuk	Narssarssuaq			Qugssuk		
SiO_2	53.21	52.34	51.91	51.55	52.00	51.34	53.70	53.79	50.86	56.51	56.80	56.51	69.19	69.25	68.91	69.12
TiO_2	0.46	0.42	0.34	0.40	0.39	0.54	0.46	0.47	0.50	0.57	0.59	0.58	0.56	0.54	0.58	0.56
Al_2O_3	10.95	12.31	8.85	10.29	9.98	8.52	10.97	11.47	8.35	14.82	14.74	14.73	14.45	14.42	14.38	14.42
Fe_2O_3	2.58	2.66	2.34	3.13	2.18	2.11	2.44	2.31	2.22	2.01	0.87	1.33	1.12	1.01	1.21	1.11
FeO	7.02	6.39	6.72	6.03	6.97	7.95	7.50	7.31	7.95	6.65	8.15	7.75	1.96	1.97	1.97	1.97
FeO*	9.34	8.78	8.83	8.85	8.93	9.85	9.70	9.39	9.95	8.46	8.93	8.95	2.97	2.88	3.06	2.97
MnO	0.17	0.15	0.17	0.16	0.16	0.18	0.16	0.17	0.16	0.14	0.14	0.14	0.04	0.04	0.04	0.04
MgO	14.74	13.70	21.08	18.49	17.84	17.27	13.30	12.79	18.31	6.29	4.97	4.98	0.69	0.66	0.65	0.67
CaO	7.30	8.21	5.93	6.82	6.77	7.83	7.49	7.77	7.04	8.29	8.59	8.59	1.96	1.97	1.97	1.97
Na_2O	1.85	2.13	1.45	1.83	1.75	1.74	1.99	1.96	1.72	2.62	3.02	2.83	3.61	3.66	3.26	3.51
K_2O	0.77	0.63	0.50	0.55	0.59	0.59	0.69	0.73	0.59	0.99	1.29	1.25	4.86	4.84	4.92	4.87
P_2O_5	0.11	0.11	0.08	0.10	0.10	0.08	0.09	0.10	0.07	0.10	0.12	0.11	0.14	0.14	0.16	0.15
l.o.i.	1.18	1.23	0.79	0.84	1.33	1.29	1.20	1.22	1.44	0.88	0.76	1.00	0.22	0.22	0.22	0.22
Sum	100.34	100.28	100.15	100.20	100.06	99.44	99.99	100.10	99.21	99.87	100.04	99.80	98.81	98.70	98.27	98.61
Rb	23	13	13	13	15		20		18	28	40	39	251	256	212	240
Ba	325	317	251	280	260		314		239	378	427	437	1280	1260	1570	1370
Pb	7	6	2	4	6		3		4	5	2	4	27	27	20	25
Sr	255	248	155	192	180		248		198	312	314	318	270	280	283	278
La	13	13	11	11	9		21		13	17	19	14	150	142	141	144
Ce	26	21	15	15	17		23		16	29	26	38	294	279	274	282
Nd	13	9	6	7	8		11		8	14	15	21	110	102	103	105
Y	10	9	8	10	9		12		9	14	15	14	44	41	43	43
Th	3	1	2	2	4		<1		3	4	2	3	33	36	31	33
Zr	61	61	51	59	60		64		58	82	94	93	481	473	526	493
Nb	3.0	3.5	1.3	2.9	2.7		3.4		3.0	4.3	4.7	4.2	22.0	22.0	24.0	22.7
Zn	98	75	69	72	77		76		72	67	77	75	42	30	43	38
Cu	56	40	46	32	34		58		801	60	52	55	2	11	14	9
Co	77	69	17	88	88		74		94	60	116	94	19	15	19	18
Ni	456	479	934	738	698		274		69	62	60	65	10	9	15	11
V	165	152	131	144	143		166		151	158	165	170	32	33	32	32
Cr	1730	1460	2860	2270	2450		1300		3220	226	86	89	11	10	10	10
Ga	15	17	11	13	12		16		13	21	20	21	20	22	21	21
Sc	28	26	22	21	26		24		19	23			3	3	4	3
Cs †													<2	<2		<2
Hf †													14	15		14.5
Sc †													4.2	4.6		4.4
Ta †													<3	<3		<3
Th †													24	28		26
U †													2.7	2.5		2.6
La †													170	170		170
Ce †													280	290		285
Nd †													100	100		100
Sm †													12	12		12
Eu †													1.6	1.6		1.6
Tb †													1.4	1.6		1.5
Yb †													3.44	3.40		3.42
Lu †													0.45	0.43		0.44

Dyke names by Berthelsen & Bridgwater (1960) are used where appropriate, or the nearest place name (Fig. 1) is indicated. Locations of samples are shown in Fig. 82.

Appendix 13. Chemical analyses of NE–SW and E–W trending mafic dykes in the Fiskefjord area

GGU	NE-SW dykes								E-W dykes							
No	328228	328229	328151	278836	283622	328147	278812	289093	278713	289092	328219	278810	289112	283384	283390	283394
	Kangeq	Eqaluk	Blåbær		Fiskefjord		Narssarssuaq		Inner Fiskefjord		S Kangeq	Qugssuk	NofUsuk		Tasiussaq	
SiO_2	51.44	51.07	53.18	52.92	49.24	49.62	53.34	52.67	50.11	49.64	49.99	50.15	50.97	50.30	49.95	50.10
TiO_2	1.05	0.88	2.21	2.37	1.59	1.37	0.62	0.60	1.74	1.49	1.56	1.00	1.11	2.25	2.08	2.27
Al_2O_3	9.25	7.99	13.73	13.13	14.50	14.05	13.41	13.80	12.70	12.82	13.46	14.33	14.23	12.69	12.80	12.65
Fe_2O_3	2.37	2.38	3.81	4.56	3.47	3.20	2.29	1.55	3.37	2.33	2.66	1.95	2.63	2.55	1.91	2.36
FeO	9.65	9.31	9.95	10.43	11.21	11.22	7.61	7.57	12.31	12.14	11.90	10.18	10.63	13.94	14.14	14.28
FeO*	11.78	11.45	13.38	14.53	14.33	14.10	9.67	8.97	15.34	14.24	14.29	11.94	13.00	16.24	15.86	16.40
MnO	0.19	0.20	0.18	0.19	0.21	0.22	0.16	0.16	0.23	0.23	0.23	0.21	0.21	0.25	0.25	0.25
MgO	10.89	13.62	3.61	3.71	6.03	7.32	9.81	8.75	5.63	6.31	5.96	6.63	6.09	5.01	5.52	4.91
CaO	10.17	10.49	7.70	7.69	9.13	8.69	9.23	10.08	9.68	10.05	9.72	11.71	10.27	9.26	9.47	9.16
Na_2O	2.38	1.96	2.50	2.61	2.35	2.14	1.99	1.94	2.29	2.13	1.99	1.87	2.23	2.36	2.34	2.30
K_2O	1.01	0.74	1.09	1.00	0.59	0.48	0.52	0.48	0.61	0.63	0.56	0.28	0.52	0.90	0.77	0.93
P_2O_5	0.15	0.12	0.49	0.50	0.28	0.22	0.08	0.08	0.17	0.15	0.16	0.07	0.14	0.25	0.21	0.25
l.o.i.	1.08	1.23	1.11	1.07	1.42	1.32	0.98	2.06	1.43	1.73	1.28	1.78	1.03	1.55	1.57	1.59
Sum	99.63	99.98	99.56	100.18	100.02	99.84	100.04	99.74	100.27	99.65	99.48	100.16	100.06	101.31	101.01	101.04
Rb				19			12	12	15	17		11	12			
Ba				523			238	243	300	224		70	252			
Pb				3			1	4	<1	2		<1	4			
Sr				380			204	192	199	198		120	227			
La				31			16	16	11	14		1	12			
Ce				57			18	23	23	24		3	18			
Nd				37			11	11	16	16		11	13			
Y				33			15	15	29	25		22	21			
Th				2			3	3	<1	2		<1	3			
Zr				166			65	67	106	89		59	70			
Nb				7.3			2.9	3.8	9.1	6.9		3.9	5.6			
Zn				156			80	77	124	118		106	89			
Cu				21			86	99	192	391		94	89			
Co				78			78	57	71	77		86	69			
Ni				38			194	174	61	71		60	46			
V				383			194	192	412	377		291	289			
Cr				39			676	490	89	135		160	97			
Ga				26			17	15	19	17		19	20			
Sc							28	30		42			35			

Dyke names by Berthelsen & Bridgwater (1960) are used where appropriate, or the nearest place name (Fig. 1) is indicated. Locations of samples are shown in Fig. 82.

Plate 1 (In pocket). Simplified geological map of the Fiskefjord area.

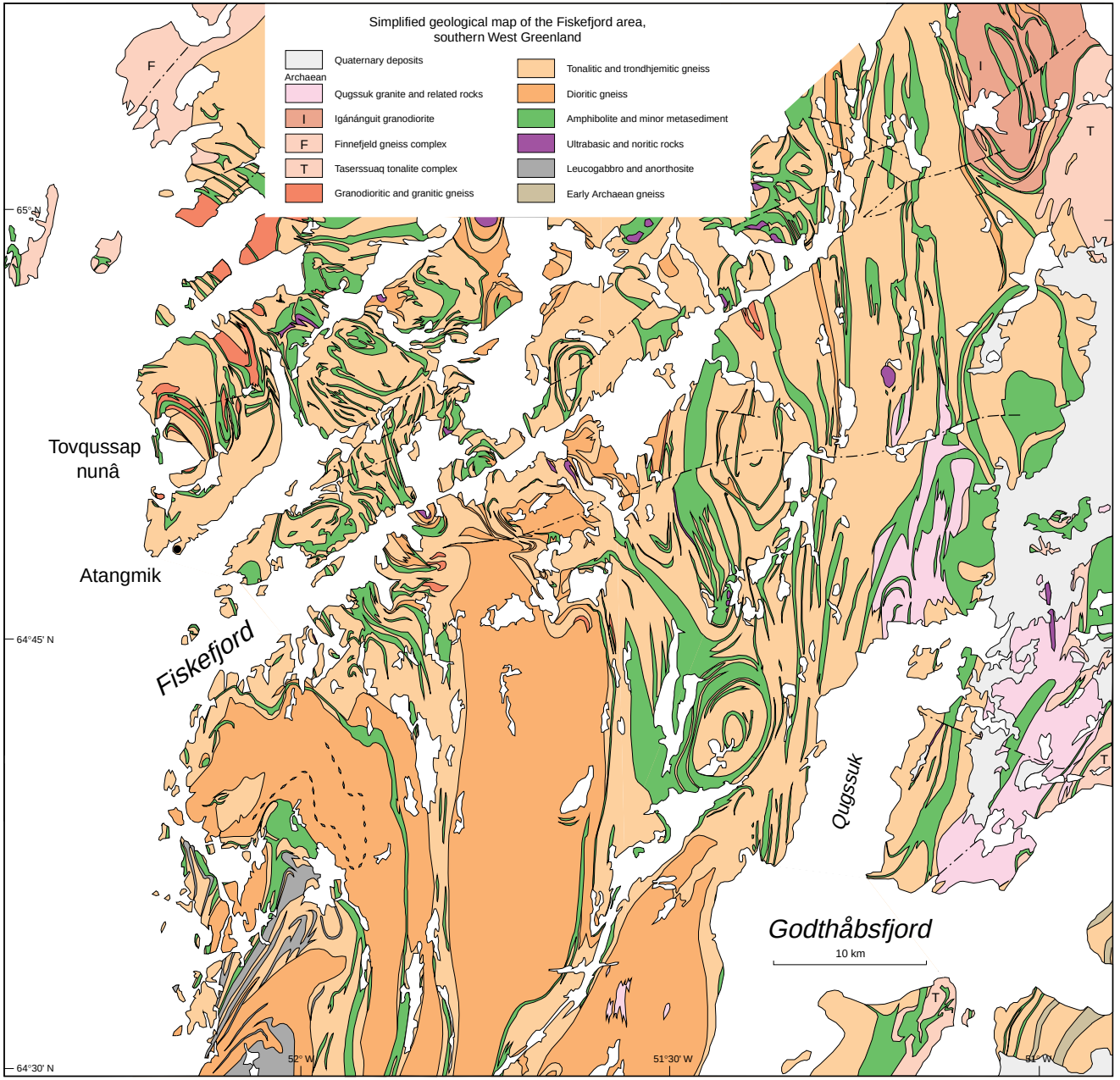
Simplified geological map of the Fiskefjord area,
southern West Greenland
Archaean
Quaternary deposits
Qugssuk granite and related rocks
Igánánguit granodiorite
Finnefjeld gneiss complex
Taserssuaq tonalite complex
Granodioritic and granitic gneiss
Tonalitic and trondhjemitic gneiss
Dioritic gneiss
Amphibolite and minor metasediment
Ultrabasic and noritic rocks
Leucogabbro and anorthosite
Early Archaean gneiss
F
I
T
65° N
Tovqussap
nunâ
Atangmik
64°45' N
Fiskefjord
Qugssuk
Godthåbsfjord
10 km
64°30' N
52° W
51°30' W
51° W